The interplay of fatty acid synthesis, metabolism, and immune function during Flavivirus infection

Alice Trenerry

ORCID ID: 0000-0002-8424-4250

from Canberra, Australia

Submitted in total fulfilment of the requirements of the joint degree of

Doctor of Philosophy (PhD)

of

The Medical Faculty

The Rheinische Friedrich-Wilhelms-Universität Bonn

and

The Department of Microbiology and Immunology

The University of Melbourne

Bonn/Melbourne, 2023

Performed and approved by The Medical Faculty of The Rheinische Friedrich-WilhelmsUniversität Bonn and The University of Melbourne

1. Supervisor: Florian Schmidt
2. Supervisor: Jason Mackenzie
Co-supervisor: Sammy Bedoui

Month and year of the original thesis submission: February 2023
Month and year of the oral examination: September 2023

Institute in Bonn: Institute of Innate Immunity
Director: Prof. Eicke Latz

Table of Contents

Abbreviations

ACC	Acetyl-CoA Carboxylase	**JAK**	Janus kinase
ACP	Acyl-carrier protein	**JEV**	Japanese encephalitis virus
AMPK	Adenosine monophosphate-activated protein kinase	**KO**	Knock-out
ASC	Apoptosis-associated speck-like protein containing a CARD	**iNOS**	Inducible nitric oxide synthase
ATP	Adenosine diphosphate	**LCFA**	Long-chain fatty acid
BBB	Blood brain barrier	**LD**	Lipid droplet
BC	Biotin carboxylase	**LDH**	Lactate dehydrogenase
BMDM	Bone marrow derived macrophage	**LPS**	Lipopolysaccharide
BSA	Bovine serum albumin	**MAVS**	Mitochondrial antiviral signalling
CARD	Caspase recruitment domain	**MCD**	Malonyl-CoA decarboxylase
CAT	Carnitine acyltransferase	**MDA5**	Melanoma differentiation-associated gene 5
CCCP	Carbonyl cyanide m-chlorophenyl hydrazone	**MHC**	Major histocompatibility complex
CDC	Centre for Disease Control	**MOI**	Multiplicity of infection
cGAS/STING	Cytosolic DNA sensing system cyclic GMP-AMP synthase/ stimulator of interferon genes	**mRNA**	Messenger RNA
CHREBP	Carbohydrate response element binding proteins	**NAD**	Nicotinamide adenine dinucleotide
CM/PC	Convoluted membrane/paracrystalline arrays	**NADPH**	Nicotinamide adenine dinucleotide phosphate
CNS	Central nervous system	**NO**	Nitric oxide
CoA	Coenzyme A	**NOS2**	Nitric oxide synthase 2
CPT-1	Carnitine palmitoyl transferase 1	**NS**	Non-structural
CRISPR	Clustered regularly interspaced palindromic repeats	**OCR**	Oxygen consumption rate

Cryo-EM	Cryogenic electron microscopy	**OXPHOS**	Oxidative phosphorylation
CT	Carboxyltransferase	**PAF**	Platelet-activating factor
DAG	Diacylglycerol	**PAMP**	Pathogen-associated molecular pattern
DAMP	Danger-associated molecular pattern	**PBS**	Phosphate buffered saline
DC	Dendritic cell	**PC**	Phosphatidylcholine
DENV	Dengue virus	**PCR**	Polymerase chain reaction
DGAT-1	Diacylglycerol O-acyltransferase	**PE**	Phosphatidylethanolamine
DMEM	Dulbecco's modified Eagle Medium	**PI**	Propidium iodide
DMSO	Dimethyl sulfoxide	**PLA2**	Phospholipase A2
DNA	Deoxyribonucleic acid	**PPAR**	Peroxisome proliferator-activated receptors
D.p.i.	Days post infection	**prM**	Pre-membrane
DRP-1	Dynamin-related protein 1	**PS**	Phosphatidylserine
dsRNA	Double stranded ribonucleic acid	**qRT-PCR**	Quantitative reverse transcription PCR
EBV	Epstein-Barr virus	**RIG-I**	Retinoic acid-inducible gene I
ECAR	Extracellular acidification rate	**RC**	Replication complex
ER	Endoplasmic reticulum	**RdRp**	RNA dependent RNA polymerase
ETC	Electron transport chain	**RIG-I**	Retinoic acid-inducible gene I
FA	Fatty acid	**RNA**	Ribonucleic acid
FABP	Fatty acid binding protein	**RNAi**	RNA interference
FACS	Fluorescent-activated cell sorting	**ROS**	Reactive oxygen species
FAD	Flavin adenine dinucleotide	**RPMI**	Roswell Park Memorial Institute
FAO	Fatty acid oxidation	**SCD-1**	Stearoyl-CoA desaturase 1
FAS	Fatty acid synthesis	**SDH**	Succinate dehydrogenase
FASN	Fatty acid synthase	**SREBP**	Sterol regulatory element binding proteins
FAT	Fatty acid translocase	**siRNA**	Short interfering RNA
FATP	Fatty acid transport protein	**ssRNA**	Single-stranded RNA

FCS	Fetal calf serum	**STAT**	Signal transducer and activator of transcription
FFA	Free fatty acid	**TAG**	Triacylglycerol
GAPDH	Glyceraldehyde 3-phosphate dehydrogenase	**TBEV**	Tick-borne encephalitis virus
gRNA	Guide ribonucleic acid	**TBS**	Tris-buffered saline
HCV	Hepatitis C virus	**TCA**	Tricarboxylic cycle
H.p.i.	Hours post infection	**TE**	Thioesterase
HRP	Horse radish peroxidase	**TLR**	Toll-like receptor
HSV	Herpes simplex virus	**TNF**	Tumor necrosis factor
IFA	Immunofluorescence assay	**USUV**	Usutu virus
IFN	Interferon	**UTR**	Untranslated region
IFN-α	Interferon alpha	**VLDL**	Very low-density lipoprotein
IFN-β	Interferon beta	**VP**	Vesicle packets
IFNAR	Interferon alpha/beta receptor	**WNV**	West Nile virus
IL	Interleukin	**YFV**	Yellow fever virus
ISG	Interferon-stimulated gene	**ZIKV**	Zika virus

List of tables

List of figures

Abstract

Macrophage activation and Flavivirus infection can both fundamentally alter cellular metabolism and change the lipid landscape of cells. Flaviviruses upregulate fatty acid synthesis to build membranous replication complexes, and can upregulate mitochondrial metabolism to fuel replication. Classically-activated pro-inflammatory macrophages actively dysregulate mitochondrial respiration and increase fatty acid synthesis, import and accumulation whilst anti-inflammatory macrophages upregulate fatty acid oxidation to fuel mitochondrial respiration. This metabolic shift in macrophages defines and drives the functional phenotype. Flaviviruses have a tropism for macrophages, yet the metabolic profile of infected cells and its link to inflammation have never been investigated. Thus, we hypothesised that virus-induced alterations on the lipid landscape would stimulate and alter metabolic pathways, potentially contributing to the inflammatory state and response of macrophages.

To test this hypothesis, we interrogated the role of fatty acid metabolism and mitochondrial respiration during infection of both macrophages and epithelial cells with West Nile (WNV) and Zika (ZIKV) virus. Our initial analyses focussed on chemical inhibition of fatty acid synthesis and oxidation, primarily targeting acetyl-CoA carboxylase (ACC - the rate limiting step of fatty acid synthesis), fatty acid synthase (FASN – the sole enzyme capable of *de novo* fatty acid synthesis) and carnitine palmitoyl transferase-1 (CPT1 – a mitochondrial enzyme integral for fatty acid oxidation). We observed that TOFA-mediated inhibition of ACC, (*i.e.* restricting *de novo* fatty acid synthesis) completely ablated the production of viral protein and infectious virus for both WNV and ZIKV, demonstrating the necessity of this pathway during infection. We observed some differential impact when we specifically inhibited different enzymatic domains of FASN using c75 and orlistat, such that orlistat demonstrated a higher degree of antiviral activity in both cell types, despite inhibiting an enzymatic activity downstream of c75.

Inhibiting fatty acid import into the mitochondria with Etomoxir caused a reduction in infectious virus production but not protein production, suggesting that

this pathway is required to fuel later steps in the viral life cycle. In addition, we observed limited induction or utilisation of lipid droplets over the course of WNV and ZIKV replication.

Intriguingly, we also observed an unexpected lipid accumulation and mitochondrial fragmentation during orlistat treatment, which has not previously been reported. This fragmentation was associated with major perturbations in mitochondrial respiration and glycolysis. These observations indicate that the antiviral effect of orlistat was not necessarily a result of fatty acid deprivation but rather another unknown (potentially mitochondria-dependent) mechanism that warrants further investigation.

Interestingly, although dysfunctional mitochondria underpin pro-inflammatory macrophage function, neither virus induced changes in mitochondrial respiration or glycolysis. Importantly, we observed that virus infection did induce macrophage polarisation as measured by upregulation of the cell surface markers CD80 and MHC-II. This polarisation occurred independently of fatty acid synthesis and oxidation, as inhibition of these pathways, even with TOFA, did not impact on macrophage status. We employed CRISPR-Cas9 to deplete human macrophages of FASN and showed again that efficient WNV and ZIKV replication critically dependent on FASN. However, despite repeated attempts we could not induce nor evaluate polarisation of these macrophages.

We conclude that the critical role of fatty acid synthesis during flavivirus infection primarily contributes to intracellular virus replication that is uncoupled to cellular metabolism and immune activation. This data highlights the potential to target fatty acid synthesis for the development of effective antivirals. Additionally, although we observed the upregulation of classical macrophage activation markers, the maintenance of metabolic homeostasis that we observed during infection may be indicative of reduced downstream immune responses, which warrants further research.

Declaration

This is to certify that:

i. This thesis comprises of only my original work towards the Doctor of Philosophy expect where indicated in the preface
ii. Due acknowledgement has been made in the test to all other material used; and
iii. This thesis is fewer than 100,000 words in length, exclusive of tables, figures, maps, references, and appendices

Preface

(I) Contribution of others

Prof Jason Mackenzie acted as primary supervisor throughout this PhD.

Turgut Aktepe provided laboratory supervision and technical guidance in the first 2 years of this PhD.

(II) Publication status

All data presented here within is unpublished material not yet submitted for publication.

(III) Acknowledgement of funding sources

This PhD has been supported financially via a Research Training Scholarship from the Australian Government and the research itself was funded by the University of Melbourne. The University of Bonn also provided a small amount of funding to cover fees and expenses associated with the joint degree, which was funded by the DAAD.

Acknowledgements

I have spent many moments over the last 4 years reflecting on what I would write in this acknowledgements section; how to possibly express my gratitude for the huge amount of support I have received throughout this PhD. This accomplishment was indeed a collaborative effort between me, my supervisors, and my friends and family, and I could not have achieved this without them.

Firstly, to my primary supervisor Jase; thank you for accepting me into your research group and giving me this opportunity. For always listening to me, assuring me, and guiding me. I experienced many really difficult and low moments throughout this process and you supported me through each and every one. I was able to count on you being able to make me feel better, and I really felt like you were in my corner. I think we have become a really strong team and I look forward to working with you in the future.

To my co-supervisors, Florian and Sammy, thank you for your advice and input always. Florian in particular, for all of the meetings and time you have invested. It was truly a shame I didn't end up in Bonn but I am grateful to still have been able to learn from you and get to know you, and to visit Bonn for a day.

To my lab members, past and present, we have really felt like a team and I truly appreciate all your support. Thank you to Turgut who taught me almost everything I learned in the first couple of years. You were such an approachable and generous teacher and mentor, and I learned so much about science and leadership from you. To the early lab members Nathan, Julio, Josh, Jordan and Harry; thank you for being so welcoming and patient. To the recent and current lab members Carol, Jess, Katelyn, Florian and Milou, thank you for all the silliness, support, and love. I feel lucky to share a space with you all and I know we will all stay in touch (group holiday to Europe??).

To my PhD committee: Damian Purcell, Axel Kallies and Sarah Londrigan. Thank you for keeping me on track, giving me reality checks when I needed them, and for your guidance. A special shoutout to Sarah who consistently went the extra mile, from helping me find a good doctor, to having coffee with me and telling it

to me straight. It truly felt like you were invested in my progress, but even more so my wellbeing, and I am grateful to have had such a strong advocate on my committee.

Lastly, and most importantly (sorry Jase), to my friends and family. Minna and Laura, you both deserve an entire thesis written above my love and gratitude for you. You supported me in every possible way – I didn't know friends could even be so good. To Arkie, Gabby, Anna, Dan and all my other incredible friends, thank you for being the best support network and the most fun people in the world - for making me feel like I was capable and reminding me that my stress wasn't everything. To my parents, Mark and Mel, and my little sister Georgia – I know we all really felt the distance during this PhD and during COVID, and I miss you every day. Your belief in me and your support has truly kept me going, and I hope I've made you proud.

List of publications

Nainu F, **Trenerry A**, Johnson K. *Wolbachia-mediated antiviral protection is cell autonomous*. J Gen Virol. 2019 Nov;100(11):1587-1592. doi: 10.1099/jgv.0.001342. Epub 2019 Oct 10. PMID: 31599711. DOI: 10.1099/jgv.0.001342. ***Equal first author.***

Monson E, **Trenerry** A, Laws JL, Mackenzie JM, Helbig K. 2021. *Lipid droplets and lipid mediators in viral infection and immunity*. FEMS microbiology reviews 45:fuaa066. DOI: 10.1093/femsre/fuaa066

Carrera J, **Trenerry A**, Simmons C, Mackenzie J. 2021. *Flavivirus replication kinetics in early-term placental cell lines with different differentiation pathways*. Virology Journal 18:251. DOI: 10.1186/s12985-021-01720-y

Mikulasova A, Gillespie LK, Ambrose RL, Aktepe TE, **Trenerry A**, Liebscher S, Mackenzie JM. 2021*. A Putative Lipid-Associating Motif in the West Nile Virus NS4A Protein Is Required for Efficient Virus Replication*. Front Cell Dev Biol 9:655606. DOI: 10.3389/fcell.2021.655606

López-Denman AJ, Tuipulotu DE, Ross JB, **Trenerry A**, White PA, Mackenzie JM. 2021. Nuclear localisation of West Nile virus NS5 protein modulates host gene expression. Virology 559:131-144. DOI: 10.1016/j.virol.2021.03.018

Chapter 1
Introduction

1.1. Flaviviridae

The *Flaviviridae* family consists of more than 100 species of positive sense, single stranded RNA genome viruses (+ssRNA) that can infect humans as well as other mammals and birds. There are four genera in this family including *Hepacivirus, Flavivirus, Pegivirus* and *Pestivirus (Simmonds et al, 2017).* These viruses contain a linear, monopartite genome, and they replicate inside the cytoplasm of host cells. Virions range from 40-60 nm in diameter and are encased in a lipid envelope. These viruses are quite diverse in their hosts and transmission pathways: *Pestiviruses* infect pigs, cattle and other mammals, and are transmitted via contact with infected secretions. *Hepacivirus* only contains one species, hepatitis C virus (HCV), and transmission in humans is through contact with infected blood. *Flaviviruses* are the biggest genus and mostly consist of mosquito-borne and tick-borne viruses (Figure 1).

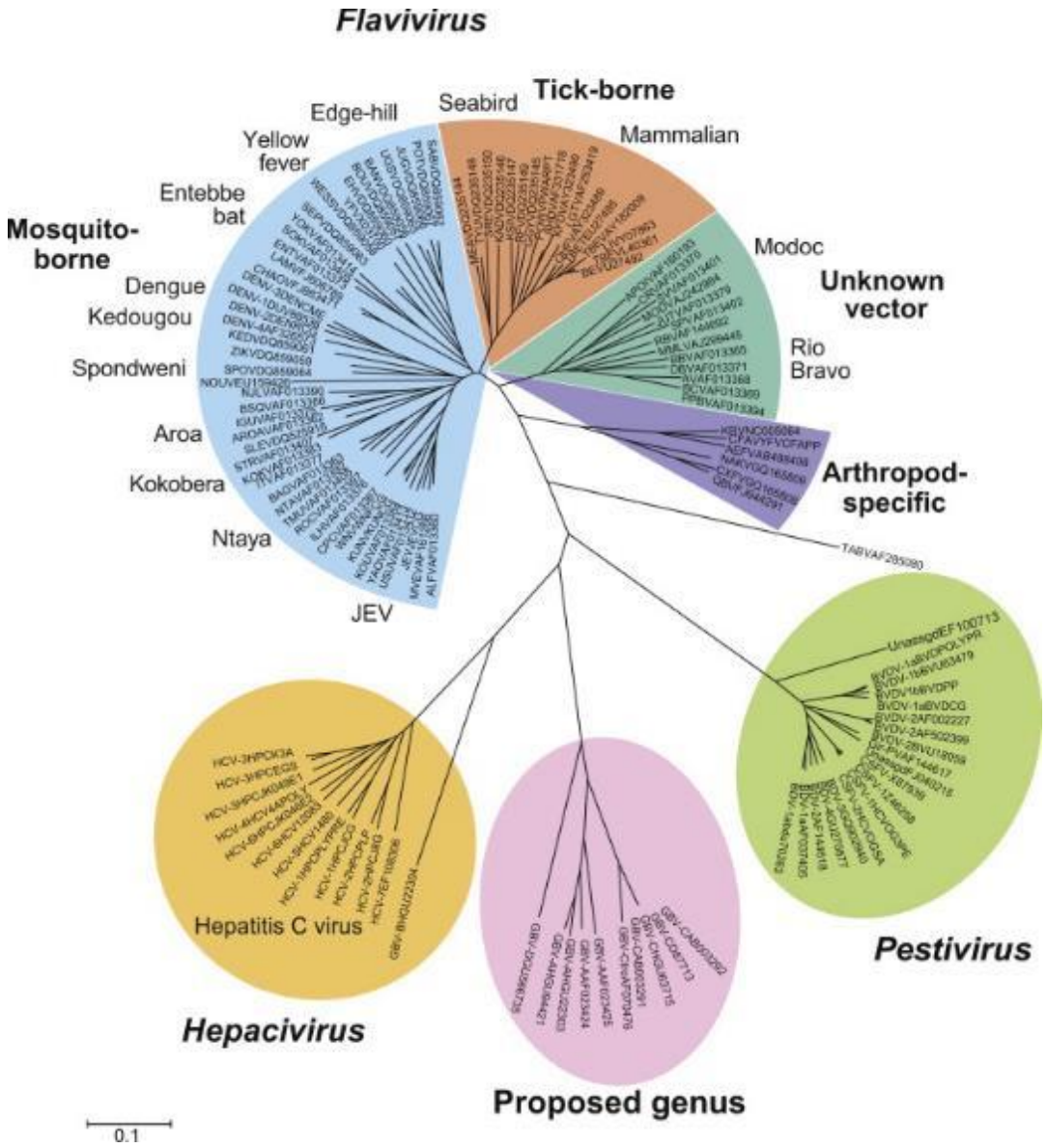

Figure 1. Classification of Flaviviridae family into genera. These classifications are based on the conserved sequences of the RNA-dependent RNA polymerase (RdRp), with the 'proposed genus' referring to Pegiviruses. The Flavivirus genus is further classified by hosts and vectors (2012).

1.2. Flavivirus genus

Flaviviruses, of the family *Flaviviridae*, are an extremely prevalent and clinically important genus of viruses. This genus comprises of over 50 different viral species, including several important arboviruses, such as dengue (DENV), Zika (ZIKV), yellow fever (YFV), Japanese encephalitis (JEV), West Nile (WNV), and

tick-borne encephalitis virus (TBEV). These viruses all pose significant risks to human health, and although about half of the world's population are living in at-risk areas of dengue infection alone (Bhatt et al, 2013), the urgency to generate effective antivirals and vaccines for these viruses is often neglected as these populations generally lie in developing countries. Current preventative measures, aside from the effective YFV and JEV vaccines, mostly fall within vector control, which often require large amounts of chemicals, and there is little evidence for their effectiveness (Bowman et al, 2016). As these viruses become only an increasing issue with global rising populations and urbanisation, the need for effective control of these viruses is striking.

1.3. West Nile virus

1.3.1. Epidemiology

WNV is a mosquito-borne Flavivirus that predominantly emerges in Africa, North America, the Middle East, Europe, and West Asia, and is the leading cause of viral encephalitis in America. It was first isolated in 1937 in the West Nile region of Uganda and has since become one of the most widely spread neurotropic arboviruses. WNV has been detected in over 65 mosquito species and 326 bird species in America alone (Hayes et al, 2005), and the introduction of the virus into North America in 1999 from a single source (named WNV New York 1999 strain; WNV_{NY99}), which lead to a large-scale dramatic outbreak, highlighted its ability to adapt to and establish itself in new environments with ease. In 2018 the highest number of cases was reported by the European union and neighbouring countries, with 2083 cases and 181 deaths (ECDC, 2019), and diseases cases in America have reached up to 5764 in a single year (CDC, 2019). Australia also has an endemic strain of the virus, termed WNV strain Kunjin virus (WNV_{KUN}), which was first identified in 1960 in Northern Queensland from a *Culex annulirostris* mosquito. Its name is derived from the aboriginal tribe of Kowanyama, who resided near where the virus was isolated, and has a 98.1 % a.a homology to the more pathogenic WNV_{NY99} strain (Westaway et al, 2002).

1.3.2. Transmission

The virus itself is maintained in a bird-mosquito transmission cycle through the *Culex* genus of mosquito. Whilst pathogenesis of the avian host is usually asymptomatic, cases of neurological disease and clinical symptoms have been previously reported, particularly during the WNV_{NY99} outbreak. The cycle begins with mosquitos becoming infected by feeding on infected birds, where the virus must first cross to the midgut of the mosquito. Here it is amplified, and disseminated to the periphery, and eventually reaches the salivary glands, where it can be transmitted to another host during feeding. High viral load in the salivary glands is integral to successful transmission of the virus. The infection of humans and horses are incidental, and they are considered 'dead end' hosts (see Figure 2), as the viral load in these hosts does not reach high enough levels to be re-transmitted to mosquitoes (Bowen & Nemeth, 2007). Outbreak epicenters appear to be on migratory bird routes but can also be imported. Although the virus is primarily transmitted through the bite of an infected mosquito, reports of interhuman transmission through blood transfusions and organ transplants have also occurred (Pealer et al, 2003; Winston et al, 2014)

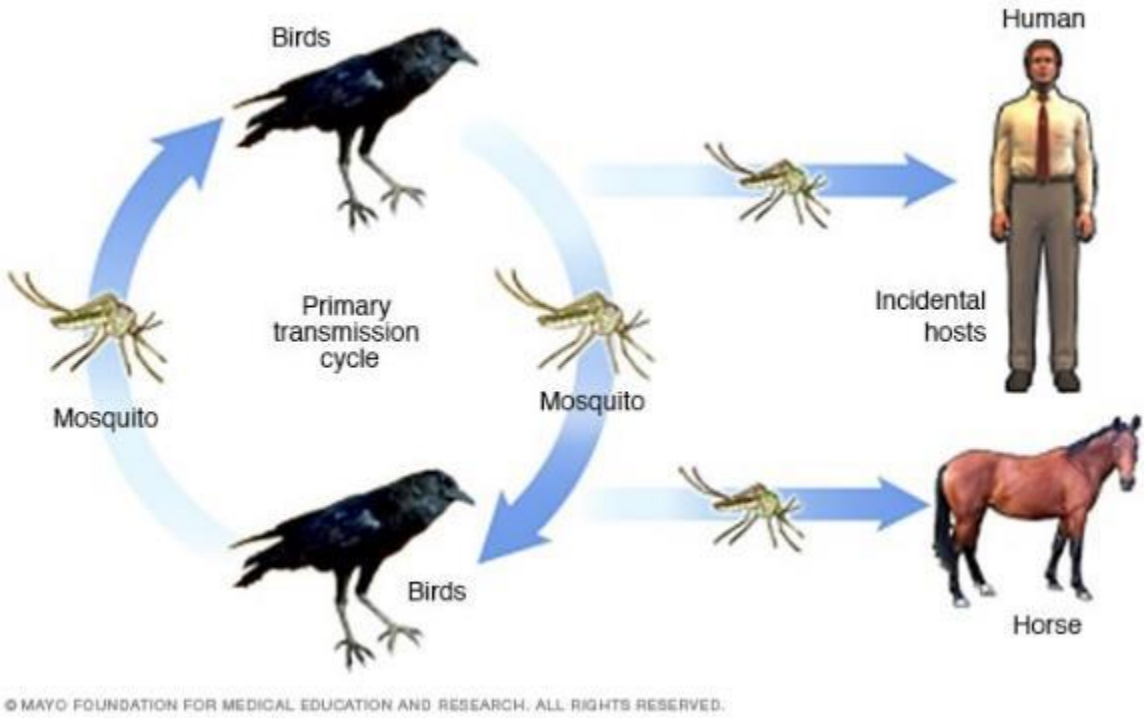

Figure 2. Transmission cycle of West Nile virus. Mosquitos bite infected avian hosts, which leads to infection of the mosquito. The arthropod host can then go on to infect humans and horses, which are incidental hosts as they cannot replicate the virus to high enough titres to re-infect mosquitos.

1.3.3. Pathogenesis

Seroprevalence studies have indicated that the majority of infections with WNV are asymptomatic (80 %), with about 20 % of cases presenting as mild febrile disease, with an incubation period in mammalian hosts varying from 2-14 days. Onset of symptoms is usually abrupt and lasts 3-6 days, and can manifest in the following symptoms: headache, fever, tiredness, body aches, vomiting, nausea and rashes. Approximately 1:150 infections also result in severe neuroinvasive disease as the virus crosses the blood-brain barrier (BBB), resulting in a range of symptoms affecting the brain and central nervous system (CNS). Again, these symptoms usually appear abruptly, and can range from milder self-limiting states of confusion, to more severe symptoms such as encephalitis, meningitis or acute flaccid paralysis, which can cause death if untreated (O'Leary et al, 2004; Petersen & Marfin, 2002). The mortality rate for severe disease is 10 %, and age, comorbidities and immunosuppression are risk factors increasing chances of death.

Although the exact mechanisms of pathogenesis and dissemination are not completely understood, rodent models have provided us with some valuable insight. From what is known, the mechanism of entry into host cells is quite conserved amongst Flaviviruses. Upon introduction of the virus to the skin via the bite of an infected mosquito, the virus is suspected to initially replicate in keratinocytes, skin resident dendritic cells (DCs) and Langerhans DCs (Byrne et al, 2001). These infected cells then migrate to the draining lymph nodes to produce primary viremia, and from there it is disseminated to peripheral tissues, namely kidney, spleen and epithelial cells, where virus production takes place. Depending on the load produced by the secondary viremia, the virus can be cleared from the serum and peripheral tissues and invade the CNS, resulting in severe neurological disease. To infect the CNS, WNV must overcome the BBB, and the mechanism via which this happens remains to be fully elucidated. Current data suggests that WNV could increase the permeability of the BBB which could facilitate its entry, which is mediated by the induction of cytokines such as tumour necrosis factor (TNF)-α, interleukin (IL)-6 (Leis et al, 2020) and TLR3 signalling (Kong et al, 2008a; Wang et al, 2004). It may also be possible that paracellular entry is at play, which could include the passive diffusion of virions (not infected cells) across the BBB, or through the trafficking of infected monocytes (Garcia-Tapia et al, 2006; Samuel & Diamond, 2006).

1.4. Zika virus

1.4.1. Epidemiology

ZIKV is another mosquito borne Flavivirus first isolated from a monkey in Uganda, Africa in 1947. From the 1900s until 2007, rare and sporadic cases were reported in Africa and Asia with people suffering mild disease, and little research had been undertaken on this virus. In 2007, ZIKV was reported for the first time outside of Africa and Asia, and caused a large outbreak on Yap Island in Micronesia (Duffy et al, 2009), with an estimated 72 % of the population infected over a 3 year period (Musso et al, 2014). In 2013, ZIKV had migrated to French Polynesia, where the largest outbreak so far was recorded, with over 30,000 people infected by 2014. It was during this outbreak that neurological symptoms were first

reported, including an increase in Guillain-Barré syndrome (Cao-Lormeau et al, 2016).

ZIKV then disseminated through the South Pacific, and in 2015 it became an undeniable public health threat as it caused an explosive outbreak in Brazil. However, It is possible that ZIKV had been circulating in Brazil prior to this, and due to the similarity between the clinical manifestations of ZIKV with DENV and WNV, which were endemic to Brazil, it may have initially gone unnoticed. Infection spread to North America, and cases in returned travelers were reported all over the world, including Australia, Japan, China, and Israel. Cases detailing microcephaly and other birth detects were accumulating, and several countries issued health warnings for pregnant women travelling to endemic areas. In 2016 ZIKV was declared by the World Health Organization as a Public Health Emergency of International Concern, however reported cases began to decline in 2017. In July 2021, an increase in reported cases in India occurred, mainly in the state of Kerala, and as of November 2021 there had been 89 reported cases, including 17 children and 1 pregnant woman.

1.4.2. Transmission

Like WNV and DENV, ZIKV is primarily spread through the bite of infected *Aedes aegypti* and *Aedes albopictus* mosquitos, and although it was originally isolated from lower primates, it is now maintained in a human-mosquito-human transmission cycle and has no other known animal reservoirs. The ability of this arbovirus to spread laterally from human-to-human increased global concern, as this phenomenon is not often seen with Flaviviruses or other arboviruses. Most notably, the outbreak in Brazil resulted in increasing reports of pregnant women passing ZIKV to their unborn fetus, and in many cases, this caused microcephaly and other severe fatal brain defects. ZIKV has also been found in the breast milk of infected mothers, but transmission via this route has not been confirmed. There is also limited evidence showing ZIKV can be sexually transmitted, even in asymptomatic cases, and can also be transferred through blood transfusions (Levi, 2017; Magnus et al, 2018; Musso et al, 2014).

1.4.3. Pathogenesis

Similar to WNV, an estimated 80 % of ZIKV infections are asymptomatic, and most symptomatic cases present as mild and self-limiting. Mild disease is characterized by rash, fever, headache, muscle pain and conjunctivitis. Severe ZIKV infection can result in multi-organ failure, thrombocytopenia, and neurological symptoms, however in contrast to other Flaviviruses, neurological symptoms generally manifest in fetuses compared to adults. As mentioned above, infection in pregnant women can result in microcephaly and congenital malformations, which may be a result of ZIKV preferentially infecting neural progenitor cells. The ability of ZIKV to cross the placental barrier and infect unborn babies is an extremely unusual and alarming feature of its pathogenesis. This involves the virus crossing both the placental barrier and the BBB, and the mechanisms underlying this ability remain to be fully elucidated. *In vitro* models suggest that the mechanisms are cell-specific; in human placenta trophoblast cells, ZIKV increased permeability of the monolayer by disrupting cellular tight junctions, and in addition, ZIKV was able to cross both the placental and BBBs via transcytosis (Chiu et al, 2020).

1.5. Treatment options for Flavivirus infections

Despite a large proportion of the world's population living in at-risk areas of Flavivirus infection and their ability to cause explosive outbreaks, to date there are minimal vaccine and therapeutic options available. Most treatment options target symptomatic infections and are not specific to Flaviviruses, and mainly include hydration and fluid management, and monitoring of the patient. Antivirals such as Ribavirin, which have proved effective against other RNA viruses such as influenza, respiratory syncytial virus and Hanta virus (Gilbert et al, 1985; Huggins et al, 1986; Taber et al, 1983), are mostly ineffective at reducing Flavivirus symptoms, as are the use of steroids or other non-steroid anti-inflammatory drugs (Gibbons & Vaughn, 2002). As it stands there are prophylactic vaccines for YFV, JEV, TBEV and DENV, however safety and efficacy data has raised concerns for some of these vaccines, highlighting the need for continuous research into this field. Currently there exists no approved vaccines or treatments for either WNV or ZIKV, but the last few years have seen

several clinic trials for potential ZIKV vaccines, including live-attenuated, adenovirus-vector, DNA and virus-like particle vaccines, which are still in development (Geerling et al, 2020; Han et al, 2021; Muthumani et al, 2016; Tebas et al, 2017).

Other efforts to reduce the burden of Flavivirus disease are focused on controlling the mosquito vector itself. This includes classic forms of personal protection and vector population control, such as the use of insect repellents, mosquito nets and widespread use of insecticides. Although these first-line control measures are important, none confer full protection, and evidence has shown that mosquitoes can develop resistance to insecticides (Gan et al, 2021). Another unique mechanism of Flavivirus prevention is through the weaponization of an insect bacterium called *Wolbachia.* This intracellular bacterium lives symbiotically in up to 60 % of insect populations, and when experimentally introduced via transfection into *Aedes aegyptii,* has the demonstrated ability to reduce levels of DENV and other Flaviviruses in the vector in a laboratory setting (Moreira et al, 2009). This has translated extremely successfully to the field, with the release of *Wolbachia*-containing mosquitoes in Indonesia reducing dengue incidence by 77 %, and an 86 % reduction in dengue hospitalizations (Utarini et al, 2021). *Wolbachia* can also reproductively manipulate its host, causing sterilization and an inability of uninfected female mosquitos to reproduce, and this facet has also been utilization a mechanism for reducing mosquito populations (Binnington & Hoffmann, 1989; Hertig, 1936; Hoffmann et al, 2011; Riegler et al, 2005; Schmidt et al, 2017; Turelli & Hoffmann, 1991).

The prevalence of these viruses, the spectrum of disease they cause, and the risk of future outbreaks make research into preventing and treating these viruses essential. This research needs to be diverse and include investment in discovery research, so we can uncover new targets for therapeutics, and understand the nuances between different Flaviviruses. This, combined with continual research into vaccine development and drug repurposing will ensure we are better prepared for future outbreaks of both known and unknown Flaviviruses.

1.6. Flavivirus life cycle

1.6.1. Entry

Members of the Flavivirus genus have an enveloped, spherical virion particle that has icosahedral symmetry. Mature virions are highly organised particles approximately 50 nm in diameter, consisting of a host-derived lipid bilayer, enclosing a capsid which contains the viral genome (Kuhn et al, 2002). The mature virion is decorated with surface proteins that mediate fusion and entry, namely the envelope (E) and pre-membrane (prM)/membrane (M) proteins. Host surface markers that mediate entry can be specific to different Flaviviruses, but generally include heat shock proteins (DENV, JEV) (Salas-Benito et al, 2007; Taguwa et al, 2015; Valle et al, 2005), carbohydrate molecules (Aoki et al, 2006; Hilgard & Stockert, 2000; Miller et al, 2008b), lectins (Cheng et al, 2010), claudin-1 cell receptors (Che et al, 2013), Dendritic Cell-Specific Intercellular adhesion molecule-3-Grabbing Non-integrin (DC-SIGN) (Davis et al, 2006a; Davis et al, 2006b) and $\alpha_v\beta_3$ integrins (reviewed in (Laureti et al, 2018)). Contact with these host markers via the E protein on the surface of the virion particle allows the viruses to enter cells via endocytosis mediated by clathrin-coated pits. For DENV, there is evidence of viral particles moving along the membrane to condense into pre-existing clathrin pits (van der Schaar et al, 2008), creating an invagination which eventually buds off the cytosolic side of the plasma membrane to form clathrin-coated vesicles. Following the shedding of the clathrin-coat, these virion-containing endocytic vesicles are delivered to and internalised by early endosomes. Maturation of the early to late endosome causes a pH shift which triggers a conformational change in the E protein to promote fusion of the viral and endosomal membranes (which is dependent on the lipid composition of both membranes (Moesker et al, 2010; Stiasny & Heinz, 2004; Umashankar et al, 2008; Zaitseva et al, 2010a)), and eventual release of viral nucleic acids into the cytosol.

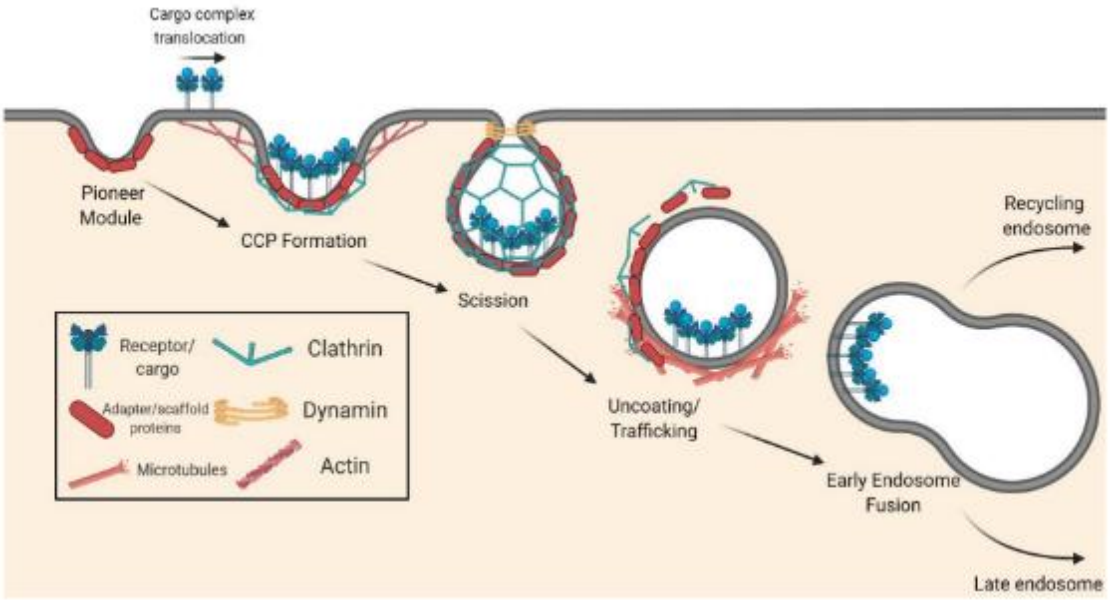

Figure 3. Flavivirus entry via clathrin-mediated endocytosis. Flavivirus entry begins with attachment of the viral envelope glycoprotein to a cell surface receptor. Particles likely diffuse along the surface of the cell until they reach an existing clathrin-coated pit. The clathrin-coated pit is excised from the plasma membrane via scission mediated by dynamin. The virus now exists in a clathrin-coated vesicle, and this endocytic vesicle is transported to early endosomes. Maturation of the early to late endosome brings a pH shift, which triggers fusion of the viral and endosomal membranes, creating a pore out of which the viral nucleic acid is released. *(Carro & Cherry, 2021)*

1.6.2. Genome

Flaviviruses have a single strand, positive sense, capped RNA genome that is approximately 11kb long (Lindenbach et al, 2013). These viruses contain a single open reading frame (ORF) that encodes for one large polyprotein, which is proteolytically cleaved by host and viral proteases into 10 smaller proteins. This includes 3 structural (**C**apsid, **Pr**e-**M**embrane and **E**nvelope) and 7 non-structural proteins (NS1, NS2A, NS2B, NS3, NS4A, NS4B, NS5). The Flavivirus genome is quite simple and encodes only what is necessary for survival. The first three (structural) proteins are the first to be translated and make up the virion particle. The capsid protein (C) packages the viral RNA into a nucleocapsid, and is important for mature virion formation. The envelope (E) and pre-membrane (prM) proteins are membrane-associated proteins embedded in the surface of the virions, and are important for attachment, membrane fusion and assembly of viral

particles. The cleavage of prM into M is a crucial step for mature virion formation, and is dependent on the host cell endoprotease furin (Mackenzie & Westaway, 2001; Wengler & Wengler, 1989).

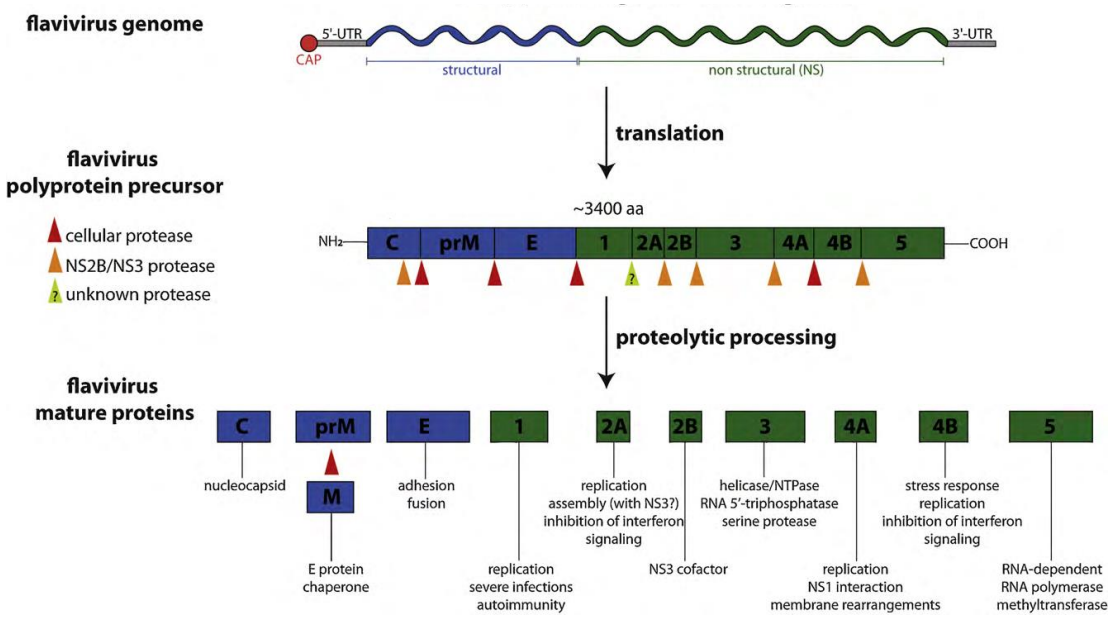

Figure 4. Organization of the Flavivirus genome. Flavivirus genomes consists of a single 11kb polyprotein that undergoes proteolytically processing by host signalase and viral NS2B-NS3 complex, resulting in 3 structural (C, prM, E) and 7 non-structural proteins (1, 2A, 2B, 3, 4A, 4B, 5). Each of these proteins are multifunctional and the full suite of their functions have not yet been fully elucidated. (Pastorino et al, 2010)

1.6.3. Non-structural proteins

The remaining non-structural proteins make up the replication complex and are involved predominantly in RNA replication and immune regulation (Westaway et al, 2002), although the full spectrum of their functions remain to be elucidated.

NS1 is a highly conserved 45 kDa protein that is generally localised to the ER lumina where it exists as a monomer or dimer, but can also be secreted as a hexamer (Flamand et al, 1999). This protein is believed to be multifunctional and aid in viral replication, however its exact functions are not fully known. The crystal structure of NS1 revealed distinct domains for membrane association for the dimer, as well as interactions with the immune system (Akey et al, 2014). NS1 is localised to the sites of viral replication (replication complexes) during infection,

where it colocalises with dsRNA, a replication intermediate for (+)ssRNA viruses (Mackenzie et al, 1996a; Westaway et al, 1997). There is evidence that once secreted, NS1 plays a role in immune regulation by inhibiting the complement system (Macdonald et al, 2005), and has also been implicated in the activation of TLR4 signalling (Modhiran et al, 2017). High levels of secreted DENV NS1 are also associated with more severe disease; whereby the secreted NS1 can trigger a vascular leak resulting in shock and often death (Beatty et al, 2015).

NS2A is a small, hydrophobic and multifunctional protein. It binds to the 3' end of the UTR on the viral genome with high specificity as well as to the replication complex (Leung et al, 2008). This diverse protein performs roles in modulating host cell immune responses (Munoz-Jordan et al, 2003), as well as virion assembly/secretion (Kummerer & Rice, 2002). Evidence also suggests that NS2A is involved in packaging newly synthesized viral RNA into immature virions; as it was observed that 3 residues on NS2A could bind to the 3'UTR of DENV RNA (Leung et al, 2008).

NS2B is an integral transmembrane protein that primarily functions as a co-factor for NS3. It has a conserved central hydrophilic region that has shown to be significant enough to activate NS3 protease, and mutations in this region led to inhibited viral replication (Arias et al, 1993; Chambers et al, 1993; Zuo et al, 2009). It is proposed to aid in anchoring NS3 to the endoplasmic reticulum membrane (Chambers et al, 1993; Clum et al, 1997), however emerging roles viral particle formation are being discovered (Li et al, 2016).

NS3 is the second largest viral protein at 70 kDa, and is a multifunctional protein containing a protease, helicase, and NTPase domain, and forms a complex with cofactor NS2B. The protease domain of NS3 is only active when forming this NS3-NS2B heterodimeric complex (Chappell et al, 2008), and the first function of this complex is to proteolytically cleave the precursor to release all the structural and non-structural viral proteins (Lindenbach et al, 2007). The helicase domain is involved in genome replication and RNA synthesis (Le Breton et al, 2011; Lescar et al, 2008), and DENV NS3 also has an ATP-independent RNA annealing function (Gebhard et al, 2012).

NS4A (16 kDa) and NS4B (27 kDa) are small, hydrophobic proteins that are strongly associated with ER membranes. Little is known about their function, however recent evidence suggests that these proteins are instrumental in inducing membranous changes required for replication (Ambrose & Mackenzie, 2011a; Dalrymple et al, 2015a; Miller et al, 2007; Roosendaal et al, 2006b), and NS4A contains a lipid-binding motif that is essential for replication (Mikulasova et al, 2021). Other evidence suggests that NS4A and NS4B operate co-operatively to block host interferon response and NS4B also interacts with the helicase domain of NS3 to dissociate it from a single strand RNA (Zou et al, 2015). There is also evidence suggesting NS4A can modulate autophagy to protect cells from apoptosis (McLean et al, 2011), and can modulate the host unfolded protein response as a means of immune evasion (Ambrose & Mackenzie, 2011b).

NS5 (90 kDa) is the largest and most highly conserved protein amongst Flaviviruses, and contains both RNA dependent RNA polymerase (RdRp) and methyltransferase domains which are connected by a flexible linker (Ackermann & Padmanabhan, 2001; Lu & Gong, 2013). The methyltransferase activity also actively participates in RNA capping, and methylation of the RNA aids in prevention of host recognition (Potisopon et al, 2014; Zhao et al, 2015). NS5 also has various roles in modulating the innate immune response; it is an extremely potent antagonist of the JAK-STAT pathway (Lubick et al, 2015), with different Flaviviruses displaying different mechanisms of suppression in this pathway. DENV and ZIKV NS5 inhibits IFN-α through proteasomal degradation of STAT2 (Ashour et al, 2009; Mazzon et al, 2009; Morrison et al, 2013), and WNV NS5 supressed interferon-α/β receptor (IFNAR) surface expression and maturation (Laurent-Rolle et al, 2010; Lubick et al, 2015).

1.6.4. Replication

Replication processes remain quite conserved between +ssRNA viruses. Flaviviruses enter cells via receptor-mediated endocytosis and fusing with the host cell membrane, allowing the nucleocapsid and viral RNA to be released into the cytoplasm (Rey et al, 1995). The genome essentially acts as mRNA and is translated by the host ribosome into a polyprotein, the processing of which takes

place on the endoplasmic reticulum (ER) membrane. After translation the viral polyprotein is proteolytically processed into the mature viral proteins by both host and viral-encoded proteases. During replication, the +ssRNA genome acts as either template for the production of both -ssRNA (which is used to generate even more +ssRNA copies), or as a template for the synthesis of the polyprotein by the RdRp. +ssRNA viruses also contain an RNA cap at the 5' end, which has a dual function in both aiding in the initiation of translation and protecting the mature mRNA from degradation by host endonucleases.

It is hallmark of most, if not all of these viruses, regardless of the host they infect, to induce the formation of host-derived replication complexes (RCs), which provide a membranous compartment favourable for replication. While *pestivirus* and *hepacivirus* replication takes place in a 'membranous web', forming vesicles in a membranous matrix (Egger et al, 2002), Flaviviruses induce the construction of two to three morphologically distinct membrane structures; vesicle packets (VPs) and convoluted membrane/paracrystalline arrays (CM/PCs) (Mackenzie et al, 1996b; Ng, 1987; Westaway et al, 1997). Immunostaining of these structures has revealed constellations of viral and host proteins that are specific to each structure, suggesting that they perform distinct functions (Mackenzie, 2005; Mackenzie et al, 1999; Mackenzie et al, 1998; Roosendaal et al, 2006a; Westaway et al, 1997). VPs are spherical membrane structures ranging from 70 to 100 nm in diameter (see Figure 3). They contain the dsRNA (a replication intermediate), as well as NS3 and NS5 which contain the catalytic activities necessary to replicate and cap the genome (Cortese et al, 2017; Junjhon et al, 2014; Mackenzie et al, 1996a; Mackenzie et al, 1998; Miorin et al, 2013; Westaway et al, 1999; Westaway et al, 1997), and are therefore proposed to constitute the replication complex (see Figure 4).

CM/PCs are the proposed sites for translation; newly synthesised RNA is translocated here, where it most likely undergoes proteolytic processing by NS2B3 (protease) and host signalase (Westaway et al, 1997). The presence of CM/PCs is generally found after the latent period of replication and evidence has shown that there is a certain threshold of RNA replication required before the

construction of these membranes (Mackenzie et al, 2001). These structures are highly ordered, and Cryo-EM has revealed their morphology as randomly folded membranes, with specific structure and shape induced by different lipids and proteins. As mentioned previously, the expression of NS4A alone is enough to induce the formation of these structures. These structures are contiguous with the endoplasmic reticulum, although *trans*-Golgi markers are also seen in the CM/PCs (Mackenzie et al, 1999).

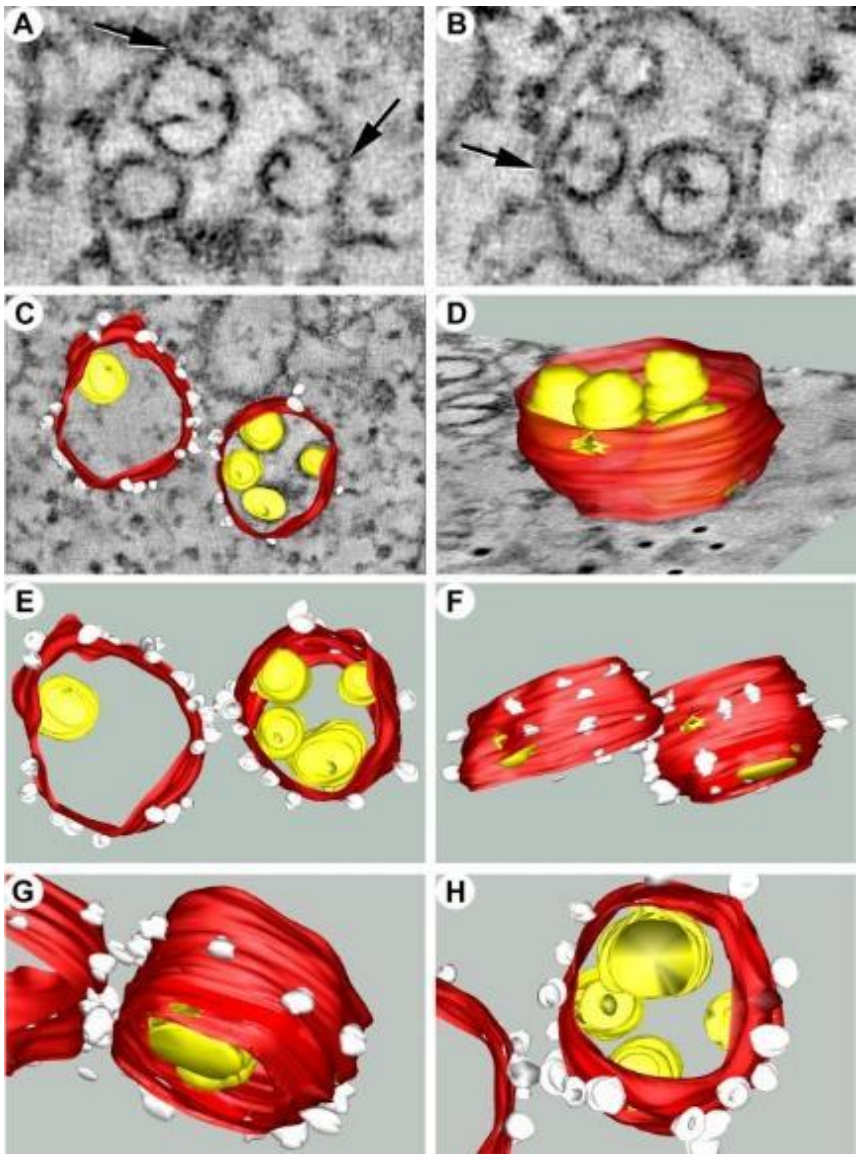

Figure 5. WNV_{KUN} replication complexes visualised via electron tomography. A) Vesicle packets enclosed by the rough endoplasmic reticulum

(ER). **B)** Neck-like structures tether vesicles to the ER membrane. **C)** 3D surface model of WNV replication complex showing association of individual vesicles (yellow) with the rough ER membrane (red), and decorated with ribosomes (white). **D-F)** Rotated views of the WNV replication complex, showing pores in the membrane which connect these structures to the cytoplasm. *(Gillespie et al, 2010)*

Whilst the roles of these membranous compartments are still shrouded in some mystery, comprehensively understanding their roles and how they are formed could aid in creating antiviral therapeutics that target viral replication. The VPs are postulated to be the replication complexes as they contain the genetic material and proteins required for replication. dsRNA is concealed in these VPs, which allows the virus to avoid detection from pattern recognition receptors (Overby et al, 2010; Uchida et al, 2014), as well as antiviral proteins PKR and MxA (Hoenen et al, 2007a). Containing these replicative components within small membrane structures also means they are condensed, which aids in increasing the efficiency of replication (Mackenzie, 2005). The induction of these membranous replication complexes is obviously integral to the life cycle of these viruses and require the subversion of host lipids to do so. Elucidating which lipids play a central role in the formation of these RCs, and how they are manipulated during infection will advance our understanding and ability to target viral replication.

1.6.5. Virion formation and budding

Although we know broadly how Flaviviruses mature and egress, we still know very little about the mechanisms that drive these processes, and the processes appear to differ slightly between Flaviviruses (Hase et al, 1987a; b). Virion morphogenesis occurs on the ER membrane, adjacent to replication complexes (Mackenzie & Westaway, 2001), and this proximity likely increases efficacy of this process (see Figure 6). Currently no packaging signal has been identified that triggers virion formation, but the process begins when viral RNA and C proteins assemble to form nucleocapsid cores (or NCs). The exact process of transport of RNA and C protein are unclear, but there is evidence suggesting NS2A aids in shuttling RNA along the ER (Leung et al, 2008). These accumulate in the ER

lumen, and eventually bud off, encapsulated by the ER membrane which is studded with E and prM proteins. This is the immature virion particle, which is about 60nm in diameter and has trimeric spikes of prM-E on the outside. The protein spikes are then glycosylated, and the immature virion translocates from the ER to the Golgi where it undergoes maturation and cleavage of prM to M via furin, which is believed to be essential for infectivity. The mature virion is a 50 nm particle and exits through the secretory pathway (Mackenzie & Westaway, 2001).

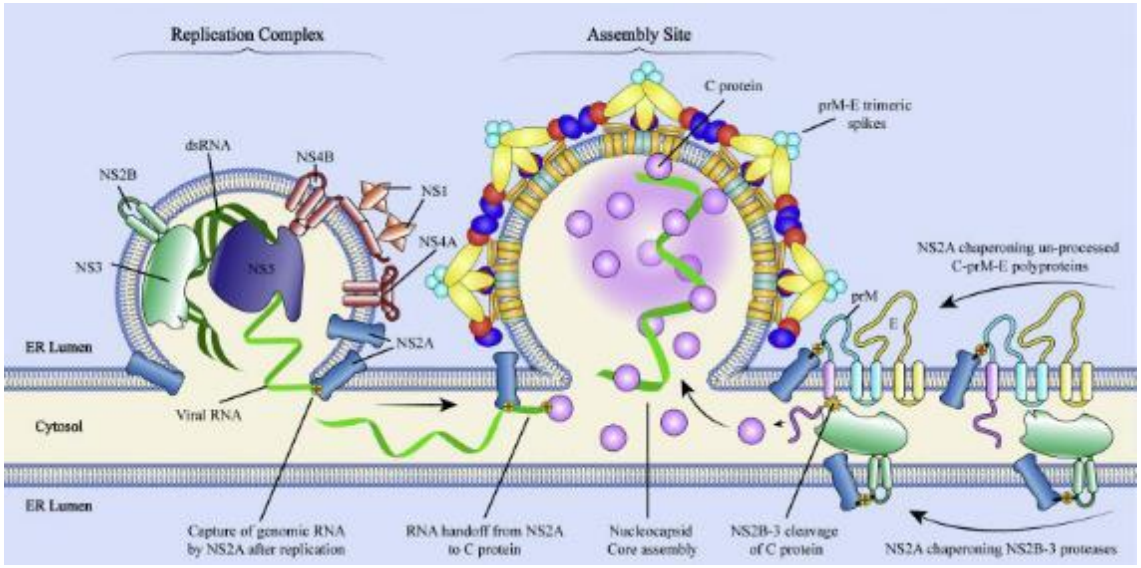

Figure 6. Schematic of the Flavivirus replication and assembly strategies on the endoplasmic reticulum. The Flavivirus replication complex (RC) involves the invagination of the host endoplasmic reticulum (ER) membrane, and several viral proteins have been implicated in the induction of these structures including NS4A, NS4B and NS1. These RCs are believed to be the sites of viral replication as they contain viral dsRNA, as well as the viral non-structural proteins. Virion particles are also believed to be assembled on the ER, but the mechanisms are not well understood. Assembly begins with the shuttling of viral RNA along the ER by NS2A. Association of viral RNA with the C protein then occurs, which forms nucleocapsid cores (NCs). These NCs accumulate and are eventually encapsulated by prM-E trimeric spikes, and this immature virion eventually buds off and is transported to the golgi network where it undergoes maturation *(Nicholls et al, 2020)*

1.7. Flaviviruses and the innate immune system

The innate immune system is the body's first line of defence against invading pathogens, and also aids in the establishment of adaptive immunity. To clear an infection, the host needs to have a means of detecting the pathogen, of transmitting signals to surrounding cells, and to disable and clear the pathogen. Cells use intracellular and extracellular pattern recognition receptors (PRRs) to recognize pathogen associated molecule patterns (PAMPs), as a generalized, rapid mechanism to detect pathogens. Those that recognize Flaviviruses include endosomal toll-like receptors (TLR3 and TLR7), which recognize dsRNA and ssRNA respectively (Barton & Medzhitov, 2003), and cytosolic sensors retinoic acid-inducible gene I (RIG-I), and melanoma differentiation-associated gene 5 (MDA5), both of which sense dsRNA (Fredericksen et al, 2008). Sensing dsRNA by RIG-I and MDA5 leads to the activation of the mitochondrial antiviral signalling (MAVS) pathway (Lazear et al, 2013; Stone et al, 2019). Recognition by each of these receptors ultimately leads to the production of type I interferon (IFN), and the release of pro-inflammatory cytokines (Nasirudeen et al, 2011). Unexpectedly, DENV can also be detected via cytosolic DNA sensing system cyclic GMP-AMP synthase/ stimulator of interferon genes (cGAS/STING). Infection results in the disruption of mitochondrial morphodynamics and the release of mitochondrial DNA, which can be recognised by cGAS/STING, again resulting in the production of type I IFN (Aguirre & Fernandez-Sesma, 2017).

Type I IFNs are a group of cytokines that are integral to the immune response against most pathogens. They are secreted by infected cells early in infection and trigger downstream signalling cascades, including activating antigen presenting cells and the adaptive immune system. This group comprises mainly of IFN-α and IFN-β, which are released from infected cells where they bind to transmembrane receptors (IFNAR) on neighbouring cells. This activation can lead to the transcription of hundreds of IFN-stimulated genes (ISGs) via the Janus kinase signal transducer and activator of transcription pathway (Randall & Goodbourn, 2008), which are diverse and can interfere with the viral life cycle at every stage (reviewed in (Au-Yeung & Horvath, 2018). IFN-α/β have been demonstrated to be integral for preventing Flavivirus infection; mice deficient in type I IFN were far

more susceptible to infection and death compared to wild type controls (Aliota et al, 2016; Dowall et al, 2016; Lazear et al, 2016; Miner et al, 2016; Rossi et al, 2016; Yockey et al, 2016), and treatments both *in vivo* and *in vitro* with IFN-α/β can prevent and reduce infection (Hoenen et al, 2007b; Mackenzie & Westaway, 2001; Samuel et al, 2006)

Flaviviruses, like all viruses, have evolved mechanisms to circumvent some of the innate immune responses aimed at eradicating them. Flavivirus non-structural proteins are potent antagonists of the IFN response, and the mechanisms and proteins driving this are continuously being unravelled; WNV NS1 induces the proteosomal degradation of RIG-I and MDA5 and blocks translocation of IRF3 (Zhang et al, 2017) and DENV NS4A and NS4B can inhibit the phosphorylation of TBK1 and IRF3 (Dalrymple et al, 2015b). NS5 can supress IFN signalling via multiple mechanisms that differ between strains (reviewed in (Best & Pierson, 2017) and (Thurmond et al, 2018)), including WNV and DENV NS5-mediated of the degradation of STAT2 (Ashour et al, 2009; Grant et al, 2016; Kumar et al, 2016; Morrison et al, 2013). DENV NS2B can also inhibit the IFN response by targeting cGAS for lysosomal degradation, preventing the detection of mitochondrial DNA by the cells (Aguirre et al, 2017). It is clear that the Flavivirus evasion of innate immunity is complex, and the more we know about how these viruses dodge our immune defences, the better equipped we are to fight them.

1.8. Lipids and the Flavivirus life cycle

Lipids are a diverse group of organic molecules that comprise the foundations of living structures and influence function. They are defined by their solubility in organic solvents such as chloroform, acetone, and benzene, and are insoluble in water. Lipids are primarily synthesized from fatty acids and are energy-rich molecules that serve innumerous functions in a physiological context. Historically, they were considered to have roles limited to membrane structure and as energy reservoirs, however over the years more diverse functions have been uncovered. In addition to being key regulators of energy storage and metabolism, they have emerging roles in cellular trafficking, cell signalling and inflammation, cell division,

and hormone regulation. Dysregulation of lipid synthesis and metabolism can lead to a range of pathophysiological conditions, and is it undeniable that lipids play important roles during infection with pathogens, and can act as either pro-host and pro-pathogen factors.

Viruses carry little genetic information and have evolved to manipulate innumerous host pathways to benefit their survival, and often require lipids for entry, genome replication, virion particle assembly and egress (Koyuncu et al, 2013; Limsuwat et al, 2020; Long et al, 2019; Pombo & Sanyal, 2018). Although most viruses utilise cell surface proteins or sugars to mediate entry, some species can exploit lipids on the plasma membrane to use as receptors to initiate infection (Agnello et al, 1999; Campanero-Rhodes et al, 2007; Izquierdo-Useros et al, 2012; Roth & Whittaker, 2011; Taube et al, 2010; Tsai et al, 2003). DENV, WNV and alphaviruses also require specific lipid composition of endosomes to facilitate correct endosomal fusion and subsequent uncoating (Kielian et al, 2010; Moesker et al, 2010; Zaitseva et al, 2010b). One of the primary utilities of lipids during infection is to build membranous replication structures. Viruses upregulate fatty acid synthesis as well as the synthesis of particular lipid classes to give these membranes the correct structure and shape; HCV and picornaviruses increase levels of a phospholipid species called phosphatidylinositol-4-phosphate PI(4)P to directly contribute to RC formation (Alvisi et al, 2011; Berger et al, 2009). DENV, WNV, HCV, respiratory syncytial virus (RSV), Vaccinia virus and severe acute respiratory syndrome coranaovirus 2 SARS-CoV-2 all upregulate FASN or cholesterol synthesis for the same purpose (Chu et al, 2021; Greseth & Traktman, 2014; Martín-Acebes et al, 2011b; Oem et al, 2008; Ohol et al, 2015; Park et al, 2009a).

Several lipid species, including ceramide, cholesterol, fatty acids, phospholipids and sphingomyelin have been shown to be integral to viral survival, and interact with Flaviviruses at every stage of their life cycle (see Figure 7). DENV and WNV both increase levels of ceramide and other sphingolipids during infection, and this is thought to aid in membrane curvature and vesiculation during RC formation (Aktepe et al, 2015; Hannun & Obeid, 2018). Similarly, lipidomics studies have

revealed that WNV upregulates phospholipase A2 (PLA2) activity, which in turns increases the production of lyso-PChol which is sequestered to the RC (Liebscher et al, 2018). Inhibiting cholesterol and fatty acid synthesis have all been shown to impact replication of several Flaviviruses (Mackenzie et al, 2007; Medigeshi et al, 2008; Rothwell et al, 2009), and emerging roles in infection are being discovered for these lipids.

Viral envelopes are generally acquired via the budding of cellular membranes (different viruses use different membranes), and as such require tight association with lipid synthesis and cellular machinery. Although much remains to be uncovered about the lipid requirements of viral morphogenesis and egress, DENV and HCV capsid proteins are specifically recruited to lipid droplets, which is thought to be the sites of viral assembly and contributes to the production of infectious viral particles (Miyanari et al, 2007; Shavinskaya et al, 2007). In addition to entry, replication and virion formation, viruses such as DENV also upregulate the catabolism of fatty acids from lipid droplets to generate energy to fuel their replication processes (Heaton & Randall, 2010; Lee et al, 2008), and can manipulate lipids as a means of negating host immune responses, all of which will be discussed in subsequent sections.

In the following sections we will describe in detail the biochemical processes of fatty acid synthesis and oxidation, and then describe the ways in which these specific pathways are manipulated by Flaviviruses.

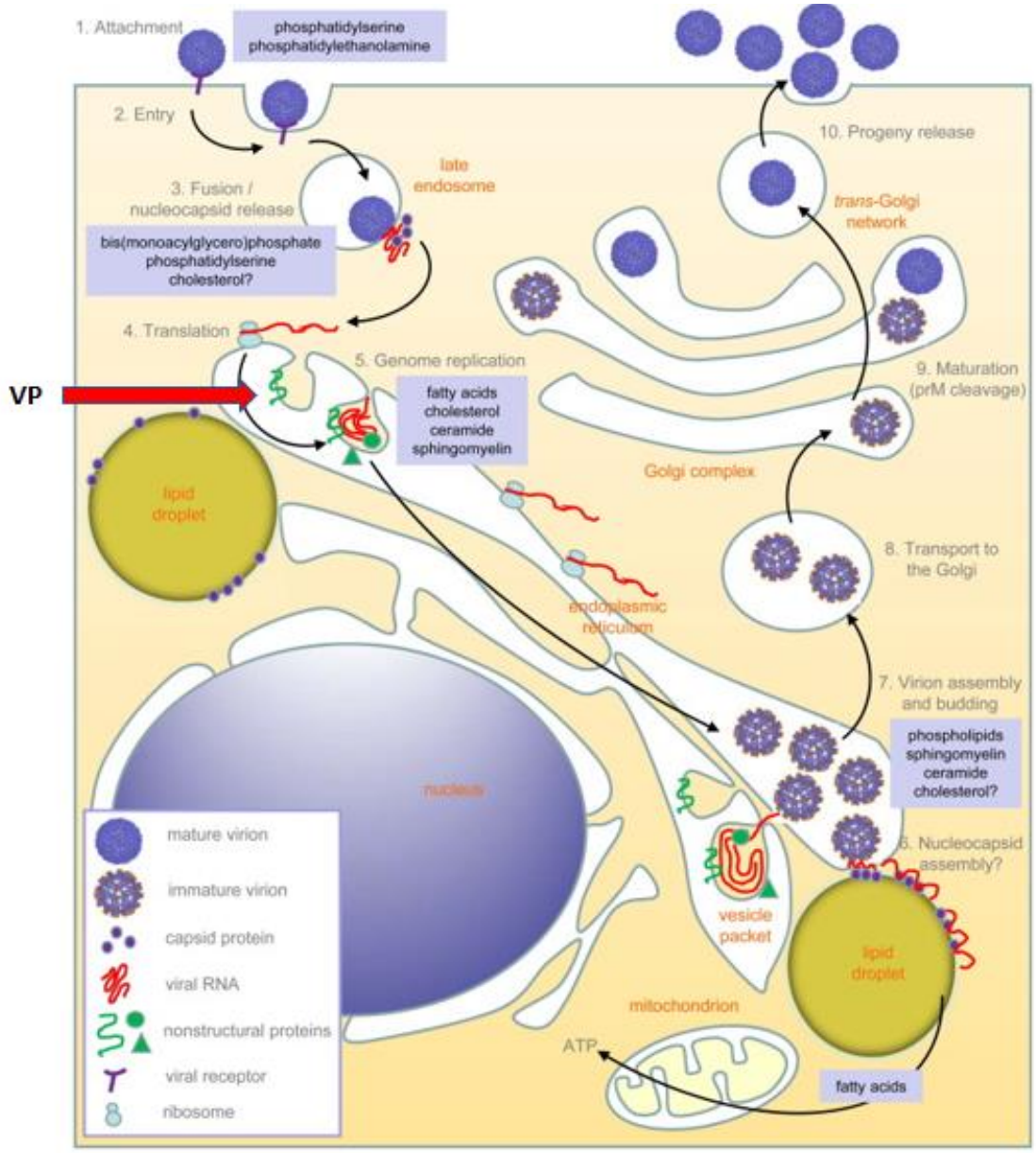

Figure 7. Schematic representation of the Flavivirus life cycle and the lipids that are subjugated by the virus at each stage. From entry via lipid based receptors, to the highjacking of membranes for replication and particle assembly and egrees. The importance of the ER as a replication platform can be seen, and a vesicle packet (VP) can be visualised by the red arrow *(Martin-Acebes et al, 2016)*

1.9. Fatty acid synthesis

Fatty acid biosynthesis is an integral anabolic reaction in most organisms and is an important component for cell growth, differentiation, and homeostasis. The

primary purpose of fatty acid synthesis is for energy storage. Excess carbohydrates in the body are converted to fatty acids, and are esterified into triglycerides and stored in hepatic and adipose tissue, however many other functions exist. The products of this pathway can be converted into other lipids, which can be utilised for membrane architecture, metabolised in the mitochondria to provide energy for cellular processes, and can also act as signalling molecules. Whilst the majority of fatty acids in humans are obtained from the diet, the ability of cells to *de novo* synthesise fatty acids and derivative lipids is an important process conserved amongst all cell types, and across many organisms. This process generally occurs when blood glucose levels are high, indicating a 'fed state' where cells have excess acetyl co-enzyme A (acetyl-CoA), which can be directed to fatty acid synthesis and storage instead of energy production.

De novo fatty acid synthesis is the process of using acetyl-CoA and malonyl-CoA as substrates to produce a long fatty acid chain. The primary product of this pathway is palmitate, which is a 16 carbon long-chain fatty acid. There are two enzymes which control this pathway – acetyl-CoA carboxylase (ACC), and fatty acid synthase (FASN). The primary function of ACC is to convert acetyl-CoA to malonyl CoA, which is then fed into the fatty acid synthase (FASN) pathway to produce palmitate (Wakil et al, 1983). ACC therefore controls the rate limiting step of fatty acid synthesis, while FASN produces the fatty acid product. Downstream of the FASN pathway, the palmitate product can be modified to produce other fatty acids, through enzymes that catalyse the desaturation, chain elongation, or α-hydroxylation of palmitate. All of these fatty acids can then be stored in lipid droplets, or used as building blocks for more complex lipids which can be transported around the body and perform diverse functions (see Figure 8).

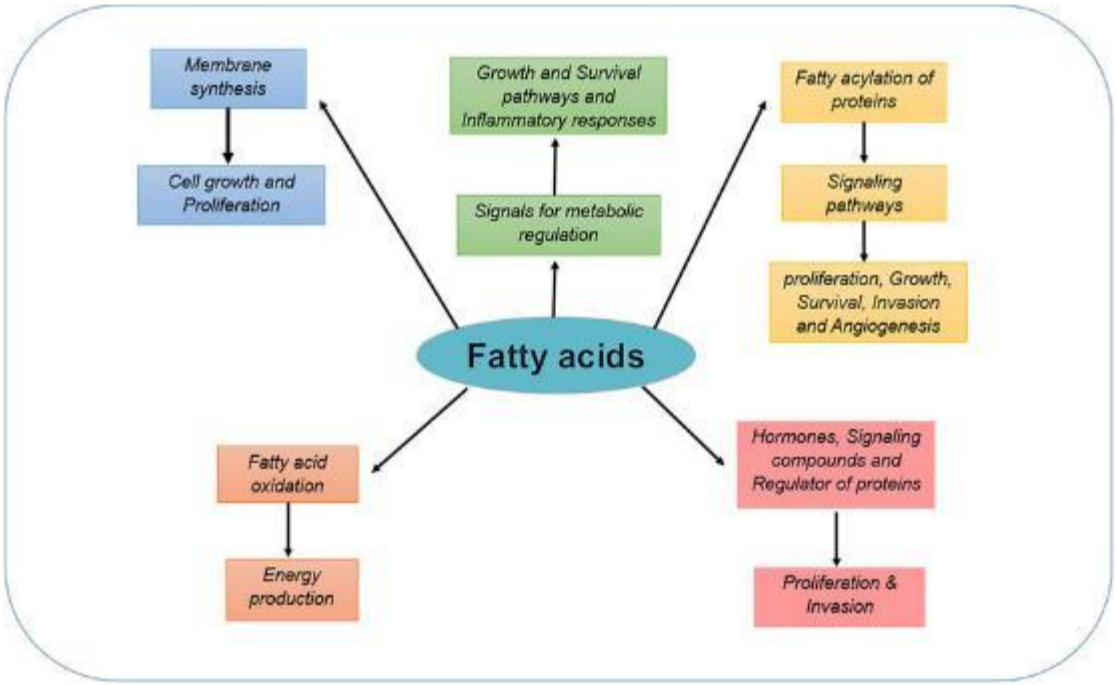

Figure 8. Diverse functions of fatty acids in humans. Fatty acids are ubiquitous, indispensable biomolecules that play many roles in human physiology. In addition to functioning as energy storage molecules, fatty acids are integral for membrane synthesis, regulation of proteins, signal transduction and certain immune pathways. *(Amiri et al, 2018)*

1.9.1. Acetyl-CoA carboxylase

Acetyl-CoA is an intermediate molecule that is critical and central to metabolic and fatty acid/lipid synthesis pathways in many organisms. In addition to its necessity as a substrate for fatty acid synthesis, it plays a complex and cyclical role in all cellular respiratory pathways. Acetyl-CoA is synthesized via the oxidation of pyruvate and is an essential substrate for the citric acid cycle and is also generated during β-oxidation and the breakdown of some amino acids. Acetyl-CoA cycles through these synthetic and metabolic pathways depending on both the glucose levels and energy demands of cells. When glycolysis levels (and subsequent ATP levels) are high, acetyl-CoA is diverted from the citric acid cycle and fatty acid synthesis is increased. Excess acetyl-CoA is converted to malonyl-CoA by ACC via a carboxylation reaction, which is therefore the initial and committed step in fatty acid synthesis.

ACC is a biotin-dependent enzyme and has two catalytic activities which work in succession to yield the final malonyl-CoA product; this enzyme acts upon acetyl-

CoA produced from the TCA cycle, and irreversibly catalyses the carboxylation of malonyl-CoA from acetyl-CoA through its biotin carboxylase (BC) and carboxyltransferase (CT) activities (Wakil et al, 1983). As this enzyme influences both acetyl-CoA and malonyl-CoA levels, it is a central regulator of many pathways, including lipogenesis. ACC exists in two isoforms with differing subcellular locations and functions; ACC1 is cytosolic and generally enriched in lipogenic tissues (such as adipose, liver and lactating mammary tissue), while ACC2 is anchored to the outer mitochondrial membrane where it regulates β-oxidation and is expressed more so in high metabolic tissues such as skeletal muscle and heart (Barber et al, 2005; Brownsey et al, 1997; Kim et al, 1996; Widmer et al, 1996).

ACC itself is regulated allosterically through citrate levels and long chain fatty acyl-CoAs (LCFA-CoAs). An accumulation of citrate signals high glycolysis levels, and the citrate is broken down and converted to acetyl-CoA via citrate lyase. Citrate itself allosterically activates ACC by inducing polymerisation of the enzyme (Beaty & Lane, 1983; Munday, 2002; Tong & Harwood, 2006). LCFA-CoAs indicate a surplus of fatty acids and signal for fatty acid oxidation, and allosterically inhibits ACC through depolymerisation. Hormonal regulation of ACC, and therefore FASN, can occur by insulin, glycogen and epinephrine. The latter two stimulate the production of protein kinase A (PKA), which phosphorylates ACC, causing it to depolymerise. Conversely, insulin stimulates the activity of phosphoprotein phosphatases which dephosphorylate and inactivate ACC. Insulin and other growth factors can also stimulate a family of transcription factors called sterol regulatory element binding proteins (SREBPs), which can transcriptionally regulate lipogenic genes including ACC and FASN (Bertolio et al, 2019; Shimano & Sato, 2017; Wilentz et al, 2000). In a similar vein, high glucose levels can stimulate carbohydrate response element binding proteins (ChREBPs), which can promote the expression of ACC1 and FASN (Ortega-Prieto & Postic, 2019).

Malonyl-CoA, as well as being a substrate for fatty acid synthesis, can also act as an inhibitor of fatty acid oxidation by inhibiting carnitine-palmotyl-transferase-

1 (CPT-1), an enzyme that produces acyl-carnitines which can shuttle fatty acids from the cytosol to the mitochondria. This allosteric form of regulation ensures that fatty acid synthesis and oxidation are not simultaneously occurring (Zang et al, 2005). ACC therefore indirectly regulates fatty acid oxidation by controlling intracellular malonyl-CoA levels. In addition, another enzyme, malonyl-CoA decarboxylase (MCD) can catalyse the decarboxylation of malonyl-CoA to acetyl-CoA, and is located in the cytosol as well as mitochondria and peroxisomes. In unison the two enzymes can control malonyl-CoA levels and regulate CPT-1 and mitochondrial respiration (Lopaschuk et al, 2010).

1.9.2. Fatty acid synthase

Fatty acid synthase (FASN) is a multifunctional, cytoplasmic enzyme, and in humans represents the only enzyme that can catalyse the *de novo* synthesis of fatty acids. FASN is not expressed uniformly throughout the body; it is constitutively expressed in most cells but at low levels in normal tissues due to its downregulation via dietary lipids (McCarthy & Hardie, 1984; Weiss et al, 1986). Higher expression of FASN occurs in tissues with specialised storage functions, such as adipocytes and liver (Berndt et al, 2007), and tissues with high metabolic requirements, such as the lung, brain and breast. The regulation of fatty acid synthesis is extremely important for development, as FASN knockout *in vivo* in mice is embryonic lethal (Chirala et al, 2003). FASN overexpression is hallmark of several tumours, and indicates poor prognosis for breast, ovarian, and prostate cancers (Cerne et al, 2010; Daker et al, 2013; Grunt et al, 2009; Zhou et al, 2012). As a result, FASN inhibition as a potential anticancer agent has been thoroughly explored.

Rather than just a single enzyme, FASN is a large homodimeric enzymatic complex that consists of two identical protein subunits which are 272 kDa each. It has multiple catalytic domains and utilises metabolites acetyl-coenzyme A (acetyl-CoA) and malonyl-coenzyme A (malonyl-CoA) to create palmitate in a cyclical loop in the presence of NADPH. The different catalytic domains of FASN and the intermediate metabolites can be visualised in Figure 9. The cycle begins with acetyl-CoA and malonyl-CoA being adjoined to acyl-carrier protein (ACP) by

the first enzyme, malonyl or acetyl-CoA transacylase (MAT). The ketoacyl synthase domain condenses these molecules into acetoacetyl-ACP, which is then reduced, dehydrated and reduced again by the following three enzymes. This cycle is repeated, with malonyl-CoA donating two carbons each cycle, until a 16-carbon palmitate chain (16:0) is produced, after which the final product is cleaved by a thioester hydrolase (thioesterase or TE domain). The TE domain is particularly significant as it is the chain-terminating step and determines the final fatty acid product. It has a maximal affinity for 16-carbon acyl chains, with a drastic decline in affinity for chain lengths greater than 18 or less than 16 carbons (Lin & Smith, 1978; Mattick et al, 1983; Pazirandeh et al, 1989). Studies in a human breast cancer cell line found that the pool of *de novo* fatty acids synthesised by FASN comprised of 80 % palmitate and 10 % each of myristate and stearate (Kuhajda et al, 1994). TE is connected via a flexible linker to the preceding ACP domain, and studies physically separating the TE domain from this complex have shown that TE loses its chain-length specificity, and fatty acids of 20-22 carbons or greater are attached to the ACP domain (Singh et al, 1984).

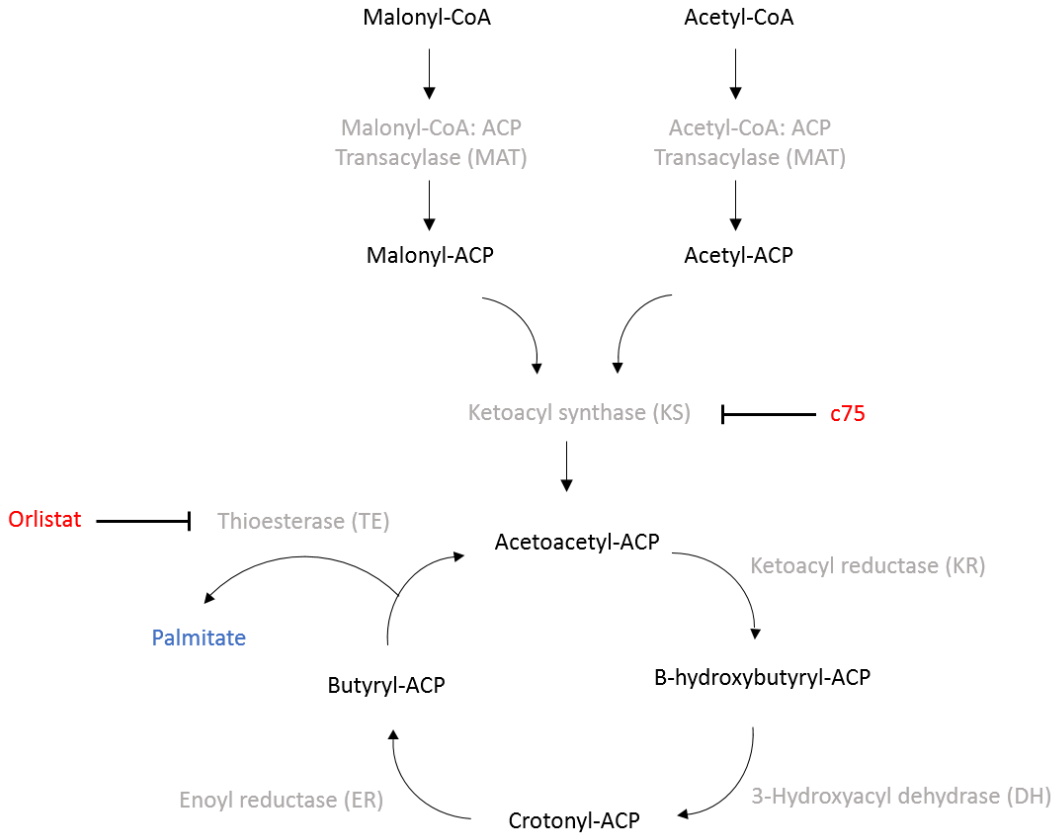

Figure 9. Schematic diagram of palmitate production via the fatty acid synthase (FASN) pathway. This enzyme has seven different catalytic domains that work in a cyclic loop to produce palmitate. Each domain generates an intermediate metabolite, and substrates are carried from one domain to the next via an acetyl-carrier protein (ACP). Two common inhibitors of FASN, orlistat and c75, are indicated in red with an arrow pointing to the specific catalytic domain that they inhibit. Image adapted from *(Carroll et al, 2018a)*.

1.9.3. Production of alternate fatty acids

Whilst the primary product of the FASN pathway is palmitate, this end product can undergo further modifications to give rise to other fatty acids. Palmitate homeostasis is a tightly controlled process in tissues and an imbalance can lead to several physio-pathological conditions including atherosclerosis, cancer and neurogenerative disorders (Tse et al, 2018). The 16-carbon palmitate chain can be elongated into stearate (18:0) through the addition of two carbons, a process which primarily takes place on the ER and involves several membrane-bound enzymes. Whilst the elongation process is similar to that of FASN, it is performed by individual proteins which may be physically associated (Hlousek-Radojcic et

al, 1998; Jakobsson et al, 2006). The palmitate precursor must first be activated to palmitate-CoA by long-chain-fatty-acid--CoA ligase 1, and an elongase enzyme complex sequentially adds C2 moieties from malonyl-CoA to generate the longer fatty acid chain. The most common product of this process is stearate (18:0), but other fatty acids can also be produced, such as arachidate (20:0), behenate (22:0), lignocerate (24:0) and cerotate (26:0). Palmitate and stearate can also undergo desaturation through the action of stearoyl-CoA desaturase (or Δ-9 desaturase) to produce the unsaturated fatty acids palmitoleate and oleate, a homeostatic process which aids in protecting the cells from ER stress and apoptosis (Borradaile et al, 2006; Busch et al, 2005; Collins et al, 2010; El-Assaad et al, 2003).

Free fatty acids are rarely found in organisms and can contribute to cell toxicity. Instead, synthesised fatty acids are converted into esters, of which there are 3 main types: triglycerides, cholesterol esters and phospholipids. Triglycerides are comprised of 3 fatty acids (predominantly saturated but can be unsaturated), esterified to a glycerol backbone. There are a few different pathways for triglyceride synthesis, however the Kennedy pathway is the predominant form and produces about 90 % of liver triglycerides (Moessinger et al, 2014). Following synthesis via the FASN pathway, palmitate is activated to palmitoyl-CoA by acyl-CoA synthases. The glycerol precursor, *sn*-glycerol-3-phosphate, is the main source of glycerol backbone and arises from the catabolism of glucose. Therefore, the presence of glucose is often a limiting factor for the production of triglycerides. Triglyceride synthesis occurs predominantly in the liver and in adipocytes, however they can be secreted from the liver directly into the bloodstream as very low-density lipoproteins (VLDLs). This serves as a transport mechanism to deliver lipids to peripheral tissues and can also transport signalling molecules that trigger signalling cascades in cells.

Phospholipids represent one of the most integral structural components in all cells, and are synthesized from fatty acids and glycerol and differ from triglycerides by a phosphate head group. They are amphiphilic; they contain a hydrophobic head group and a hydrophilic fatty acid tail, and it is this property

which lends this class of lipids the ability to create boundaries and compartmentalise cells. The shape, size, charge and composition of phospholipids can affect the structure and stability of the membranes they form. Phospholipids can aid in the stabilisation of proteins embedded in the membrane, they can act as a reservoir for signalling molecules, and can facilitate the absorption and storage of lipids. There are 3 main types of phospholipids that account for about 90 % of the total phospholipid content in humans: phosphatidylcholine (PC), phosphatidylethanolamine (PE) and phosphatidylserine (PS). Phospholipids are synthesized on the cytosolic side of the ER membrane and involve several enzymes, and begins with the synthesis of phosphatidic acid which acts as a backbone for the synthesis of more complex phospholipids (reviewed in (Fagone & Jackowski, 2009)).

1.9.4. Lipid droplets

Lipid droplets (LDs) are lipid-enriched, cytosolic storage organelles that exist within most eukaryotic cells, and they are the primary means of fatty acid storage in cells. As such, they can regulate metabolism, energy homeostasis and inflammatory processes. LDs display a hydrophobic core, enclosed by a phospholipid bilayer and contain fatty acids and neutral lipids, and are decorated with proteins (see Figure 10). They are dynamic organelles, and their size can change depending on the energy demands of the cell (Cohen et al, 2015; Suzuki et al, 2011). Excess lipids can be stored in these reservoirs and released under stress via lipolysis (through the action of lipases) or lipophagy (through autophagy) (Schott et al, 2019). By sequestering cytoplasmic free fatty acids (FFAs), LDs aid in protecting the cell from lipotoxicity; FFAs can disrupt membrane integrity as well as being incorporated into other potentially cytotoxic lipid species (Listenberger et al, 2003; Nguyen & Olzmann, 2017; Senkal et al, 2017). The dysregulation of LDs can therefore result in the development of metabolic diseases associated with lipotoxicity, such as type 2 diabetes and fatty acid liver disease (Greenberg et al, 2011; Krahmer et al, 2013; Olofsson et al, 2011). Until recently, LDs were viewed as obligate cellular inclusions with little functionality besides a lipid repository, however they are slowly being revealed as important cellular as well as immune regulators. LDs can protect against ER

stress and mitochondrial damage during autophagy (Chitraju et al, 2017), and can mitigate harmful effects of oxidative stress. In subsequent sections we will discuss the emerging roles of lipid droplets in immune functions.

These multifunctional organelles are primarily comprised of TAGs (the major fatty acid storage molecule) and sterol esters surrounded by the phospholipid bilayer, but can also contain other lipids including ceramides and DAGs. Their synthesis occurs on the ER membrane, and this biosynthetic pathway is still not completely understood. The current model for LD biogenesis is as follows; it is believed that, via diffusion, fatty acids begin to accumulate between the bilayers of the ER, generating a bulge, or lens, that eventually forms a sphere and buds off due to differences in surface tension of the LD monolayer and the ER lumen (reviewed in (Chen & Goodman, 2017; Jackson, 2019). The newly synthesised LD buds off into the cytoplasm, encapsulated by the ER membrane, although the composition of this new membrane is different in its composition to the ER membrane, as proteins are embedded into the LD monolayer both during and after biogenesis (Bersuker & Olzmann, 2017). Currently between 100-150 proteins have been identified to localise to LDs, and these can range in diversity, including enzymes needed for their formation (including ACC) as well as degradation, several metabolic enzymes, and many cell signalling and trafficking proteins (Bersuker & Olzmann, 2017; Bersuker et al, 2018; Krahmer et al, 2011; Wilfling et al, 2013). Lipid droplets are transient and heterogenous; their FA makeup, protein composition, size and shape can vary from one tissue type to the next, from one cell to the next, and they are constantly undergoing synthesis and depletion based on diverse cellular signals. The homeostatic nature of these organelles, as well as their roles in inflammation and infection, highlights their significance and the need to understand the mechanisms underlying their synthesis and regulation.

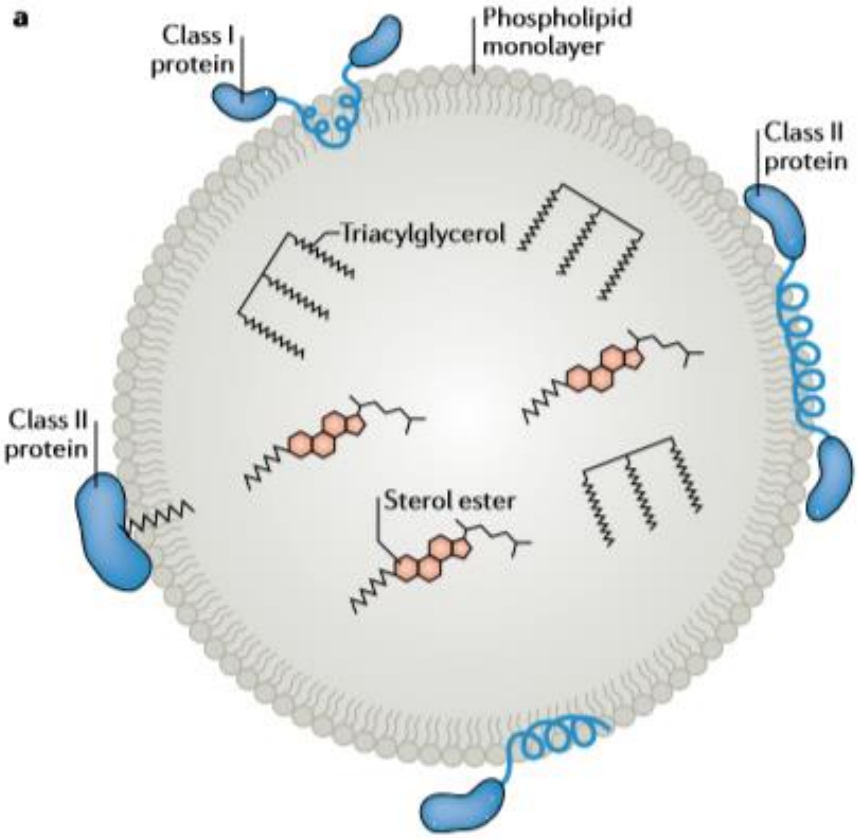

Figure 10. The structure of a neutral lipid droplet. A phospholipid monolayer encloses a core of neutral lipids, primarily triacylglycerol and sterol esters. Proteins are embedded either at the biogenesis state on the endoplasmic reticulum, or after *(Olzmann & Carvalho, 2019)*.

1.9.5. Cellular fatty acid transport

For fatty acids to perform their diverse functions, they need a means of being transported into and around cells, and into the mitochondria. It was once thought that fatty acids travelled through cell membranes via passive diffusion, but more recently several membrane-bound proteins have been identified that aid in and regulate this process (reviewed in (Kampf & Kleinfeld, 2007) and (Bonen et al, 2007)). These proteins are essential for mediating lipid flux, metabolism and inflammation, and defective proteins can lead to a number of metabolic diseases including insulin resistance, diabetes type-2 and hepatic steatosis. The proteins involved in uptake of extracellular fatty acids include fatty acid scavenger receptor CD36, a family of plasma membrane fatty acid binding proteins (FABPs), and several fatty acid transport proteins (FATPs) (see Figure 11 for a general overview of this process). CD36, also know at fatty acid translocase (FAT), is an

integral membrane protein found mostly on the surface of cells with high metabolic capacity, including adipocytes, monocytes, microglia, erythrocytes, skeletal muscle, and spleen cells (Febbraio et al, 2001). Expression levels of the receptor are elevated in the livers of patients with type-2 diabetes, resulting in increased lipid uptake and contributing to the pathogenesis of this disease (Koonen et al, 2007). CD36 recognises several ligands including LCFAs, VLDLs, collagen, thrombospondin and phospholipids (Baillie et al, 1996; Fernandez-Garcia et al, 2009; Tandon et al, 1989), and its scavenger functions have been implicated in the regulation of innate immunity (Cho et al, 2005; El Khoury et al, 2003; Harb et al, 2009; Janabi et al, 2000; Park et al, 2009b) and pathogen recognition (Hoebe et al, 2005; Means et al, 2009), metabolism and angiogenesis (Jiménez et al, 2000).

Mammalian FABPs exist in several isoforms, each with a different and specific localisation, and can be either intracellular or extracellular. FABPs have been shown to bind several hydrophobic ligands including fatty acids, retinoids, vitamins and haeme (Storch & Thumser, 2010). The full spectrum of their tissue-specific functions remains to be elucidated, but emerging evidence has shown their ability to direct fatty acids towards different intracellular fates, including lipid storage, peroxisomes, targeting FAs to different catabolic and anabolic pathways, mediating gene expression, and phospholipid synthesis (reviewed in (Storch & Thumser, 2010)).

Another enzyme involved in fatty acid transport is carnitine palmitoyltransferase-1 (CPT-1), which acts as a central regulator of β-oxidation. CPT-1 is a mitochondrial enzyme that catalyses the formation of acyl carnitines, which allow long-chain fatty acids to be shuttled into the mitochondria (short chain FAs are able to diffuse through the mitochondrial membrane). Fatty acids that are synthesised *de novo,* transported into cells or generated from the breakdown of other lipids or storage molecules, are present in the cytosol and must first be converted to fatty acyl-CoAs before they can be transported into the mitochondria, where they can be utilised as a substrate for energy production. This esterification reaction is performed by fatty acyl-CoA synthases, which are

specific for fatty acids of different chain lengths, and are ATP-dependent. Once esterified, fatty acyl-CoAs can either be converted into acyl-carnitines by CPT-1 through the conjugation with a carnitine molecule, or utilised in lipid biosynthetic pathways. Short-chain fatty acyl-CoAs can passively diffuse through the mitochondrial membrane, but LCFAs require conversion to acyl-carnitines for this to occur. The acyl-carnitines are then transported across the mitochondrial membrane by an integral mitochondrial protein, carnitine translocase, which exchanges the acyl-carnitine for a free carnitine molecule. Another integral enzyme, CPT-2, exists within the mitochondria and catalyses the inverse reaction to CPT-1 by converting the fatty acyl-carnitines back into fatty-acyl CoAs so they can enter the β-oxidation pathway. Malonyl-CoA is a potent allosteric inhibitor of CPT-1, and ACC2 is found associated with CPT-1, which most likely allows efficient regulation of the enzyme (Abu-Elheiga et al, 2000).

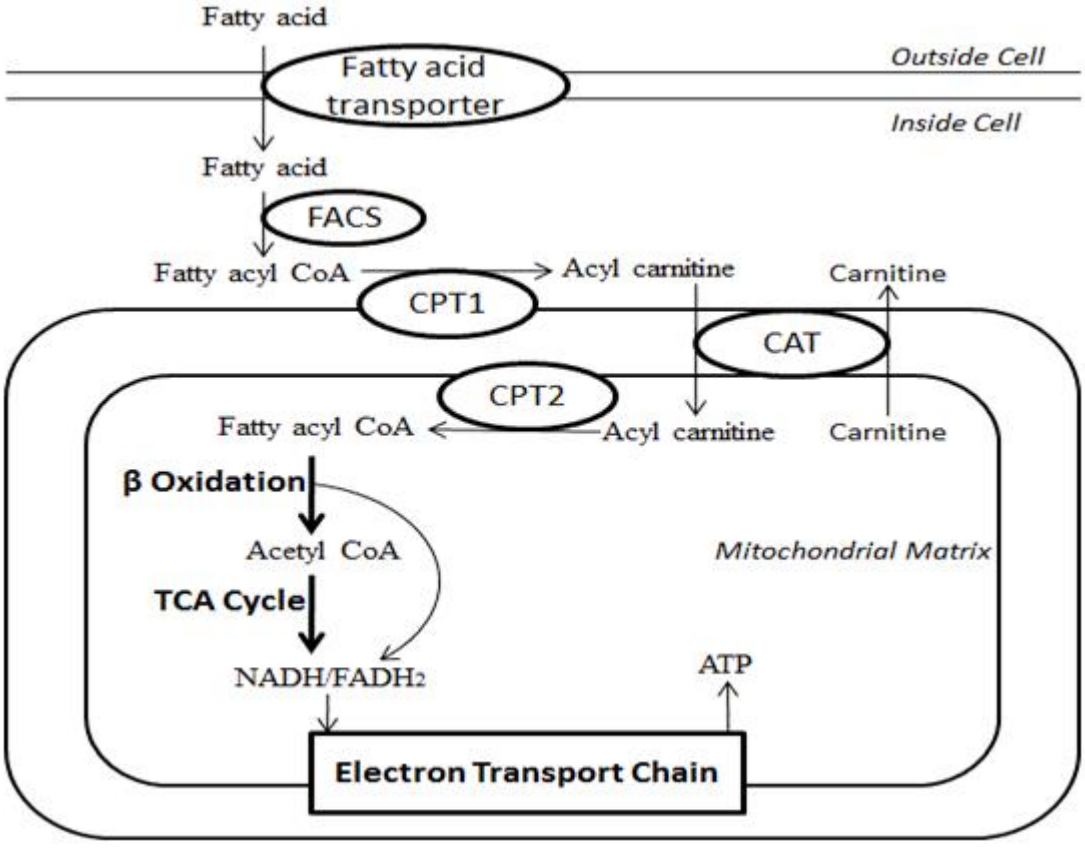

Figure 11. Schematic representation of the general mechanisms of fatty acid transport into and around cells. Fatty acids enter cells via fatty acid transporters present in the plasma membrane. Once in the cytosol, fatty acyl-CoA

synthase adds a CoA group to the fatty acid, resulting in a long chain fatty acyl-CoA. On the outer mitochondrial membrane, carnitine palmitoyl transferase 1 (CPT-1) recognizes the fatty acyl-CoA and converts it to a long chain fatty acyl-carnitine; a necessary step for the transport of the fatty acid moiety across the mitochondrial membrane where it will be oxidized. Carnitine translocase (CAT) transports the acyl-carnitine to the inner mitochondrial membrane, where it is converted back to a fatty acyl-CoA but CPT-2, and can participate in β-oxidation *(AOCS, 2021)*

1.10. Mitochondrial fatty acid synthesis

In addition to the cytosolic pathway of FAS that is regulated by ACC and FASN, there is another form of FAS that is far more mysterious and occurs in the mitochondria. As mitochondria are derived from a bacterial evolutionary lineage, mitochondrial fatty acid synthesis pathway (mtFASII) is one conserved feature that is largely similar to that of modern-day bacteria. mtFASII differs from cytosolic FASN in its enzymatic structure – rather than a single, multifunctional complex, mtFASII consists of individual proteins that catalyse each step. The substrate of this pathway is malonate, and in mammalian cells the final product is FAs with a chain length of up to 14 carbons (myristate), but can be up to 16 carbons in other organisms, however FA synthesis via this pathway does not contribute to cellular lipids. It remains to be elucidated why this mitochondrial FAS pathway is conserved in mammalians cells, and it may have important functions that are yet to be discovered. Knockdown of individual mtFASII components has resulted in mitochondrial dysfunction in the form of reactive oxygen species (ROS) production, decreased respiration rates, and changes in mitochondrial morphology (Brody et al, 1997; Feng et al, 2009; Kastaniotis et al, 2004; Miinalainen et al, 2003), suggesting that this pathway is integral to the overall function of this organelle. One known important function of this pathway appears to be through the production of lipoic acid, which is a co-factor for several enzymes, most of which are involved in cellular respiration. Inhibiting mtFASII components led to an overall decrease in cellular lipoic acid levels, and reduced levels of protein lipoylation (Brody et al, 1997; Witkowski et al, 2011).

1.11. Cellular respiration

Cellular respiration is the broad term for the suite of metabolic reactions that cells use to generate energy, in the form of ATP, from oxygen or nutrients. ATP is the energy currency of cells; it has 3 phosphate groups and therefore a net negative charge, and it exchanges energy through its dephosphorylation to ADP. In a general sense, all of the food you intake is broken down in the intestinal system into sugars, fats and amino acids, and distributed throughout the body where they can be absorbed and act as substrates for cellular respiration. These metabolic processes are overwhelmingly complex and stringently regulated, but can be broken down into three individual but interconnected stages; glycolysis, the citric acid cycle (or Krebs cycle or TCA cycle), and oxidative phosphorylation. While each of these processes yield ATP, they vary greatly in efficiency, with oxidative phosphorylation generating the bulk of the energy during cellular respiration but requiring substrates produced by glycolysis and the TCA cycle.

Simplified formula: Glucose + oxygen = CO_2 + H_2O + ATP

1.11.1. Glycolysis

Glycolysis is the process of converting glucose (the substrate) to pyruvate, which yields 2 ATP molecules per glucose molecule, and is a highly conserved, ancient metabolic process (Romano & Conway, 1996). Glucose is a simple 6-carbon sugar that circulates through the blood as blood sugar, and is transported into cells via glucose transporters, and occurs when blood-glucose levels are high. Glycolysis occurs in the cytoplasm, and involves 10 different reactions catalysed by 10 different enzymes, and uses the electron carrier nicotinamide adenine dinucleotide (NAD+) to transport electrons from one reaction to the next. This process can occur aerobically (with the presence of oxygen), in which case pyruvate gets converted into 2-carbon molecule acetyl-CoA, or anaerobically, where the lack of oxygen results in pyruvate being converted to lactic acid.

Simplified formula: Glucose → pyruvate + 2 ATP + 2 NADH

1.11.2. The citric acid cycle

The 2 ATP molecules produced per glucose molecule during glycolysis is simply not enough to meet the energy demands of many organisms, so they have evolved additional metabolic pathways to do this. The citric acid cycle utilizes acetyl-CoA as a substrate, which is derived from the pyruvate produced by glycolysis, and produces ATP, NADH, NAD+ and carbon dioxide, which are used as substrates for oxidative phosphorylation. This process occurs in the mitochondria and is a cycle of 8 reactions, catalysed by 8 different enzymes. Before the cycle can begin, pyruvate must enter the mitochondrial membrane where it is converted to acetyl-CoA in three steps: first, pyruvate is decarboxylated, then oxidized to an acetyl group, and then transferred to the co-enzyme A, resulting in acetyl-CoA. Some often consider the oxidation of pyruvate to acetyl-CoA a separate step to the citric acid cycle.

In addition to glycolysis, acetyl-CoA can also be derived from the catabolism of fatty acids through β-oxidation. As previously discussed, fatty acids can enter the mitochondria as acyl-carnitines through the action of CPT-1, and once translocated across the membrane via CAT, are converted back into fatty-acyl-CoAs by CPT-2 so they can enter the β-oxidation pathway. β-oxidation, like fatty acid synthesis, occurs in a cyclic pathway that shortens, instead of extends, two carbons at a time, producing NADH, $FADH_2$ and acetyl CoA, and involves the action of four enzymes. This produces one acetyl-CoA per cycle, and the overall amount of acetyl-CoA that can be derived from a fatty acid depends on its chain length. This process is regulated both allosterically and transcriptionally. Each enzyme can be allosterically inhibited by the acyl-CoA intermediate they produce, and additionally by NADH and acetyl-CoA levels (Eaton, 2002; Schulz, 1994). β-oxidation can be transcriptionally regulated by several factors including peroxisome proliferator-activated receptors (PPARs) and transcription factor PGC-1α, which act on several proteins involved in β-oxidation including FATP, CD36 and CPT-1 (Huss & Kelly, 2004). The FADH and NADH produced via this process are fed into the electron transport chain during oxidative phosphorylation, and the acetyl-CoA is fed through the citric acid cycle.

The very first step of the citric acid cycle occurs when the acetyl group is removed from acetyl-CoA and transferred to oxaloacetate by citrate synthase, which produces citrate, the substrate for the citric acid cycle. The cycle takes place in the mitochondrial matrix (see Figure 12) and is a closed loop with oxaloacetate being regenerated in the final step of the process. It is an aerobic process and is a series of redox, dehydration, hydration and decarboxylation reactions catalysed by different enzymes, all of which are soluble except for succinate dehydrogenase, which is embedded in the inner mitochondrial membrane. The resulting products, per acetyl-CoA molecule from this process, are 1 ATP, 3 NADH, 1 FADH2 and CO_2. Although, like glycolysis, this generation of ATP is generally not enough to meet the energy constraints of most organisms, these by-products are fed into and are integral for oxidative phosphorylation, which produces the bulk of the energy during cellular respiration.

Simplified formula: pyruvate → acetyl-CoA → 3 NADH + FADH2 + ATP

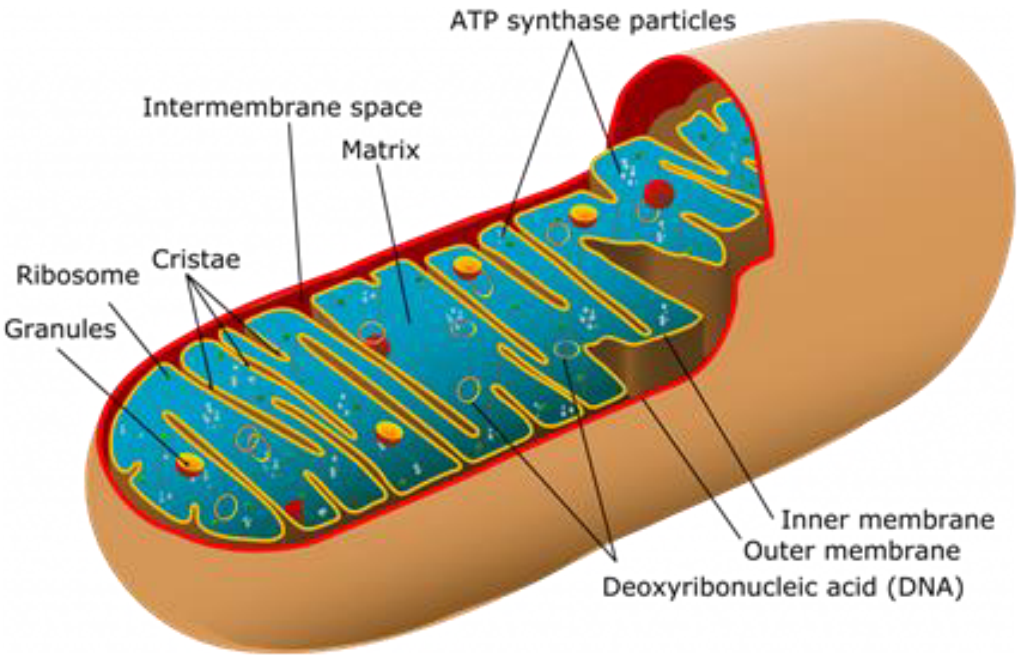

Figure 12. Schematic representation of mammalian mitochondria. Mitochondria have a double membrane structure (an outer membrane and an

inner membrane) that are comprised of phospholipids and proteins, and are separated by an intermembrane space. The inner membrane contains many folds, called cristae, which increase the surface area of the organelle. The mitochondrial matrix is a viscous liquid and is where the tricarboxylic acid cycle (TCA cycle) occurs. Oxidative phosphorylation occurs in the inner mitochondrial membrane, through a series of reactions catalyzed by proteins embedded in this membrane.

1.11.3. Oxidative phosphorylation

Oxidative phosphorylation is a highly efficient energy-producing process that is the primary source of energy for many tissues. This process involves the oxidation of the energy-carrying coenzymes generated from glycolysis and the citric acid cycle (NADH, FADH2), and overall yields 26-28 ATP per glucose molecule. The electrons produced from these oxidation reactions are fed into the electron transport chain, which is a series of 4 mitochondrial complexes that transfer electrons from one acceptor to the next, with each having an increasingly greater affinity for electrons (see Figure 13). This does not generate ATP, but instead pumps hydrogen ions into the intermembrane space. This results into a proton gradient – where there is a higher concentration of hydrogen ions in the intermembrane space vs the mitochondrial matrix. This is a form of stored energy, and the energy is released via proton movement through a protein complex called ATP synthase, which is located in the inner membrane. As protons move through this complex, ATP synthase adds a phosphate group to ADP to produce ATP, which is a highly efficient process which produces the bulk of ATP of cellular respiration.

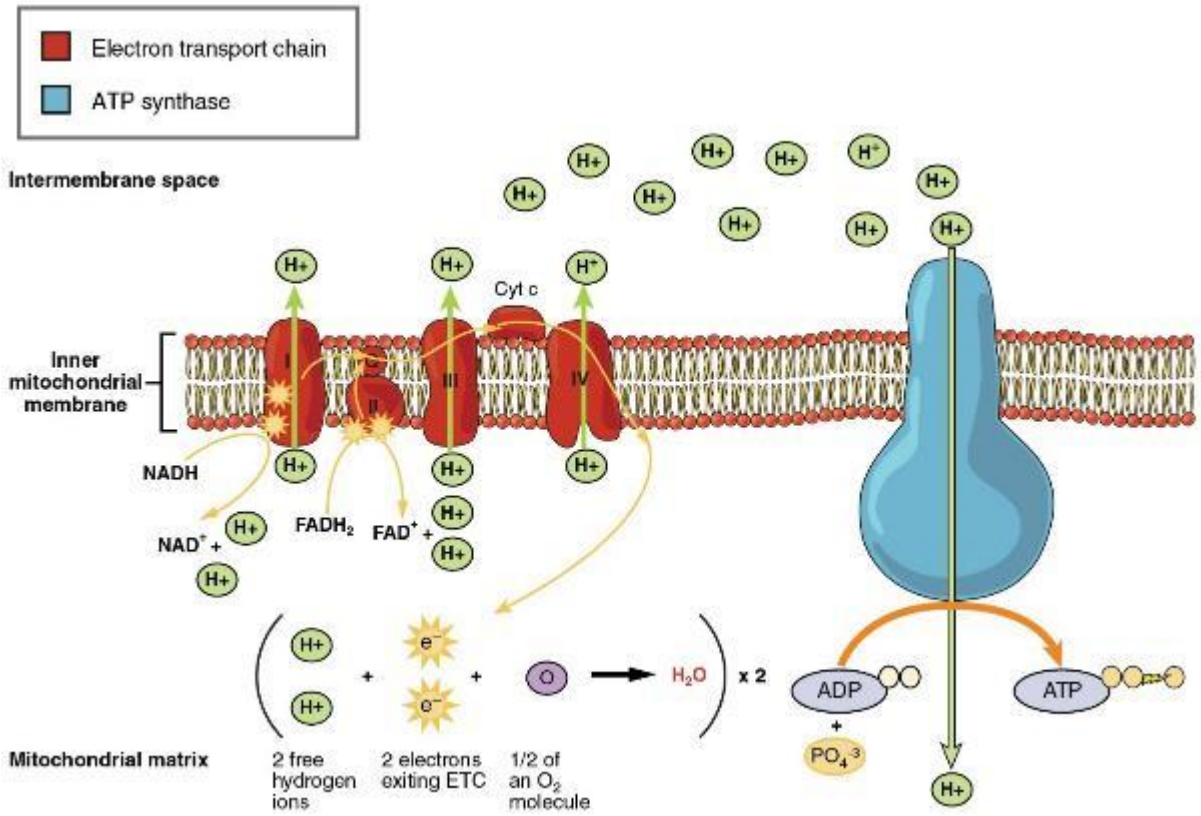

Figure 13. Movement of electrons through the electron transport chain (ETC) and ATP synthase. The ETC consists of 4 protein complexes that transfer electrons from one acceptor to the next, generating energy that is used to pump hydrogen ions from the inner mitochondria matrix to the intermembrane space. This produces a proton gradient, which results in proton movement through ATP synthase, which converts ADP to ATP, which is the energy currency of cells *(College, 2013)*.

1.12. The role of fatty acid synthesis and metabolism during infection

As obligate parasites, most viruses lack the machinery to synthesis lipids and must commandeer many lipid synthesis and metabolic enzymes in order to complete their life cycle. We know that lipid reorganisation and subversion of lipid pathways is a hallmark of Flavivirus infection, and we are slowly uncovering the reasons for this. RNA interference (RNAi) genome-wide screens of WNV and DENV-infected human cells revealed 305 host proteins that are involved in infection, including several proteins related to metabolic processes and lipid synthesis and degradation (Krishnan et al, 2008). It is clear from studies with these, and other viruses, that lipid synthesis pathways are central to viral

replication and survival (Koyuncu et al, 2013; Limsuwat et al, 2020; Long et al, 2019; Pombo & Sanyal, 2018). The emerging field of lipidomics has allowed insight into how these viruses utilise host lipids for their own pathogenesis. Flaviviruses, like most positive strand RNA viruses, orchestrate a drastic rearrangement of host cellular lipids, with between 15 % and 85 % of metabolites detected being different between infected and uninfected mosquitoes, depending on which cellular location is analysed (Perera et al, 2012). ZIKV infection in placental cells also demonstrated that infection impairs lipid homeostasis, with FASN and FAT/CD36 transcription increased and the lipid profile of cells is altered compared to uninfected cells (Chen et al, 2020). A study of DENV-infected cells also showed an increase in several metabolic-related genes during infection including FASN, ACC1, CPT-1, SCD-1 and DGAT-1 (Tongluan et al, 2017). The primary utility of these lipids is most likely to construct membranous replication complexes, although several other roles throughout the viral life cycle exist. Here we will describe some of the reported ways that viruses hijack these pathways, with a particular focus on Flaviviruses.

1.12.1. ACC

As ACC and FASN both control *de novo* fatty acid synthesis studies, they are often, but not always studied in conjunction. Whilst ACC has additional functions in regulation fatty acid oxidation and mitochondrial respiration, FASN regulates fatty acid chain lengths and has multiple catalytic domains that can produce intermediate metabolites. Studies with WNV and Usutu virus (USUV) using TOFA, a small chemical inhibitor of ACC1, showed a reduction in the cellular lipids required for infection (including TAGs, DAGs, cholesterol, ceramide, and some phospholipid species), and a subsequent inhibition of viral replication in Vero cells (Merino-Ramos et al, 2015). Inhibition of ACC has not had as clear of an effect on ZIKV virus replication; one study showed TOFA reduced viral replication of another mosquito-borne virus – Semliki Forest virus – but had no significant effect on ZIKV replication in A549 cells (Royle et al, 2017). A different study however, found the ACC inhibitors PF-05175157, PF-05206574 and PF-06256254 all significantly reduced replication of WNV_{NY99}, ZIKV and DENV in Vero cells, and further reduced WNV viral load in a mouse model of infection

(Jiménez de Oya et al, 2019). Electron microscopy (EM) and immunofluorescence images of infected cells saw a reduction in viral-induced membrane structures and dsRNA accumulation, suggesting that reduction of lipid synthesis induced by TOFA was resulting in impairment of replication complex formation. These results are promising and suggest that ACC may be a druggable target to reduce replication of different Flaviviruses, however more research needs to be done to confirm this, particularly for ZIKV.

1.12.2. FASN

FASN has been studied extensively as a target for metabolic disease and viral pathogenesis, and also heavily in cancer research. Subsequently there are several inhibitors available to each of the catalytic domains of this complex, and more are in development. When treated with pharmacological inhibitors of FASN, or siRNA knockdown of FASN, both DENV and WNV levels are drastically reduced (Heaton et al, 2010; Liebscher et al, 2018; Martín-Acebes et al, 2011a; Tongluan et al, 2017). It is proposed that FASN is commandeered primarily to generate fatty acid substrates for viral replication complex morphogenesis. Heaton et al 2010 showed via immunofluorescence that FASN was redistributed to sites of viral replication, and this was instigated via a direct interaction with NS3 (Heaton et al, 2010). Inhibiting FASN also attenuates WNV proliferation and disrupts replication complex formation, however an association with NS3 has not been found. Whilst it appears that it is being utilised to generate fatty acids to incorporate into these VP and CM/PC structures, FASN is multi-faceted and can contribute and interact with infection in many diverse ways. The role of FASN in ZIKV infection is again not clear – one study showed no difference in viral accumulation when treated with cerulenin (Royle et al, 2017), however this was the only FASN inhibitor that was tested and is a natural, more cytotoxic analogue of the synthetic FASN inhibitor c75 which is far more commonly used. Another study has recently reported an effect of orlistat on ZIKV replication, however only under particular treatment conditions (Hitakarun et al, 2020) The heavy reliance on the FASN pathway by other Flaviviruses and other studies showing FASN upregulation during ZIKV infection (Chen et al, 2020), suggests that further research may implicate a role for FASN in ZIKV infection.

FASN has also been implicated in the life cycles of numerous other pathogens, including bacteria, fungi and other viruses, showing a broad-spectrum utilisation and reliance on *de novo* lipogenesis during infection. Respiratory syncytial virus (RSV) and other respiratory viruses are susceptible to FASN inhibition, and palmitate was shown to be necessary for replication, protein levels, viral particle formation and release of infectious virus (Ohol et al, 2015). The utilisation of FASN by Hepatitis C virus (HCV), another member of the *Flaviviridae* family, has been extensively studied, revealing that FASN is upregulated during infection and has roles in every stage of the viral life cycle including entry (Agnello et al, 1999; Alvisi et al, 2011; Nasheri et al, 2013; Yang et al, 2008). One study in particular observed an association between HCV NS5B and FASN via a pull-down assay, saw co-localisation of FASN and NS5B in viral replication complexes and lipid rafts, and observed FASN directly increase the RdRp activity of NS5B (Huang et al, 2013). Taken together it appears that FASN is a common pro-viral factor and is deliberately utilised by viruses to aid in replicative processes.

In addition to FASN, downstream enzyme SCD-1 has also been implicated in viral infection, including HCV, DENV and ZIKV (Gullberg et al, 2018; Hishiki et al, 2019; Lyn et al, 2014; Nguyen et al, 2014; Nio et al, 2016). SCD-1 is an extremely important enzyme that is essential for the production of unsaturated fatty acids, which make up the building blocks of phospholipids, TAGs and cholesterol esters. The substrates of SCD-1 are stearoyl-CoA and palmitoyl-CoA (the direct products of the FASN pathway), and the products of this reaction are oleoyl-CoA and palmitoleoyl-CoA. Unsaturated fatty acids by nature contain at least one double bond, which gives the fatty acid chain a ‘kink’ and can contribute to membrane curvature and increase fluidity. Chemical inhibition or siRNA knockdown of SCD-1 in Huh-7 cells significantly reduced DENV and ZIKV viral titre and mRNA levels, and this effect could be rescued with exogenous unsaturated fatty acids (Hishiki et al, 2019). Clearly in addition to *de novo* synthesis of fatty acids via FASN, viruses also require the ability to alter FA species in a manner that benefits their survival.

1.12.3. Lipid droplets

Lipid droplets are specifically targeted by several different pathogens during infection. It is believed that they act as energy reservoirs for viruses, but emerging evidence also suggests roles in replication, virion assembly, and they have also been implicated in the host innate immune response. Several viruses induce lipid droplet biogenesis quite rapidly upon infection, including HCV (Barba et al, 1997), DENV (Samsa et al, 2009), ZIKV (Monson et al, 2021a), herpes simplex virus (HSV) (Monson et al, 2021a) and Influenza A virus (Episcopio et al, 2019; Monson et al, 2021a). Currently there is little known about the mechanisms underpinning the LD induction for each of these viruses, and in some cases it is unclear whether their formation is pro-viral and intentionally driven by viral factors, or if their induction is part of the host immune response. A 2020 study found that induction of LDs with several viruses occurred as early as 2 hours post infection and was associated with an increased IFN response which was essential to control the replication of ZIKV and HSV-1 (Monson et al, 2021a). The interplay of LDs with the immune system is a promising field that is in its infancy, and will be discussed further throughout this thesis.

From what we have observed of viral interactions with LDs it appears they may play roles in both replication and assembly of different viruses. The Flavivirus capsid protein, which mediates assembly of the virion and has been shown to interact with host lipid structures (Faustino et al, 2014; Faustino et al, 2015), has been observed to associate with LDs during DENV (Samsa et al, 2009), WNV (Martins et al, 2019), ZIKV (Shang et al, 2018), JEV (Sarkar et al, 2021) and HCV (Camus et al, 2013; Harris et al, 2011) infection, suggesting that this organelle is widely important for this stage of the viral life cycle. Samsa et al 2009 showed that DENV upregulates LD content upon infection and found that dissociating the lipid-binding amino acid sequence in the capsid protein led to the mislocalisation of the protein, and resulted in a reduction in viral RNA (Samsa et al, 2009). During ZIKV infection in placental cells, the virus upregulates FASN and DGAT-1 to increase LD accumulation and size (Chen et al, 2020). Interfering with DGAT-1 reduced LD content and viral replication, demonstrating that LDs are associated with infection in a pro-viral manner. The reason for this is unclear, however like

DENV it is proposed that they provide a platform for virion assembly or to increase metabolism (Chen et al, 2020). DENV has also shown a specific interaction with VLDLs and high density lipoproteins (HDLs) in the blood, and may form lipo-viroparticles which shuttle new viral particles into the extracellular space and to new target cells (Benfrid et al, 2022; Faustino et al, 2014). Specifically, secreted DENV NS1 has been shown to form stable complexes with HDL and low density lipoproteins (LDLs), which trigger the inflammatory response of macrophages (Benfrid et al, 2022).

In addition to virion assembly and exit, LDs have also been implicated in other aspects of the Flavivirus life cycle. Although ZIKV and DENV have induced LD accumulation in some studies, other have found the reverse, with ZIKV reducing LD content in hepatic cells, and DENV in hepatic and kidney cells (García et al, 2020; Heaton & Randall, 2010). It has been observed by several groups that DENV induces autophagy in a pro-viral manner to release the contents of these LDs (termed lipophagy), which increases the β-oxidation and overall metabolic rate of cells. The process by which DENV does this remains largely unknown; however it is believed that NS4A and NS4B are involved (Klemm et al, 2011). Although not directly related to LDs, another study found that inhibiting autophagy pathways for both DENV and ZIKV affected both intracellular viral RNA levels, and resulted in the production of non-infectious virions, indicating that the autophagy of LDs is important for genome replication and virion packaging (Mateo et al, 2013). The authors proposed that DENV and ZIKV may regulate autophagy as a means of efficiently switching between lipid catabolism and biosynthetic pathways to support infection. As our knowledge expands of the involvement of LDs in cellular processes emerge, it is likely that the roles of LDs during infection will continue to be uncovered.

1.12.4. Mitochondria and metabolism

As well as lipid biogenesis, viruses induce specific alterations to mitochondrial dynamics and can change the metabolic profile of infected cells. It is common for cells, before infection, to be in a metabolically quiescent state, and there are several viruses that drive cells toward glycolysis (aerobic glycolysis or the

Warburg effect), as a means of reducing FAO and boosting FAS. This effect has been observed for HIV, influenza A, human cytomegalovirus (HCMV), and ZIKV (Chen et al, 2020; Hollenbaugh et al, 2011; Ritter et al, 2010; Vastag et al, 2011). In placental cells, ZIKV disrupts the mitochondrial network and lowers mitochondrial respiration, which leads to an accumulation of lipids and also appears to disrupt the innate immune response (Chen et al, 2020). Contrarily, DENV upregulates autophagy pathways to release fatty acids from LDs (Heaton & Randall, 2010; Lee et al, 2008) and increases mitochondrial elongation through impairment of fission protein DRP-1 (Barbier et al, 2017). This results in boosting of β-oxidation and a subsequent increase in ATP production. DENV NS3 has also been shown to specifically bind to GAPDH to directly lower rates of glycolysis (Silva et al, 2019). Reports of DENV infection in fibroblasts however, suggest that DENV upregulates glucose uptake and glycolysis and inhibiting these pathways attenuates replication (Fontaine et al, 2015). Whilst it is clear that many viruses induce metabolic alterations, this appears to be very cell-type and species dependent.

1.13. Lipids, metabolism and immunity

In addition to viruses modulating cellular metabolism, immune cells such as macrophages and dendritic cells rapidly undergo metabolic reprogramming in response to pro-inflammatory stimuli such as cytokines or pathogens. This is to meet the new energy demands of their inflammatory functions, and some intermediate metabolites produced in the mitochondria can also serve as inflammatory signals. Triggers for this change in inflammatory and metabolic states can start with the detection of PAMPs, or from inflammatory signals produced by other cells *e.g.* IFN, and can aid in the clearance of pathogens. In the same way that cells can shift their metabolic profile in response to stimuli, it is believed that the metabolic profile of a cell can in turn influence its phenotype, which may have far-reaching consequences in inflammatory diseases. This field at the interface of intracellular metabolism and immune pathways is termed immunometabolism, and has implications for obesity, autoimmunity, cancer, and

infection. The intricacies of the interplay between viral infection and immunometabolism are understudied, and it is likely these interactions vary greatly between different species and cell types. Here we will describe what is known about the impact of metabolic pathways on immune functions, and further discuss what is known about the interplay of these pathways with infection.

1.13.1. Lipid droplets, lipid mediators and lipid rafts

Lipids and fatty acids can have abundant effects on immune function; they can interact with nuclear receptors, can modulate lipid rafts, act as lipid mediators which effect signalling cascades, and they can form lipid droplets which can house innate immune proteins and behave as signalling platforms. Although the induction of lipid droplets in response to infection appears to be beneficial for the replication of some viruses as previously discussed, induction of LDs during ZIKV and HSV-1 infections were found to be essential for robust IFN signalling. Curtailing LD content in infected cells reduced the ability of cells to produce IFN and lead to higher viral titres (Monson et al, 2021a). Additionally, recent studies have shown that several ISGs localise to LDs, and that one protein in particular, viperin, may require this LD localisation to restrict viral replication (Helbig et al, 2011; Saitoh et al, 2011). Indeed, LDs are readily and actively produced in immune cells including macrophages, dendritic cells and neutrophils. This data suggests that lipid droplets may act as important hubs for innate immune signalling, and it's possible that viral manipulations of these LDs are a mechanism for immune evasion.

Lipid rafts are lipid-rich, highly ordered membrane domains that are enriched with sphingolipids and cholesterol and have various functions. They influence membrane fluidity and compartmentalisation and are important for membrane protein trafficking and signal transduction. Several studies have shown that lipid rafts can facilitate viral entry for diverse pathogens, including SARS-CoV-2, echovirus 1 (EV1), HIV-1, measles virus, Ebola virus and Epstein–Barr virus (EBV), as well as exit (influenza virus) (Chazal & Gerlier, 2003; Ripa et al, 2021; Sviridov & Bukrinsky, 2014; Wang et al, 2008). Additionally to the plasma membrane, lipid rafts can be present on the membranes of organelles and can

aid in endocytic vesicle fusion (Sindbis and Semliki viruses) (Ahn et al, 2002; Phalen & Kielian, 1991).

Perturbation of lipid biosynthetic pathways has been shown to inhibit certain innate signalling pathways, predominantly through the disruption of lipids rafts and LDs. TLR4-mediated signalling, a pattern recognition receptor that recognises several PAMPs including DENV NS1, can be disrupted via FASN inhibition. One study found that FAS and cholesterol synthesis are linked by a shared metabolite, acetoacetyl-CoA, and inhibiting FASN resulted in lower levels of this metabolite, which reduced cholesterol synthesis. Consequently, reduced cholesterol levels impaired the formation of lipid rafts, which TLR4 is dependent on for signalling (Carroll et al, 2018a). The authors found overall that inhibition of FASN, cholesterol synthesis and TLR4 signalling led to a defective ability of macrophages to mount an inflammatory response when stimulated with LPS (Carroll et al, 2018a). The connection between fatty acid synthesis, TLR4 signalling and NS1 during infection is yet to be investigated. Cholesterol-rich lipid rafts are also important for IFN-stimulated STAT antiviral signalling, and it was found that the redistribution of cholesterol by WNV from the plasma membrane to viral RCs, resulted in a downregulation of this signalling pathway (Mackenzie et al, 2007). This clearly demonstrated that the perturbation of lipid pathways may not only benefit viral replicative processes, but may also be a mechanism of immune evasion.

Lipid mediators are lipids that can directly function as potent signalling molecules, and are often associated with immune functions (reviewed in (Monson et al, 2021b)). They can be rapidly synthesised from existing cellular membranes when required, and are found both packaged into LDs during biosynthesis or can be directly synthesised via LDs. Lipid mediators can be divided into 3 classes. Class I includes eicosanoids (prostaglandins and leukotrienes), which cannot be stored but can be synthesised on demand from the poly unsaturated fatty acid arachidonic acid. Eicosanoids have diverse regulatory roles and during viral infection have been shown to be both pro-viral and anti-viral (Coulombe et al, 2014; Harbour et al, 1978; Rossen et al, 2004). Class II are membrane-derived

lipid mediators and mostly consist of phospholipids and sphingolipids and include lysophosphatidic acid (LPA) and lysophospholipids such as platelet-activating factor (PAF). This class has only been shown to be pro-viral, enhancing replication of DENV, HIV, RSV and HCV (Caini et al, 2007; Lima et al, 2006; Souza et al, 2009; Villani et al, 1991). Class III are generally derived from omega-3 and omega-6 fatty acids and include resolvins and protectins, which contribute to the resolution of inflammatory processes and regulate the functions of Class I lipid mediators (Mittal et al, 2010; Molfino et al, 2017; Serhan, 2014). In contrast to Class I and I, Class III have only been demonstrated to have pro-host functions during infection (Cilloniz et al, 2010; Morita et al, 2013; Rajasagi et al, 2013; Richardson et al, 2005; Shirey et al, 2014). It is clear that fatty acids play a diverse and complex role in the regulation of immune signalling, and can be used as tools by both the host immune system as well as by pathogens.

1.13.2. Citric acid cycle

In some cases, it has been demonstrated that immune cells undergo metabolic changes in the form of breaks in the TCA cycle which can contribute to the clearance of pathogens. In ZIKV infected neuronal cells, infection triggers the transcription of immune responsive gene 1 (IRG1), which increases the production of itaconate, a TCA cycle intermediate that can inhibit succinate dehydrogenase activity (SDH) (Daniels et al, 2019). Inhibition of SDH causes a metabolic shift and generates an antiviral metabolic state that restricts ZIKV replication in neuronal cells. Similarly, in pro-inflammatory myeloid cells, DRP-1-driven mitochondrial fission results in two breaks in the TCA cycle, which produces succinate. Accumulation of succinate in the mitochondria leads to ROS production and increased cytokine production, including TNF-α and IL-1β (Krzak et al, 2021; Mills et al, 2016; Zuo & Wan, 2020). This represents a novel immunometabolism mechanism and highlights how metabolic intermediates can have antiviral functions.

1.13.3. Macrophages

One of the most well-characterised models of immunometabolism exists within macrophages. Whilst the characterisation of macrophage phenotypes is

complex, with a diverse range of functions and genetic and metabolic signatures, they can more or less be categorised into two different states for simplicity: M1 (pro-inflammatory or 'classically activated') or M2 (anti-inflammatory or 'alternatively activated') (Carroll et al, 2018a; Parisi et al, 2018; Shapouri-Moghaddam et al, 2018; Van den Bossche et al, 2017). In these extreme states, pro-inflammatory M1 macrophages are more involved in pathogen defence and elimination and can present antigens to T cells and secrete inflammatory cytokines, whilst anti-inflammatory M2 macrophages are involved in homeostatic functions such as tissue repair and regulation, and can release anti-inflammatory mediators, increase phagocytosis of apoptotic cells and induce collagen production (Mantovani et al, 2013; Viola et al, 2019). These macrophages have very distinct transcriptional and metabolic profiles (summarised in Figure 14); upon activation, M1 macrophages show increased TAG synthesis and lipid accumulation (Dierendonck et al, 2022; Feingold et al, 2012; Funk et al, 1993), enhanced glycolysis and impaired oxidative phosphorylation (Freemerman et al, 2014; Fukuzumi et al, 1996; Funk et al, 1993; Hard, 1970). The shift to glycolysis occurs as this form of energy production can be mobilised quickly to maximise cellular response to stimuli, and M1 macrophages also display breaks in the TCA cycle, allowing the accumulation of citrate, succinate and itaconate which can trigger anti-microbial functions (reviewed in (Viola et al, 2019)). M2 macrophages, conversely, rely mostly on β-oxidation for their energy (the consumption of fatty acids (Nomura et al, 2016b)), which is a more efficient form of energy production better suited to the long-term activities of these macrophages (Odegaard & Chawla, 2011).

To date, most of the research into pathogen-drive metabolic shifts in macrophages has been performed in the context of bacterial LPS, and little is currently known about the impacts of viral infections on macrophage metabolism and polarisation. The role of glycolysis in HIV is currently unclear, with findings that GLUT1 expression and glycolysis are both upregulated (Palmer et al, 2014) and downregulated (Sen et al, 2015), suggesting that the metabolic state during HIV infection may depend on the timeline of infection and the differentiation state of the macrophages (Palmer et al, 2016). Despite the tropism of Flaviviruses for

macrophages, and the knowledge that infection of this cell type may contribute to viral spread and severe symptoms (Wan et al, 2018), the relationship between metabolism and immune function is extremely understudied in these cells. Studies in other cell types including placental cells, fibroblasts and liver cells show contrasting metabolic manipulations, as previously mentioned. Understanding of the induction and subversion of metabolic and inflammatory processes in macrophages may help us to understand the immunopathological mechanisms underpinning Flavivirus hyper-inflammation and encephalitis, and allow us to better target these pathways therapeutically.

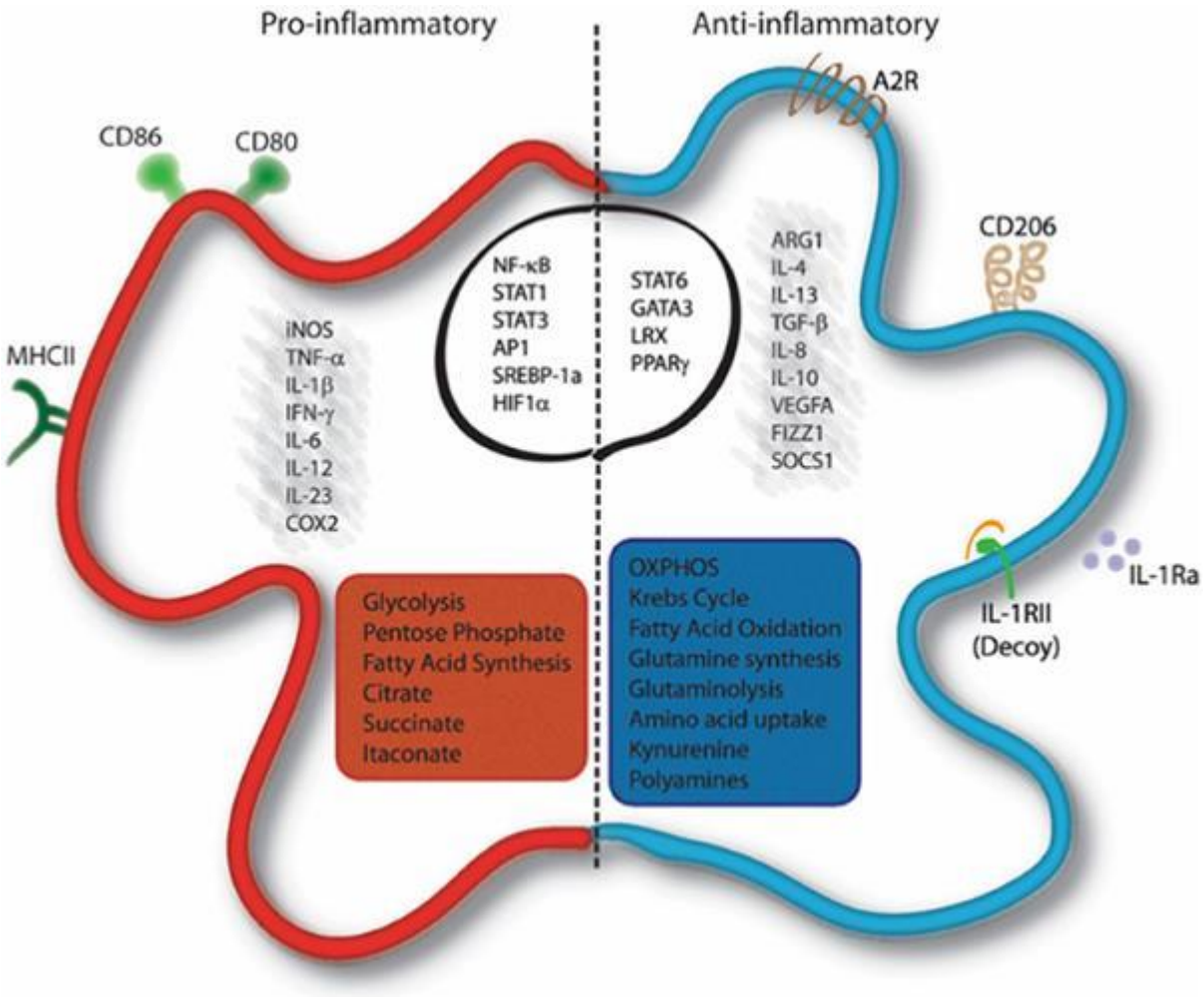

Figure 14. The transcriptional, metabolic and cytokine profile of pro-inflammatory and anti-inflammatory macrophages. Pro-inflammatory macrophages are activated by LPS and IFN-γ and are categorised by the

expression of specific surface markers, cytokine production, and transcription factors. They also have a specific metabolic profile, include upregulated glycolysis and fatty acid synthesis. Anti-inflammatory macrophages are generally induced by IL-4 or IL-13 and rely on oxidative phosphorylation, and exhibit differential expression of surface markers, transcription factors and cytokines. *(Viola et al, 2019)*

1.13.4. Inflammasomes

Inflammasomes are large multiprotein intracellular signalling platforms, that detect pathogens and mount a highly inflammatory response, which results in a rapid form of cell death called pyroptosis. They are activated by a diverse range of triggers and their dysregulation can lead to a number of autoinflammatory diseases and they are implicated in sepsis. The inflammasome generally consists of the following domains: caspase-1, an enzyme responsible for cleaving pro-IL-1β, pro-IL-18 and Gasdermin-D into their mature forms, a caspase recruiting domain (CARD) and a pyrin domain (PYD). A subset of nucleotide-binding domain, leucine-rich repeat containing (NLR) proteins have been shown to be cytoplasmic mediators of some inflammasomes. The NLRP3 inflammasome is expressed by myeloid cells and lacks a CARD domain, and instead must recruit pro-caspase-1 through its adaptor molecule apoptosis-associated speck-like protein (ASC). NLRP3 can be activated by a range of stimuli, from danger-associated molecular patterns (DAMPs) to pathogen-associated molecular patterns (PAMPs). Fatty acid synthesis has been demonstrated to induce the activation of the NLRP3 inflammasome (Moon et al, 2015b), whilst FAO has been implicated in NLRP3 activation in macrophages (Moon et al, 2016).

Flaviviruses have also been implicated in the activation of the NLRP3 inflammasome during infection. ZIKV NS5 protein has been shown to bind with NLRP3 to facilitate its assembly in macrophages and dendritic cells, which in turns increases production of IL-1β and IL18 (Wang et al, 2018). DENV has also been shown to induce NLRP3 activation in M1 macrophage. Similarly, mice with impaired ASC domains showed an impaired immune response to WNV, and greatly reduced levels of IL-1β. These findings suggest a key role for the NLRP3 inflammasome in Flavivirus host immune defence. Whether the stimulation of FASN during infection contributes to inflammasome activation, or if Flaviviruses

have evolved a way to perturb the activation of this highly inflammatory cascade, is currently unclear.

1.14. Thesis aims

The utilization of lipid biosynthetic and metabolic enzymes is integral to the survival of many viruses, but the exact requirements differ between viruses and cell types. These pathways may prove ideal targets for therapeutics; however we must first gain a comprehensive understanding of the metabolic needs of specific viruses, and the impacts inhibiting these pathways may have on host immunity. So far, *de novo* fatty acid synthesis has been identified as a key pathway for Flavivirus replication. Flaviviruses are known to drastically alter the lipid landscape of infected cells and can also completely modify host cellular metabolism. In macrophages, fatty acids play pro-inflammatory roles, and the concentration of metabolites is a forceful driver of macrophage phenotype and function. Thus, we hypothesized that alterations in the lipid landscape of infected macrophages may lead to an alteration in immune responses. Despite Flaviviruses having a tropism for macrophages, the metabolic profile of Flavivirus-infected macrophages has never been categorized. Our overarching aim was therefore to determine if fatty acids were a strict requirement for flaviviruses, despite having pro-inflammatory roles in immune cells, and to determine if metabolic changes induced by the virus could be linked to altered immune responses. The specific aims for this thesis are to:

1. Investigate the dependence on fatty acid synthesis during infection in an epithelial vs macrophage cell line
2. Investigate the effect of infection on the metabolic profile of infected cells
3. Determine if the viral manipulation of fatty acid metabolism contributes to the polarisation of macrophages.

Chapter 2
Materials and methods

2.1. Cell Maintenance

Vero cells (monkey kidney epithelial cells) and RAW264.7 cells (mouse immortalised bone marrow macrophages) (ATCC) were maintained in DMEM media (Gibco) supplemented with 10 % foetal calf serum (FCS) (Gibco) and 1 % GlutaMAX (Gibco) and kept at 37 °C. THP-1 cells (ATCC) were maintained in RPMI 1640 media supplemented with 10 % FCS, 1 % GlutaMAX and 1 % sodium pyruvate and kept at 37 °C.

Differentiation and polarisation of THP-1 cells. Prior to experimentation, THP-1 cells were treated with phorbol 12-myristate 13-acetate (PMA) at 50 ng/ml to differentiate them into a macrophage-like state. Cells were seeded in wells and treated for 24 hours, before media was replaced with fresh media not containing PMA, and allowed to rest for another 24 hours. Differentiation was gauged via attachment to the surface of the wells, and non-adherent cells were removed (washed off with media) prior to experimentation. For experiments requiring the polarisation of cells into either an inflammatory (M1) or anti-inflammatory (M2) phenotype, the cells were treated with either LPS (10 ng/mL) and IFN-γ (50 ng/mL) (Australia Biosearch #570202) in combination, or IL-4 (20 ng/mL) (Miltenyi Biotech Australia # 130-093-921), for 24 hours post-differentiation and rest.

Polarisation of RAW264.7 macrophages. For the experiments requiring the polarisation of these macrophages into an inflammatory state, cells were stimulated with LPS (100 ng/mL or 1 ug/mL) and IFN-γ (1 IU/uL) for 24 hours. As there is no effective protocol for M2 polarisation in this cell type, untreated cells were used a proxy-control for this phenotype.

2.2. Virus culture and infection

Virus propagation. The African strain of ZIKV – MR-766 – was kindly provided by VIDRL. WNV_{KUN} MRM61C strain and ZIKV viral stocks were propagated in Vero cells. Confluent T175 flasks were infected (for ZIKV at an MOI of 0.5, for WNV at

an MOI of 0.1), and cells were harvested when flasks had reached approximately 70 % cell death for WNV, and 30 % cell death for ZIKV, which was generally 48-72 hours post infection. Supernatant was collected from these flasks and centrifuged at max speed (11400 g) for 15 minutes on the Allegra X-12R tabletop centrifuge (Beckman Coulter). The supernatant was then harvested and stored at -80 °C, and viral titre was determined via plaque assay.

Plaque assay. $1x10^5$ Vero cells were seeded in 12-well plates and incubated overnight, and only infected if wells reached ~50-60 % confluency. A 10-fold serial dilution was performed using virus stock, or supernatant collected from experiments, using serum-free DMEM. Plates were then incubated for 1.5 or 2 hours for WNV and ZIKV respectively, with plates being rocked every 10 minutes to avoid dehydration of cell monolayer. Following this incubation, virus was removed and 1mL of overlay was added, which contained 1.8 % CMC (50 % v/v), FCS (2.5 % v/v), HEPES (2.5 % v/v), NaHCO3 (1.5 % v/v), GlutaMAX (1 % v/v), sodiumpyruvate (1 % v/v) and 2x DMEM (41.5 % v/v). Plates were then incubated for 4 days at 37 °C, after which they were fixed using 10 % formalin (Sigma) for 1 hour at room temperature. The formalin and overlay were then removed, and cells were stained using 0.5 % crystal violet for 30 minutes. Crystal violet was then removed, and wells were washed x2 with tap water before being left to dry. Plaques were then counted in duplicate, and the following equation was used to calculate viral titre:

$$\text{PFU/mL} = \frac{\text{\# of plaques x dilution factor}}{\text{Volume plated}}$$

Infection of cells. For all experiments in Vero cells, the cells were infected at an MOI of 2 for WNV, and an MOI of 1 for ZIKV. THP-1 cells were infected at an MOI of 0.1 or 5 for both viruses, and RAW264.7 cells were infected at an MOI of 5 for both viruses. Vero cells and RAW264.7 cells were seeded the day before infection, and THP-1 cells were seeded 3 days before infection, to allow for differentiation. Cells were inoculated with serum-free media containing virus and left to infect at 37 °C for 2 hours, rocking plates every 10 minutes, before inoculum

was replaced with media containing 2 % FCS and left to incubate at 37 °C for the duration of infection.

2.3. Antibodies

Secondary antibodies (Alexa-flour 488, 594 or 647) were from Invitrogen and purchased from Life Technologies or Sigma. Details for all primary antibodies used throughout these studies are listed below.

Table 1. Primary antibodies used to target viral and host proteins

Antibody	Clone	Assay used	Source
Rb-Calnexin	Polyclonal	Western blot	Abcam (ab22595)
Rb-Fatty acid synthase	Polyclonal	Western blot, IFA, flow cytometry	Abcam (ab22759)
Ms-dsRNA (J2)	Monoclonal	IFA	Focus Bioscience (Ab01299-2.0)
Ms-dsRNA (IgM)	Monoclonal	IFA	Prof Roy Hall
Rb-NS3	Monoclonal	IFA	Prof A. Khromykh
Ms-E (4g2)	Monoclonal	Western blot	Prof Roy Hall
CD68	Monoclonal	Flow cytometry (THP-1)	Dako (M0718)
CD80	Monoclonal	Flow cytometry (THP-1)	Australian Biosearch (305218)
hMMR/CD206	Monoclonal	Flow cytometry (THP-1)	R&D Systems (685641)
CD86	Monoclonal	Flow cytometry (THP-1)	BD Horizon (563158)
HLA-DQ	Monoclonal	Flow cytometry (THP-1)	BioLegend (318106)

CD80	Monoclonal	Flow cytometry (RAW264.7)	BioLegend (104707)
CD206	Monoclonal	Flow cytometry (RAW264.7)	BioLegend (141704)
CD86	Monoclonal	Flow cytometry (RAW264.7)	BioLegend (105028)
MHC-II	Monoclonal	Flow cytometry (RAW264.7)	BioLegend (107627)

2.4. Harvesting cell lysates and supernatant

For all drug treatment experiments, cells were harvested in 3 different ways: supernatant was collected for a plaque assay, lysates were taken for a western blot, and cells were lysed with TRIzol™ reagent (ThermoFisher) for RT-qPCR. Briefly, cell supernatant was harvested and centrifuged at 400 g for 5 min at 4 °C. Supernatant was transferred to a new tube and stored at -80 °C for a plaque assay. Trypsin was used to collect Vero cells, while cell scrapers were used for THP-1 and RAW264.7 cells. Cells were spun down and washed with PBS twice and then split into two tubes. For one of the tubes, cells were lysed in 60 µl of lysis buffer (1 % Triton X-100 v/v, 50 mM Tris-HCl, pH 7.4, 1 mM EDTA, 150 mM NaCl) with Protease Inhibitor III Cocktail (Astral Scientific). Supernatants were snap frozen at -20 °C and heated to 95 °C for 10 minutes before being used for an assay. For the remainder of the cells, 500 µl of TRIzol™ reagent was added and cells were lysed, for subsequent RT-qPCR.

2.5. Cytotoxic assay

LDH cytotoxic assay. To determine if the FASN inhibitors (c75 and orlistat) were eliciting a cytotoxic effect on the cells, a CytoTox 96® Non-Radioactive Cytotoxicity Assay (Promega) was utilised, as per the manufacturer's protocol. This assay quantitively measures the release of lactase dehydrogenase (LDH) from cells, a cytosolic enzyme released upon cell lysis. Cells were seeded in a 96-well plate either 1 (Vero) or 3 (THP-1) days before the beginning of the assay. Cells were then treated with varying concentrations of each drug, in triplicate.

Concentrations ranged from 10 µm to 200 µm for each drug. Plates were left to incubate with the drugs at 37 °C for a total of 48 hours, as this is the longest period they would be left for during infection. After this time, 3 untreated wells were treated with lysis buffer provided by Promega for 45 minutes, to create a 'total lysis' control. 50 µl aliquots were then transferred from each well to new 96 well plates, in duplicate for each sample. 50 µl of CytoTox 96® Reagent was then added to each well, and then incubated in darkness at room temperature. After this, 50 µl of stop solution was added to each well, and the plates were read with a ClarioStar plate reader at 490 nm absorbance. Results were calculated using the following formula:

$$\text{Percent cytotoxicity} = 100 \times \frac{\text{Experimental LDH Release}}{\text{Maximum LDH Release}}$$

Propidium iodide (PI) cell death assay.

Cells were seeded into Corning® black-walled 96-well plates (#CLS3603) and left to attach overnight. Cells were then either left uninfected, or infected with WNV or ZIKV and treated with varying concentrations of each drug for 24 hours (Vero and RAW264.7 cells) or 3 days (THP-1 cells). Triton-X at 10 % was used as a control for total cell lysis, and propidium iodide was added to each well at a final concentration of 1 µg/mL. A ClarioStar® Plus microplate reader (BMG Labtech) was used to measure the fluorescence of PI at 535 nm over this time, with measurements acquired every 6 minutes. Fluorescent values were graphed using GraphPad Prism 8.

2.6. Transfection of viral non-structural proteins

Vero cells were transfected with constructs containing either WNV_{KUN} NS4A or ZIKV NS4A. Cells were seeded on coverslips in 24-well plates and left to attach overnight. The following day, Lipofectamine 3000 (ThermoFisher) was diluted 1:25 in Opti-MEM™ Medium. 1 µg of plasmid DNA and 2 µL of P3000 reagent were then diluted in 25 µL of Opti-MEM™ Medium. These were left for 2 minutes, during which time the cell culture medium was replaced with fresh medium containing 2 % FCS. The Lipofectamine mixture and the DNA mixture were then

mixed and incubated at room temperature for 10-15 minutes. The mixture was then added drop-wise to the cells, and left to incubate at 37 °C for 24 hours.

2.7. Lipid rescue experiments

To determine if the supplementation of fatty acids could rescue the inhibitory effects of our FASN inhibitors, we exogenously added in different types of fatty acids. 100 µM of palmitic acid (Sigma) or oleic acid (Sigma) were mixed at a 2:1 molar ratio with fatty-acid free BSA (Sigma) in DMEM and warmed to 37 °C. For the palmitic acid mixture, often a white precipitate formed upon addition of powder to media, which could usually be dissolved by vortexing. Fatty acid-BSA mixtures were then added to cells and left for 24 hours.

2.8. Immunofluorescence (IFA)

For immunofluorescence assays, cells were seeded on coverslips in 24-well plates. For THP-1 cells, cells were seeded on coverslips that had been pre-treated with 500 µL of poly-l-lysine for 10 minutes, washed twice with H_2O and then allowed to dry for 1 hour. After the appropriate infection time (24, 36 or 48 hours), cells were fixed in the wells with 4 % paraformaldehyde for 15 minutes. After fixation, cells were permeabilised with 0.1 % Triton-X/PBS and blocked with 0.2 M glycine for 7 minutes at room temperature. Primary antibodies were diluted in PBS and 1 % BSA and added to parafilm, where the coverslips were incubated cell-side down on the antibody mixture for 1 hour at room temperature, away from light. Coverslips were then returned to the wells and rinsed and washed with a 1 % BSA/PBS mixture twice. A secondary antibody mixture was then created as above, and coverslips were inverted again on parafilm and allowed to incubate for 45 minutes at room temperature. After secondary incubation, cells were washed and incubated with Hoechst (Life Technologies) at 1:5000 for 5 minutes to stain nuclei. The coverslips were returned to the wells and either washed with H_2O or PBS (for BODIPY-stained samples) before being mounted onto slides. Slides were then imaged on the ZEISS LSM700 or LSM780 confocal microscope.

Lipid droplet staining for IFA. For experiments involving lipid droplet visualisation, cells were incubated with BODIPY™ 493/503 (Life Technologies), which binds to neutral lipids that accumulate within lipid droplets. This step was performed after

the secondary antibody staining for IFA. A working solution of 1 mg/mL in ethanol was made fresh every ~6 months and stored at 4 °C. This working solution was diluted 1:500, and 500 µL of this was added to each coverslip and incubated at room temperature in the dark for 30 minutes. This solution was removed, and coverslips were washed 2x with PBS before nuclear stain was added. As a control to ensure lipid droplet staining was successful, oleic acid, a mono-unsaturated fatty acid that is a potent inducer of lipid droplet formation, was added to cells at a concentration of 30 µM and left for the duration of the experiment.

Mitotracker staining for IFA. For experiments requiring visualisation of mitochondria, cells were incubated with MitoTracker™ Red CMXRos (Invitrogen) which stains viable mitochondria. This occurred prior to harvesting cells. Supernatant was removed from wells and replaced with 500 µL warm (37 °C) media containing MitoTracker™ Red CMXRos at a dilution of 1:5000, for 30 minutes in a 37 °C incubator.

2.9. Western blotting

Western blots were run on samples to determine the amount of viral and host proteins in our samples. Polyacrylamide gels were cast using TGX™ FastCast™ Acrylamide Kit, 10 % (Biorad #1610173). Gels were loaded into the tanks and covered with tris-glycine running buffer (25 mM Tris, 190 mM glycine and 0.1 % SDS v/v). Sample was loaded into each well and run at 120V for approximately 1 hour 30 minutes, or until the loading dye had run off the gel. After this, the gel was soaked in transfer buffer (25 mM Tris, 190 mM glycine and 40 % methanol v/v) and sandwiched between filter paper and PVDF membrane (BioRad #1620177). The transfer was run for 70 minutes at 100V. The membranes were then transferred to 50ml tubes containing TBS-T and rinsed, before being blocked in 5 % skim milk, diluted in TBS for 2 hours at room temperature. Primary antibodies were then added to the membranes and incubated overnight at 4 °C on a rotator. The next day, the blot was washed 4x with TBS-T before a HRP-conjugated secondary antibody was added at 1:10 000 dilution (in TBS-T), and incubated for 2 hours at room temperature on a rotator. Membranes were then

washed another 4x with TBS-T before chemiluminescence was measured using an Amersham Imager 600 (GE Healthcare).

2.10. RT-qPCR

RNA extraction from cells was performed using RiboZol™ RNA Extraction Reagent (AMRESCO), as per the manufacturer's instructions. After extraction, samples were DNase treated with Promega RQ1 RNase-free DNase, as per the manufacturer's instructions (Promega). SuperScript® III Reverse Transcriptase Kit was then used for cDNA synthesis using the manufacturers protocols (ThermoFisher Scientific Inc), using gene-specific primers for host and target genes.

cDNA templates were analyzed via RT-qPCR, using Platinum SYBR Green qPCR SuperMix-UDG kit (TheromoFisher), according to the manufacturers protocols. Gene-specific forward and reverse primers were used for WNV, and viral accumulation was measured by comparing the relative abundance of this gene to the reference gene Rpl13 The QuantStudio7 Real Time PCR System (ThermoFisher) was used with the following cycle: 50 °C for 2 minutes, 95 °C for 2 minutes, followed by 40 cycles of 95 °C for 10 seconds, 60 °C for 20 seconds and 72 °C for 20 seconds.

Table 2. Primer sequences for RT-qPCR

Primer name	Sequence (5' to 3')
Rpl13A F	CTCAAGGTCGTGCGTCTGAA
Rpl 13A R	CTGTCACTGCCTGGTACTTCCA
FASN F	ACGTACTGGCCTACACCCAGG
FASN R	TGAACTGCTGCACGAAGAAGCATAT
WNV_{KUN} F	TCAAGAATAACTTGGCGATCCA
WNV_{KUN} R	TCACCTAGGACCGCCCTTT
ZIKV F	CTGTGGCATGAACCCAATAG
ZIKV R	ATCCCATAGAGCACCACTCC

2.11. CRISPR

The CRISPR/Cas9 lentiviral system was used to generate FASN knockout THP-1 cells, using a protocol adapted from the Hartland Lab at the University of Melbourne (written by Max Chao Yang).

Guide RNAs (gRNAs) were designed to target different enzymatic domains of FASN, to give us the biggest chance of knocking out the gene. 3 gRNAs were designed per cell line, and the sequences and targets can be seen in Table 1 below. We first cloned these gRNAs individually into a pFgh1tUTG-mCherry doxycycline-inducible lentiviral vector, then generated lentiviral particles in HEK293T cells, and used this virus to infect a THP-1 cell line that stably expressed BFP-Cas9. A cell sorter was used to identify and collect cells that displayed fluorescence of both mCherry and BFP, and knockout validation was performed using both PCR and western blotting methods.

Table 3. CRISPR guide RNAs directed to human fatty acid synthase gene.

	Sequence	**PAM**	**Location**
Vero gRNA 1	GAGTTCTGGGACAACCTCAT	CGG	Ketoacyl-synthase domain
Vero gRNA 2	GGAGGGTGTGTTTGCCAAGG*	AGG	Acyl transferase domain
Vero gRNA 3	TCACGGACATGGAGCACAAC**	AGG	Thioesterase domain
THP-1 gRNA 1	CCTCACCAGGTACGAGCAGC	CGG	5' UTR
THP-1 gRNA 2	GGAGGGTGTGTTTGCCAAGG*	AGG	Acyl transferase domain
THP-1 gRNA 3	TCACGGACATGGAGCACAAC**	AGG	Thioesterase domain

Cloning gRNAs into lentiviral vector. Firstly, primer duplexes were created from the forward and reverse gRNAs. The pFgh1tUTG-mCherry doxycycline-inducible lentiviral vector was then digested using NEB Buffer and BsmBI for 2 hours at 37

°C, and then dephosphorylated. Annealing was then performed using NEB T4 PNK and T4 ligation buffer under the following conditions in a thermocycler: 37 °C for 30 min, then 95 °C for 5 min and then ramped down to 25 °C at 5 °C/min. The ligation reaction was then performed using T4 DNA Ligase and T4 Ligation Buffer, and incubated for 4 °C overnight.

Creating competent cells. A starter bacterial culture was prepared through the inoculation of 3mL of Luria-Bertain (LB) broth with a single colony of DH5α bacteria, which was left to incubate overnight on a shaker (180 rpm) at 37 °C. The following day, the optical density (OD) of the starter culture was measured, and diluted to 0.1 UOD/mL in 50 mL of fresh LB broth. This culture was incubated for a further 2-3 hours on a shaker at 37 °C, until the OD had reached between 0.4 – 0.6 (the exponential growth phase). The bacterial culture was then placed on ice for 5 minutes to stop growth, and then centrifuged at 4 °C for 15 minutes at 3000 rpm. Supernatant was then discarded, and the bacterial pellet was resuspended in 25 mL of $CaCl^2$ and incubated for 30 minutes on ice. Following this, cells were centrifuged at 3000 rpm for 15 minutes at 4 °C, and then supernatant was discarded. The pellet was then resuspended in 2 mL of 0.05 M $CaCl_2$ and glycerol (15 % v/v), aliquoted, and kept on ice for a further 15 minutes. Finally, competent cells were snap frozen using dry ice, and stored at -80 °C.

Transforming competent cells. A standard heat shock method was used to transform our gRNA into the competent cells we made. Our ligated plasmid reactions were mixed with 100 µl of competent cells, and incubated on ice for 30 mins. After this, samples were put in heat block at 42 °C for 2 mins, and then ice for 1 minute. 1 mL of SOC media was then added to each mixture, and the tubes were placed on a shaker at 37 °C for 1 hour. Mixture was then plated using beads onto Luria ampicillin plates and left to incubate overnight at 37 °C. The following day, 5 single colonies from each plate were patched onto a new plate and again left to incubate overnight at 37 °C. The following day, 5 single colonies per gRNA were patched onto a new Luria ampicillin plate, and left to incubate at 37 °C overnight. After this, individual colonies (6 per gRNA) were selected and used to inoculate 10 mL of LB broth supplemented with ampicillin, which was again left

overnight at 37 °C on a shaker. These cultures were then centrifuged, and a Miniprep kit was used to extra and purify plasmids.

Miniprep of colonies. Minipreps were carried out as per the manufacturers protocol (Bioneer AccuPrep® Plasmid Mini Extraction Kit). After the colonies were miniprepped, they were sent away to AGRF for sequencing, to determine if the gRNAs had been inserted into the vector.

Lentiviral particle production. gRNA lentiviral particles were generated in Hek293T cells. Cells were seeded in a 10 cm dish the day before transfection. Lentiviral packages (pMDL, pRSV-REV and pVSV) were then combined with gRNA vector. 25 µl of FuGene was then mixed with 550 µl of OptiMEM media and incubated at room temperature for 5 minutes. Plasmids were then added to this mixture and incubated for a further 25 minutes. Finally, this mixture was added to the Hek293T cells and left for 48 hours at 37 °C. Supernatant/virus was then harvested using a 10 mL syringe, and the media was replaced with fresh media. Supernatant was filtered through a 0.45 µm filter and added to 1.5 mL Eppendorf tubes and stored at -80 °C.

Infection of Cas9-expressing THP-1 cell line with gRNA lentiviral particles. A stably expressing mCherryCas9 THP-1 cell line was obtained from the Villadangos Lab at the University of Melbourne. 1.5 mL of Cas9-THP1 cells (containing about 2 x 10^6 cells) were seeded in 6-well plates. 1.5 mL of virus-containing media was then added to the cells, and plates were spun down at 1800 rpm for 1 hour at room temperature. Cells were then placed in a 37 °C incubator for 24 hours. Media was replaced every 24 hours for the following 3 days before being considered virus-free. Transduction was confirmed using a fluorescent microscope, and cells were then sorted for mCherry fluorescence.

Single cell cloning and validation of knockouts. Knockouts were induced via treatment with doxycycline (1 µg/mL) in media for 3 days, and then sorted based on mCherry-BFP fluorescence. Cells were sorted into individual wells of 96 well plates containing media, at a concentration of ~1 cell per well. In total there was approximately 3 plates for each gRNA (~9 plates in total). Plates were left to

incubate, replenishing media every 4-5 days, and once individual clones reached confluency in the 96-well plate, they were further expanded into 6-well plates and subsequently 25 cm^2 ventilated flasks. Gradual validation began with PCR genotyping, as follows: ~ $2x10^5$ cells were harvested for each clone, spun down at 1800 rpm, and supernatant was removed. Pellet was then resuspended in 30 µl of PBND buffer (50 mM KCl, 10 mM Tris-HCl (pH 8.3), 2.5 mM $MgCl_2$, 0.1 mg/mL gelatin, 0.45 % v/v NP40, 0.45 % v/v Tween 20) containing 200 µg/ml of Proteinase K. Lysates were transferred to a PCR tube and incubated in a thermocycler for 1 hour at 55 °C followed by 10 minutes at 95 °C. PCR was then performed using FASN-specific primers (Table 2), Taq polymerase and dNTPs, with the following cycle: 95 °C for 30 seconds, then 3-35 cycles of 95 °C for 30 seconds, 60 °C for 30 seconds, 72 °C for 60 seconds, terminal extension at 72 °C for 5 minutes, and a hold step at 12 °C. PCR products were then run on a 0.8 % agarose gel. Clones with a promising knockout phenotype were further validating using the anti-FASN antibody via western blot, as described above.

2.12. Flow cytometry

Cells were harvested, either by trypsin (Vero), scraping (THP-1) or washing (RAW264.7), spun down at 500 g for 5 minutes, and resuspended in cold FACS buffer (PBS + 1 % FCS + 2 mM EDTA). Cells were transferred to a 96-well plate where they were incubated with a Fixable Viability Dye (Invitrogen) for 10 minutes on ice to allow for discrimination of live and dead cells. Cells were washed 2x with FACS buffer, and samples being stained for surface markers were incubated with 50 µl of primary antibody (diluted in FACS buffer) for 1 hour in the dark, at 4 °C. Cells were washed 2x again to remove residual antibody, and then fixed with 4 % PFA for 15 minutes on ice, and washed again. For samples requiring intracellular staining, cells were additionally permeablised using 0.5 % Triton-X for 20 minutes on ice. Cells were then incubated with 50 µl primary unconjugated antibody mixture as above. Cells were washed 2x and then stained with the appropriate secondary antibody for 30-45 minutes. After 2 final washes, cells were resuspended in 200 µL of FACS buffer and kept at 4 °C until flow cytometry could be performed. Samples were run and data was collected on a BD LSR Fortessa Cell Analyser and data was analysed using FlowJo analysis software.

Mitotracker and BODIPY staining for flow cytometry. Mitotracker staining for flow cytometry was as above for IFA and was performed prior to cells being harvested. For BODIPY staining, this was also performed as per the IFA section, after both primary and secondary antibody steps, with the volume adjusted to be 50 µl per well in the 96-well plate format but using the same dilution factor.

2.13. Seahorse XF Mito Stress Test

Several parameters of mitochondrial respiration were assayed using the Seahorse XF Cell Mito Stress Test Kit (Agilent Technologies), as per the manufacture's protocols. Briefly, assay medium was prepared two days before infection, using Seahorse XF DMEM base media with 1 mM pyruvate, 2 mM glutamine and 10 mM glucose, and adjusted to a pH of 7.4 and filtered. On the day prior to infection, the Seahorse XF Cell Culture Microplate (96-well) was coated with poly-L-lysine (Sigma) and cells were seeded one day prior to infection in a total of 80 µl per well in regular DMEM + 10 % FCS. An initial optimisation experiment was performed to determine the optimal seeding density, aiming for 90-100 % confluency on the day of the experiment. For Vero cells this was $1x10^4$ and for RAW264.7 cells this was $2.5x10^4$. A titration was also performed to determine the ideal concentration of carbonyl cyanide m-chlorophenyl hydrazone (CCCP) that did not diminish oxygen consumption rate response of cells. Stocks of compounds were also prepared at the concentrations in Table 4. Prior to the day of the assay, cells were infected and sensor cartridge was hydrated overnight at 37 °C in a non-CO_2 incubator. On the day of the assay, the Agilent Seahorse XFe/XF Analyzer was firstly turned on to allow it to warm up to the correct temperature. Working solutions of the compounds were prepared and media was warmed to 37 °C. Media was then removed from the plates, and gently replaced with 180 µl of the Seahorse media per well. Plates were then left to temperature normalise in a non-CO_2 incubator for 1 hour. During this time, compounds were loaded into the appropriate ports of the sensor cartridge (see below). The experiment was set up using Wave software and Mito Stress Test template on the Seahorse XFe/XF Analyzer, and a 30-minute calibration was performed. After this time, the microplate was added to the machine and the Mito Stress Test was

performed. Data was analysed using the Report Generator provided by Agilent, and GraphPad Prism 8.

Table 4. Concentrations of compounds used in the Seahorse XF Cell Mito Stress Test

	Drug	Stock concentration	Final concentration in port	Volume to add to port	Final concentration in well
Port A	Oligomycin	50 mM	20 µM	20 µL	2 µM
Port B	CCCP	20 mM	11 µM	20 µL	1.1 µM
Port C	Antimycin A	20 mM	3.6 µM	20 µL	0.3 µM
	Rotenone	10 mM	6 µM		0.5 µM

2.14. FASN activity assay

This assay was a spectrophotometry-based assay that measures the consumption of NADPH, and was performed as described in Puig et al. (Puig et al, 2009). Briefly, Vero, THP-1 or Huh7.5 cells were seeded and treated with FASN inhibitors (c75 and orlistat) or left untreated for 24 hours. Huh7.5 cells were used as a control as they have a higher expression of FASN, according to ProteinAtlas.org. Cells were harvested using trypsin, centrifuged, washed in cold PBS and finally resuspended in PBS. Particle-free supernatant was then generated via sonication of cells for 30 minutes at 4 °C. Protein content was measured using a Bradford assay, and supernatants were diluted to 1ug/mL. After temperature equilibration, supernatants were incubated with the reaction buffer, following by the FASN substrate malonyl-CoA, to achieve the following final concentrations: 200 mmol/L potassium phosphate buffer (pH 7.0), 1 mmol/L EDTA, 1 mmol/L DTT, 30 µmol/L acetyl-CoA, 0.24 mmol/L NADPH, and 50 µmol/L malonyl-CoA (Puig et al, 2009). Measurements were made using a

spectrophotometer at 340 nm, and basal levels of NADPH oxidation were measured for 3 minutes prior to the addition of malonyl-CoA, and 10 minutes following.

2.15. Bradford assay

For experiments requiring the quantification of protein, a Bradford assay was performed using the Bio-Rad Protein Assay Dye Reagent Concentrate and standard procedures. Briefly, the concentrate was diluted 1:5 with H_2O and filtered. To generate a standard curve, standards of BSA were created at the following concentrations: 0 µg/mL, 50 µg/mL, 165 µg/mL, 275 µg/mL, 386 µg/mL and 500 µg/mL. In duplicates, 10 µL of standard of 10 µL of sample were added to the wells of a 96-well plate. 200 µL of diluted reagent was then added to each well, and incubated at room temperature in the dark for more than 5 minutes, but no longer than 1 hour. Absorbance at 595 nM was then measured using a ClarioStar spectrophotometer, and a standard curve was plotted and used to calculate the unknown protein concentrations.

Chapter 3
Dissecting the lipid requirements of Flaviviruses through chemical inhibition of lipid pathways

3.1. Introduction

Whilst viruses lack the machinery required for lipid synthesis and energy production, they have evolved sophisticated mechanisms to ensure they co-opt these vital pathways from their host. Flaviviruses are known to subvert lipid and metabolic pathways for their replicative cycle, and the remodelling of host cellular membranes to produce replication complexes during Flavivirus infection is known to be integral to viral replicative efficiency as well as immune evasion (Kikkert, 2020; Paul & Bartenschlager, 2015; van den Elsen et al, 2021). The increase in efficiency stems from the concentration of genetic material, and these complexes provide a physical barrier between immunogenic viral replicative material, and host nucleases, proteases and PRRs that can detect and degrade viral matter. As mentioned previously, Flavivirus RCs manifest as 3 continuous structures, VP and CM/PC (Mackenzie et al, 1996b; Westaway et al, 1997), and for WNV these membrane arrangements can begin to be observed at the end of the latent period, approximately 9-10 hours post infection (Ishak et al, 1988; Ng, 1987; Ng & Hong, 1989). This process is intimately tied to lipid synthesis, and our lab and others have contributed much knowledge to the specific requirements needed for viral membrane morphogenesis (Aktepe & Mackenzie, 2018; Heaton et al, 2010; Leier et al, 2018; Liebscher et al, 2018; Martín-Acebes et al, 2011b; Tongluan et al, 2017).

Fatty acids, cholesterol, phospholipids, and sphingolipids are the main classes of lipids that have been identified as contributing to RC formation. As different lipid species can impose differential effects on membrane curvature and fluidity, the correct composition of these lipids is essential for the efficient functioning of these complexes. Ceramide, a sphingolipid, is synthesised in the ER from serine and palmitoyl-CoA and can induce negative membrane curvature due to its conical shape, and is important for WNV replication (Aktepe & Mackenzie, 2018).

Phospholipids, particularly lyso-PChol, can elicit positive membrane curvature and contribute to RC formation for WNV, and it is believed that both ceramide and lyso-PChol are necessary to elicit the curvature required for VP formation from the ER. FAs contribute to membrane fluidity rather than shape; saturated FAs are more rigid and decrease fluidity, whilst unsaturated FAs contain at least one *cis* double bond, resulting in less densely packed phospholipids and increasing fluidity, as well as contributing to membrane thermostability. To proliferate host membranes so dramatically and successfully, viruses likely require the specific regulation of several lipid enzymes. As FAs provide substrates for the synthesis of membranes and complex lipids and have roles in immune function that are relevant for subsequent chapters, we focussed specifically on delineating the role of *de novo* FAS and FAO during infection.

Thus far the *de novo* FAS pathway appears to be a consistent requirement for WNV and DENV infection, with perturbation of FASN attenuating replication of these viruses in several cell types (Heaton et al, 2010; Liebscher et al, 2018; Martín-Acebes et al, 2011a; Tongluan et al, 2017). The role of FASN during ZIKV infection is less clear; one study found no effect of inhibiting FASN with cerulenin (Royle et al, 2017), however as this inhibitor is highly cytotoxic it's possible the concentration used incompletely inhibited this enzyme. Contrarily, a recent paper reported an increase in FASN as well as fatty acid translocase (FAT) expression in placental cells upon ZIKV infection (Chen et al, 2020), and an additional report has observed a role for ACC during ZIKV replication in a mouse model of infection (Jiménez de Oya et al, 2019). A 2020 study additionally observed a decrease in ZIKV replication with orlistat but only under certain treatment conditions (Hitakarun et al, 2020). It is believed that the primary fate of these fatty acids is for the morphogenesis of viral membranes, with FASN inhibition reducing RC complex formation and viral RNA replication. Throughout this study we assessed the role of FAS in WNV and ZIKV replication; our aim was to confirm the requirement for this pathway for WNV in our cell type of interest (Veros), and to expand on the limited knowledge of the role of this pathway during ZIKV infection. We additionally wanted to investigate the fate of these newly synthesised FAs and how they contribute to the viral life cycle, *i.e.* are they being utilised for RC

formation, as substrates for mitochondrial respiration, or driving LD formation and contributing to viral assembly? If *de novo* FAS proves to be a consistent requirement for infection, this could have positive implications for therapeutics targeting these viruses.

Small chemical inhibitors have been used in a diverse range of applications to perturb FAS function *in vitro* and *in vivo*. Some of these drugs are FDA approved and were originally developed to combat diet-induced obesity, and more recently the discovery of FASN as a pro-tumorigenesis gene has led to the development of natural FASN inhibitors that have increased effect on enzymatic activity and minimised off-target effects. Since FASN is upregulated in tumour cells but has a constitutively low expression in most other cell types, its specific targeting can result in the death of tumour cells whilst leaving other cells unaffected (Ventura et al, 2015). It therefore may prove an efficient target for pathogens or inflammatory processes in cells which specifically upregulate or stimulate this enzyme. The *de novo* FAS pathway constitutes several enzymatic domains that catalyse distinct reactions and work in concert to produce the final FA product. The development of inhibitors that target these different domains has resulted in a greater understanding of the contributions of each domain to overall enzymatic activity, as well as their role in the activation of different metabolic pathways.

Throughout this study we utilised four different chemical inhibitors of metabolic pathways; 3 inhibitors of *de novo* FAS (TOFA, c75 and orlistat), and one inhibitor of FAO (etomoxir), which can be visualised in Figure 15. TOFA, or 5-(tetradecyloxy)-2-furoic acid, is a cell-permeable small molecule inhibitor of ACC. Within the cell, TOFA is converted to the ester TOFyl-CoA, which binds to and allosterically inhibits ACC (Halvorson & McCune, 1984; McCune & Harris, 1979). As ACC catalyses the conversion of acetyl-CoA to malonyl-CoA, the primary substrate for the FASN pathway, TOFA treatment effectively inhibits the rate limiting step of FAS. This inhibitor can decrease the accumulation of FFAs intracellularly and completely inhibit *de novo* FAS (Guseva et al, 2011; Harada et al, 2007; Ma et al, 2019). An increase in OXPHOS has also been observed during treatment with TOFA, as this inhibitor reduces cellular malonyl-CoA pools, the

metabolite that regulates CPT-1 (Huang et al, 2016; Otto et al, 1985). Conversely, other groups have observed a decrease in OXPHOS with this inhibitor, an observation which likely results from the sequestering of intracellular CoA (Octave et al, 2020; Otto et al, 1985). TOFA is a potent FAS inhibitor and its effects on FAO have only been observed under certain conditions and likely depend on the concentrations of both TOFA and FAs in the system.

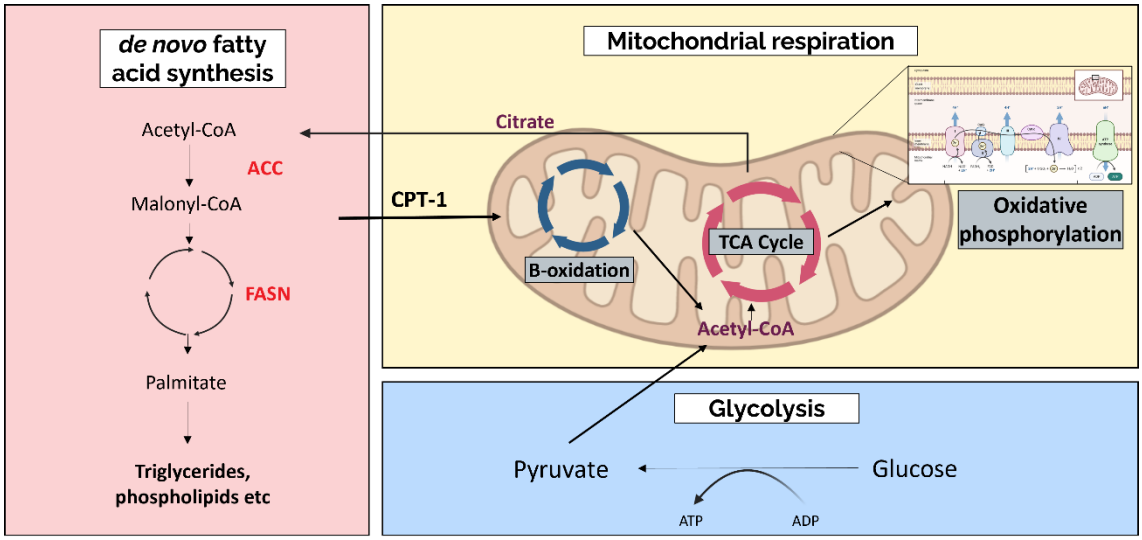

Figure 15. Cellular respiration and the enzymes and inhibitors investigated throughout this study. De novo fatty acid synthesis is the process of converting acetyl-CoA and malonyl-CoA to a long-chain fatty acid, usually palmitate, which can be used to generate more complex lipids. This process is controlled by two enzymes: acetyl-CoA carboxylase (ACC), which converts acetyl-CoA to malonyl-CoA, which are then fed through the fatty acid synthase pathway (FASN) to produce the final fatty acid product. Under excess fatty acid conditions, fatty acids are transported to the mitochondria with the aid of carnitine-palmitoyl transferase 1 (CPT-1), which converts long-chain fatty acyl-CoAs to acyl-carnitines, so they may cross the mitochondrial membrane. Fatty acids are broken down in the mitochondria through the process of β-oxidation, with acetyl-CoA being the metabolic product, which is then fed through the tricarboxylic acid cycle (TCA cycle), which then in turns provides substrates for oxidative phosphorylation. Fatty acids are not the only source of acetyl-CoA for mitochondrial respiration; pyruvate produced from the glycolytic pathway being converted to acetyl-CoA via oxidative decarboxylation. Throughout this study we used TOFA to inhibit ACC, c75 and orlistat to inhibit FASN, and etomoxir to inhibit CPT-1.

C75 (α-methylene-β-butyrolactone) is a small molecule inhibitor of FASN and is a synthetic, stable derivate of cerulenin (Kuhajda et al, 2000). It targets the β-ketoacyl-synthase activity of FASN, which is the second functional domain in this pathway, and effectively blocks the binding of malonyl-CoA to this domain and prevents chain elongation (Kuhajda et al, 1994; Kuhajda et al, 2000). Studies using [U-^{14}C]acetate have shown that treatment with this inhibitor can result in a reduction of phospholipids and triglycerides of up to nearly 90 %, and reduces cellular free fatty acid pools by 44 % (Kuhajda et al, 2000). Although blocking the β-ketoacyl domain can result in the accumulation of malonyl-CoA, c75 has paradoxically been shown to stimulate CPT-1 activity and increase OXPHOS, likely by competing with malonyl-CoA due to their similar structure (Thupari et al, 2002). C75 is one of the most commonly utilised inhibitors of the FASN pathway and has been a useful tool to dissect the role of FASN in tumorigenesis, inflammatory disease and infection of many pathogens (Aliyari et al, 2022; Buckley et al, 2017; Chu et al, 2021; Flavin et al, 2010; Liu et al, 2021; Matsuo et al, 2014).

Orlistat (or tetrahydrolipstatin) is also an inhibitor of the FASN pathway, but targets the catalytic activity of the thioesterase domain (TE), which is the terminal domain of this pathway. The TE domain is in the serine hydrolase family, and hydrolyses the thioester bond between the growing fatty acyl chain and the phosphopantetheine of the ACP carrier molecule. This domain therefore regulates the chain length of the final FA product, but has specificity for chain lengths of 16-18 carbons (Lin & Smith, 1978; Mattick et al, 1983; Pazirandeh et al, 1989). One study has demonstrated that this inhibitor can reduce cellular FAS by up to 75 % within 30 minutes of treatment and reduces overall lipid accumulation (Kridel et al, 2004), and in cancer cells treatment can result in ER stress and apoptosis as well as inhibit growth (Dowling et al, 2009; Little et al, 2007). Orlistat is an FDA approved drug for the treatment of obesity, due to its function as a pancreatic and gastric lipase inhibitor, and its ability to inhibit FASN was a secondary novel discovery. This drug has poor systemic bioavailability and is almost exclusively metabolised in the gastrointestinal wall (Padwal &

Majumdar, 2007), however can penetrate membranes efficiently and have intracellular affects (Ko & Small, 1997).

Lastly, we utilised the CPT-1 inhibitor etomoxir to assess the role of FAO in the replication of our viruses. As mentioned previously, CPT-1 is a mitochondrial enzyme that converts long-chain fatty acyl-CoAs to acyl-carnitines, a process that is required to transport FAs across the mitochondrial membrane to participate in β-oxidation. Etomoxir is a small molecule inhibitor that was developed for the treatment of metabolic and cardiovascular diseases and has been used experimentally to inhibit FAO by up to 90 % and reduce OXPHOS (Yao et al, 2018). High concentrations of this inhibitor (≥200 μM), however, can have off-target effects including inhibition of mitochondria complex 1, and depletion of intracellular free CoA levels (Divakaruni et al, 2018).

In this study we aimed to utilise these inhibitors to ascertain the role of FA pathways in WNV and ZIKV infection, and to determine if FA utilisation by these viruses correlated to changes in mitochondrial metabolism. Overall, we saw a dependence of both viruses on *de novo* FAS, which was required for efficient RC formation, but the subversion of this pathway did not alter mitochondrial respiration or glycolysis. Further, we did not observe any effect of infection on LD formation, suggesting that *de novo* FAs are not contributing to the formation of these organelles in this cell type, and are likely being directly incorporated into growing membranes. We additionally made some unexpected observations with orlistat, including lipid accumulation and mitochondrial fragmentation, which have provided us insight into the specificity of FA utilisation by these viruses.

3.2. Results

3.2.1. FASN is not upregulated during infection and is not sequestered to viral replication complexes

As FASN has shown to be indispensable for the replication of many viruses, we first sought to determine the localisation and expression of FASN during infection with WNV and ZIKV in Vero cells. We performed immunofluorescence and stained for FASN, dsRNA as our viral marker, and Hoechst as a nuclear marker.

As FASN is a cytoplasmic enzyme, within uninfected cells we observed an even, diffuse staining throughout the cytoplasm (Figure 16a). Upon infection with WNV and ZIKV, we saw a high proportion of cells become infected as indicated by dsRNA staining, and although we do not see the expression of FASN altered (either by quantified fluorescent signal from IFA images or via flow cytometry) (Figures 16a and b), we observed a degree of co-localisation between dsRNA and FASN as indicated by orange hues. This was particularly obvious for WNV, with dsRNA staining revealing distinct perinuclear puncta (see arrows in Figure 16g), with FASN being present at these sites. As dsRNA is localised exclusively to viral replication complexes (specifically VPs), we could extrapolate that FASN is co-localising with the replication complexes of WNV and ZIKV. This co-localisation was not significant, however, with a Pearson's coefficient below 0.5 for both viruses. As the distribution of FASN was not noticeably altered during infection, it is difficult to ascertain from this result whether the virus is actively sequestering FASN to RCs as has been observed for DENV (Heaton et al, 2010), or if this co-localisation is passive and a result of the ubiquitous nature of this protein. The fluorescent intensity values of the images in Figure 15a and flow cytometry data from infected cells were used to deduce the impact of infection on the expression levels of FASN (Figures 16b and c). We observed that neither virus induced significant changes in FASN expression, however this data does not rule out the possibility that the activity of this enzyme is being stimulated by the virus. We made several attempts to assess the activity of a FASN enzyme, using a common assay derived from the literature (Puig et al, 2009), but unfortunately were not able to establish this assay.

In addition to infected cells, we also transfected cells with constructs encoding for WNV or ZIKV NS4A-GFP and stained for FASN to investigate a potential relationship between NS4A and FASN. We chose NS4A as this protein, when expressed individually, can induce alterations to membranes that are contiguous with CM/PC structures observed during infection (Mikulasova et al, 2021; Roosendaal et al, 2006a). We aimed to investigate if the overexpression of this protein resulted in the alteration of FASN distribution, and to determine if there was co-localisation between the two proteins. In mock-transfected cells (Figures

17a-d) we again saw a diffuse, cytoplasmic staining for FASN. In transfected cells, we observed significant co-localisation between FASN and WNV-NS4A and ZIKV-NS4A, as indicated by yellow-orange hues in the merged panels (Figures 17e-l; Pearson's coefficient = 0.608 for WNV and 0.694 for ZIKV). WNV-NS4A additionally appears to change the distribution of FASN; as FASN is not uniformly spread throughout the cells as is the case in the adjacent untransfected cells, and more closely resembles the staining pattern of NS4A. NS4A and FASN both localise to very distinct, donut-shaped perinuclear puncta which is the well-described morphology of WNV replication complexes. Taken together, this data suggests a relationship between FASN and the replication complexes of WNV and ZIKV, but further protein-protein interaction studies are needed to confirm whether this is completely facilitated via the viral NS4A protein. Our data is so far consistent with the hypothesis that these viruses require FASN to provide fatty acid substrates for membrane morphogenesis, a process which may be facilitated by the viral NS4A protein.

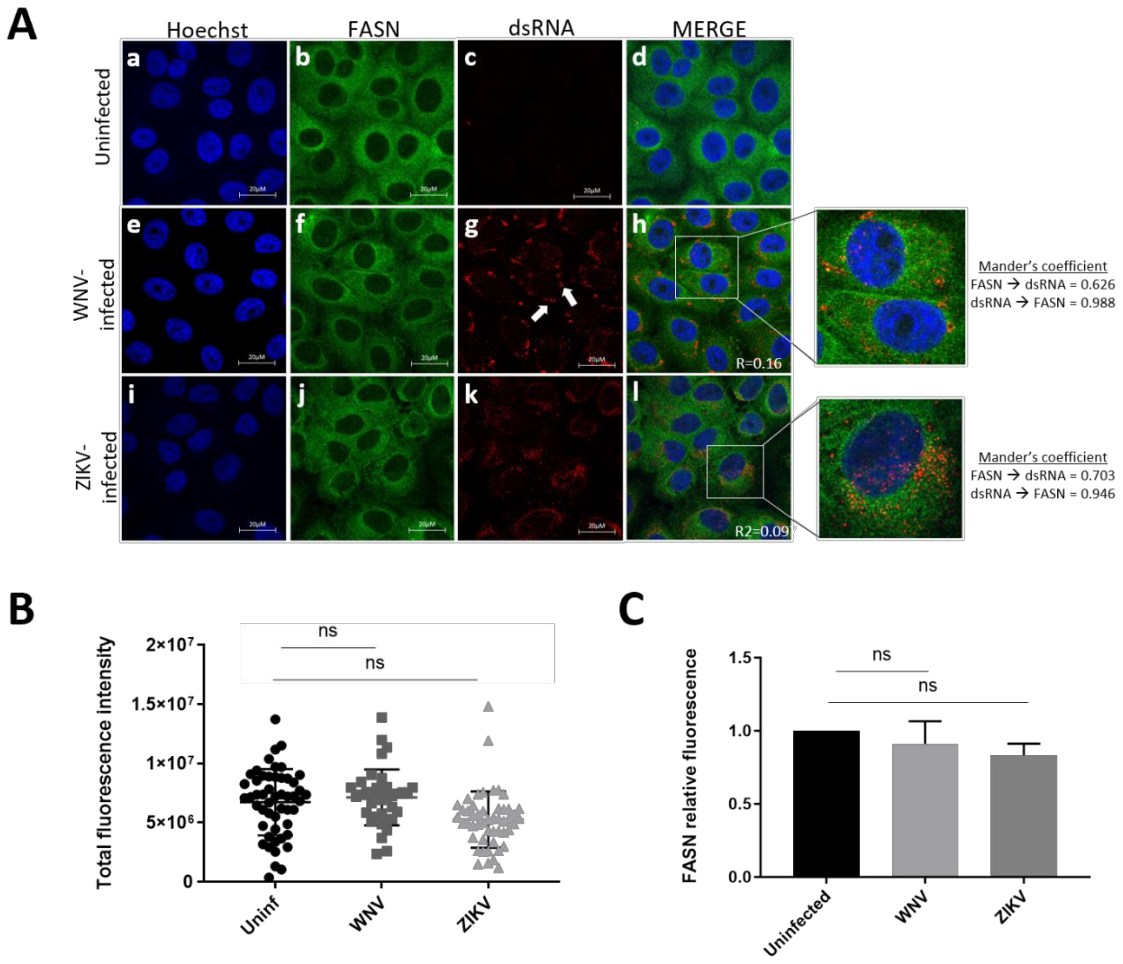

Figure 16. Expression of fatty acid synthase is not altered during infection, but the protein co-localises with viral replication complexes. Vero cells were infected with either WNV or ZIKV for 24 hours and **(A)** fixed and analysed via immunofluorescence, staining for Hoechst (blue), FASN (green) or dsRNA (red), with orange-yellow hues indicating co-localisation, which was measured using both Mander's co-efficient and JaCOP plugin software on ImageJ. **(B)** Immunofluorescence images were used to calculate total fluorescent intensity was calculated from 55 uninfected, 39 WNV-infected and 50 ZIKV-infected cells, using a macro and ImageJ. **(C)** Cells were also stained with an anti-FASN antibody and analysed via flow cytometry, with error bars indicative of 3 biological replicates (n=3, +/- SEM) and a paired t-test was used to determine significance (GraphPad Prism 8).

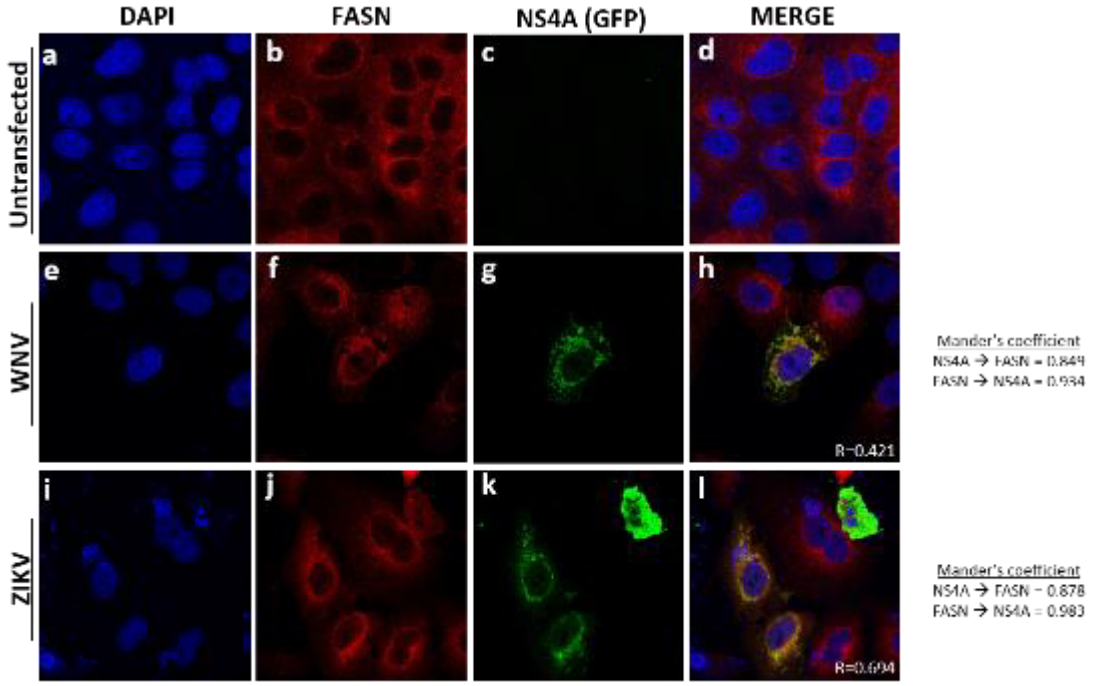

Figure 17. Transfection of Veros cells with plasmids containing Flavivirus non-structural proteins reveals that NS4A co-localises with FASN. Cells were either mock-transfected (panels a-d) or transfected with cDNA plasmids that encoded for WNV NS4A-GFP (panels e-h) or ZIKV NS4A-GFP (panels i-l) for 24 hours, before being fixed and labelled with DAPI (blue) or FASN (red). The merged images are provided and co-localisation is visible as orange-yellow hues, Mander's coefficient and the JaCOP plugin software on ImageJ was used to calculate the degree of co-localisation.

3.2.2. Inhibiting fatty acid synthesis pathways perturbs viral replication

To confirm that fatty acid synthesis is required for replication of WNV and ZIKV, we utilised several small chemical inhibitors of this pathway. We treated cells for 24 hours (post infection) with TOFA to inhibit ACC, which is the rate-limiting step of fatty acid synthesis, is upstream from FASN activity and completely inhibits this pathway. We also treated cells for the same period with two inhibitors of the FASN pathway, c75 and orlistat, which both inhibit distinct partial catalytic activities of this enzymatic complex (see Figure 9). In addition, we also blocked fatty acid transport to the mitochondria through treatment with etomoxir, which blocks CPT-1, to allow us insight into the fate of the fatty acids produced via the FASN pathway. All compounds were used at concentrations that were non-toxic to cells

as assessed by the Cytotox 96 assay or propidium iodide uptake assay (see Appendix A).

When we inhibited the rate-limiting step of fatty acid synthesis with TOFA, we saw a complete ablation of viral replication; we were unable to detect any viral protein expression via western blot (Figure 18a) and did not detect any infectious virus in the supernatant via plaque assays (Figure 18b) for either virus. This suggests that FAS is important for early replicative stages of infection. When we inhibited the ketoacyl synthase domain of FASN with c75, we observed about a 40 % reduction in WNV NS1, and about a 65 % reduction in ZIKV NS1 (Figure 18a). Surprisingly we saw no significant effect of c75 on viral titre for WNV, but a significant reduction was observed for ZIKV (Figure 18b). Interestingly, we saw an even greater reduction in viral replication with orlistat compared to c75, despite this drug inhibiting a catalytic domain downstream of c75. For WNV, we observed about a 70 % reduction in NS1 expression but again no effect on viral titre. Orlistat had an even greater impact on ZIKV replication, with an observed reduction in expression of >98 % for NS1, and an approximate 1 log drop in viral titre which correlates to a 90 % reduction (Figures 18a and b).

Finally, when we inhibited CPT-1 using etomoxir, we saw no significant impact on viral protein expression, but observed a significant drop in infectious virus production (>50 % for both viruses) (Figures 18a and b). This suggests that FAO is not required for replicative processes but may play a role in viral assembly and egress. Overall, this data suggests that fatty acid synthesis is indispensable for replication of WNV and ZIKV, and that ZIKV appears to have a greater reliance on these pathways. Additionally, the orlistat data suggests that infection might rely on the particular catalytic activity of the TE, which is inhibited by orlistat.

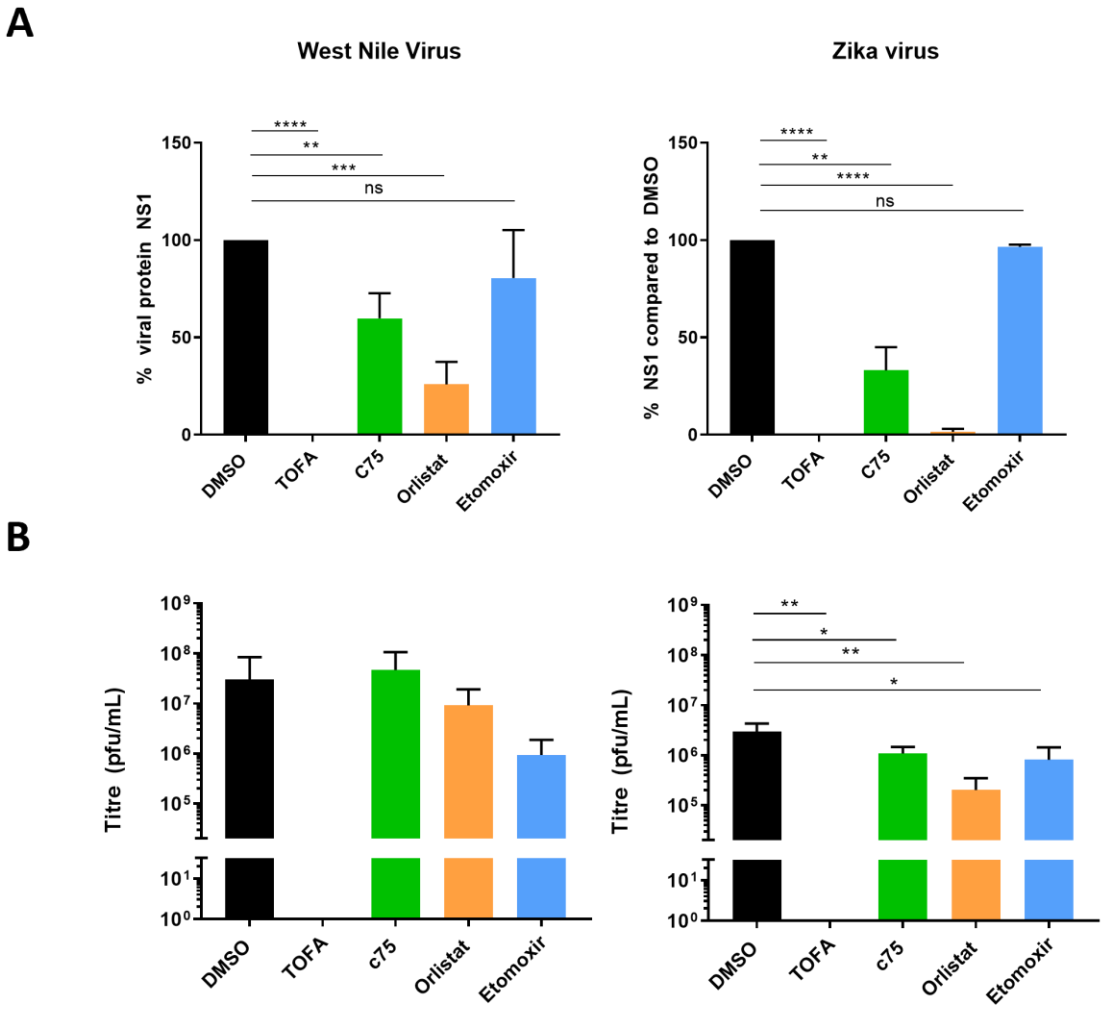

Figure 18. Inhibition of fatty acid synthesis, but not oxidation, significantly perturbs viral replication. Vero cells were infected with WNV or ZIKV and treated with inhibitors for 24 hours before lysates and supernatant were collected for each sample. Inhibitors were used as the following concentrations: TOFA = 50 μM, c75 = 30 μM, orlistat = 100 μM, etomoxir = 100 μM. **(A)** Expression of viral NS1 was assessed by western blotting using antibodies against Flavivirus NS1 and host ER marker calnexin, and relative expression for NS1 was quantified via densitometry from 4 independent replicates (n=4, error bars +/- SEM). **(B)** Supernatants from the cell culture were analysed via plaque assay to determine levels of virion secretion, calculated as pfu/mL and normalised to the DMSO vehicle control. Error bars are representative of 4 biological replicates (n=4, +/- SEM) and asterisk (*) indicate a significant change compared to the DMSO vehicle control as determined by paired t-test (GraphPad Prism 8). * = $p \leq 0.05$, ** = $p \leq 0.005$, *** = $p \leq 0.0005$, **** = $p < 0.0001$.

3.2.3. Inhibiting FASN disrupts replication complex formation

To determine if the inhibition of FAS affected the ability of WNV and ZIKV to construct RCs, we performed immunofluorescence, by staining with dsRNA to visualise viral RCs and treating the infected cells with our inhibitors. As seen previously, WNV resulted in a high proportion of infected cells (>80 %) and induced the formation of distinct, spherical, organelle-like structures, which are representative of RCs (Figure 19) (Gillespie et al, 2010; Mackenzie et al, 1996b; Welsch et al, 2009). When treated with FASN inhibitor c75, and to a greater extent with orlistat, we see a reduction in the number of infected cells and the dispersion of these tight perinuclear RCs. For ZIKV, we do not observe the same distinct structures during infection, however treatment with c75 and orlistat greatly reduced dsRNA staining. Overall, this suggests that FAS is required for the construction of viral RCs, most likely by directly providing FA substrates that the viruses utilise for membrane morphogenesis.

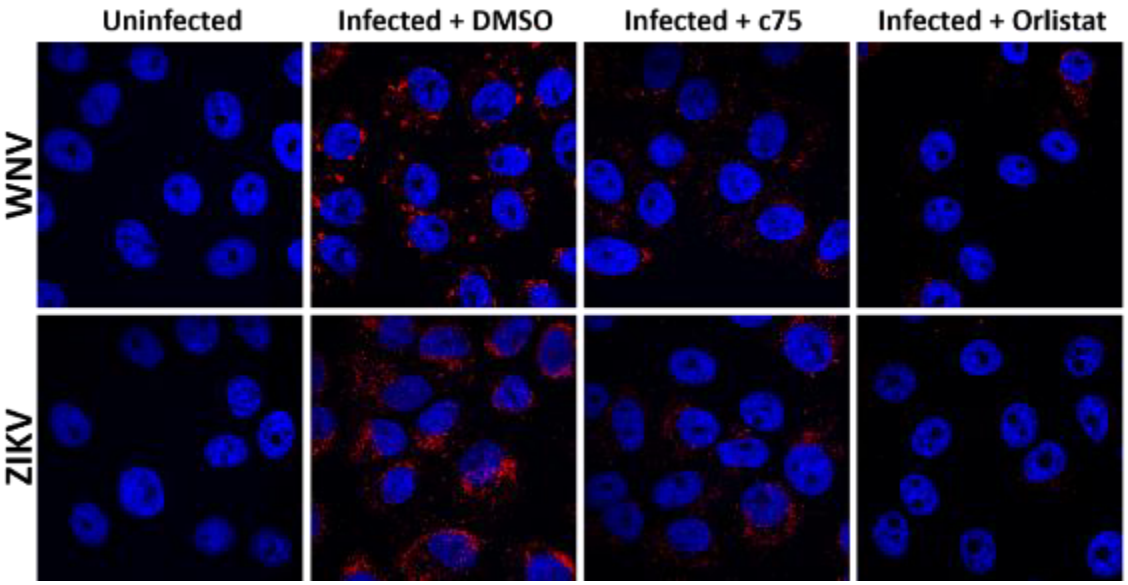

Figure 19. Treatment of Flavivirus infected Vero cells with FASN inhibitors disrupts replication complex formation. Vero cells were infected with WNV (MOI 2) and ZIKV (MOI 1) for 24 hours in the presence of FASN inhibitors c75 (30 μM) and orlistat (100 μM), and DMSO was used as a vehicle control. Cells were fixed with PFA and immunolabelled with an anti-dsRNA antibody to visualise replication complexes. Cells were counterstained with DAPI to visualise nuclei,

and imaged on a Zeiss confocal microscope, and Zen Blue software was used to analyse and enhance fluorescence.

3.2.4. Infection does not dramatically alter cellular respiration

Many viruses, including DENV, have been demonstrated to induce changes in cellular metabolic pathways to benefit their own replication. Whilst our data with etomoxir suggested that FAO is not important for viral replicative processes, fatty acids are not the only substrate for mitochondrial respiration. Therefore, we further probed the metabolic profile of infected cells using a Seahorse XF Analyser and Seahorse XF Mito Stress Test kit. This is a widely accepted method of assaying mitochondrial respiration and allowed us the ability to measure several parameters of mitochondrial function at once (See Figure 20a). The Mito Stress Test measures both oxygen consumption rates (OCR, expressed as pmol/min), which is indicative of mitochondrial respiration, and extracellular acidification rate (ECAR, expressed as pmol/min), which measures proton flux and is generally indicative of glycolysis, although CO_2 production can also contribute to this measurement. The system has in-built drug ports that allow the injection of different inhibitors at specific time points, which artificially alter the metabolic capabilities of the cells and allow us to measure different parameters. Before the injection of any drugs, basal OCR and ECAR were first measured, giving us insight into the energetic demands of the cells under normal conditions. Oligomycin was the first inhibitor injected and inhibits ATP synthase. This completely inhibits ATP production and allows us to infer how much ATP the cells were producing. FCCP was the second inhibitor that was injected and is an uncoupler that completely collapses the proton gradient. This allows uninhibited movement of electrons through the ETC and is indicative of the highest possible rate of respiration the cell is capable of (maximal respiration). The last injection involves two simultaneously injected inhibitors, rotenone, which is a complex I inhibitor and antimycin A, which is a complex III inhibitor (see Figure 13). This completely shuts down oxidative phosphorylation and allows us to calculate spare respiratory capacity (SRC), which is reflective of the ability of cells to

respond to increased energy demand resulting from stress, as well as non-mitochondrial oxygen consumption.

We seeded and infected cells directly on the Seahorse XF 96 microplate, and measured OCR and ECAR after 24 hours of infection. We used Wave software and the Seahorse XF Cell Mito Stress Test Report Generator to gain a comprehensive understanding of the effect of infection on several parameters of mitochondrial respiration. Overall, we saw no significant effect of infection on cellular respiration (see Figures 20b and c). Infection did not alter basal or maximal respiration, and had no significant effect on SRC, indicating that infection did not reduce the metabolic fitness of cells. Additionally, neither WNV nor ZIKV significantly altered rates of extracellular acidification, suggesting glycolytic rates remained stable (Figure 20b). Overall, this data indicates that WNV and ZIKV do not perturb metabolic homeostasis during infection in this cell type. Although these viruses rely on the synthesis of FAs for replication, it does not appear that they are relying on *de novo* FAS to boost mitochondrial respiration, which is consistent with what we observed during treatment with etomoxir.

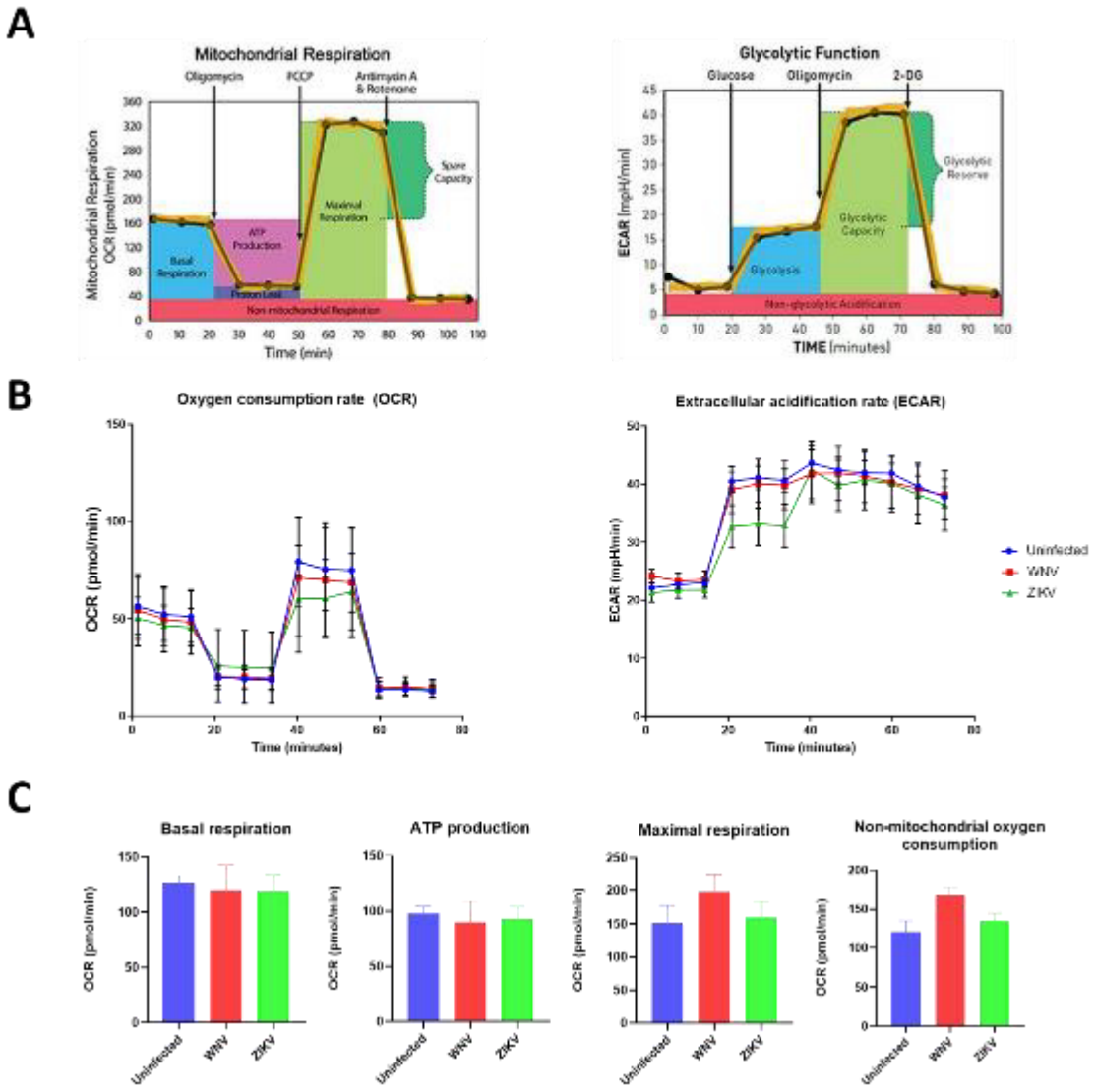

Figure 20. OCR and ECAR rates are not significantly impacted during Flavivirus infection of Vero cells. Vero cells were seeded onto Seahorse XF96 Cell Culture Microplate and infected for 24 hours with WNV (MOI 2) and ZIKV (MOI 1), before rates of OCR and ECAR were measured using the Seahorse XF Mito Stress Test Kit. **(A)** Schematic of the inhibitors used and parameters measured using the Mito Stress Test Kit. **(B)** OCR and ECAR rates of infected cells. The compounds were injected at the time points indicated in **(A)** and each data point is the mean of 3 technical replicates of 2 independent biological replicates (n=2) with error bars indicating S.D. **(C)** Bar graph representation of each of the parameters, using data extracted from **(B)** and analysed using the Seahorse XF Cell Mito Stress Test Report Generator and Prism. Statistical significance was determined using an ordinary one-way ANOVA (GraphPad Prism 8).

3.2.5. Lipid droplets are not induced during infection

As lipid droplets function primarily as storage molecules for fatty acids and other lipids, we hypothesised that inhibiting FAS may result in the depletion of these molecules, reducing the pool of fatty acids available to the virus and potentially interfering with other processes such as viral assembly. As there exists conflicting evidence about the roles of lipid droplets in Flavivirus infection, we also wanted to ascertain the utilisation of these organelles during infection in our vero cell model. We performed an infection timecourse, staining for lipid droplets at 2, 6, and 24 hours post infection, and stained cells with antibodies to the viral E protein and a neutral lipid stain called BODIPY, and visualised lipid droplet accumulation via immunofluorescence and flow cytometry. Although the induction of lipid droplets early in infection has been reported for DENV and ZIKV (Monson et al, 2021a), we did not observe the same phenomena with WNV and ZIKV in Vero cells at any of the timepoints examined (Figures 21a and b).

Additionally, we generally observed very low lipid droplet content within this cell type. Due to the transient nature of LDs, we observed a degree of variation in LD content over the replicates, however overall, we observed infection was possible in the absence of LDs, suggesting that LD presence and content is not an essential factor for replication in vero cells. To ensure that this observation was not related to issues with the BODIPY staining process, we included an oleic acid control; oleic acid is a potent inducer of LD formation (Eynaudi et al, 2021; Nakajima et al, 2019; Rohwedder et al, 2014), and when cells were treated with 100 µM of this fatty acid, we observed a very distinct rise in LD content as early as 2 hours post treatment. After 24 hours of treatment, every cell on the coverslip was displaying a very high lipid load, confirming the efficacy of BODIPY as an LD stain, and the propensity for this cell type to form LDs. We additionally performed immunofluorescence with our FAS inhibitors, however as we saw minimal LD content, and minimal impacts of our inhibitors in this regard. This suggests to us the FAs being produced by the FASN pathway during infection are most likely being immediately incorporated into growing RCs, without the need for an intermediate storage step, and suggests they may not be essential for viral assembly. This lipid droplet data, in combination with our Seahorse oxygen

consumption rate data, suggest that the metabolism of LDs is dispensable for replication.

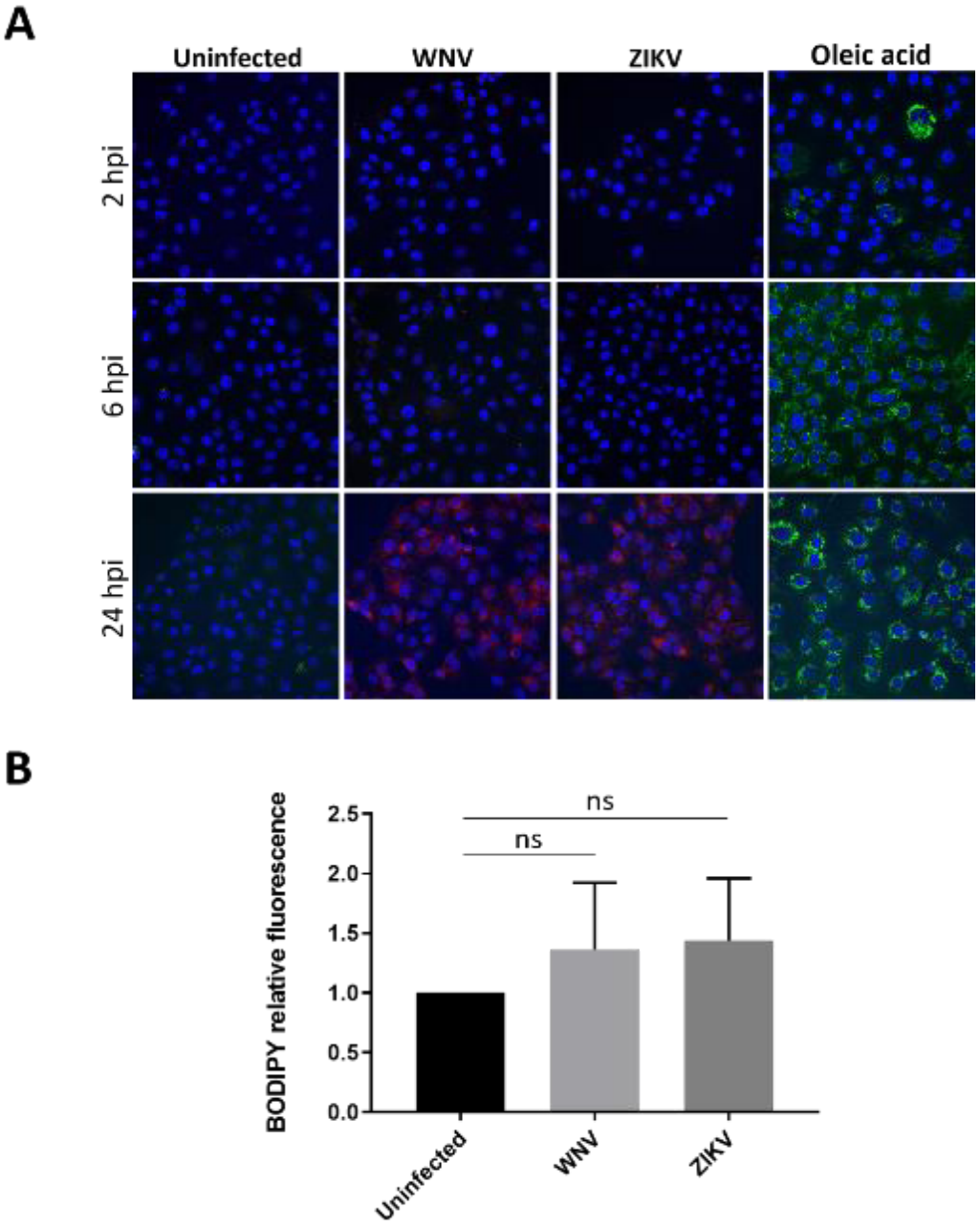

Figure 21. Lipid droplets are not induced during infection with WNV and ZIKV. (A) Vero cells were seeded onto coverslips and infected with WNV and ZIKV, left uninfected, or left uninfected and treated with 100 μM of oleic acid, before being fixed at either 2, 6, 12 or 24 hours post infection (h.p.i). Samples were stained with BODIPY to visualise lipid droplets (green), antibodies to the

viral envelope protein (red) and DAPI (blue). Images were taken on a Zeiss confocal microscope at 20x magnification, and Zen Blue software was used for analysis. **(B)** Cells were infected for 24 hours or left uninfected, stained with an anti-NS1 antibody to determine infected cells, and BODIPY to measure lipid droplet content, and analysed via flow cytometry using a BD LSR Fortessa Cell Analyser. Cells were analyse using FlowJo software, and gated for infection and relative values were calculated using the mean fluorescent intensity values, and normalised to uninfected cells. Error bars are indicative of the S.E.M. of 3 biological replicates (n=3), and significance was determined using a paired t-test (GraphPad Prism 8).

3.2.6. Lipid droplets are induced during treatment with orlistat, but not c75

Despite observing low levels of LD content in our Vero cell model, we unexpectedly observed a drastic and consistent accumulation of LDs during orlistat treatment via immunofluorescence. We again stained with antibodies against dsRNA and used BODIPY to visualise LDs, and observed an accumulation of LDs in both infected (Figure 22 f and i) and uninfected cells (Figure 22 c) treated with orlistat. These figures represent images taken at 24 hours post infection with orlistat treatment, and is representative of 4 biological replicates (n=4). As c75 and orlistat both inhibit FASN, c75 acts as a control to demonstrate that this increase in LD content was not a general consequence of FASN inhibition. Indeed, we expected to see a decrease in LD content with these inhibitors as we are blocking *de novo* FAS. Although early biochemical research indicated the specificity of orlistat's lipase inhibition for pancreatic and gastric lipases (Borgström, 1988; Hadváry et al, 1988; Hadváry et al, 1991), recent reports have revealed orlistat's propensity to inhibit many cellular lipases, and it has since been referred to as a 'pan-lipase inhibitor' (Clifford et al, 2000; Kumar & Bhandari, 2015; Rajan et al, 2021; Smith et al, 1996; Yasser et al, 2010). Although it has shown no specificity to PLA2, a lipase that breaks down phospholipids, a recent report has demonstrated its ability to inhibit adipose triacylglycerol lipase (ATGL) with high potency (Iglesias et al, 2016). ATGL is required for LD hydrolysis, so treatment with orlistat likely renders these cells incapable of breaking down these organelles.

Our LD data in both uninfected and infected cells indicates that under our experimental conditions, Vero cells harbour low levels of stored FAs. This, combined with the fact that we observe such potent LD accumulation in orlistat-treated cells but not under any other condition, suggests that FAs are still being synthesised during orlistat treatment. Overall, this unexpected result suggests that orlistat's antiviral capabilities may be partially attributed to its lipase activity, as these viruses are likely unable to access stored FAs, but further indicates that inhibiting the TE domain of FASN may not comprehensively inhibit *de novo* FAS.

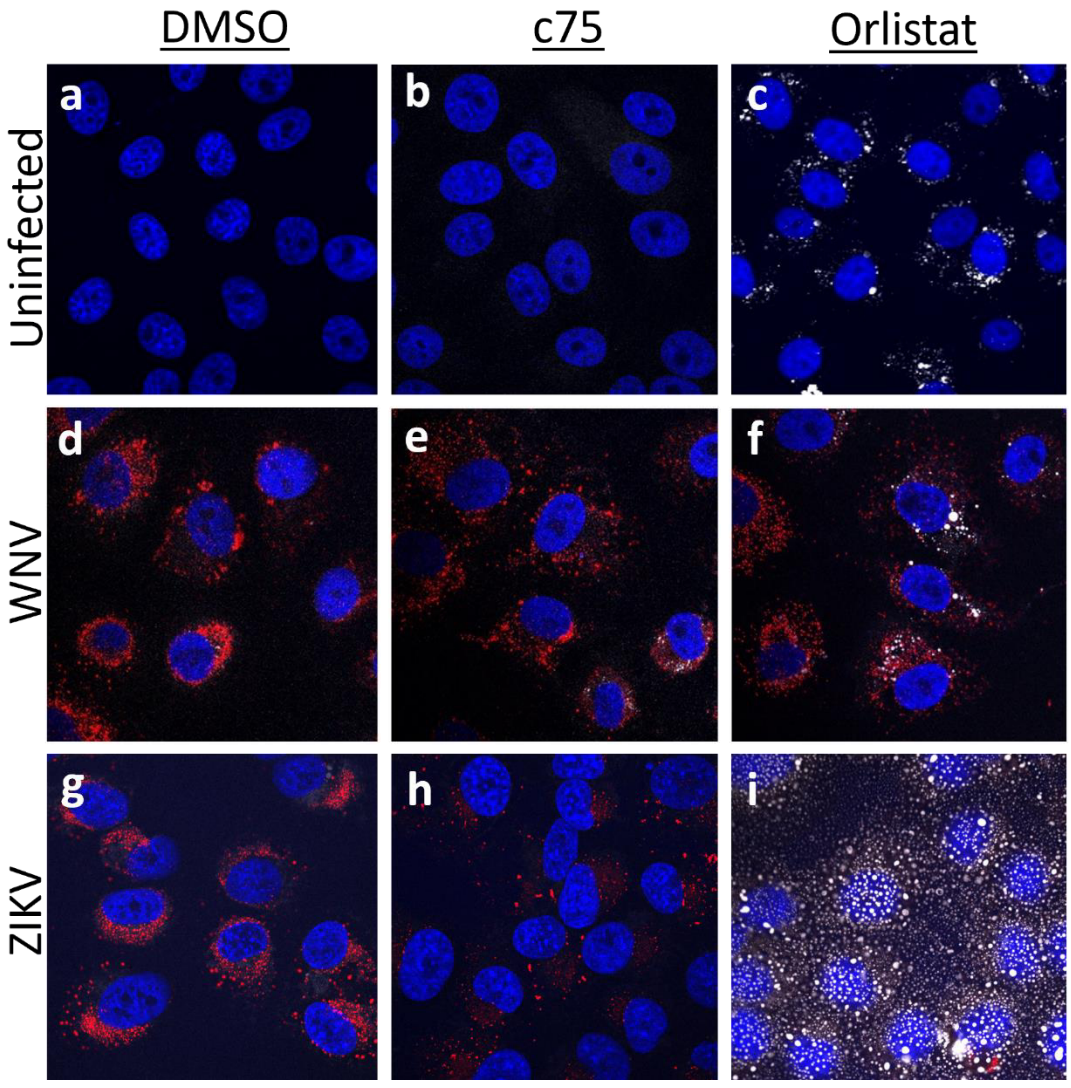

Figure 22. Lipid droplets are induced and accumulate in WNV infected cells in response to treatment with orlistat. Cells were seeded and infected on

coverslips (MOI 2), and treated with fatty acid synthase inhibitors c75 (30 μM) and orlistat (100 μM) for 24 hours. DMSO was used a vehicle control for infected cells, and after 24 hours cells were fixed with PFA and immunolabelled with antibodies specific for dsRNA (red), BODIPY (grey) or nuclei were counterstained using DAPI (blue). Images were taken on a Zeiss confocal microscope and analysed using Zen Blue software. These images are representative of a minimum of 4 biological replicates (n=4) where induction of lipid droplet formation with orlistat was observed.

3.2.7. Orlistat induces mitochondrial fragmentation and dysregulates metabolism in Vero cells

Our LD results suggested that orlistat may be disrupting lipid homeostasis within cells which could be related to its antiviral mechanism. To explore this further, we investigated other pathways that may be affected by FAS dysregulation or LD accumulation. As orlistat is likely preventing the breakdown of intracellular FAs, we postulated that this drug may be impacting mitochondrial respiration. Additionally, some studies have shown that accumulation of certain species of FAs(primarily palmitate and other saturated FAs) can induce mitochondrial fragmentation and dysfunction (Borradaile et al, 2006; Eynaudi et al, 2021; Penzo et al, 2002; Sergi et al, 2021). To assess if orlistat treatment resulted in any mitochondrial changes or defects, we performed immunofluorescence using a mitochondrial stain to visualise morphology, and Seahorse to quantify mitochondrial respiration. For IFA, we utilised a stain called MitoTracker™ Red CMXRos, which is dependent on mitochondrial membrane potential and accumulates within mitochondria with intact membranes. In cells treated with orlistat, and either uninfected or infected with WNV (see Figure 23) or ZIKV (data not shown), we observed significant induction of mitochondrial fragmentation. In uninfected and untreated cells, we observe a heterogenous population of mitochondria, but generally they existed as elongated, tubular, reticular structures, which are indicative of normal mitochondrial respiration. When we infected cells, with either WNV or ZIKV, we observed no distinguishable changes in morphology, which supports our previous Seahorse findings that infection does not significantly alter rates of mitochondrial oxygen consumption (see Figure 20). However, treatment with orlistat induced a complete shift in mitochondrial

morphology, with essentially every cell displaying small, individual, spherical puncta instead of elongated networks (Figures 23c and d).

Fragmented mitochondria to this extent are generally indicative of dysfunction, and our Seahorse assay confirmed that this morphology was correlated to a huge reduction in OCR in both uninfected (see Figure 24) as well as infected cells (Figures 25 and 26). Inhibition of ATP synthase using oligomycin yielded no decrease in OCR, suggesting that orlistat was completely inhibiting ATP production from this pathway. We included c75 again as a control for FASN inhibition and did not observe a significant reduction in OCR or ECAR. This suggests that the dysfunction seen with orlistat is not simply a consequence of FASN inhibition but is specific to orlistat treatment. Orlistat interfered with every parameter of mitochondrial respiration measured, including significantly increasing proton leak and decreasing coupling efficiency. As an increase in proton leak is generally indicative of damaged mitochondria, we believe orlistat is inducing mitochondrial damage, however the mechanism by which it does this is unknown. In addition to significantly perturbing oxygen consumption rates, orlistat also drastically reduced ECAR compared to both untreated and c75-treated cells, suggesting that this inhibitor also interferes with rates of glycolysis. Overall, it appears that orlistat is generally inhibiting cellular respiration and inducing a metabolically quiescent state in these cells, which may not be conducive to viral replication.

As orlistat appeared to be preventing the break down and subsequent oxidation of FAs, we could postulate that the reduction in OCR we observe is attributed to this. However, treatment of cells with our FAO inhibitor etomoxir did not yield this same reduction in OCR, suggesting that these cells are not relying on the oxidation of FAs to fuel mitochondrial respiration. This is supported by our LD data showing low basal levels of LDs, which does not increase upon infection. We instead hypothesise that the induction of mitochondrial fragmentation by orlistat may instead be a result of the accumulation of FAs within these cells.

It is a well-documented phenomena that excess free FAs can result in cellular stress and cause apoptosis, and our results are consistent with orlistat inducing

lipotoxicity. During our experiments we consistently observed a level of cell detachment during orlistat treatment, so we wanted to rule out the possibility of orlistat inducing apoptosis. If orlistat was killing infected cells, then the reduction in viral replication could be partly attributed to this. We performed a cytotoxicity assay using propidium iodide (PI), which can enter and accumulate within cells with compromised membranes, and measured PI fluorescence using a spectrophotometer. Readings were taken over a 24-hour period, and our results revealed that orlistat did not induce cell death in uninfected or infected cells (Figure 27), despite potentially inducing lipotoxic effects.

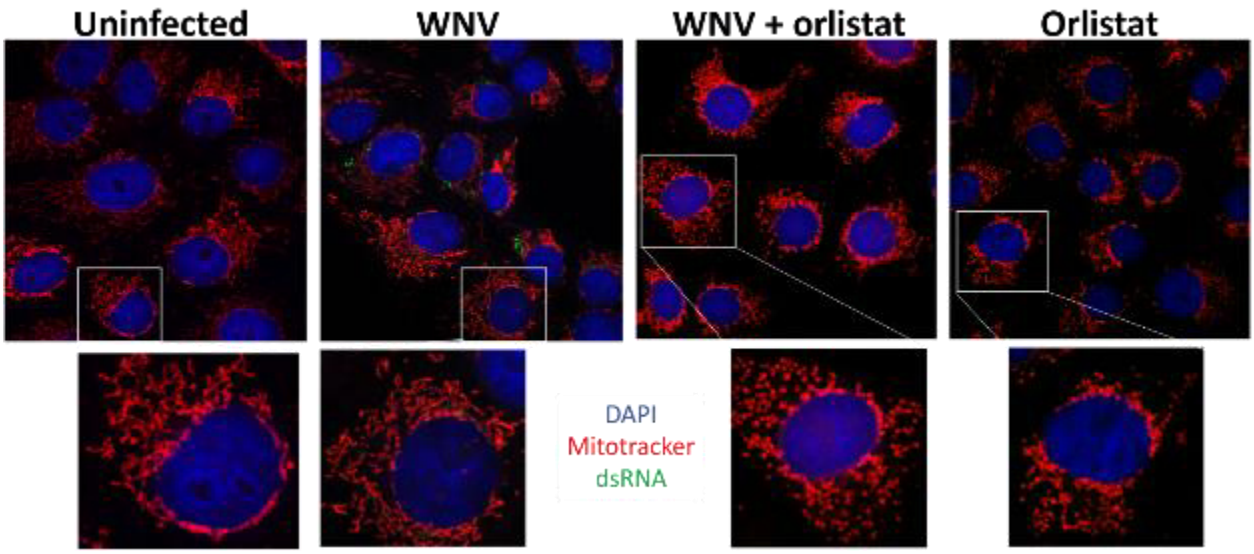

Figure 23. Immunofluorescence reveals treatment with orlistat causing drastic mitochondrial fragmentation.

Cells were seeded on coverslips and either left uninfected, infected with WNV and/or treated with orlistat for 24 hours, after which they were labelled with MitotrackerRed (red), fixed and dsRNA (green), and nuclei were counterstained with DAPI (blue). Images were taken on a Zeiss confocal microscope and analysed using Zen Blue software. These images are representative of the observations made over 3 biological replicates (n=3).

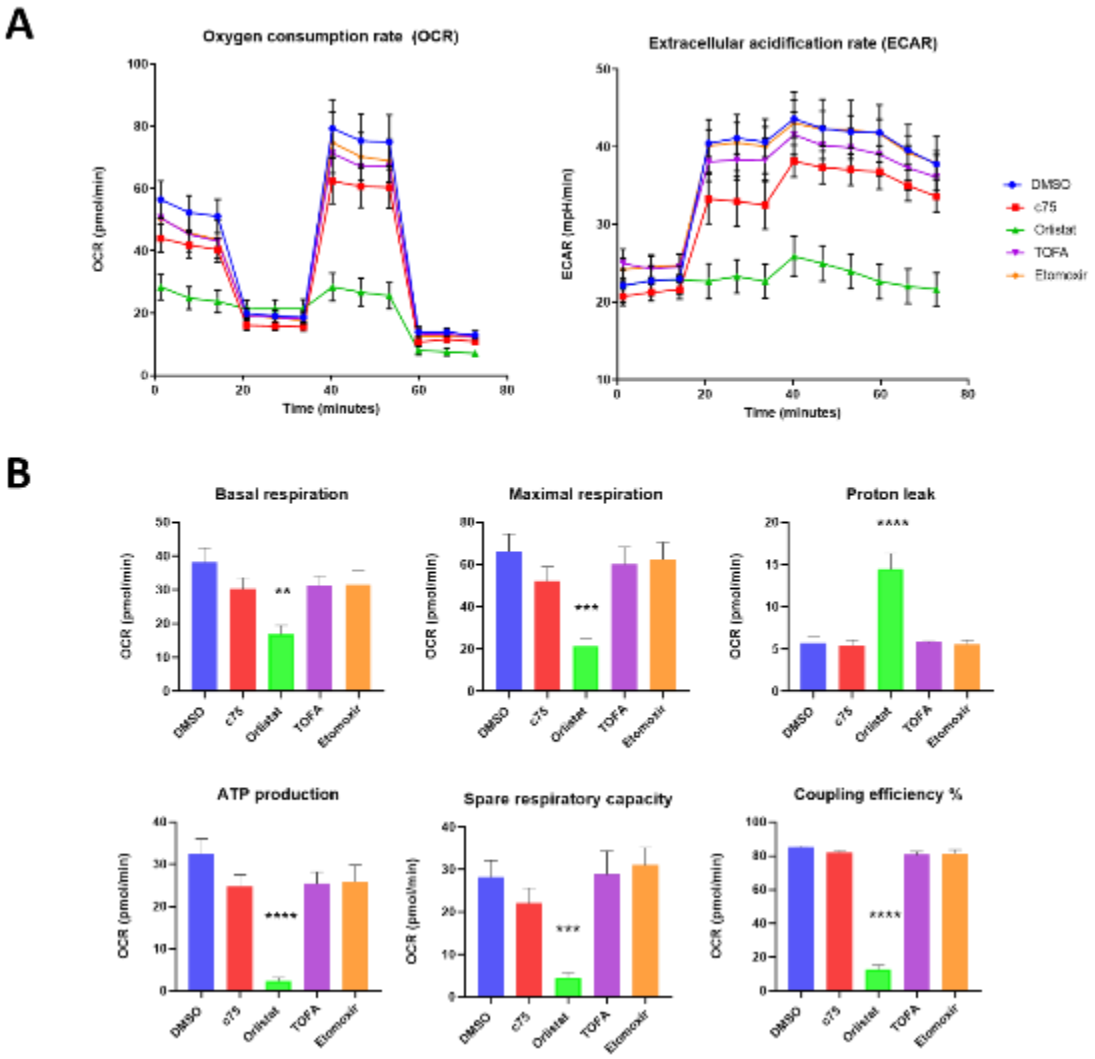

Figure 24. Orlistat completely dysregulates oxygen consumption and extracellular acidification rates in uninfected cells. Vero cells were seeded onto Seahorse XF96 Cell Culture Microplate and treated with metabolic inhibitors for 24 hours at the following concentrations: c75 = 30 μM, orlistat = 100 μM, TOFA = 10 μM, etomoxir = 100 μM, and DMSO was used as the vehicle control. Rates of OCR and ECAR were then measured using the Seahorse XF Mito Stress Test Kit and a Seahorse XF Analyser. **(A)** OCR and ECAR rates of infected cells. The compounds (oligomycin, CCCP, antimycin A and rotenone) were injected at the time points indicated in Figure 20a and each data point is the mean of 3 technical replicates of 2 independent biological replicates (n=2) with error bars indicated S.E.M. **(B)** Bar graph representation of each of the parameters, using data extracted from **(A)** and analysed using the Seahorse XF Cell Mito Stress Test Report Generator and Prism. Significance was determined using an ordinary one-way ANOVA with multiple comparisons (GraphPad Prism 6), and indicated on graphs with asterisks (*). ** = $p \leq 0.005$, *** = $p \leq 0.0005$, **** = $p < 0.0001$.

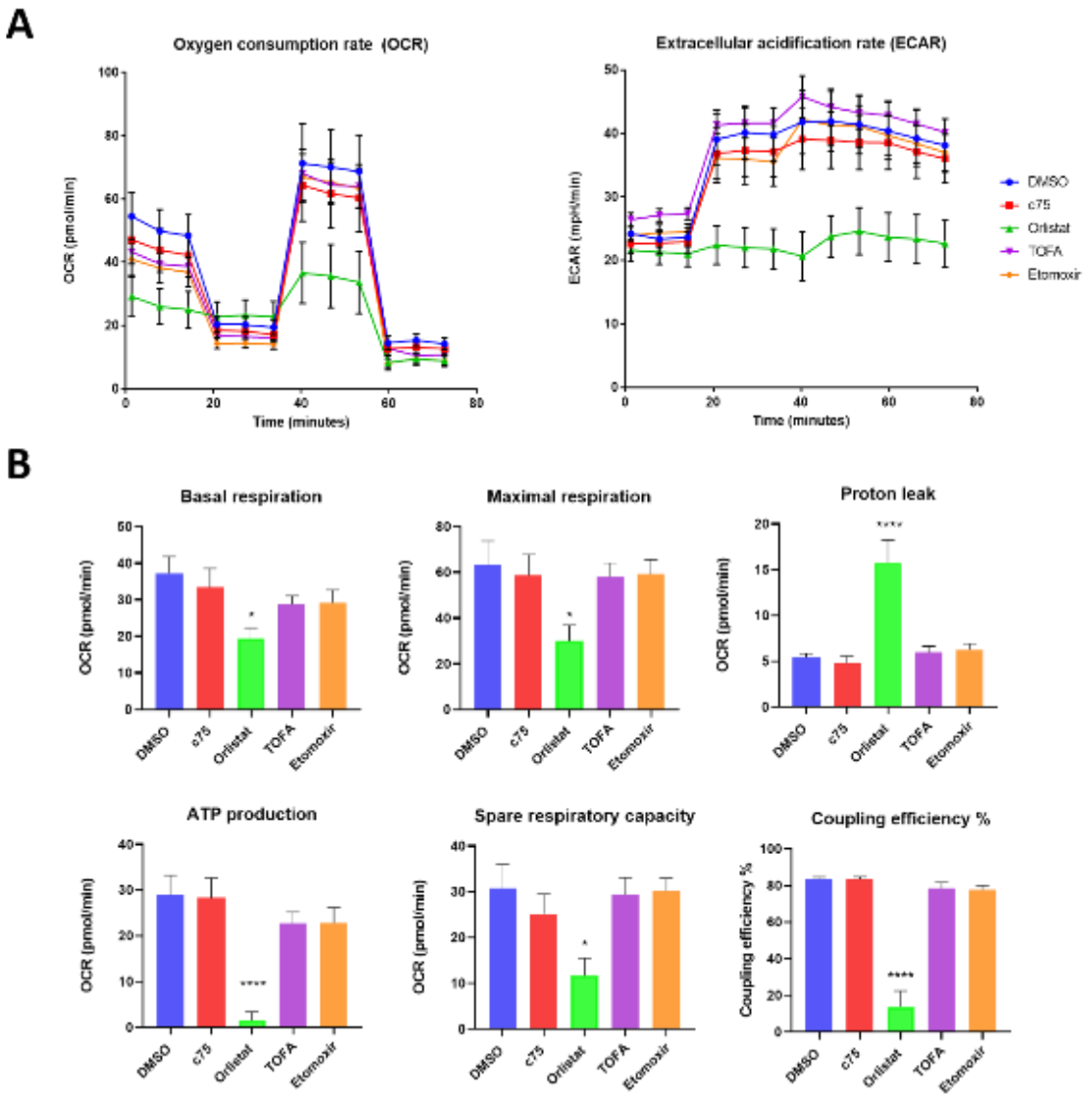

Figure 25. Orlistat completely dysregulates oxygen consumption and extracellular acidification rates in West Nile virus-infected cells. Vero cells were seeded onto Seahorse XF96 Cell Culture Microplate, infected with WNV at an MOI of 2, and treated with metabolic inhibitors for 24 hours at the following concentrations: c75 = 30 μM, orlistat = 100 μM, TOFA = 10 μM, etomoxir = 100 μM, and DMSO was used as the vehicle control. Rates of OCR and ECAR were then measured using the Seahorse XF Mito Stress Test Kit and a Seahorse XF Analyser. **(A)** OCR and ECAR rates of infected cells. The compounds (oligomycin, CCCP, antimycin A and rotenone) were injected at the time points indicated in Figure 20a and each data point is the mean of 3 technical replicates of 2 independent biological replicates (n=2) with error bars indicated S.E.M. **(B)** Bar graph representation of each of the parameters, using data extracted from **(A)** and analysed using the Seahorse XF Cell Mito Stress Test Report Generator and Prism. Significance was determined using an ordinary one-way ANOVA with

multiple comparisons (GraphPad Prism 6), and indicated on graphs with asterisks (*). * = p ≤ 0.05, **** = p <0.0001.

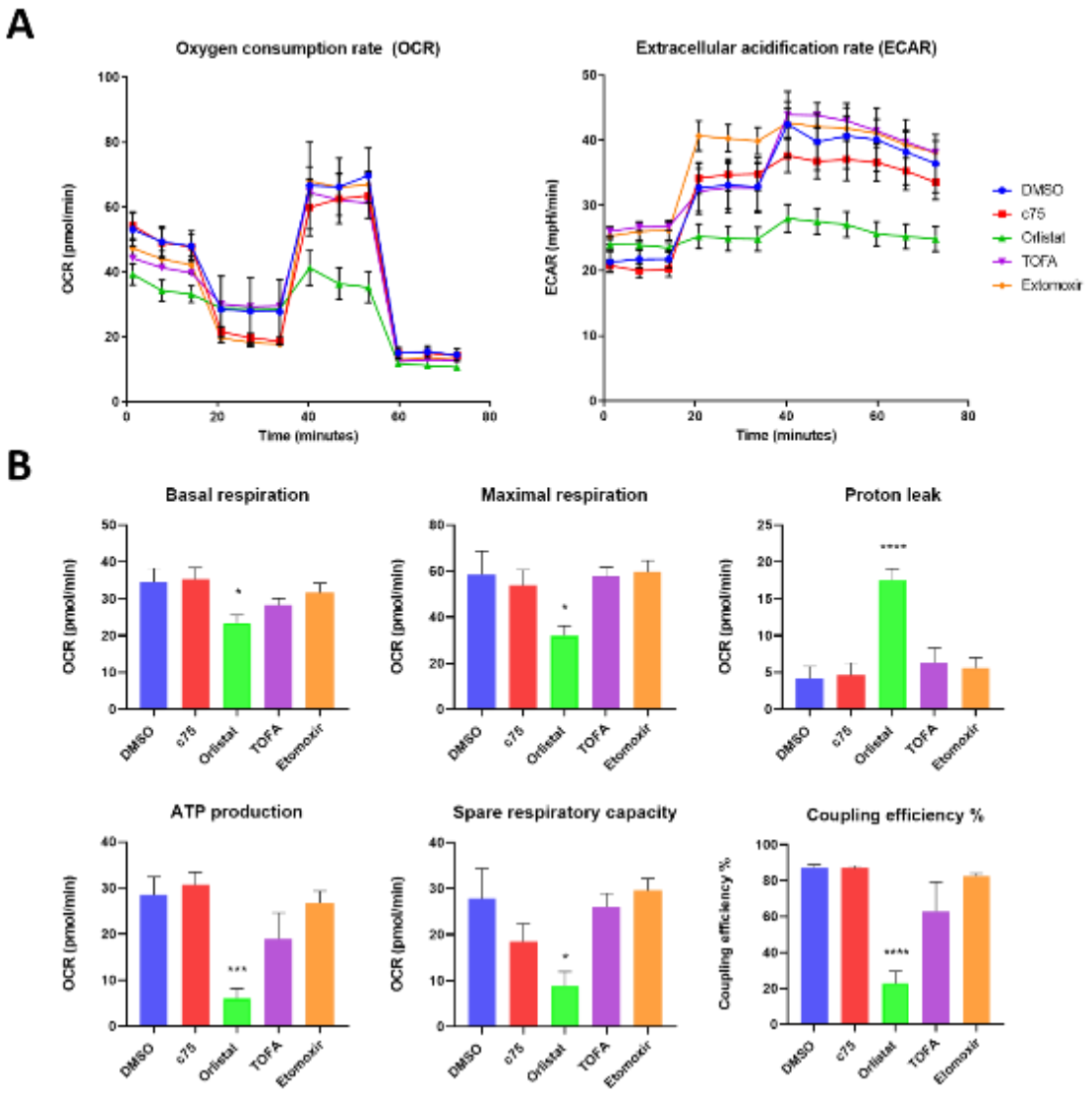

Figure 26. Orlistat completely dysregulates oxygen consumption and extracellular acidification rates in Zika virus-infected cells. Vero cells were seeded onto Seahorse XF96 Cell Culture Microplate, infected with ZIKV at an MOI of 1, and treated with metabolic inhibitors for 24 hours at the following concentrations: c75 = 30 μM, orlistat = 100 μM, TOFA = 10 μM, etomoxir = 100 μM, and DMSO was used as the vehicle control. Rates of OCR and ECAR were then measured using the Seahorse XF Mito Stress Test Kit and a Seahorse XF Analyser. **(A)** OCR and ECAR rates of infected cells. The compounds (oligomycin, CCCP, antimycin A and rotenone) were injected at the time points indicated in Figure 20a and each data point is the mean of 3 technical replicates of 2 independent biological replicates (n=2) with error bars indicated S.E.M. **(B)** Bar graph representation of each of the parameters, using data extracted from

(A) and analysed using the Seahorse XF Cell Mito Stress Test Report Generator and Prism. Significance was determined using an ordinary one-way ANOVA with multiple comparisons (GraphPad Prism 6), and indicated on graphs with asterisks (*). * = p ≤ 0.05, *** = p ≤ 0.0005, **** = p <0.0001.

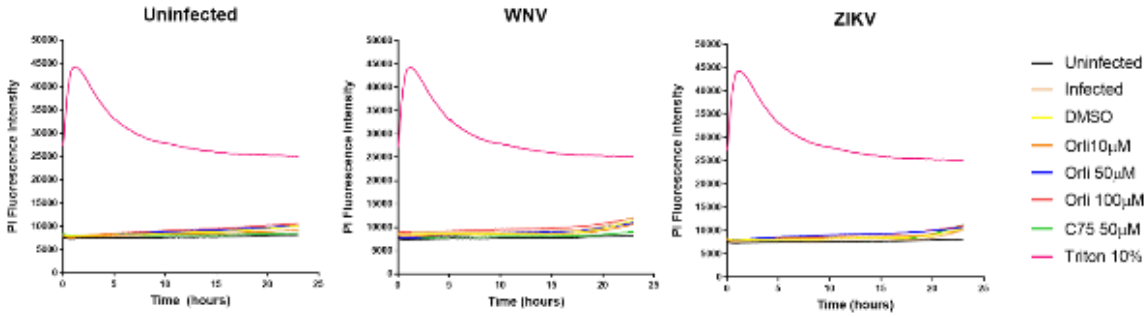

Figure 27. Orlistat does not induce cell death in Vero cells during infection with WNV and ZIKV. Vero cells were seeded in a 96-well plate and either infected with WNV (MOI 2) or ZIKV (1), or left uninfected, and subsequently treated with the FASN inhibitors c75 and orlistat at indicated concentrations. 10 % Triton-X was used as a control for total cell lysis. Propidium iodide (PI) was added to each well at a concentration of 1 µg/mL, and PI fluorescence was measured using a ClarioStar Plus Microplate Reader over a 24 hour period at 37 °C and 5 % CO_2. Fluorescent intensity was then graphed using GraphPad Prism 8 (n=3).

3.2.8. Orlistat-induced mitochondrial fragmentation is exacerbated by palmitic acid, and partially rescued by oleic acid

Orlistat inhibits the TE domain of FASN, which is responsible for halting the elongation of the FA chain at 16-carbons to release palmitate and therefore controls chain length specificity. We hypothesised that orlistat treatment may therefore not completely inhibit FA synthesis, and instead may be resulting in the production of FAs with different chain lengths. It is possible that these particular FA species are unable to be utilised by the virus, converted into other FAs, or broken down by the cell, causing their accumulation in LDs, and could potentially be exerting lipotoxic effects on cells. Indeed, one of the main functions of LDs is to sequester toxic lipid species from the cytosol. There are many studies that have investigated the differential effects of palmitate (a saturated FA) and oleic acid (an unsaturated FA) on LD formation and mitochondrial dynamics, and have

found that palmitic acid, but not oleic acid, is poorly incorporated into LDs, causes mitochondrial fragmentation and induces apoptosis (Eynaudi et al, 2021; Listenberger et al, 2003; Nolan & Larter, 2009; Sergi et al, 2021; Tse et al, 2018). Although we believe that orlistat is specifically inhibiting palmitate synthesis/release of palmitate from the FASN enzymatic complex, it's possible that alternate FAs being produced could be eliciting lipotoxic effects on the cells. As oleic acid has previously been demonstrated to rescue mitochondrial fragmentation and lipotoxic effects caused by palmitate, we performed an experiment to determine if oleic acid could rescue the mitochondrial fragmentation caused by orlistat. We also used palmitic acid as a control to confirm that that this FA induced mitochondrial fragmentation in Veros.

Cells were seeded on coverslips and left untreated, or treated with orlistat in the presence or absence of either palmitate and oleic acid, and stained with MitotrackerRed and BODIPY to visualise mitochondria and LDs respectively. In orlistat treated cells with no lipid treatment, we again observed concurrent LD accumulation and mitochondrial fragmentation (Figures 28A panels b and c). Orlistat treatment resulted in a significant decrease in mitochondrial footprint (mitochondrial area), mean branch length, and number of branches (Figure 28B). When we treated cells with palmitic acid (but not orlistat), we observed weak LD induction, severe mitochondrial fragmentation, and cell detachment and changes in nuclear morphology that were indicative of cell death (Figure 28A panel d and 28B). When we treated with palmitic acid and orlistat concurrently, we observed each of these same effects (Figures 28A panels e and f, 28B). Addition of oleic acid to cells induced a high lipid droplet load, as well as the formation of more elongated, tubular mitochondria, indicative of increased mitochondrial respiration (Figure 28A panel g, 28B). Treatment of oleic acid and orlistat concurrently appeared to partially rescue the fragmented mitochondria (Figures 28A panel h and i); with an increase in mitochondrial footprint and network branches, but no increase in mean branch length (Figure 28B). The remaining fragmentation in these cells is likely a result of general lipid overload in these cells. Overall, this data has demonstrated the distinct effects that different FA species can exert on cells. Our observation that orlistat and palmitic acid treatment both result in

mitochondrial fragmentation, the former of which can be partially rescued by oleic acid treatment, supports our hypothesis that orlistat treatment is resulting in the production of toxic FA species leading to mitochondrial damage.

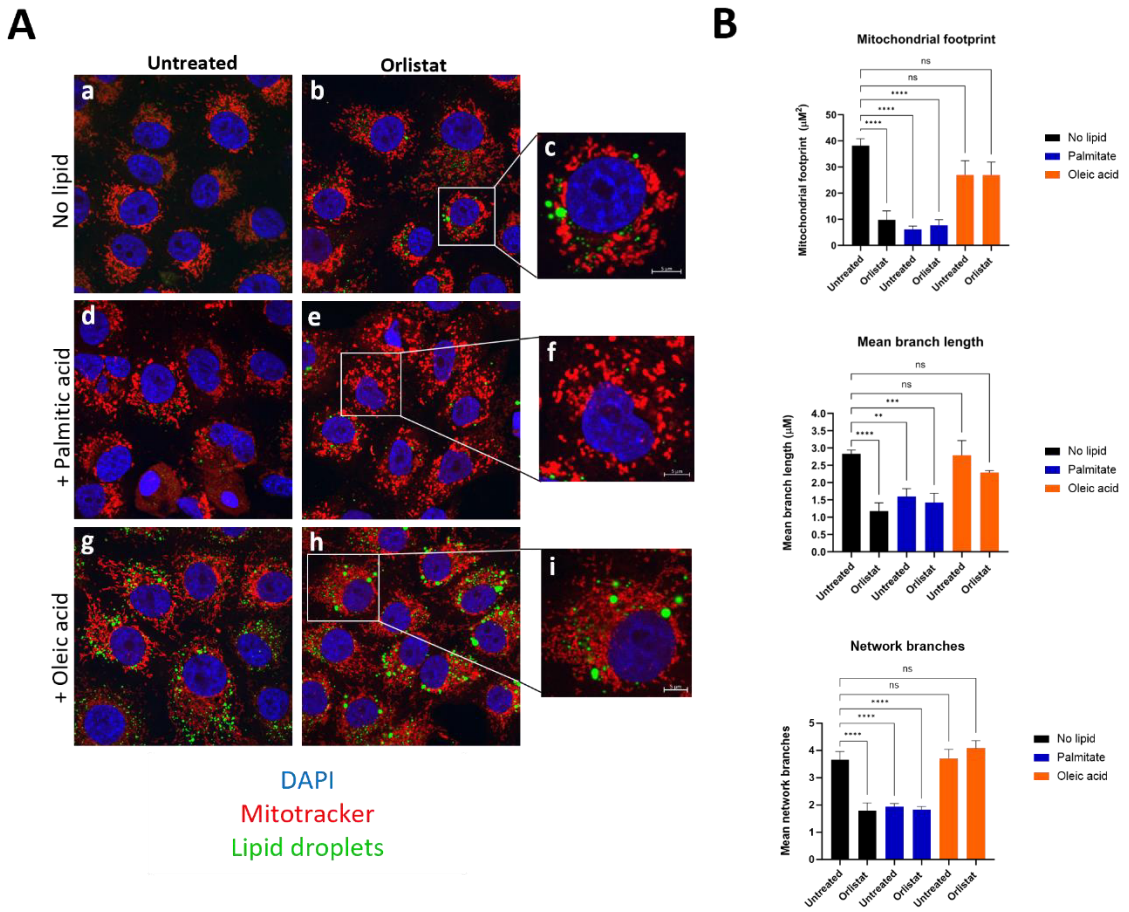

Figure 28. Mitochondrial fragmentation is induced with orlistat treatment, and can be partially rescued by exogenous addition of oleic acid, but not palmitic acid. Cells were seeded on coverslips and untreated or orlistat-treated cells were incubated with either no lipid, or oleic (100 μM) or palmitic acid (100 μM) for 24 hours, after which they were stained with MitoTracker™ Red CMXRos (red) for 30 minutes, fixed and counterstained with Hoechst (blue). Before mounting, cells were stained with the fluorescent dye BODIPY™ 493/503 (Invitrogen) to visualise lipid droplets (green). **(A)** Images were taken on a Zeiss confocal microscope and analysed using Zen Blue software. These images are representative of the observations made over 3 biological replicates (n=3). **(B)** Quantification and categorization of mitochondrial morphology using MiNa Single Image macro (Github). Analyses were performed on minimum of 10 cells per treatment. Error bars are S.E.M and statistical significance was interpreted as * = $p \leq 0.05$, ** = $p \leq 0.005$, *** = $p \leq 0.0005$.

3.2.9. *Exogenously adding fatty acids rescues the inhibitory effect of c75, but not orlistat*

In addition to assessing the effects of different FAs on mitochondria, we further aimed to assess the effects of these FAs on viral replication and determine if the addition of exogenous FAs (namely oleic acid) could rescue the inhibitory effects seen with either drug. We hypothesised that if the viral inhibition caused by c75 was due to a reduction in the bioavailability of lipids for replication, then these exogenous FAs would supplement this deficiency and restore viral replication. For orlistat-treated cells, based on the mitochondrial morphology data, we hypothesised that the addition of palmitate may be detrimental to viral replication, but the addition of oleic acid may rescue potential lipotoxic effects of orlistat and restore viral replication to some degree.

We exogenously added palmitic acid and oleic acid to infected cells, and measured the effect of these FAs on viral protein expression (NS1) via western blot, and on infectious virus production via a plaque assay. Overall, treatment with palmitate had a significant inhibitory effect on the replication of both WNV and ZIKV (Figure 29a), resulting in a reduction in NS1 expression of ~50 % for both viruses. The addition of oleic acid during infection led to a ~35 % increase in NS1 expression for WNV, and ~10 % for ZIKV, but this trend was not significant. In Figures 29b and c, the addition of palmitate in the presence of our FASN inhibitors resulted in a greater reduction in NS1 expression compared to the no lipid control. Conversely, the addition of oleic acid resulted in a rescue of viral inhibition caused by c75, but surprisingly not of orlistat. Although there was not a significant difference for ZIKV between the DMSO no lipid control, and orlistat + oleic acid treated cells, the trend was clear and overall, we observed less NS1 expression in the orlistat + oleic acid treated cells. These results were further confirmed using plaque assays to measure infectious virus production (Figure 29d). Taken together, this data suggests that both palmitate and orlistat are detrimental to cellular functions and are most likely creating a microenvironment within cells that is not amenable to viral replication.

Overall, our data is consistent with the previous studies, in both Veros and other cell types, indicating that *de novo* FAS is essential for Flavivirus replication. We

confirmed this for ZIKV in this cell type, and demonstrated that the fate of these FAs is primarily for viral membrane morphogenesis. Our data additionally suggests that orlistat does not completely halt FA synthesis, and we have identified novel cellular effects of this inhibitor, including LD formation and mitochondrial dysfunction. We believe that these effects are at the root of orlistat's antiviral effect in this study, however more work is needed to confirm the exact mechanism.

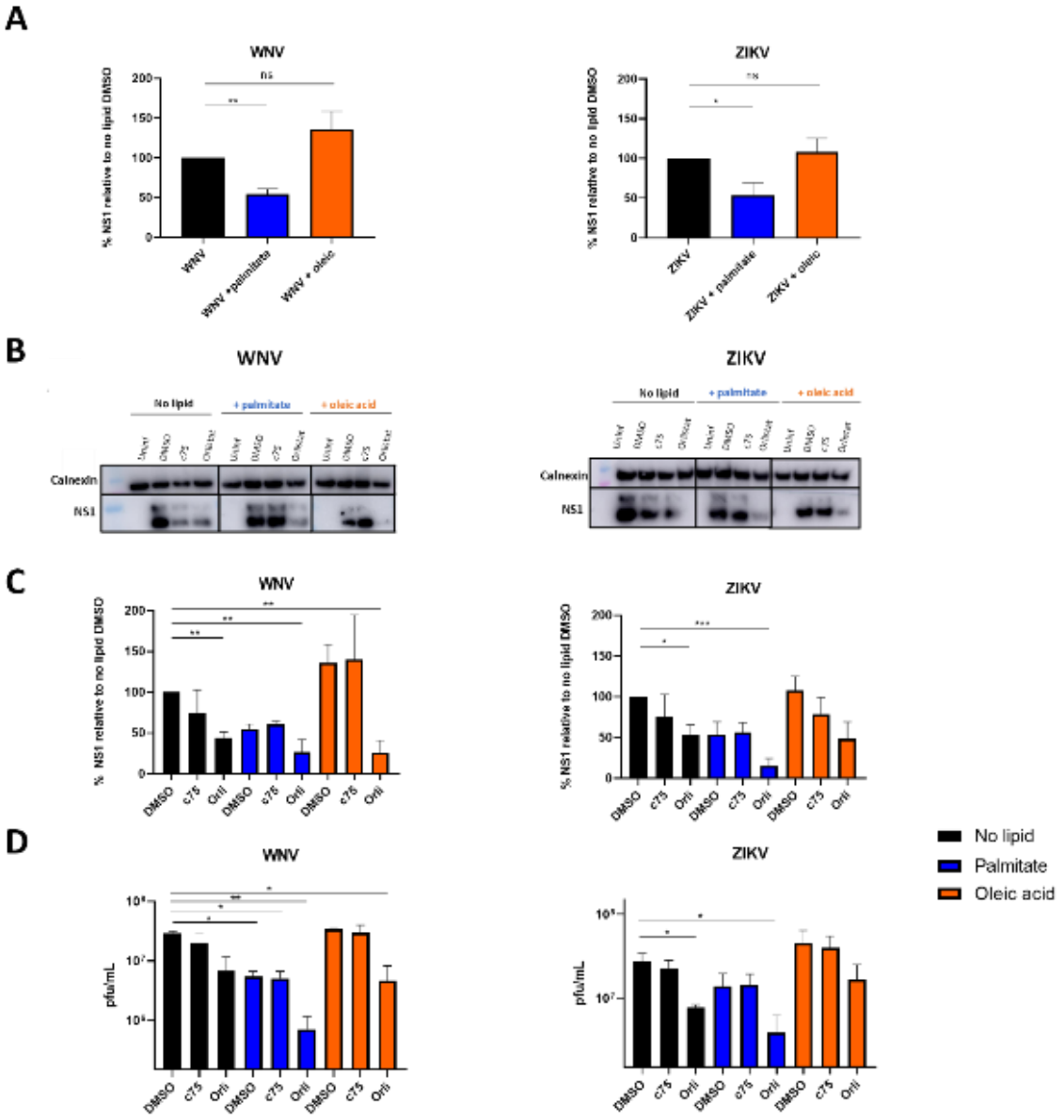

Figure 29. The addition of palmitic acid is detrimental to viral replication, and exogenously adding oleic acid rescues the inhibitory effects on viral replication induced by c75, but not orlistat. Vero cells were infected with WNV (MOI 2) or ZIKV (MOI 1) and either left untreated, treated with c75, or treated with orlistat, and either in the absence or presence of either palmitic acid (100 μM) or oleic acid (100 μM). **(A)** The effect of palmitic acid or oleic acid on viral protein NS1 expression for WNV and ZIKV, assayed via western blot and quantified via densitometry using ImageJ (n=3). **(B)** Western blot analysis of a lipid rescue experiment performed with WNV and ZIKV in the presence of FASN inhibitors and palmitic or oleic acid. **(C)** Quantification of the lipid rescue western blot represented in (B) via densitometry using ImageJ. Error bars are representative of 3 independent biological replicates (n=3, +/- SEM) (GraphPad Prism 8). **(D)**

Plaque assay results from lipid rescue supernatants (n=2 +/- SEM). * = p ≤ 0.05, ** = p ≤ 0.005, *** = p ≤ 0.0005.

3.3. Discussion

As +ssRNA viruses have a limited genome size they must rely on the commandeering of host pathways and machinery to complete their life cycle. For Flaviviruses, the commandeering of lipid pathways is essential for the construction of membranous replication complexes required for efficient genome replication. Whilst there has been progress in uncovering the host factors required for the formation of Flavivirus RCs, there remains much to be elucidated about these processes. In understanding the molecular mechanisms underpinning viral replication, we are able to develop therapeutics to target pathways integral to viral survival and ease the burden of these diseases. In this chapter, we aimed to further elucidate the reliance of WNV and ZIKV on fatty acid metabolism, using small chemical inhibitors of these pathways. Overall, we demonstrated that fatty acid synthesis, but not oxidation, is indispensable for viral replication in Vero cells. We also found that infection is not dependent on lipid droplet presence within cells, and that infection overall does not perturb mitochondrial respiration. Our results with orlistat indicate that this inhibitor does not reduce overall lipid synthesis or accumulation, and its antiviral effects may be a result of lipotoxicity induced by this inhibitor.

During this study we observed a degree of co-localisation between dsRNA and FASN, but as the distribution and expression of FASN did not change upon infection, we could not confirm that FASN was actively being recruited to sites of replication, as has been seen with DENV in Huh-7.5 cells (Heaton et al, 2010). Despite this, it remains possible that WNV and ZIKV may still rely on FAs produced by the FASN pathway without actively sequestering the enzyme, as FAs produced in the cytosol are generally transported to either the mitochondria for oxidation, or to the ER for lipid or lipid droplet synthesis. As viral replication complexes are derived from ER membranes, the FAs may be transported here by normal cellular processes, or these viruses could highjack FA transport

proteins such as FATP1 or FATP2, a possibility worth investigating in the future. We additionally hypothesised that the viruses may be stimulating FASN activity rather than upregulating its expression, and we attempted to assess this by establishing an assay for FASN activity, based on previous publications (Puig et al, 2009), however our attempts were unsuccessful. The co-localisation of FASN and NS4A is further evidence of a role for FASN in viral replication complex formation, and may give us some mechanistic insight into the utilisation of FASN by these viruses, however further work involving protein-protein interaction studies needs to be done to confirm this.

Previous studies have found that *de novo* synthesised FAs are integral for DENV and WNV replication (Heaton et al, 2010; Martín-Acebes et al, 2011b; Merino-Ramos et al, 2015; Tongluan et al, 2017), but there have been conflicting results for ZIKV (Jiménez de Oya et al, 2019; Royle et al, 2017). Our results clearly demonstrate that this pathway is indispensable for replication of WNV and ZIKV in this cell type. Our results reveal that inhibiting the rate limiting step of FAS (the conversion of acetyl-CoA to malonyl-CoA by ACC) completely attenuates viral replication; as upon treatment of infected cells with TOFA resulted in no intracellular viral protein accumulation, or the production of infectious virus in the supernatant, suggesting that FAS is likely important for early replicative processes. Inhibiting FASN with c75 and orlistat significantly reduced replication of both viruses, but to a lesser extent than inhibiting ACC with TOFA. This may be indicative of only partial inhibition of FAS with c75 and orlistat, or alternatively that enzymatic activities upstream of c75 are important. Interestingly, we observed an impact of c75 and orlistat on NS1 protein expression, but no significant impact on viral titre, which may indicate that these inhibitors are impacting NS1 specifically but not overall infection. In the future, to confirm this, we would assay the impact of these inhibitors on other viral proteins, including E. Further, as secreted NS1 is lipid-associated, we would like to measure secreted NS1 levels in response to our inhibitors.

As the inhibition of ACC with TOFA depletes cellular malonyl-CoA pools, some groups have observed an increase in oxidative phosphorylation with this inhibitor.

As malonyl-CoA allosterically inhibits CPT-1, ACC is therefore a central regulator of FAO, and we hypothesised that inhibiting ACC could affect mitochondrial respiration which may be contributing to its antiviral effect. Our Seahorse data, however, indicated that TOFA did not significantly perturb mitochondrial respiration (Figure 25, 26 and 27). This was not surprising given our LD data showing that Vero cells harbour very few lipid droplets (Figure 22 and 23), so even if CPT-1 was uninhibited, the pool of intracellular FAs available for FAO would likely be very small. We can therefore conclude that the antiviral effect of TOFA was most likely a product of the complete restriction of *de novo* FAS.

The role for FAs in DENV infection has been shown to be dualistic in nature; *de novo* synthesised FAs co-fractionate with viral RCs and are likely used to build or expand these structures, and additionally DENV upregulates the oxidation of FAs to boost metabolism for replicative processes. Our immunofluorescence data suggested that *de novo* FAs contribute to and are necessary for viral RC formation (Figure 19), and our metabolic data indicated that neither WNV nor ZIKV increased mitochondrial respiration, suggesting that FAO is not upregulated (Figure 20). The inhibitory effect we observed with etomoxir on virus particle production, however, suggests that a certain level of mitochondrial respiration (or energy production) may be necessary for viral particle formation and release. Overall, this data provides strong evidence that the role of FAS during infection in this cell line is primarily limited to the morphogenesis of RCs, but a certain level of energy production may be required for virion assembly and release for both viruses. As ZIKV has been demonstrated to induce metabolic rearrangements in placental cells (Chen et al, 2020), we do not exclude the possibility that the role of FAs may differ between cell types. It's possible that the minimal effects of viral infection on LD content and FAO may be a consequence of the low lipid content in this cell type; the virus may prioritise diverting FAs to RCs as this may be the most necessary component for replication, but perhaps in a cell type or condition with high lipid content, this result could vary and include broader uses of FAs, namely to fuel energy production.

It has been observed by some groups that LDs are induced upon infection with both DENV and ZIKV (Chen et al, 2020; Cloherty et al, 2020; Monson et al, 2021a; Samsa et al, 2009), or induced in response to dsRNA stimulation (Monson et al, 2021a). LDs play complex roles during infection, and can be pro-host or pro-viral which appears to be virus and cell-type specific. In our study we did not observe the induction of LD formation at any of the time points investigated. Other studies have found that this induction of LDs can occur in an IFN-independent manner, making it unlikely that our observations are due to Vero cells lacking the ability to produce IFN. Although kidneys have a high metabolic rate, the overall low cellular content of LDs in Veros was not altogether surprising as this is an epithelial cell line, and LD presence and accumulation is generally higher in specialised cells with higher metabolic capacity and needs. Our observation that viral replication appears to be able to occur in a cellular environment lacking LDs, suggested that the replication and assembly of WNV and ZIKV can occur independently of LDs. However, as LDs are highly transient organelles and undergo periods of expansion and depletion (reviewed in (Olzmann & Carvalho, 2019), it remains possible that we simply did not detect their presence at the time points observed.

An interesting and novel observation in this study was the detection of LDs during treatment with orlistat, which was observed in both uninfected and infected cells (Figures 22 and 23). Orlistat is an FDA-approved drug and has been a focus of cancer research for years, however this phenomenon had never been reported until recently (Farley et al, 2022). Whilst the presence of these LDs could hypothetically be attributed to orlistat's lipase activity, if orlistat was concurrently inhibiting FAS, there would be few FAs to store in these organelles. We thus sought to rationalise the seeming inability of orlistat in reducing *de novo* FAS. Orlistat's use as an anti-obesity drug stems from its ability to inhibit gastric lipases, thus preventing the absorption of FAs, but subsequent research led to the revelation that orlistat was also a potent inhibitor of the FASN TE domain (Kridel et al, 2004). The function of the TE domain is to cleave the thioester bond between the growing fatty acyl chain and the carrier molecule ACP, to release the final free fatty acid product (Joshi et al, 2005). This domain has been

repeatedly demonstrated to have a high specificity for C_{16} (palmitate) and C_{18} (stearate), and early biochemical work has shown that the complete loss of the TE domain results in a loss of chain-length selectivity, and fatty acids of shorter and longer chain lengths were produced, namely C_{20} (arachidate) and C_{22} (behenate) (Chakravarty et al, 2004; Wakil et al, 1983). Although it has not been demonstrated, we hypothesised that the inhibition of the TE domain of FASN with orlistat does not completely inhibit FAS, but results in a loss of chain-length specificity, producing FAs of longer or shorter chain lengths. We further hypothesised that these FAs are unable to be utilised by the virus, and perhaps by the cell, leading to their accumulation in LDs, and orlistat's lipase activity may be preventing these LDs from being broken down.

It is now common knowledge that saturated free FAs can exert lipotoxic effects on cells, and are sequestered to LDs in order to protect the cells from these effects (El-Assaad et al, 2003; Engin, 2017; Nolan & Larter, 2009; Oh et al, 2018). Unsaturated FAs, such as oleic acid, do not induce these lipotoxic effects, and have indeed been found to reverse the detrimental effects of saturated FAs (Busch et al, 2005; Eynaudi et al, 2021; Listenberger et al, 2003; Nolan & Larter, 2009; Thombare et al, 2017), namely via the sequestration of these toxic FA species to LDs (Eynaudi et al, 2021; Listenberger et al, 2003). The lipotoxic effects exerted by saturated FAs such as palmitate include mitochondrial fragmentation and dysfunction, ROS production, ER stress and apoptosis. In this study we observed obvious mitochondrial fragmentation with both orlistat and palmitic acid treatment, and for orlistat this was in conjunction with a drastic reduction in mitochondrial respiration (Figures 25, 26 and 26). As orlistat significantly reduces both proton leak and coupling efficiency, it appears that orlistat might be actively damaging mitochondria rather than simply depriving them of fatty acid substrates. Conversely, the monounsaturated FA oleic acid induced mitochondrial elongation and partially rescued the effect on mitochondrial morphology observed with orlistat. Taken together, it seems apparent that orlistat does not altogether reduce FA synthesis, but may increase levels of saturated FAs within cells, which are sequestered to LDs in an attempt to reduce lipotoxic dysregulation of mitochondria.

The conversion of saturated FAs to monounsaturated FAs is a conserved cellular process aimed to reduce these lipotoxic effects. A group of enzymes called fatty acid desaturases are responsible for this, via the removal of two hydrogen atoms which results in a double bond. This understanding led us to question why these cells were not upregulating this process during orlistat treatment in order to mitigate the toxicity caused by the saturated FAs. In our further research of the literature, we found a probable reason. There are four fatty acid desaturases in humans, Δ9 desaturase, Δ6 desaturase, Δ5 desaturase, and Δ4 desaturase, and each have a different substrate specificity. Δ9 desaturase, also known as SCD-1, is responsible primarily for the conversion of stearate and palmitate to oleate and palmitoleate, whilst the other 3 desaturases act upon dietary-derived FAs. Early biochemistry research revealed that SCD-1 has substrate specificity for FAs with chain lengths of 14 to 19 carbons, with a dramatic loss in activity for anything above that (Enoch et al, 1976; Paton & Ntambi, 2009). If orlistat is producing FAs with chain lengths of 20+ carbons, then the ability of cells to convert them to unsaturated FAs is extremely minimal.

Flaviviruses require a specific composition of lipids to produce the correct curvature and confirmation for viral RCs (Aktepe & Mackenzie, 2018). The conversion of saturated to monounsaturated FAs is an integral step for the synthesis of more complex lipids, particularly phospholipids, and Flavivirus replication is dependent on the activity of SCD-1 for RNA replication (Gullberg et al, 2018; Hishiki et al, 2019). If orlistat is indeed producing FA species that cannot be desaturated and converted to phospholipids, then this would likely disrupt viral RC formation. In other work into the effects of ER damage in type 2 diabetes, palmitate overload of cells swiftly increases the saturated FA content of the ER membrane, resulting in compromised membrane morphology and integrity (Borradaile et al, 2006). This may additionally explain why we observed consistent cell detachment (but not cell death) with orlistat treatment, as saturated FAs can decrease membrane fluidity and affect cell adhesion (Schaeffer & Curtis, 1977). Taken together, we hypothesise that orlistat treatment results in the production of FAs with unusual chain lengths (20-22 carbons or more), which is

disrupting viral replication potentially via multiple mechanisms (see Figure 30 for a summary), including:

1. Disrupting replication complex formation through the deprivation of FA substrates for phospholipid synthesis
2. Increasing saturated FA content of ER and RC membranes, disrupting their morphology and integrity
3. Increasing circulating FFA levels, resulting in damage to mitochondria and disrupting metabolic homeostasis, generating a metabolic quiescent state that is not amenable to viral replication
4. Inducing lipotoxic effects in the form of ROS production, which could be inducing ER stress and disrupting replication complexes

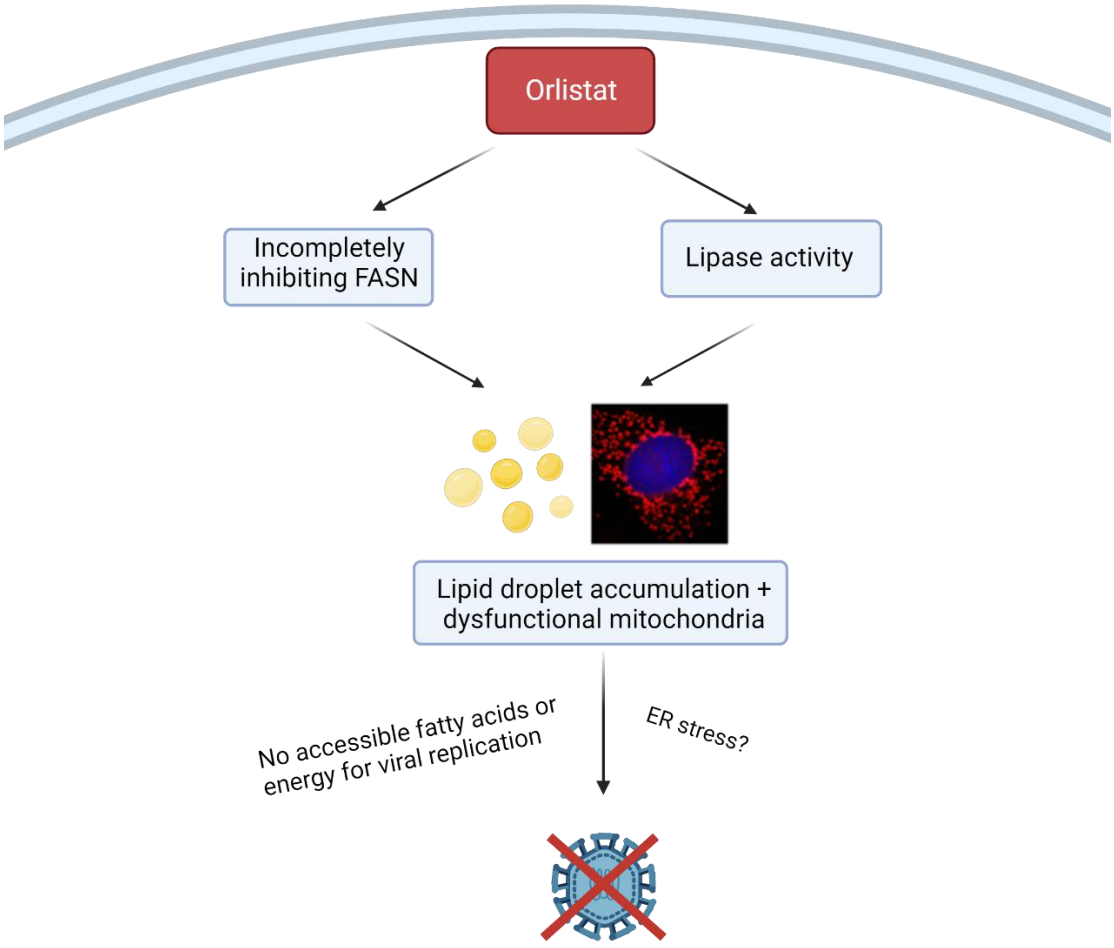

Figure 30. Model describing the potential antiviral action of orlistat in Vero cells. We hypothesise that orlistat prevents palmitate synthesis specifically, but

does not completely inhibit fatty acid synthesis. This, combined with orlistat's pan-lipase activity, results in lipid droplet accumulation, and subsequent mitochondrial fragmentation as a result of lipotoxicity and inaccessible fatty acid stores. This generates a metabolically quiescent state that is not amenable to Flavivirus infection.

Strangely, when we exogenously added in oleic acid, we saw an increase in viral replication overall, but did not observe a rescue of viral replication in orlistat-treated cells (see Figure 29). We hypothesised that the monosaturated FA might sequester the FA species produced during orlistat treatment to LDs, reducing lipotoxic effects, whilst supplementing the FAs required for viral RC formation. Whist oleic acid has been demonstrated to sequester palmitic acid to LDs and reverse lipotoxic effects, little is known about the effect of oleic acid on longer chain saturated FAs (C20-22+), as they are quite uncommon. It's possible that the combination of orlistat and oleic acid treatment is resulting in a condition of lipid overload, whereby oleic acid is potently inducing LD formation, but there is still a level of circulating saturated free FAs that are contributing to cellular stress and preventing viral replication. If orlistat is inducing mitochondrial dysfunction even in the presence of oleic acid, it's possible the energy levels of the cells are not meeting the energy demands for viral replication. It's also possible that although orlistat and oleic acid were added simultaneously, orlistat could be absorbed quicker by the cells, interfering with very early replicative processes, and the absorption of oleic acid occurs too late to rescue replication. Overall, it would appear that oleic acid is unable to completely ameliorate the potentially lipotoxic effects of orlistat, but it remains possible that orlistat is affecting cellular processes that we have not accounted for. In the future, this is something we would like to examine further. As well as assessing the impact of orlistat on ROS production and ER stress, we would also like to take a more global approach to identify novel effects of this drug using transcriptomics and/or proteomics. Overall, we believe our data is indicative of orlistat being an inefficient inhibitor of *de novo* FAS. Whilst orlistat likely renders the FASN complex incapable of synthesising palmitate, solely inhibiting the final functional domain is this pathway does not appear to halt fatty acid chain initiation, elongation, or overall FAS. Though we were unable to determine the impact of our inhibitors on the

enzymatic activity of FASN, experiments performed by others in cancer cells revealed orlistat reduced FASN activity (as assessed by NADPH oxidation) by only 23 %, at a concentration of 150 μM (Deepa et al, 2010). Instead of ablating overall FASN activity, our hypothesis is that the treatment of orlistat leads to the production of unusual FA species, which are exhibiting lipotoxic effects on the cells. We confirmed the effect of orlistat on mitochondrial function, and we additionally planned on investigating the effect of orlistat on ER stress, which has been observed in cancer cells (Little et al, 2007), but were unable to complete these experiments in time.

To confirm our hypotheses surrounding orlistat, we would also ideally perform some lipidomics to determine the specific lipid composition of orlistat-treated cells, and electron microscopy to confirm orlistat's effect on membrane morphology. Previous lipidomic analyses have highlighted distinct differences in the phospholipidome induced by c75 and orlistat, which supports our results with these inhibitors; in HeLa cells, c75 induced no effect on PE species, whilst orlistat resulted in a strong decrease in PE species, and a strong increase in PC species (Jeucken & Brouwers, 2019). It is known that the ratio of PE:PC is important for membrane integrity, and changes in this ratio in the mitochondria can affect energy production. This could provide another explanation behind the mitochondrial dysfunction observed in our system, and subsequent effect on viral replication, and lipidomic analyses will be key to fully ascertain this.

Overall, this study has contributed to our knowledge of the metabolic requirements needed for efficient replication of WNV and ZIKV, as well as providing potentially valuable insight into the cellular effects of a common FDA-approved drug. We have demonstrated the importance of the FAS pathway and shown that the primary fate of FAs in this cell type is for membrane morphogenesis, and that these viruses sequester FAs without perturbing other metabolic processes. Our findings with orlistat have provided us insight into specificity of FAs required for viral replication, and supports work by others showing downstream modification of FASN products are vital for RNA replication. This knowledge of WNV and ZIKV replication could aid in the development

specific antiviral approaches for these and similar viruses, and we hope that these novel cellular effects of orlistat may inform previous and current research using this FDA approved inhibitor.

Chapter 4
Investigating the bipartite role of fatty acids in infection and immune responses in macrophages

4.1. Introduction

Macrophages play an indispensable role in innate immunity and pathogen defence and display a high degree of plasticity. These cells can detect and respond to stimuli by shifting to a specific phenotypic and functional state, a process generally referred to as 'polarisation' or 'activation'. These activation phenotypes exist on a spectrum, but for simplicity can be broadly categorised into two extreme states - 'pro-inflammatory' or 'M1' macrophages and 'anti-inflammatory' or 'M2' macrophages. Polarisation occurs in response to certain stimuli (LPS, IFN-γ for M1, and IL-6, IL-10, IL-4 for M2), that bind to receptors (generally TLR4, IFNyR, JAK1/2) and activate transcription factors (STATs, PI3K etc). For M1 macrophages, this results in the transcription of ISGs and activation of the innate immune response, which aids in pathogen clearance. Polarisation towards the M2 phenotype results in the transcription of genes involved in tissue repair, angiogenesis, and other homeostatic functions.

These macrophage functional states have distinct metabolic signatures, which not only aid in defining them, but are also regulators of these discrete responses. In response to pro-inflammatory stimuli, M1 macrophages display increased glycolysis, increased TAG synthesis and LD accumulation, an impaired TCA cycle, and dysregulated OXPHOS (see Figure 31). Glycolysis is believed to be upregulated as this form of energy can be mounted rapidly to support acute inflammatory functions, with inhibition of this pathway resulting in impaired phagocytosis, ROS production and cytokine signalling (Freemerman et al, 2014; Michl et al, 1976; Pavlou et al, 2017). Recent evidence has directly connected this form of metabolism to inflammatory signalling pathways, including IL-1β and TNF-α production (Jiang et al, 2016; Millet et al, 2016; Moon et al, 2015a; Tannahill et al, 2013; Xie et al, 2016). Pro-inflammatory macrophages also exhibit two breaks in the TCA cycle, leading to the accumulation of citrate, itaconate and succinate, which have microbiocidal activities (Michelucci et al, 2013; Naujoks et

al, 2016), and frees up acetyl-CoA which can contribute instead to FAS (Infantino et al, 2013). Acetyl-CoA can also be utilised for the production of NO, ROS and prostaglandins, all of which have antiviral functions and are important for pro-inflammatory macrophage activation (Infantino et al, 2011; O'Neill, 2011).

Anti-inflammatory macrophages, conversely, rely on the oxidation of FA substrates and increased OXPHOS (see Figure 31). This is the most efficient energy pathway in our cells and provides sustained energy to support tissue repair and other anti-inflammatory functions. One of the key regulators of the metabolic switch between pro- and anti-inflammatory macrophages is the regulation of mitochondrial respiration via inducible nitric oxide synthase (iNOS). Pro-inflammatory macrophages upregulate iNOS expression resulting in increased nitric oxide (NO) production, which damages mitochondria, dampens OXPHOS and results in the accumulation of FAs (Bailey et al, 2019; Rosas-Ballina et al, 2020). Anti-inflammatory macrophages conversely have a fully functional respiratory redox chain, which allows them to upregulate the oxidation FAs and increase OXPHOS (Figure 31). Although the exact mechanisms of the upregulation of OXPHOS are not well defined, blocking NO production can effectively alter the metabolism of macrophages and reprogram them towards an anti-inflammatory phenotype (Van den Bossche et al, 2016). This demonstrates how these metabolic changes can drive the functional phenotype of these cells.

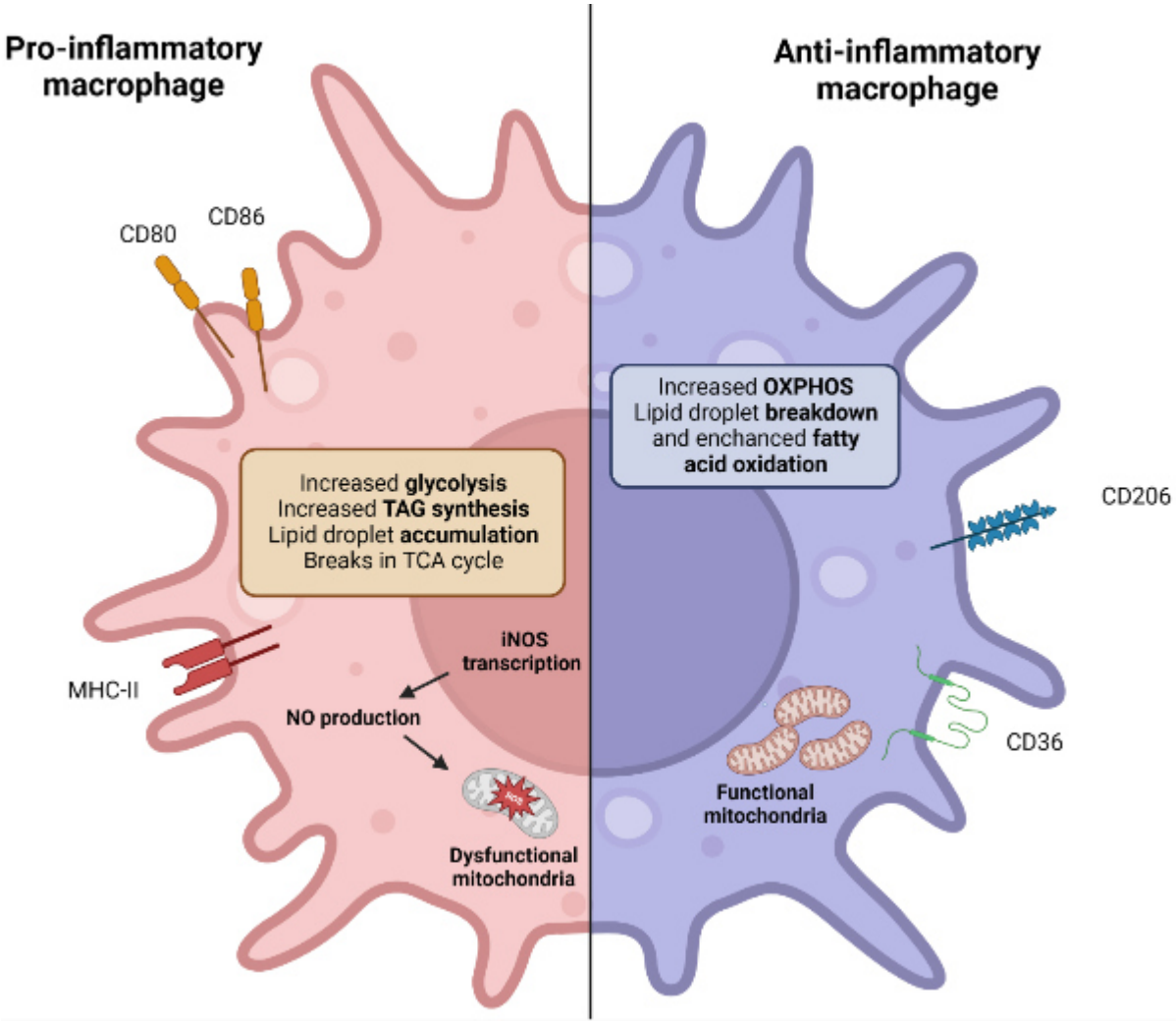

Figure 31. The metabolic signature of pro-inflammatory versus anti-inflammatory macrophages. Macrophages exhibit phenotypic plasticity and can detect stimuli and shift to a particular activation state in response, which is driven by shifts in metabolism. Pro-inflammatory macrophages are generally induced via the stimulation of LPS and IFN-γ, and undergo an increase in glycolysis, and actively dysregulation mitochondrial respiration via an increase in NO production from iNOS. They also exhibit breaks in the TCA cycle and increase in TAG synthesis and lipid droplet accumulation. Anti-inflammatory macrophages, conversely, upregulate the oxidation of fatty acids and predominantly rely on oxidative phosphorylation as their energy pathway.

The role of FAs in macrophage activation and immunometabolism has been an emerging area of research, and have distinct roles in both pro- and anti-inflammatory functions. As it stands, the catabolism of FAs is associated predominantly with anti-inflammatory activation, and FA synthesis is associated

with pro-inflammatory functions. During the pro-inflammatory activation of macrophages, LDs accumulate within cells and have even been used as a marker for the activation of macrophages and neutrophils (Bozza et al, 2009), but the mechanisms underlying this, and the purpose of this accumulation, remains unclear. Until very recently, it was uncertain whether the induction of LD formation was simply a consequence of both increased *de novo* FAS and a downregulation of FAO, or if these LDs, and FAs, were directly contributing to the inflammatory response of these macrophages. More research into this field has revealed 3 potential ways that LDs/FAs could be contributing to the immune response:

1. Recent evidence shows that LDs can house innate immune proteins and may act as platforms for different immune signalling cascades, including TLR7 and TLR9 signalling (Bosch et al, 2020)
2. LDs may act as reservoirs of FAs to be converted to inflammatory mediators and increase cytokine signalling (Dierendonck et al, 2022; Monson et al, 2021b)
3. FAs contribute to the formation of lipid rafts which are essential for many innate and adaptive immune signalling pathways (Carroll et al, 2018a; Kulkarni et al, 2022; Varshney et al, 2016)

Although LDs are a marker of macrophage activation and likely participate in immune responses, there are currently mixed reports on the contribution of *de novo* FAS to the formation of these LDs. Earlier papers reporting the use of carbon-labelled acetate tracing found an increase in *de novo* FAS in murine models of sterile inflammation and in human macrophages that contributed to lipid accumulation (Everts et al, 2014; Feingold et al, 2012; Im et al, 2011; Posokhova et al, 2008). Additionally, Srebp1-a, a regulatory protein involved in regulating FAS and cholesterol synthesis at the transcriptional level, positively regulates pro-inflammatory functions and is induced in LPS-treated mice. Mice with deficiency in Srebp1-a were unable to synthesise lipids and had lower secretion of cytokines and defective inflammasome signalling (Im et al, 2011). Contrastingly, a recent paper using ^{13}C-labeled glucose found that the increase

in TAGs was derived from increase glucose and exogenous FA import, rather than de novo FAS (Rosas-Ballina et al, 2020). Other studies have also found an increase in FA uptake via CD36 and glucose uptake via GLUT1 during pro-inflammatory macrophage activation, which contributed to LD accumulation (Feingold et al, 2012), although CD36 has also been implicated as an M2 marker (Orecchioni et al, 2019; Pennathur et al, 2015; Woo et al, 2016). Whilst lipid accumulation and FAS increase is a consistent observation in activated macrophages, the source and functions of these FAs may differ depending on stimuli and experimental conditions.

Aside from LD formation, other studies have implicated FASN as a mediator of pro-inflammatory macrophage functions. In mouse bone marrow derived macrophages (BMDMs), inhibiting FASN with c75 was found to reduce levels of IL-1β, TNF-α, and IL-6 secretion in response to LPS (Carroll et al, 2018a). The authors went further and made the novel discovery that FAS and cholesterol synthesis are linked via an intermediate metabolite of the FASN pathway, acetoacetyl-CoA, the production of which was inhibited with c75 treatment. The resulting disruption in cholesterol synthesis reduced the efficiency of lipid raft formation and associated TLR4 signalling, muting macrophage polarisation (Carroll et al, 2018a). In a diabetes model of infection, it was observed that *de novo* FAS was required for M1 macrophage activation, as synthesised FAs altered plasma membrane composition and allowed for the retention of cholesterol within the cells (Wei et al, 2016). Exogenous FAs altered the plasma membrane composition via the incorporation of unsaturated FAs, resulting in less inflammatory signals, highlighting the need for intrinsic FAS for macrophage activation. FASN and its products have also repeatedly been implicated in inflammasome activation (Gianfrancesco et al, 2019; Moon et al, 2015b; Wen et al, 2011).

To date, work on macrophage immunometabolism has almost exclusively been performed in the context of LPS/IFN-γ or sterile inflammation. The role metabolism and FAs play in both inflammation and Flavivirus infection in macrophages has not yet been explored. We understand from previous

observations in other cell types that both *de novo* FAs and LDs play integral roles in the Flavivirus life cycle, including replication complex formation, genome replication, and virion particle assembly. We additionally know that Flaviviruses can alter metabolism to support their replicative needs. For DENV, this manifests in increased oxidation of FAs and mitochondrial respiration in hepatic cells (Heaton & Randall, 2010), but upregulation of glycolysis has been reported in fibroblasts (Fontaine et al, 2015). For ZIKV, very recent research has demonstrated that the dysregulation of mitochondrial respiration may underpin inflammation and pathogenesis in both placental cells and *in vivo* (Chen et al, 2020; Yau et al, 2021).

Arguably, all Flaviviruses have a tropism for macrophages, and this cell type has been implicated in both pathogenesis as well as in effective viral clearance. It was previously observed that depletion of macrophage levels in mice resulted in an acceleration of WNV infection. Under these conditions, more mice displayed encephalitis and overall there was a 50 % increase in mortality, clearly demonstrating the importance of macrophages in immunity to WNV (Ben-Nathan et al, 1996). Contrastingly, migration of macrophages to the CNS and subsequent inflammatory activation has also been demonstrated to contribute to neuropathological damage and severe disease during WNV and DENV infection (Ashhurst et al, 2013; Getts et al, 2008; Yen et al, 2008). Many others have demonstrated both a protective or pathological role of inflammatory mediators including TNF-α, IL-6 and iNOS (Chen et al, 2007; Davison & King, 2011; Wang et al, 2007; Yeung et al, 2012), which seem to depend on both timing and concentration, but we postulate that other factors may be involved.

During infection, Flaviviruses drastically alter the lipid and metabolic landscape of infected cells. As macrophage activation phenotypes have stringent metabolic requirements which both support and define their functions, in this study we aimed to investigate if WNV and ZIKV altered the metabolic profile of infected cells, and to determine if these metabolic alterations influenced the polarisation state of macrophages. We focussed on *de novo* FAS and cellular respiration as these pathways have been strongly correlated with both successful Flavivirus

infection and effective immune responses. Our plan was to generate a FASN-knockout macrophage cell line using the CRISPR-Cas9 system, as well as chemical inhibitors of FA metabolism, to ascertain the contribution of these pathways to infection and immune responses. Overall, we confirmed that FAS is a critical requirement for Flavivirus infection of macrophages, consistent with our previous observations in Vero cells (Chapter 3). We additionally demonstrated a role for FAO in WNV and ZIKV replication, but intriguingly observed no significant virus-induced perturbations of mitochondrial respiration rates overall, and little effect on glycolysis. As perturbations in mitochondrial respiration underpin the inflammatory phenotype in pro-inflammatory macrophages, we postulated that the metabolic homeostasis induced by these viruses may be dampening immune responses. Despite this, we observed polarisation of macrophages to a pro-inflammatory state during infection, as assessed via the expression of macrophage surface markers, and we found that inhibiting FA metabolism had no effect on the expression of these markers. This indicates that *de novo* FAS, as well as FAO, is likely uncoupled to macrophage polarisation during infection. In addition to marker expression, in the future we would like to investigate if the lack of mitochondrial dysfunction in these infected macrophages results in the downregulation of cytokine signalling and production of free radicals, however overall it appears that these viruses are able to manipulate FA metabolism without further exacerbating the immune response.

4.2. Results

4.2.1. Infection is permissible and detectable in THP-1 macrophages

To begin our investigations into the role of metabolic pathways during Flavivirus infection of immune cells, we begun with a human monocyte cell model, THP-1. The THP-1 cell line has been used previously as a model for Flavivirus infection (Luo et al, 2018; Roby et al, 2016; Tiwari et al, 2017; Wen et al, 2022; Xie et al, 2015), however not in our lab or with the virus strains we were using. Thus, we first performed an optimisation experiment to determine infection kinetics, and to confirm that we could detect infection via our common assays, namely plaque assay and western blotting. As THP-1 is a monocyte-derived cell line, we began

each experiment by differentiating cells into macrophages using PMA for 24 hours, followed by removal of PMA-containing media and incubation with normal media for 24 hours (rest period). Cells were subsequently infected at 3 different MOIs (0.1, 1 and 5), and the supernatants were collected each day for 5 days for determination of infectious virus production via plaque assay. Cell lysates were additionally harvested each day for 3 dpi to determine the quantity of intracellular viral proteins. We observed an increase in infectious virus begin at 24 hpi for MOI of 0.1, indicating that virus production was taking place (Figure 32a). This increase continued until a peak in production of infectious virus occurred at 3 dpi, with a subsequent and continuous drop in titre thereafter (Figure 32a), which could be a result of the death of infected cells, or clearance of infection by these cells. An MOI of 0.1 resulted in the highest titre of about 6.5 $x10^6$ pfu/mL on day 3 for both WNV and ZIKV. Interestingly, for MOI 5 for both WNV and ZIKV, we saw maximal titre at days 1 and 2 post-infection with a decline thereafter, suggesting that the maximal amount of cells had been infected at this time point.

This mostly correlated to our western blot data, however in this experiment we could barely detect viral protein at an MOI of 0.1 via this method, but this was not an issue in subsequent experiments. For WNV, we observed a gradual increase in detectable viral envelope protein using a pan-Flavivirus anti-E antibody, peaking at day 2 and 3. For ZIKV we observed an accumulation of E protein that was higher at day 2 compared to day 3, suggesting that genome replication may cease at 2 dpi but secretion of infectious virus from cells continues until 3 dpi. This demonstrates that WNV and ZIKV may have slightly different infection kinetics in this cell type. Surprisingly, we were only able to detect infection with our most sensitive antibody, anti-E 4g2, and not with our anti-NS5 antibody which is known to detect NS5 produced from both WNV and ZIKV. For this reason, we utilised this anti-E antibody as our viral marker in subsequent experiments.

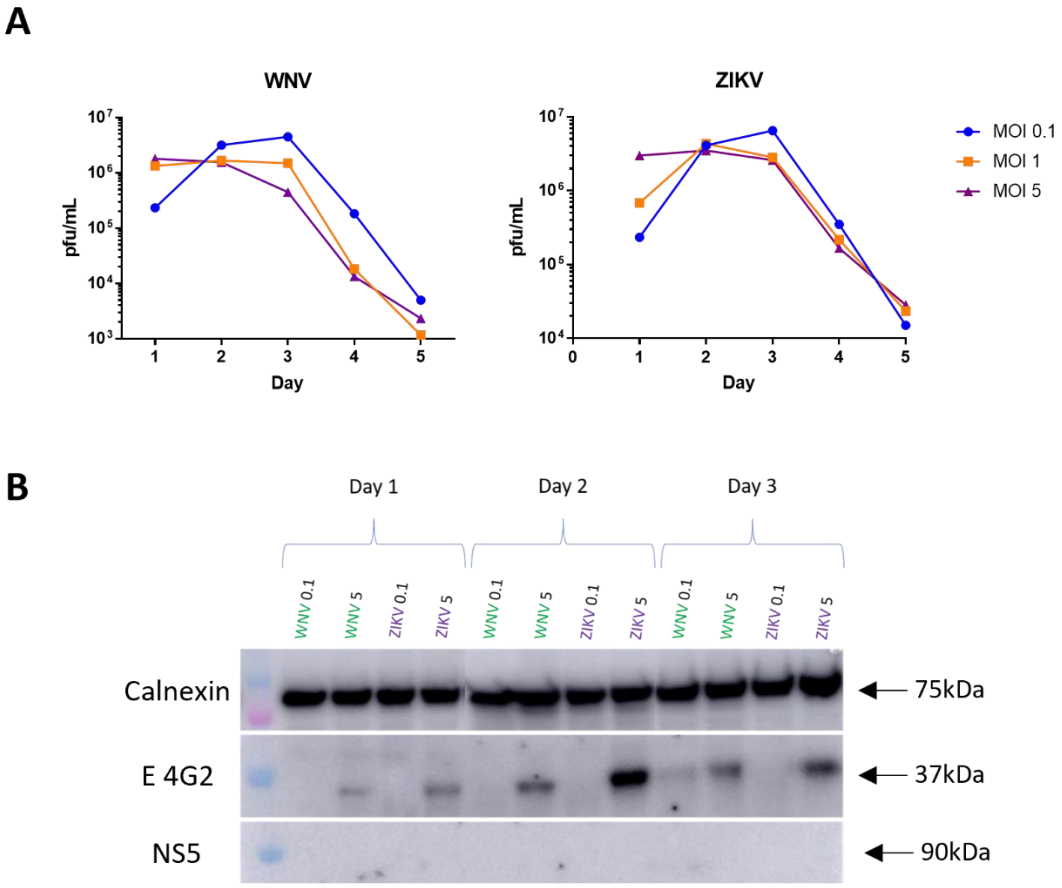

Figure 32. THP-1 cells are permissible to WNV and ZIKV infection. THP-1 cells were first differentiated with PMA for 24 hours, followed by 24 hours of rest in media not containing PMA. Cells were then infected with either WNV or ZIKV at 3 different MOIs, and supernatant and lysates were harvested at 1, 2 and 3 dpi. **(A)** Infectious virus production was measured via a plaque assay and viral titre was calculated, and graphed using GraphPad Prism 8. **(B)** A western blot was performed using the lysates and membranes were stained for viral E protein (E 4g2), viral NS5, and calnexin as the host marker.

4.2.2. FASN is upregulated during infection and is essential to Flavivirus replication in THP-1 cells

As we had observed that infection was robust and detectable in THP-1 cells we next aimed to determine if *de novo* FAS was essential for replication in this cell type. To investigate this, we assessed the impact of WNV or ZIKV infection on FASN expression using western blotting, and assessed the impact of two FASN inhibitors, c75 and orlistat, on viral replication. In our viral kinetics experiment above, we observed the most progressive increase in infectious virus production

at an MOI of 0.1 but had difficulty detecting this MOI via western blot. For this reason, we infected THP-1 cells with WNV and ZIKV at two different MOIs (0.1 and 5) to ensure we were capturing peak viral infection, and cell lysates were harvested at 3 dpi. Viral protein and FASN expression were then assessed via western blotting. Our results indicated that FASN expression was upregulated during infection, with >100 % increase in expression observed with both viruses at an MOI of 0.1, and up to a 250 % increase observed using an MOI of 5 (Figure 33a and b).

We next performed a cytotoxicity assay to determine the concentrations of each inhibitor, namely c75 and orlistat, that were tolerated by the THP-1 cells (Appendix B). To assay the impact of chemical inhibition of FASN activity on viral replication, we infected cells with WNV or ZIKV and treated cells with non-toxic concentrations of c75 and orlistat for 3 days before harvesting the supernatant to determine the viral titre via plaque assay. For WNV, we observed a significant drop of ~2 logs in viral titre upon c75 treatment, which correlates to a ~99 % reduction in infectious virus production (Figure 33c). With orlistat treatment we also observed a significant reduction in viral titre, with over a 1 log drop, equivalent to over a 90 % reduction in infectious virus. For ZIKV we surprisingly did not see a significant reduction in titre, however the trends were clear, with a 0.6 log drop in replication with c75, and nearly a 1 log drop for orlistat, correlating to a ~60 and ~90 % reduction in infectious virus, respectively (Figure 33c). Taken together with the FASN expression data, it appears that *de novo* FAS is required for the replication of both viruses in the THP-1 macrophages.

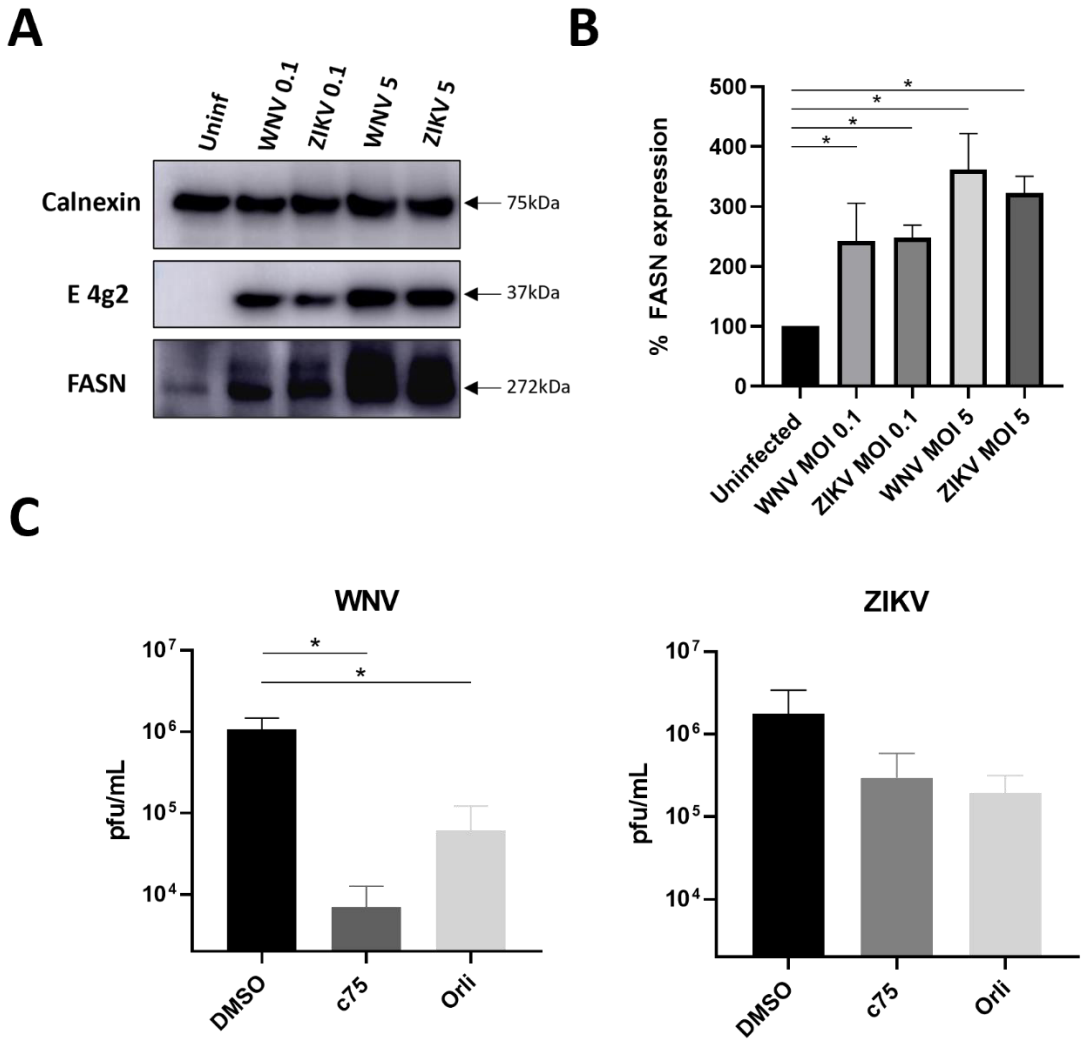

Figure 33. WNV and ZIKV infection in THP-1 cells upregulates FASN expression, and viral replication is perturbed with FASN inhibition. THP-1 cells were seeded and differentiated into macrophages via treatment with PMA for 24 hours, followed by 24 hours of rest. **(A)** Cells were then infected with WNV or ZIKV at either an MOI of 0.1 or 5, and left to infect for 3 days, after which cells were lysed and lysates were run on a western blot. Membranes were probed with either an anti-E4g2 antibody to detect viral infection, or an anti-FASN antibody to detect FASN. **(B)** FASN expression was quantified via densitometry using ImageJ software and statistical significance ($P \leq 0.05$), indicated using asterisks (*), was determined using an unpaired t-test (GraphPad Prism 8). Error bars are representative of 2 independent biological replicates (n=2, +/- SEM). **(C)** THP-1 cells were differentiated as above and infected with WNV or ZIKV at an MOI of 0.1, and treated with either c75 or orlistat for 3 days, after which supernatant was collected and viral titre was measured via plaque assay. Error bars are representative of 4 independent biological replicates (n=4, +/- SEM). Statistical

significance was determined using an unpaired t-test on the linear values (GraphPad Prism 8). * = $p \leq 0.05$

4.2.3. Initial validation of FASN-knockout THP-1 cells displayed a promising phenotype

To further confirm the role of *de novo* FAS during infection, we attempted to establish a FASN THP-1 knockout cell line using the CRISPR-Cas9 system. As FASN is a large, multifunctional protein (272 kDa), we designed guide RNAs (gRNAs) targeting 3 distinct regions of FASN (see Figure 34a) to improve the likelihood of generating successful knockout cells. gRNA1 targeted the 5' untranslated region (UTR), gRNA2 targeted the ketoacyl-synthase domain, and gRNA3 targeted the thioesterase domain. We cloned these gRNAs individually into a pFgh1tUTG-mCherry doxycyline-inducible lentiviral vector and transfected HEK293T cells with plasmid DNA to assemble lentiviral particles. Virus was harvested after 48 hours, and used to infect a THP-1 cell line stabling expressing Cas9-BFP. Cells were then sorted for mCherry fluoresence, and were subsequently treated with doxycycline to induce the gRNAs, and validated for a knockout phenotype via western blotting and flow cytometry. Western blotting revealed a very strong knockdown, but not compelete knockout of FASN for all three gRNAs upon doxycline induction (Figure 34b). This was supported by our results with flow cytometry that indicated >60 % reduction on FASN expression with the two gRNAs that we tested (Figure 34c). As FASN is ubiquitiously and constitutively expressed, and whole-body FASN knockout in mice is lethal, we presumed there may be a fitness cost associated with this knockout phenotype (Chirala et al, 2003), which may explain why we were unable to see a complete knockout.

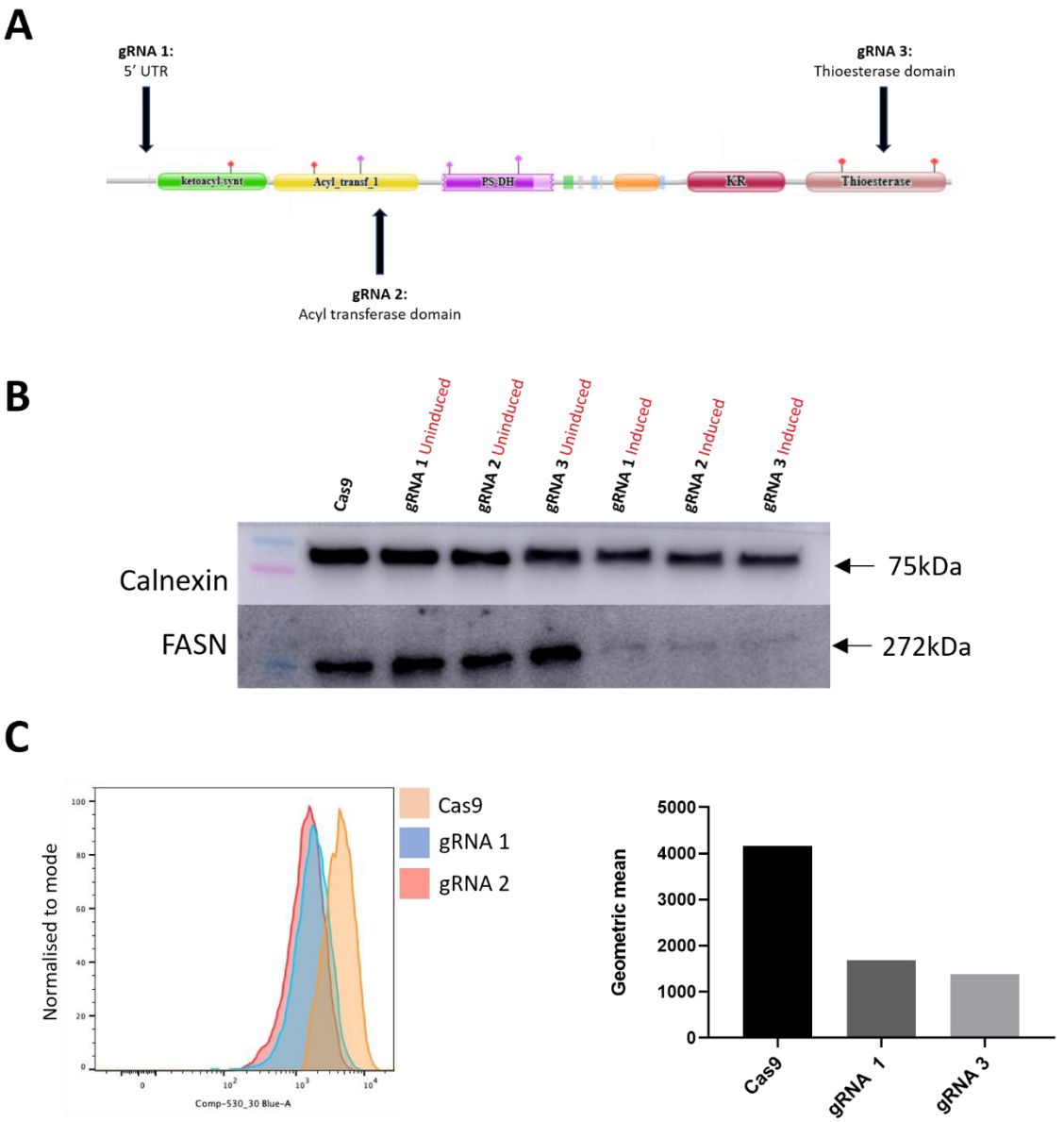

Figure 34. Validation of CRISPR-Cas9 knockout of fatty acid synthase in THP-1 cells. (A) gRNAs were designed to target three different domains of the FASN gene; the 5' UTR (gRNA 1), the ketoacyl-synthase domain (gRNA 2), and the thioesterase domain (gRNA 3). gRNAs were cloned into a lentiviral vector and transfected into Hek293T cells to produce infectious virus. This virus was used to infect a Cas9-BFP THP-1 cell line to generate the knockout cell line. **(B)** A subset of these cells were treated with doxycycline for 24 hours to induce the knockout, after which cell lysates were taken and a western blot was used to validate the knockout phenotype using an anti-FASN antibody. The original Cas9 cell line (not containing gRNAs), and the uninduced cells, were included as controls. **(C)** Doxycycline-induced cells and the original Cas9 cell line were analysed for FASN expression using flow cytometry using a BD LSR Fortessa

Cell Analyser. Cells were analysed and histograms created using FlowJo software. Bar graph was generated using GraphPad Prism 8.

4.2.4. Passaging of a heterozygous pool of knockout cells led to loss of FASN knockout phenotype

Despite the initial validation of the FASN gRNA expressing cells revealing a promising loss of FASN expression, subsequent passaging resulted in an apparent loss of this phenotype. Within a period of months, we observed a gradual increase in FASN expression with all cell lines expressing the 3 gRNAs, as assessed via western blotting (Figure 35a). As this was a heterogeneous pool of cells (not single cell-derived colonies), we surmised that this loss of phenotype was most likely due to a fitness cost of cells that had the knockout phenotype. Over time, it's likely that the cells not containing the knockout, or cells heterozygous for FASN, grew at a faster rate and resulted in an overrepresentation in the pool. We also performed immunofluorescence using our anti-FASN antibody, and observed little difference between the Cas9-THP-1 control and the putative FASN knockout cell lines, at which point we decided to reconsider our approach.

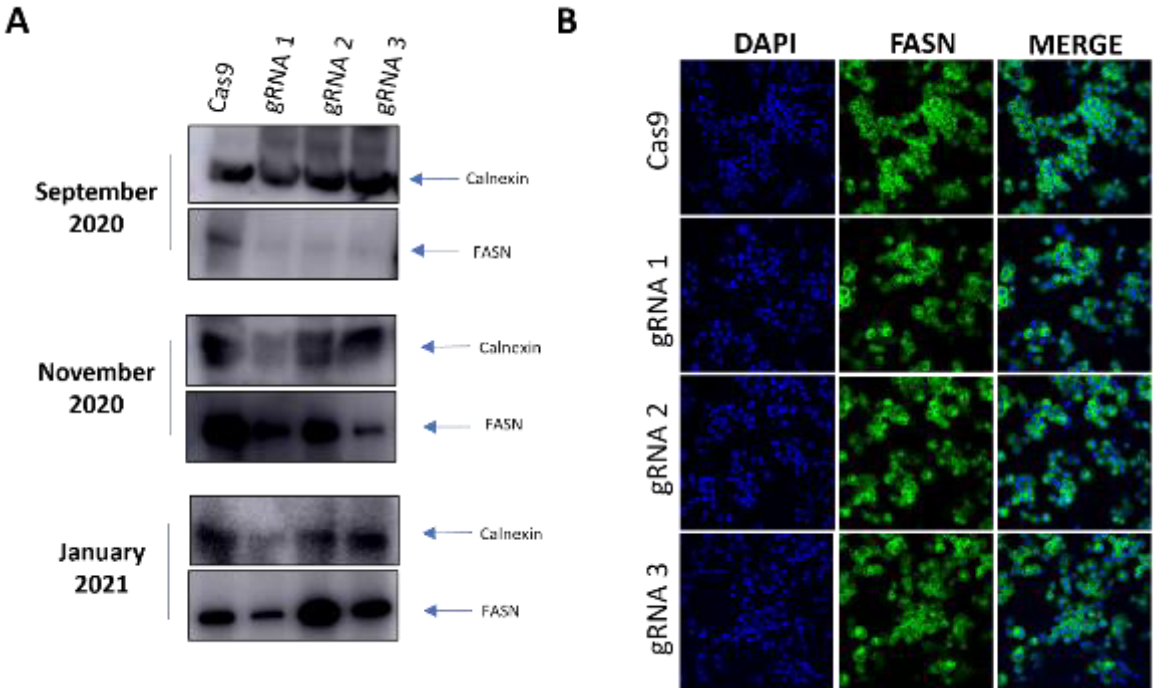

Figure 35. Continuous passaging of a pool of FASN knockout THP-1 resulted in a loss of knockout phenotype. (A) Cells were passaged over a number of months and FASN expression was continuously monitored via western blotting using an anti-FASN antibody and calnexin as the internal host control. **(B)** After months of passaging, FASN expression was also checked via immunofluorescence, immunostaining using anti-FASN antibody and nuclei were counterstained using DAPI. Images were taken on a Zeiss confocal microscope and images were analysed using Zen Blue software.

4.2.5. Validation of single cell clones indicates FASN knockout

As FASN expression increased in our pool of cells over time, we decided to isolate FASN KO cells via single cell cloning. Thus, we re-infected our Cas9 THP-1 cells with our gRNA-containing lentivirus, and sorted cells into 96-well plates at ~1 cell per well. We expanded ~80 colonies for each gRNA, induced them with doxycycline, and validated them first via PCR (Figure 36a) using FASN primers we had designed previously. This method proved to be a successful means of quickly phenotyping these cells, and we observed many promising knockouts during this initial screening and further validated these cells using western blotting (Figure 36b) Clones from gRNA 1 and gRNA 2 appeared to generate cells with the greatest level of FASN reduction, with colonies from gRNA 1 exhibiting

extremely limited FASN expression when compared to the Cas9 control. We chose a subset of these to continue with our infection experiments.

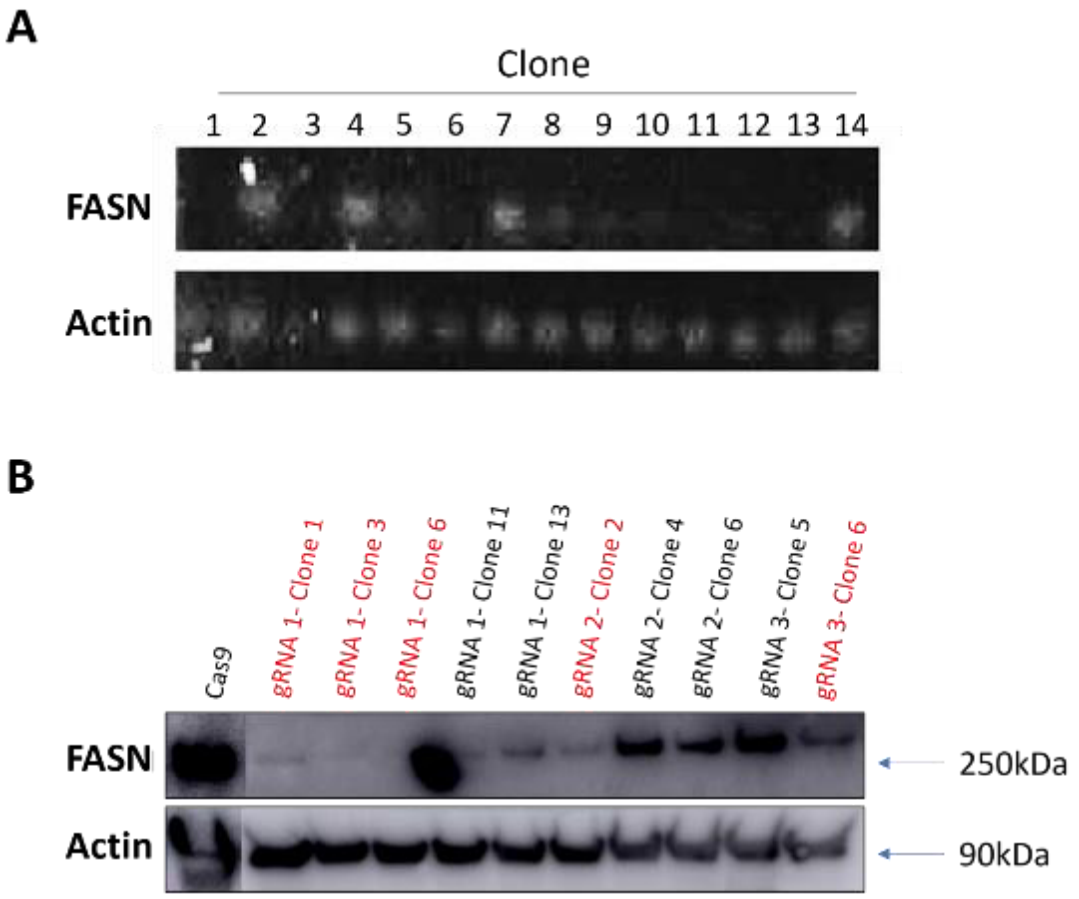

Figure 36. Validation of FASN expression in single cell clones revealed a promising knockout phenotype. Singe-cell derived clonal populations (clones) of FASN-knockout THP-1 cells were initially validated via PCR using FASN primers **(A),** then subsequently validated via western blotting using an anti-FASN antibody and an anti-calnexin antibody as the loading control **(B).**

4.2.6. Infection of single cell clones suggests FASN expression and activity is essential for replication

We infected two cell line clones that exhibited the greatest level of FASN knockout, namely gRNA 1 clone 1 (G1C1) and gRNA 1 clone 3 (G1C3), with WNV and ZIKV for 3 days and assessed infectious virus production via plaque assay. Our results revealed >60 % reduction in infectious virus for both WNV and ZIKV upon infection of the G1C1 cells, but notably we observed no infectious viral particles produced upon infection of the G1C3 cell line (Figure 37). Overall, our

data is consistent in showing that FASN is essential for replication of WNV and ZIKV in THP-1 macrophages, and that our CRISPR-Cas9 knockout approach generated two stable FASN knockout clones useful for our subsequent studies.

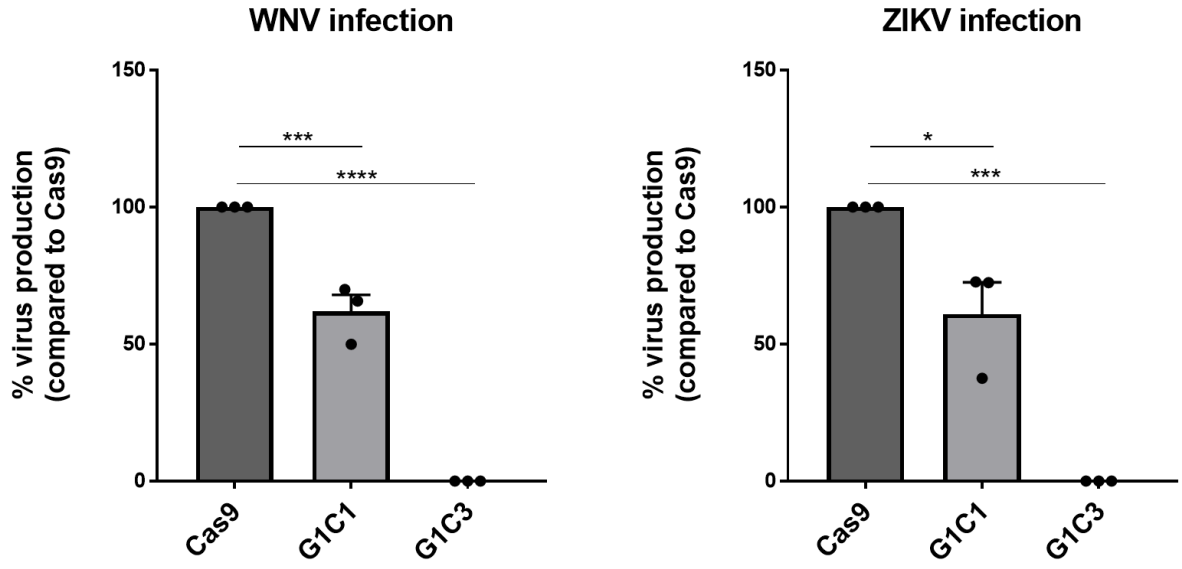

Figure 37. Infection of two FASN knockout THP-1 clones suggests FASN is indispensable for replication of WNV and ZIKV in macrophages. THP-1 cells expressing the Cas9 vector, and two generated FASN knockout cell lines were infected with WNV or ZIKV at an MOI of 0.1 for 3 days. Supernatant was subsequently harvested, and infectious virus production was measured via plaque assay. Viral titres were used to calculate the % of virus production compared to the THP-1 Cas9 control, and the results were graphed and analysed for significance using GraphPad Prism 8. Error bars are indicative of 3 independent biological replicates (n=3, +/- S.E.M) and statistical significance ($p \leq 0.05$) is indicated with an asterisk. * = $p \leq 0.05$, *** = $p \leq 0.0001$, **** = $p < 0.0001$.

4.2.7. Macrophage markers are unable to be detected in THP-1 cells via flow cytometry

After establishing a knockout cell line and confirming the reliance of FASN during infection, we next aimed to assess the role and potential contribution of FASN in promoting inflammatory activation of macrophages during infection. Our plan was to infect the WT and FASN KO cells and subsequently treat them with our FASN inhibitors, and measure the expression of pro-inflammatory and anti-inflammatory

macrophage markers via flow cytometry. We began by performing an optimisation experiment to confirm we could detect our chosen markers via this method. Based on the literature and advice, we chose several classical markers of pro-inflammatory macrophage activation (CD86, CD80, HLA-DQ), and one anti-inflammatory macrophage marker (CD206). We polarised cells to a pro-inflammatory state using LPS and IFN-γ, and to an anti-inflammatory state using IL-4, both well-established methods and markers of macrophage polarisation in this cell type (Baxter et al, 2020; Chanput et al, 2010; Chanput et al, 2013; Genin et al, 2015; Tedesco et al, 2018). However, upon performing these initial experiments we were unable to detect any significant increase in any of the markers during either stimulation (Figure 38).

We performed several rounds of optimisation, changing many parameters including PMA concentration, LPS/IFN-γ and IL-4 concentration, time of incubation with these stimulants, and concentrations of our markers, but to no avail. We additionally included HLA A-B-C (MHC-I, highly expressed in activated macrophages) as a positive control to confirm that the issue was not our harvesting or staining protocol. Upon activation with LPS/IFN-γ, we observed a drastic increase in the surface expression of HLA A-B-C, with nearly the entire population of cells expressing this marker when activated (Figure 38). This indicated that our protocol was sufficient to detect surface markers, indicating that difficulties in detecting CD86, CD80, HLA-DQ and CD206 were an inherent issue with the cell lines we were using. These antibodies were gifted to us from the Brooks Lab (Doherty Institute), who were able to detect these markers on primary human cells, so the issue was clearly low surface marker expression in the THP-1 cell type.

In the literature, it has been reported that the expression profile of markers in THP-1 cells can vary greatly. Their inflammatory profile is less pronounced than primary monocyte-derived macrophages (MDMs), and the markers used and detected varied between labs (Tedesco et al, 2018). We were aware of this during our experimental design, but chose markers and protocols that were as consistent as possible with previous studies. Despite this, we were unable to

optimise this experiment so we decided not to investigate and pursue this further. We additionally struggled to detect infection during FACS as well using several different viral markers. For these reasons combined, and in the essence of time, we decided to switch to a different macrophage cell line to complete the remaining experiments.

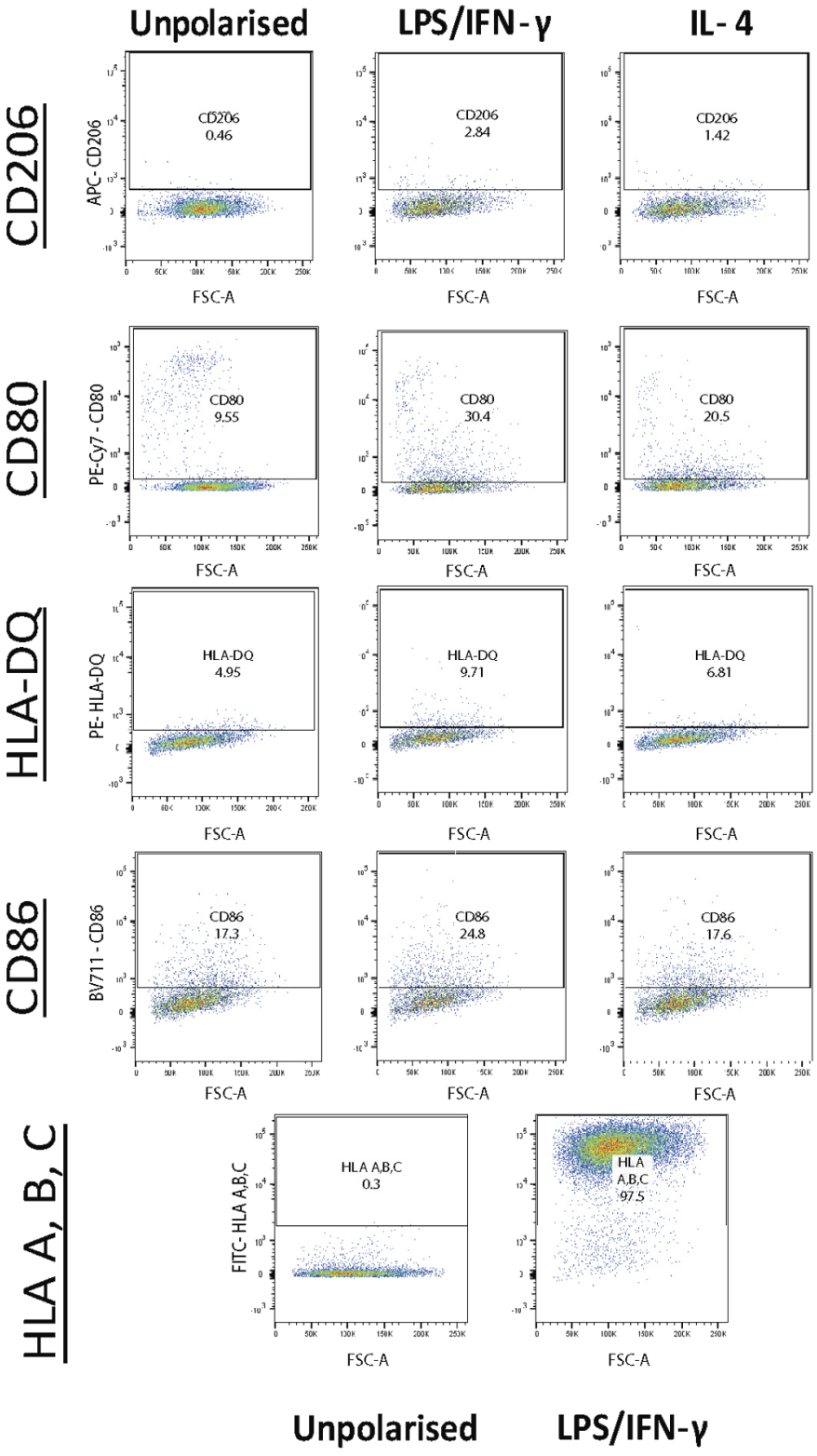

Figure 38. Classic macrophage markers are unable to be detected in THP-1 cells via flow cytometry. THP-1 cells were differentiated with PMA for 24 hours and left to rest for 24 hours, before either being left untreated or stimulated with

LPS-IFN-γ (concentration here) or IL-4 (concentration here) for a further 24 hours. Cells were then harvest and immunolabelled with antibodies to detect the pro-inflammatory markers CD80, CD86, HLA-DQ (MHC-II) or HLA-A,B,C (MHC-I), and the anti-inflammatory marker CD206. Samples were analysed for fluorescence via flow cytometry, using the BD LSR Fortessa Cell Analyser. Gating and dot plots of the fluorescence for each marker were then analysed using FlowJo software. These images are representative of at least 4 independent experiments.

4.2.8. Infection is permissible and easily detected in RAW 264.7 macrophages

After determining that our macrophage polarisation experiments were not feasible in our derived THP-1 cells, we utilised another immortalised cell line and one commonly used in our lab *i.e.* RAW 264.7 cells, a mouse macrophage cell line. The benefits of using this cell line included the absence of a differentiation step, and macrophage polarisation protocols were abundant in the literature. Additionally, mouse models of Flavivirus infection are very common to understand viral pathogenesis and host immune activation. We were able to establish that infection was permissible in this cell type, with infection easily detected at 24 h.p.i. via western blotting with our anti-NS1 antibody at both MOIs of 1 and 5 (Figure 39a). As we were only able to detect viral E in THP-1 cells (Figure 32), which is our most sensitive antibody against Flaviviruses, this data already indicated that RAW264.7 cells may be more permissible to infection. We also determined that infection was detectable via flow cytometry (Figure 39b), as this would be necessary for our macrophage polarisation experiments. After 24 hours of infection, we were able to detect NS1 expression via FACS, with up to 75 % of cells infected with WNV and 50 % for ZIKV after 24 hours of infection (Figure 39b). We additionally determined the efficacy of our viral markers in this cell type for immunofluorescence and observed that multiple antibodies that we had in-house were able to detect infection (Figure 39c). Using NS1 and dsRNA, for both viruses (data not shown for ZIKV) we observed the distinct spherical donut-like structures that are indicative of the viral RCs, suggesting that replicative processes in this cell are similar to that of human cells, and lipids are

likely required. Taken together, this data confirmed that this cell line would be an appropriate model to undertake the remaining experiments.

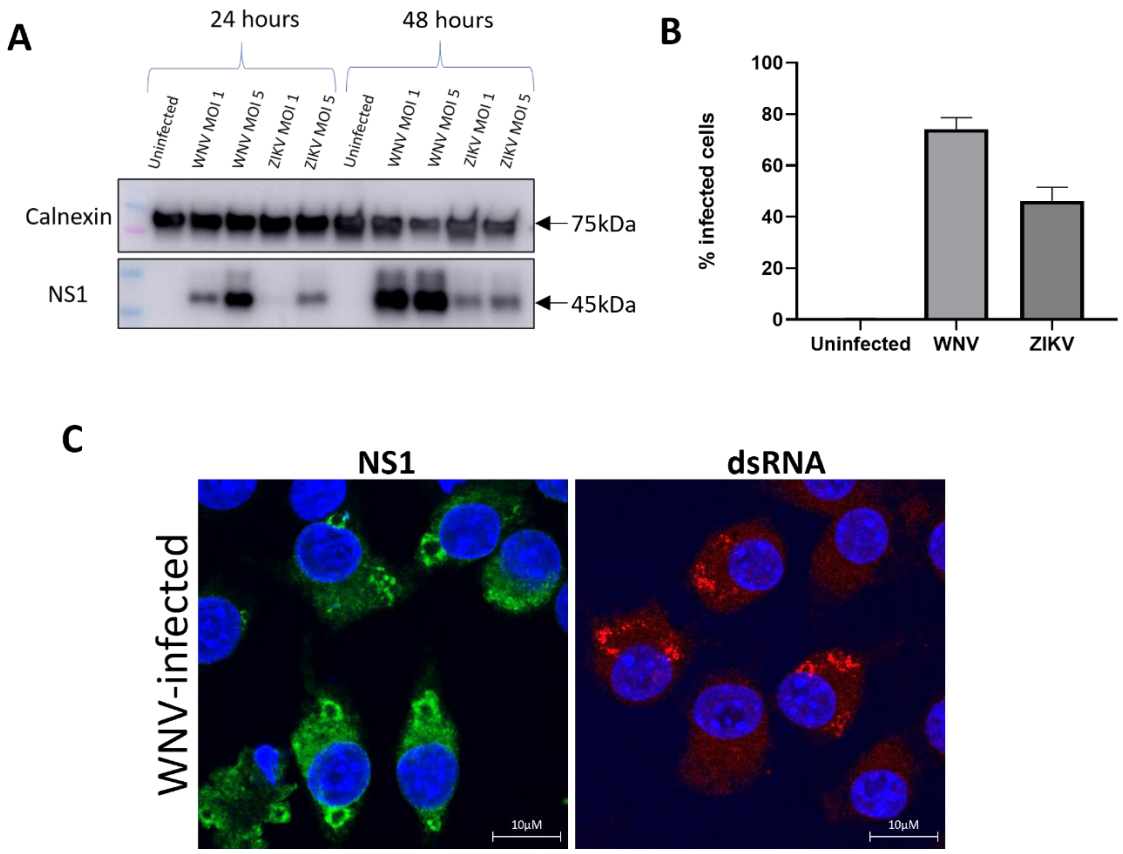

Figure 39. Infection of WNV and ZIKV is permissible and easily detected in RAW264.7 macrophages. (A) RAW264.7 cells were infected with WNV or ZIKV at an MOI of 1 or 5, and cell lysates were taken after 24 and 48 hours. Expression of calnexin and NS1 were assessed using a western blot and antibodies specific to these proteins. **(B)** Cells were infected with WNV or ZIKV at an MOI of 5 and left to infect for 24 hours. Cells were then fixed, permeabilised and stained with an anti-NS1 antibody, and analysed via flow cytometry using a BD LSR Fortessa Cell Analyser. Percentage of infected cells was determined using FlowJo software and graphed using GraphPad Prism 8. Error bars are indicative of 3 independent biological replicates (n=3, +/- SEM). **(C)** Cells were seeded on coverslips and infected with WNV or ZIKV for 24 hours at an MOI of 5, after which cells were fixed with PFA, permeablised with Triton-x and immunostained with either an anti-NS1 antibody (green), or one of two dsRNA antibodies (J2 clone (red) or IgM (grey)). Hoechst was used to stain nuclei (blue). Images were taken on a Zeiss confocal microscope and images were analysed using Zen Blue software.

4.2.9. FASN is upregulated during infection and co-localizes with viral replication complexes in RAW264.7 cells

Having confirmed detection of the viral markers was possible in the virus-infected RAW264.7 cells, we first begun to assess the role of *de novo* FAS by assessing the localisation and expression of FASN during infection. Thus, we immunostained WNV- and ZIKV-infected cells with anti-dsRNA antibodies (red) to visualise the viral RCs, anti-FASN antibodies (green), and the stain DAPI (blue) to visualise nuclei. As we have observed previously in Veros (Fig. 16a), FASN has a diffuse and cytoplasmic distribution in uninfected cells (Fig 40a, panels b, d). During infection with WNV, as seen previously, we observed very distinct donut-like RC structures in a high proportion of cells stained with the anti-dsRNA antibodies (Figure 40a, panel g). We additionally observed a degree of co-localisation between FASN and dsRNA, with yellow hues indicating co-localisation (40a, panel h). The distribution of FASN changes slightly up WNV infection, with FASN staining in a ring-like pattern around the RCs, and small vacuoles visible (40a, panel h and inset image). During ZIKV infection we again observed distinct RC structures, with co-localisation between dsRNA and FASN, but these vacuoles were not present to the same degree as for WNV (Figure 40a, panels j-l). Quantification of FASN fluorescent intensity from our IFA images indicated a significant increase in FASN expression in infected cells during infection with both viruses (Figure 40b). Overall, this data is consistent with a role for FASN in viral RC morphogenesis in murine macrophages.

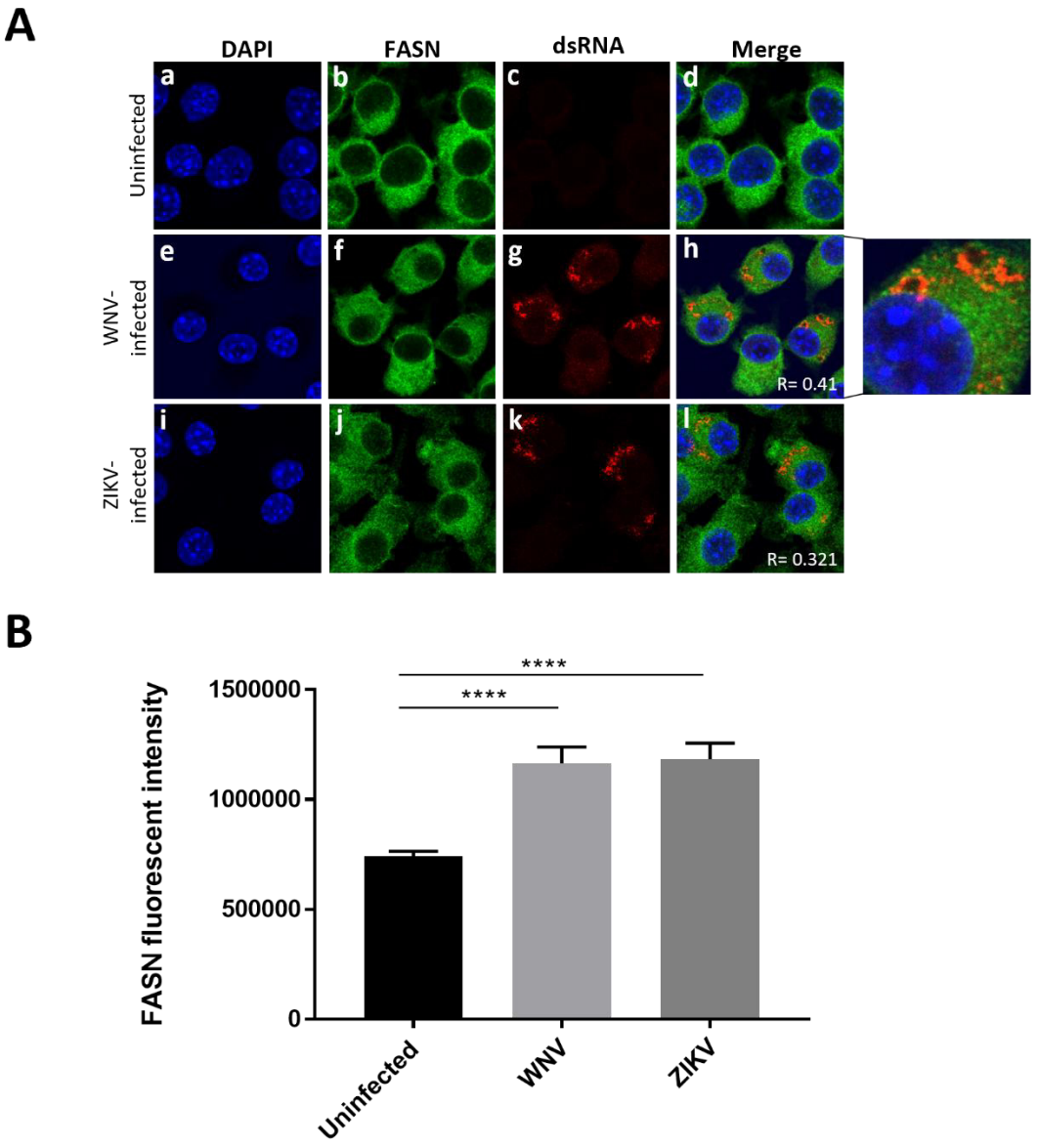

Figure 40. FASN is upregulated during infection with WNV and ZIKV and co-localises with viral replication complexes. Cells were infected with WNV or ZKV at an MOI of 5 for 24 hours. **(A)** Cells were fixed onto coverslips, permeabilised and stained with anti-dsRNA (red), FASN (green), and counterstained with DAPI (blue). Images were taken on a Zeiss confocal microscope and analysed using Zen blue software. **(B)** FASN fluorescent intensity was quantified using a macro and ImageJ software, from 470 uninfected, 72 WNV-infected and 69 ZIKV-infected cells over two independent biological replicates. Results were graphed and analysed for statistical significance using an unpaired t-test (GraphPad Prism 8). **** = $p < 0.0001$

4.2.10. Inhibiting fatty acid synthesis via ACC inhibition attenuates replication in mouse macrophages

To confirm the role of *de novo* FAS during infection, we utilised all our available inhibitors of these pathways, namely TOFA, c75, and orlistat, and additionally included etomoxir as an inhibitor of FAO, to again allow us insight into the fate of these FAs. We infected and treated RAW264.7 cells for 24 hours, harvested cell lysates and supernatant, and determined the impact of the inhibitors on infection via western blot and plaque assays. Our western blot data indicated that inhibiting the rate limiting step of FASN using TOFA severely attenuated viral replication in a dose-dependent manner for both viruses (Figure 41a and b). At the highest concentration of 10 μM, TOFA resulted in a ~95 % reduction in NS1 expression. Treatment with our FASN inhibitors c75 and orlistat, however, surprisingly did not result in a significant reduction in NS1 expression. Previous work has demonstrated a 75 % reduction and 44-90 % reduction of cellular FAs during orlistat and c75 treatment respectively. It's possible that an increase in FASN expression and activity during infection may be resulting in a relative insensitivity of these inhibitors, as postulated by others (Royle et al, 2017). To properly assess this, we would need to assay the impact of these inhibitors on FASN enzymatic activity (an assay we were unable to establish) or FA production (lipidomics). In an attempt to increase the sensitivity of the viruses to our FASN inhibitors, we additionally performed an experiment whereby we pre-treated cells for 2 hours prior to infection, to determine if this earlier blockade in FASN activity would hinder the virus to a greater extent, but this did not result in increased viral inhibition (data not shown). As our inhibitors are usually added after 2 hours of virus incubation and attachment/entry, these pre-treatment results further indicate that FASN is not required for the viral entry into cells. Interestingly, we did observe a significant reduction in NS1 expression with etomoxir for WNV, suggesting the oxidation of FAs may be important for this virus in this cell type (Figure 41a and b).

When we assessed virus production using plaque assay we observed a significant reduction with the higher concentration of TOFA, with approximately a 1 log drop (~90 % reduction) in viral titre for WNV, and slightly less for ZIKV

(Figure 41c). Interestingly, we observed a significant effect on virus production with orlistat for both viruses, suggesting that this inhibitor may affect virion particle formation or secretion, but does not interfere with earlier replicative processes. We additionally observed a significant reduction (~1 log or 90 %) with etomoxir for ZIKV but surprisingly not for WNV (Figure 41c). Overall, our data with TOFA suggests that the *de novo* FAS pathway is utilised and is essential for replication with WNV and ZIKV, which is consistent with what we observed in Veros and with what has been seen previously in the literature for other cell types. This has not, however, previously been demonstrated in macrophages. Our observations with etomoxir also suggest that FAO may be important for the replication of WNV, and virus production for ZIKV.

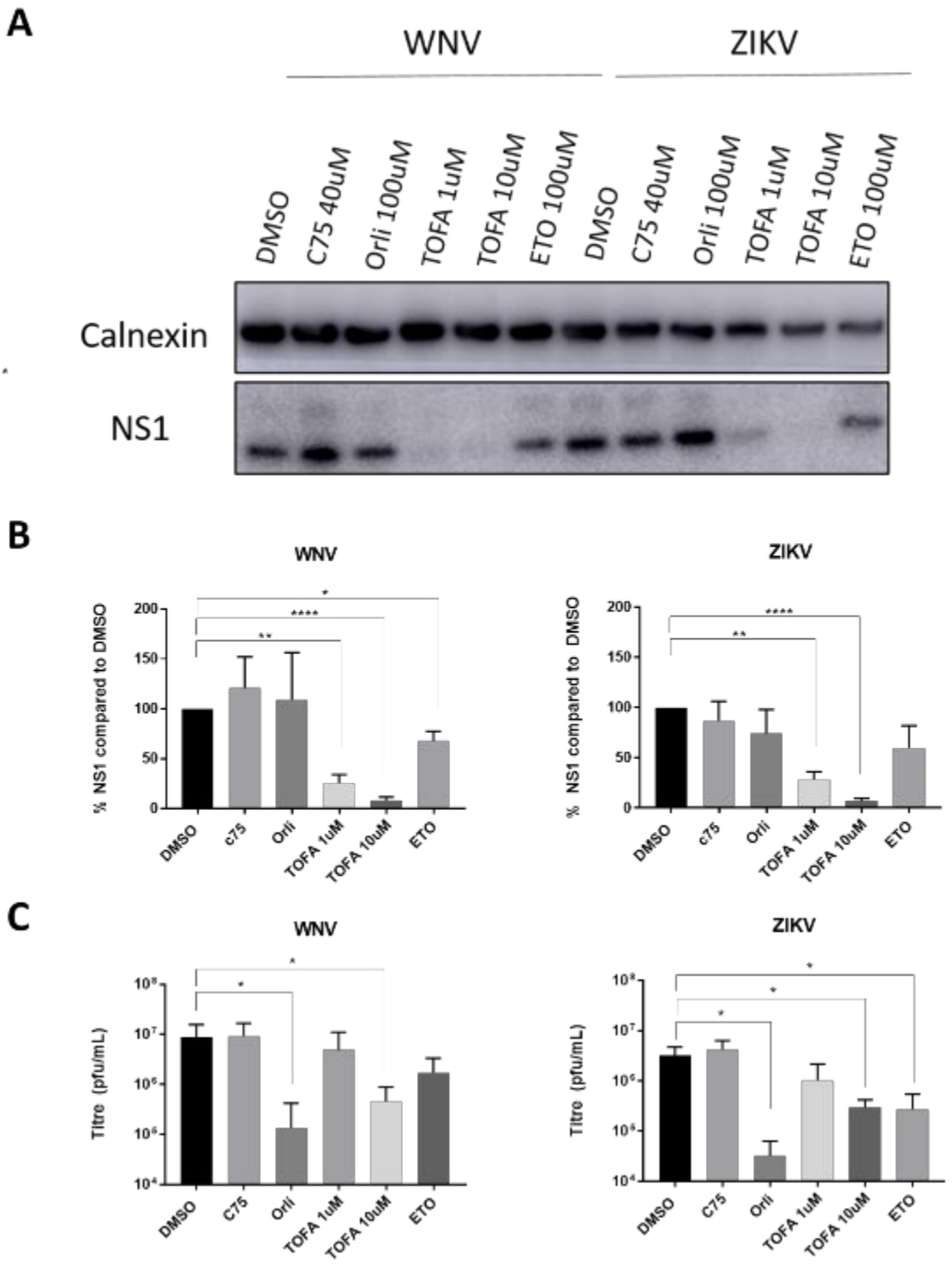

Figure 41. Inhibition of ACC, but not FASN, significantly attenuates viral replication. Cells were infected with WNV or ZIKV at an MOI of 5, treated with each inhibitor (c75=30 μM, orlistat=100 μM, TOFA as indicated, etomoxir=100 μM) and left to infect for 24 hours. **(A)** Whole cell lysates were taken and calnexin and NS1 expression were analysed via western blot, with antibodies specific to these proteins. **(B)** Protein expression was quantified from the western blot via

densitometry using ImageJ software, and error bars are indicative of 3 independent biological replicates (n=3, +/- SEM). **(C)** Supernatants were taken from infected cell after 24 hours and viral titre was quantified using a plaque assay. Error bars are indicative of the mean of 3 independent biological replicates (n=3, +/- SEM), and in all cases statistical significance was analysed using a one-way ANOVA and multiple comparisons (GraphPad Prism 8). * = $p \leq 0.05$, ** = $p \leq 0.001$, **** = $p < 0.0001$

4.2.11. Inhibiting ACC disrupts viral replication complex formation

During infection with WNV and DENV, it is accepted that *de novo* FAS contributes to replication likely through the involvement of FA substrates for viral RC morphogenesis. To assess whether inhibition of this pathway affected RC formation during WNV and ZIKV infection of macrophages, we performed immunofluorescence and stained infected cells with anti-dsRNA antibodies (Figure 42). We treated the infected cells with each inhibitor or with DMSO as the vehicle control. In the infected and DMSO-treated cells we observed that dsRNA was distributed as small perinuclear punctae indicative of viral RCs, with multiple generally visible within each infected cell (Figs 42b and h). Upon treatment with c75 or orlistat we observed no distinguishable effect compared to DMSO alone, with the dsRNA puncta visibly intact and multiple RCs observed per cell (Figure 42c, d, I and j). In contrast, when we completely inhibited FAS using TOFA we observed very little dsRNA staining and did not observe the formation of any distinct viral RCs (Figure 42e and k). We observed slightly less infected cells with etomoxir compared to the DMSO control, although the viral RCs were clearly evident (Figs 42f and l). Overall, this data is consistent with our western blot and plaque assay results, and it is evident that inhibiting FAS with TOFA is rendering the virus unable to form RCs, thereby reducing replication in the murine macrophages.

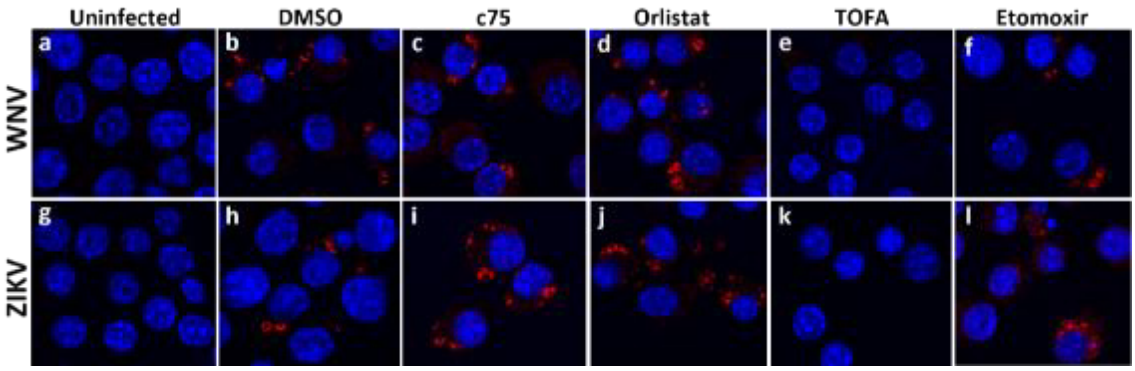

Figure 42. Inhibition of ACC using TOFA results in inability of WNV and ZIKV to form replication complexes in macrophages. RAW264.7 cells were seeded on coverslips, infected with WNV or ZIKV and treated with different metabolic inhibitors for 24 hours (c75=30 μM, orlistat=100 μM, TOFA=10 μM, and etomoxir=100 μM). Cells were then fixed, permeabilised and stained with an anti-dsRNA antibody and visualised with species-specific IgG conjugated to AF594 (red) and counterstained with DAPI to visualise nuclei (blue). Images were taken on a Zeiss confocal microscope and imaged using Zen Blue software.

4.2.12. Lipid droplets are upregulated in response to infection and pro-inflammatory stimuli

In addition to *de novo* FAS, we additionally wanted to ascertain whether WNV and ZIKV utilised LDs during replication in macrophages. The role of LDs in both infection and immunity is an emerging field, with the function of LDs differing depending on the pathogen, cell type and metabolic conditions being investigated. Indeed, even for Flaviviruses, contradicting roles have been identified in this area. LD levels have been observed to decrease during infection of hepatic cells with DENV and ZIKV (García et al, 2020; Heaton & Randall, 2010), whilst an increase in LDs in response to DENV, WNV and ZIKV infection has been documented in various other cell types (Monson et al, 2021a; Samsa et al, 2009). We additionally know that LDs can have pro-inflammatory roles, and for WNV and ZIKV have been shown to increase type-I and type-III IFN signalling and restrict viral replication (Monson et al, 2021a). LD content is also upregulated during pro-inflammatory macrophage activation. As the metabolic response of macrophages to Flavivirus infection, including LD accumulation, has not been categorised, we aimed to determine the impact of infection on LD dynamics. We

aimed to investigate whether infected macrophages would upregulate LD formation as a general inflammatory response and defence mechanism, or if infection and replication of WNV or ZIKV would exploit LDs, and potentially deplete them as an immune evasion strategy.

To investigate our aims, we utilised both flow cytometry and IFA to determine the impact of infection on LD formation and abundance. We included both LPS and LPS+IFN-γ stimulation as a positive control, to confirm that pro-inflammatory stimulation resulted in the induction of LDs in this cell type. For our flow cytometry analyses we quantified LD content at both 12- and 24-hours post-infection using BODIPY. We observed a significant increase in LD accumulation in response to both LPS and LPS+IFN-γ after 12 hours post-stimulation (1.8-1.9-fold increase respectively) (Figure 43a). We did not observe a further increase from 12 to 24 hours, suggesting that LD accumulation may be triggered in the early stages of the immune response (as early as 2 hours), as has been seen by others (Monson et al, 2021a). During infection, we observed a similar degree of LD induction at 12 hours post-infection, with a 1.6-fold increase for WNV and 1.7-fold for ZIKV (Figure 43b). During WNV infection we observed a slightly greater increase at 24 hours, and slight reduction with ZIKV compared to 12 hours post-infection, but we still observed a significant increase overall compared to uninfected cells.

Overall, it appeared that LDs accumulated within both activated (LPS and LPS+IFN-γ) and infected cells. Infection with either virus did not result in the reduction of LD content at either of the timepoints assayed, suggesting that they are likely not being metabolised by WNV and ZIKV. This data also indicates that LDs may not be exploited for replication or to enhance metabolism by the viruses, however, we have not excluded the possibility that the LDs are being utilised as platforms for viral assembly, as has been observed by others for ZIKV and DENV in different cell types (Samsa et al, 2009; Shang et al, 2018). As we see a similar level of LD induction between infected and activated macrophages, it appears likely that LD induction may be a result of general inflammatory activation of these macrophages.

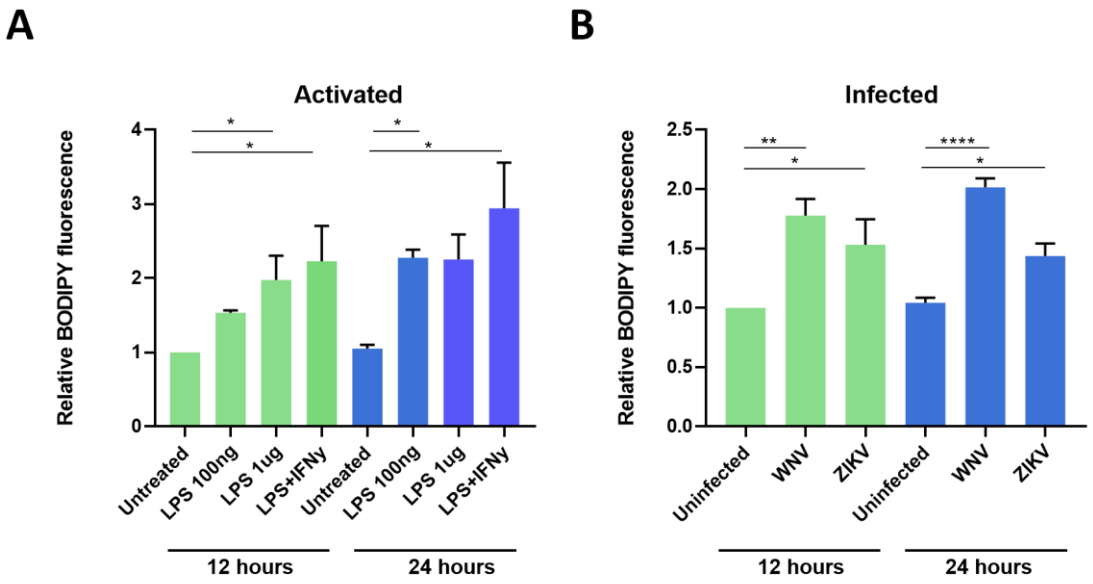

Figure 43. Lipid droplets accumulate during infection with WNV and ZIKV, and in response to inflammatory stimuli. (A) RAW264.7 cells were stimulated to a pro-inflammatory state with either LPS at varying concentrations, or with LPS (1 µg) and IFN-γ concurrently. **(B)** Another subset of RAW264.7 cells were infected with WNV and ZIKV. After 12 or 24 hours, activated or infected cells were fixed, permeabilised, and stained using BODIPY 493/503 to quantify lipid droplets. Cells were analysed via flow cytometry using a BD LSR Fortessa Cell Analyser and FlowJo, and MFI values were used to calculate relative BODIPY fluorescence. Error bars are indicative of the mean of 3 independent biological replicates (n=3, +/- SEM), and in all cases statistical significance was analysed using a one-way ANOVA and multiple comparisons (GraphPad Prism 8). * = $p \leq 0.05$, ** = $p \leq 0.001$, *** = $p \leq 0.0001$.

4.2.13. Flavivirus infection of macrophages does not perturb mitochondrial respiration

So far, we ascertained that *de novo* FAS is integral for the replication of WNV and ZIKV in macrophages, and our data with etomoxir additionally suggested that FAO may be involved in the life cycle of these viruses. As pro-inflammatory and anti-inflammatory macrophages have divergent and stringent metabolic requirements, we aimed to interrogate the impact of infection on these cellular respiration. We had originally hypothesised that Flaviviruses may upregulate mitochondrial respiration in this cell type, as has been observed with DENV in hepatic cells, potentially pushing the cells into an anti-inflammatory phenotype.

Conversely, if WNV and ZIKV were stimulating FAS and glycolysis, they could be driving an inflammatory response. As we did not observe a decrease in LD content during infection, it is unlikely that the autophagy of LDs would be contributing to increased metabolic rates. However, it is still possible that *de novo* FAS is being used to fuel mitochondrial respiration, or infected cells could be increasing the import of FAs which is boosting metabolism. To assess the impact of infection on metabolism, we used the Seahorse XF Mito Stress Test Kit, which gives a measurement of both OCR and ECAR, giving us insight into mitochondrial respiration and glycolytic rates, respectively (Figure 44). Surprisingly, our results indicated no significant change in OCR during infection at any of the parameters investigated, including basal and maximal respiration rates (Figure 44a and b). Interestingly though, we did observe an increase in spare respiratory capacity (SRC) for WNV. In contrast, we also observed a significant increase in basal ECAR for WNV, with a similar trend for ZIKV, indicating increased glycolysis upon infection (Figure 44c and d). Whilst our ECAR results were mostly consistent with the phenotype of pro-inflammatory macrophages, our OCR results are more consistent with an anti-inflammatory phenotype.

In addition to our observations with the Seahorse assay, we used immunofluorescence and flow cytometry to investigate any changes in mitochondrial morphology and mass that may be associated with infection. For these analyses we used MitoTracker™ Red CMXRos, a dye that stains mitochondria within live cells, and is dependent on mitochondrial membrane potential (Figure 45). We observed that infection of RAW264.7 cells with either WNV or ZIKV had no discernible impact on the morphology of mitochondria (Figure 45a). When we quantified MitoTracker™ Red CMXRos via flow cytometry, however, we did observe a significant increase for WNV (Figure 45b), indicating an increase in mitochondrial mass during infection. Shifts in mitochondrial respiration and physiology underpin the activation of macrophages and contribute to their inflammatory functions. It thus appears that WNV and ZIKV do not induce the same perturbations observed in pro-inflammatory macrophages, although our analyses would suggest that infection with WNV may promote more of an anti-inflammatory phenotype compared to ZIKV infection.

Although our analyses would suggest that infection with WNV may promote more of a pro-inflammatory phenotype in macrophages compared to ZIKV infection.

Polarisation of M2 macrophages is often associated with an increase in the FA scavenger receptor CD36, which increases import of FAs to fuel OXPHOS (Huang et al, 2014; Orecchioni et al, 2019; Pennathur et al, 2015). To assess the impact of infection on FA import, we assayed the expression of CD36 during infection in macrophages. Our results indicated a significant upregulation of this marker during WNV infection, but not ZIKV, highlighting differences between these two related viruses (Figure 46). As WNV also increases SRC of cells, which is a measure of the metabolic fitness of cells, it's possible that, similar to M2 macrophages, WNV is upregulating FA import to fuel OXPHOS. It is likely that upregulation of CD36 in combination with increased mitochondrial mass accounts for the increase in SRC by WNV.

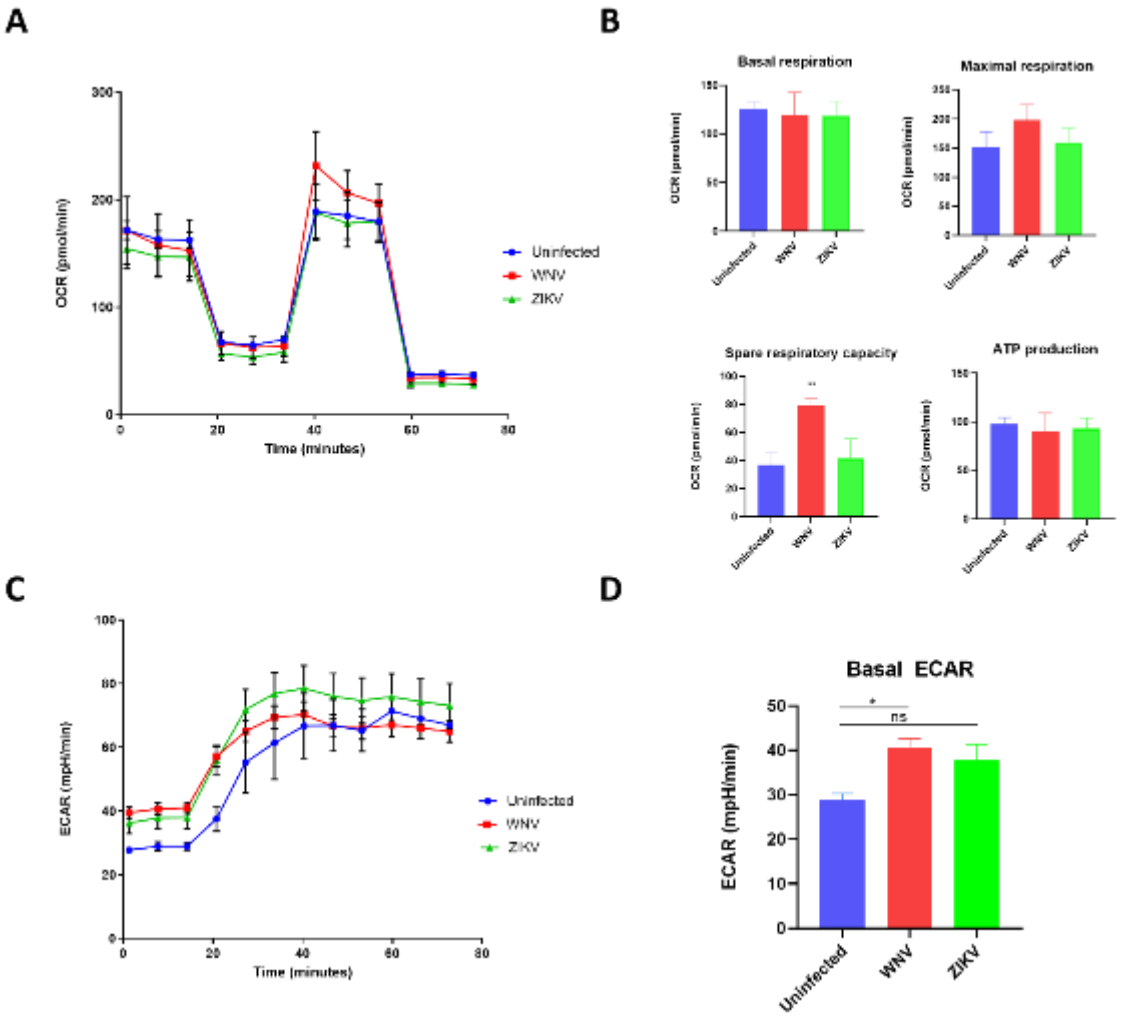

Figure 44. Infection of RAW264.7 macrophages with WNV or ZIKV has minimal impact on oxygen consumption and extracellular acidification rates. **(A)** RAW264.7 cells were seeded onto Seahorse XF96 Cell Culture Microplate and infected for 24 hours with WNV and ZIKV, before oxygen consumption rate (OCR) was measured using the Seahorse XF Mito Stress Test Kit and a Seahorse XFe96 Analyzer. Each data point is the mean of 3 technical replicates of 2 independent biological replicates (n=2) with error bars indicating S.E.M. **(B)** Bar graph representation of each of the parameters, using data extracted from **(A)** and analysed using the Seahorse XF Cell Mito Stress Test Report Generator and GraphPad Prism 8. Statistical significance was determined using an ordinary one-way ANOVA (GraphPad Prism 8). **(C)** Extracellular acidification rate (ECAR) measurement from the experiment in **(A). (D)** Bar graph representation of basal ECAR, analysed using the Seahorse XF Cell Mito Stress Test Report Generator and Prism. Statistical significance was determined using an ordinary one-way ANOVA (GraphPad Prism 8). * = $p \leq 0.05$

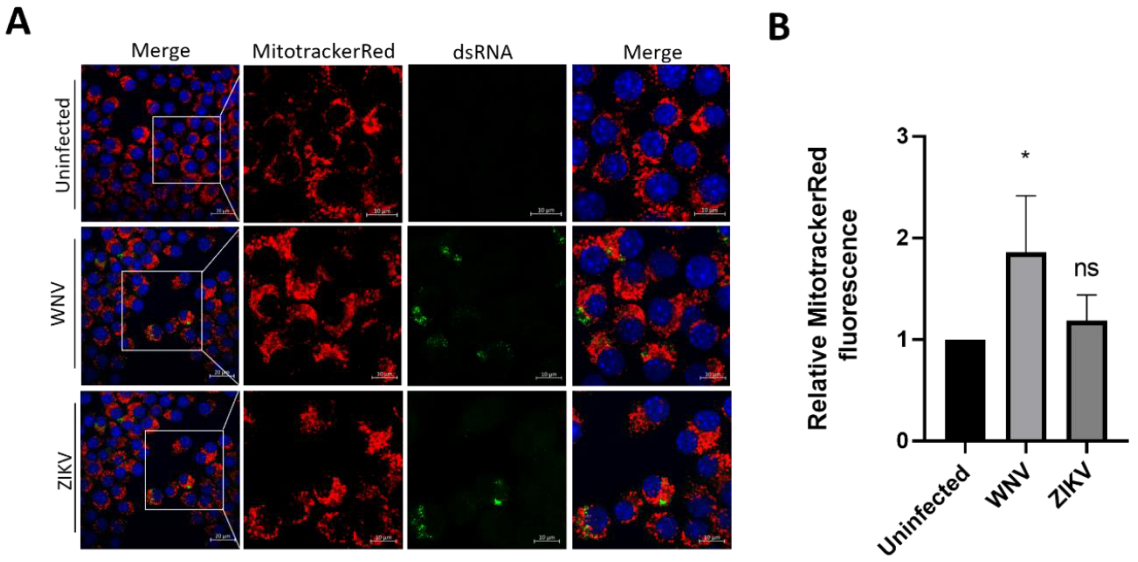

Figure 45. Infection of RAW264.7 macrophages with WNV or ZIKV does not perturb mitochondrial morphology. **(A)** Cells were seeded on coverslips and infected with either WNV or ZIKV at an MOI of 5 for 24 hours. Before fixation, cells were stained with MitoTracker™ Red CMXRos (red), and then subsequently fixed, permeabilised, and stained for anti-dsRNA (green) to visualise virus. Images were taken on a Zeiss confocal microscope and analysed using Zen Blue software (n=2). **(B)** Cells were infected as above and stained with MitotrackerRed or NS1, and analysed on a BD LSR Fortessa Cell Analyser. MitotrackerRed MFI was calculated using FlowJo software and used to calculate relative fluorescence. Bar graphs were generated using GraphPad Prism 8 and significance was determined using an unpaired t-test. Error bars are indicative of 2 biological replicates (n=2, +/- SEM). * = $p \leq 0.05$

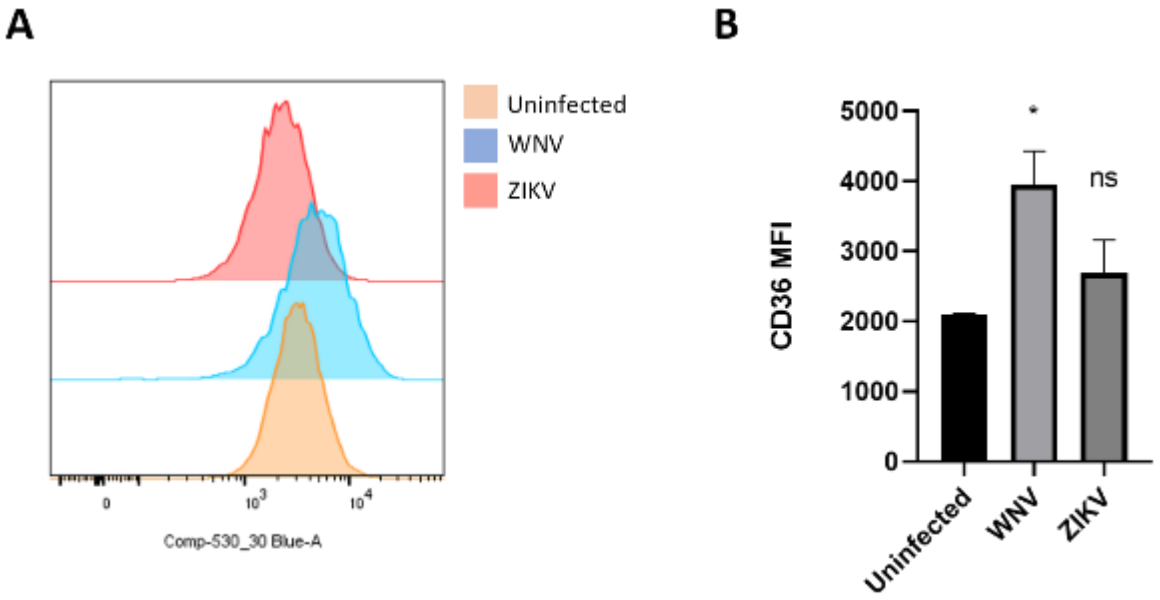

Figure 46. Infection of RAW264.7 cells with WNV, but not ZIKV, increases CD36 expression. Cells were seeded on coverslips and infected with either WNV or ZIKV at an MOI of 5 for 24 hours. After this time, cells were stained with an anti-CD36 antibody and then fixed with 4 % paraformaldehyde. Samples were then analysed via flow cytometry on a BD LSR Fortessa Cell Analyser, and **(A)** histograms of the fluorescent intensity values for each marker were generated using FlowJo software (red = uninfected, blue = WNV-infected, yellow = ZIKV-infected). **(B)** Bar graphs of MFI values were generated using GraphPad Prism 8 and significance was determined using an unpaired t-test. Error bars are indicative of the mean of 2 independent biological replicates (n=2, +/- SEM). * = $p \leq 0.05$

4.2.14. Fatty acid inhibitors have differing effects on mitochondrial respiration and glycolysis

In addition to assessing the impact of infection on metabolic rates, we assayed the impact of our metabolic inhibitors on these pathways to determine if we could link any perturbations in metabolism to decreased viral replication. We infected cells, treated with inhibitors for 24 hours, and then assessed OCR and ECAR using the Seahorse Mito Stress Test. Overall, in uninfected cells we saw a significant reduction in OCR and ECAR with orlistat, TOFA and etomoxir (Figure 47a, b, c). As etomoxir inhibits FAO, we expected we would likely see a reduction in mitochondrial respiration with this inhibitor. We observed a significant decrease

in basal respiration and ATP production with etomoxir in uninfected cells, suggesting that these macrophages are oxidising FAs in a resting state. As in Vero cells, we saw a drastic drop in both OCR and ECAR during orlistat treatment, which may be due to orlistat's potential lipase inhibition activity, and/or production of toxic FA species resulting in mitochondrial damage, as previously discussed. What was more surprising, however, was the drop in cellular respiration observed with TOFA, with both orlistat and TOFA reducing basal respiration in uninfected cells by over 60 %. It is well known that inhibition of ACC can result in the upregulation of OXPHOS, as ACC regulates cellular malonyl-CoA pools and subsequently FAO. Despite this, reciprocal effects on FAO inhibition using TOFA have been reported, which have been linked to a reduction in the availability of CoA, which is required for FAO (Otto et al, 1985). Thus, in our macrophage system is appears that TOFA is inhibiting both FAS and FAO.

Similarly to uninfected cells, we observed significantly lower levels of basal OCR and ATP production during etomoxir treatment, during both WNV (Figure 47a and d) and ZIKV (Figure 47a and e) infection, indicating that FAO contributes to energy production during infection. Intriguingly, we noted a significant effect of this inhibitor on maximal respiration, which was not observed in uninfected cells. Maximal respiration is calculated after the addition of FCCP, a drug that stimulates the ETC, resulting in the accelerated oxidation of substrates, and is indicative of the maximal capacity of these cells to produce energy via OXPHOS. The increase we observe in maximal respiration is therefore likely a result of the increased lipid content we observe in infected cells, as seen in Figure 43b and c, which would provide adequate substrates for OXPHOS. We again additionally saw perturbation of OCR and ECAR with both TOFA and orlistat treatment, which affected global ATP production as in uninfected cells. Despite seeing significant perturbations of mitochondrial respiration with three of our inhibitors, TOFA was the only inhibitor that we observed complete ablation of viral replication, through the inhibition of RC formation, viral protein production and infectious virus production. As we only see inhibition of virus production with orlistat, we can extrapolate that mitochondrial respiration is likely only required for the later stages

of viral replication, and the complete ablation of viral replication by TOFA is a result of impaired FAS.

Next, we wanted to determine if the reduction in mitochondrial respiration induced by our inhibitors was complimented by changes in mitochondrial morphology or LD accumulation, as these processes are intimately tied. We performed IFA and stained with MitoTracker™ Red CMXRos to visualise functional mitochondria, and BODIPY to visualise LDs. Our MitoTracker staining revealed that the mitochondria in our macrophages were quite condensed, and it was difficult to clearly observe differences in morphology between our inhibitors. Noticeably though, orlistat did not appear to effect mitochondria morphology as was observed in treated Vero cells (Figure 24). We did not observe orlistat-induced mitochondrial fragmentation, but clearly observed an increase in LD content (Figure 48d). Conversely, TOFA treatment appeared to induce a degree of fragmentation, but did not induce LD accumulation (Figure 48e). Interestingly, despite having less of an effect on OCR than TOFA and orlistat, etomoxir appeared to induce severe mitochondrial fragmentation (Figure 48f). This drastic degree of fragmentation would usually be indicative of completely defective mitochondria, but this was not the case as seen in our Seahorse data. As this was only the result of one replicate, we would like to repeat this experiment to confirm this result.

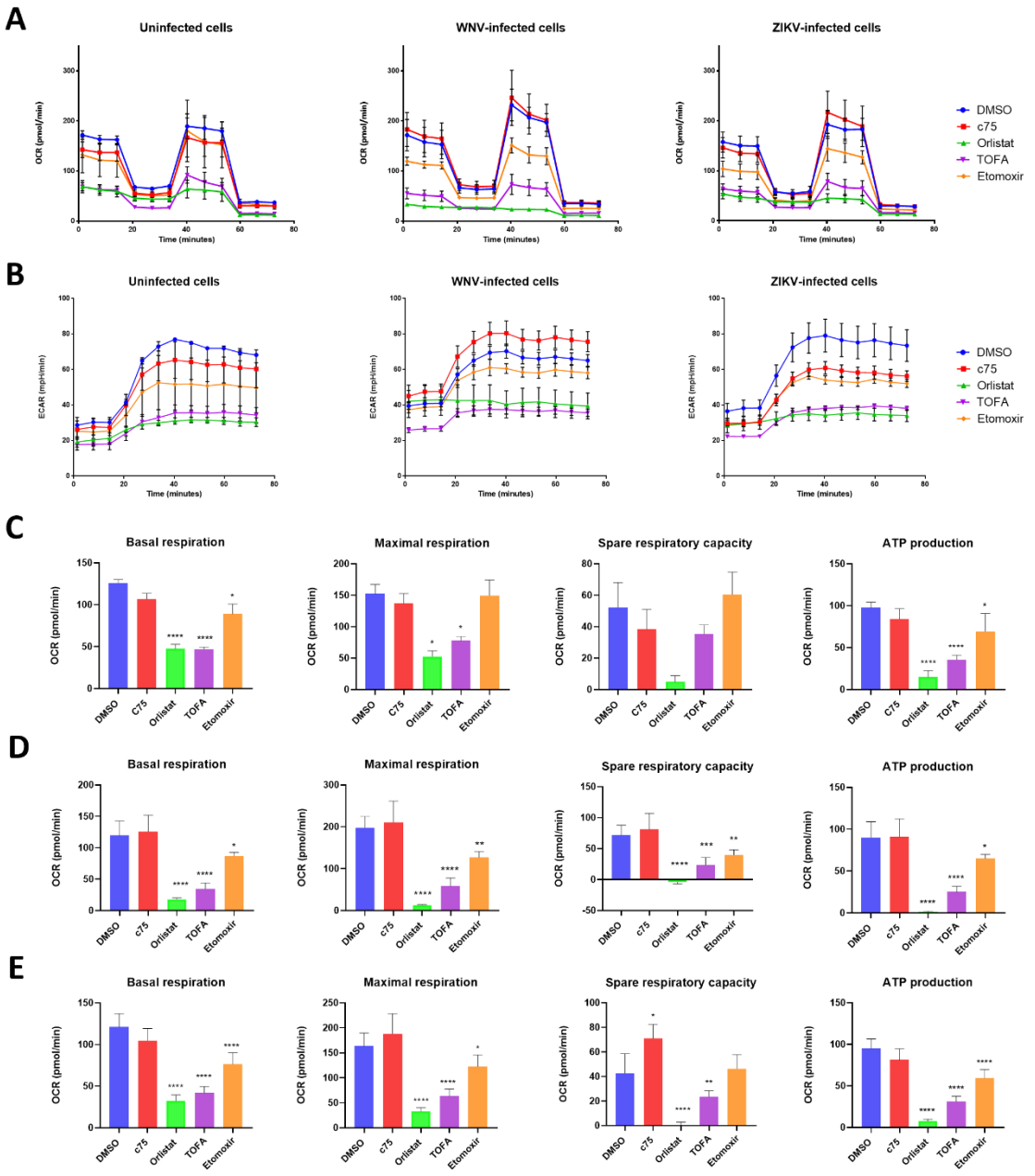

Figure 47. The effect of fatty acid synthesis and oxidation inhibitors on mitochondrial respiration and glycolysis. RAW264.7 cells were seeded onto Seahorse XF96 Cell Culture Microplate and infected for 24 hours with WNV and ZIKV, and concurrently treated with respective inhibitors for 24 hours at the following concentrations: c75 (30 μM), orlistat (100 μM), TOFA (10 μM) and etomoxir (100 μM), and DMSO was used as the vehicle control. **(A)** Oxygen consumption rate (OCR) and **(B)** extracellular acidification rates were measured using the Seahorse XF Mito Stress Test Kit and a Seahorse XFe96 Analyzer. Each data point is the mean of 3 technical replicates of 2 independent biological replicates (n=2) with error bars indicating S.E.M. **(C)** Bar graph representation of each of the parameters of OCR for WNV-infected cells, using data extracted from

(A) and analysed using the Seahorse XF Cell Mito Stress Test Report Generator and GraphPad Prism 8. Statistical significance was determined using an ordinary one-way ANOVA and multiple comparisons (GraphPad Prism 8). * = p ≤ 0.05, ** = p ≤ 0.001, *** = p ≤ 0.0001, **** = p <0.0001.

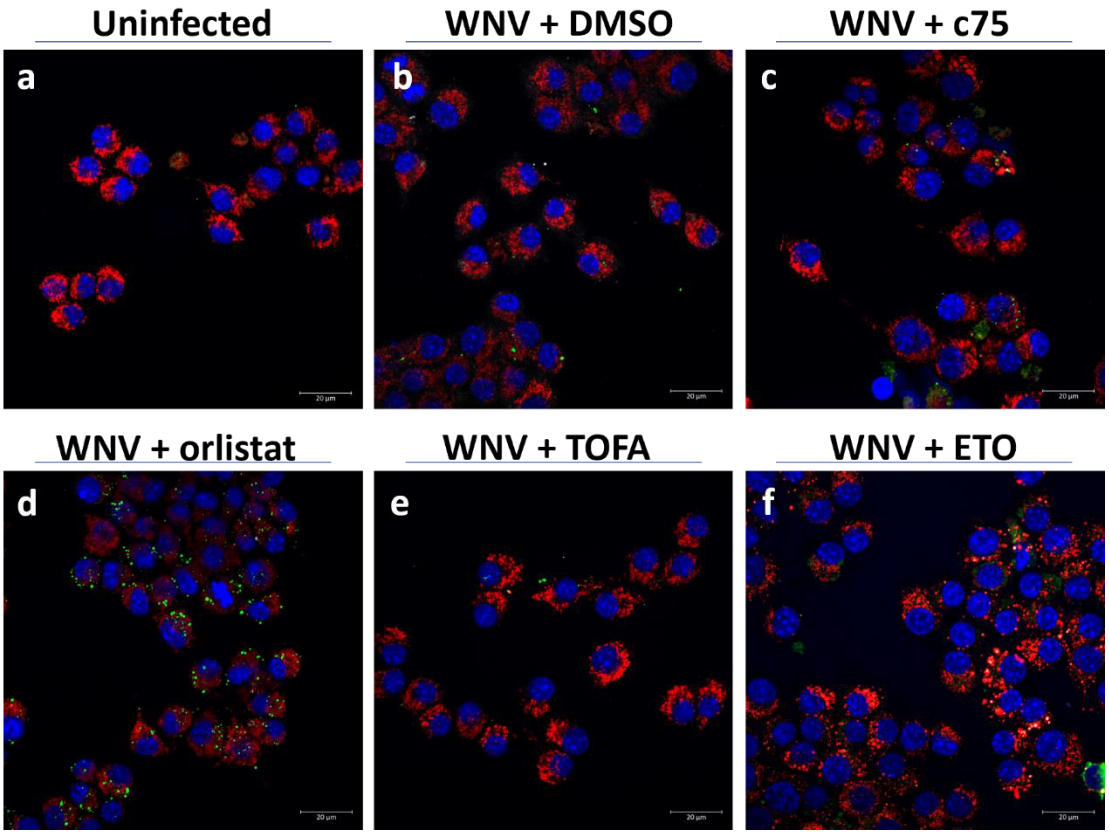

Figure 48. The impact of fatty acid synthesis inhibitors on mitochondrial morphology and lipid droplet content. RAW264.7 cells were seeded in 24-well plates onto glass coverslips and left to attach overnight. Cells were either left uninfected or infected with WNV, and treated with fatty acid synthesis and oxidation inhibitors at the following concentrations: c75 (30 μM), orlistat (100 μM), TOFA (10 μM) and etomoxir (100 μM), and DMSO was used as the vehicle control. After 24 hours, cells were incubated with MitoTracker™ Red CMXRos (red) for 30 minutes, and then subsequently fixed, permeabilised, and stained for anti-dsRNA (grey) to visualise virus. Cells were then incubated with BODIPY™ 493/503 for 30 minutes to stain lipid droplets (green). Finally, cells were counterstained with Hoechst to visualise nuclei (blue) and mounted. Images were taken on a Zeiss confocal microscope and analysed using Zen Blue software (n=1).

4.2.15. WNV and ZIKV induce an inflammatory state in RAW264.7 cells

After evaluating the impact of infection on metabolic pathways, we next aimed to determine if the manipulation of these pathways altered the functional capacity of infected macrophages. Namely, our objective was to determine if *de novo* FAS or FAO contributed to the polarisation state of macrophages during infection. Our previous observations indicated that the infected cells displayed some classical signs of pro-inflammatory activation, including increase FASN expression (Figure 40b), LD accumulation (Figures 43b and c) and Increased glycolysis (Figures 44c and d). We did not, however, observe a shift in mitochondrial respiration which generally underpins the polarisation states of macrophages. Thus, we first sought to define the inflammatory profile of infected cells by using flow cytometry to assess the surface expression of candidate M1 or M2 polarisation markers. Based on the literature (Jablonski et al, 2015; Lv et al, 2017; Pireaux et al, 2016; Taciak et al, 2018), we chose several classic M1 (CD80, CD86, MHC-II) and M2 markers (CD206). We either infected RAW264.7 cells with WNV or ZIKV, or treated cells with LPS or LPS+IFN-γ as a control for pro-inflammatory activation. As there is no established and functional protocol for M2 polarisation in this cell type, we used untreated cells as a proxy-M2 phenotype.

Overall, we observed a striking upregulation of the pro-inflammatory markers with LPS+IFN-γ treatment and observed a correspondingly downregulation of CD206 (Figure 49), confirming the efficacy of this control. During infection of these cells with WNV and ZIKV we observed a stark upregulation of CD80 (Figure 49a), but, interestingly, not CD86 (Figure 45b), despite the two being co-stimulatory molecules. We also observed a slight upregulation of MHC-II (Figure 49c), but a minimal effect on CD206 (Figure 49d). Overall, these results confirm that these viruses are inducing a pro-inflammatory state, however the magnitude of this activation is not to the same degree as we see upon LPS+IFN-γ stimulation.

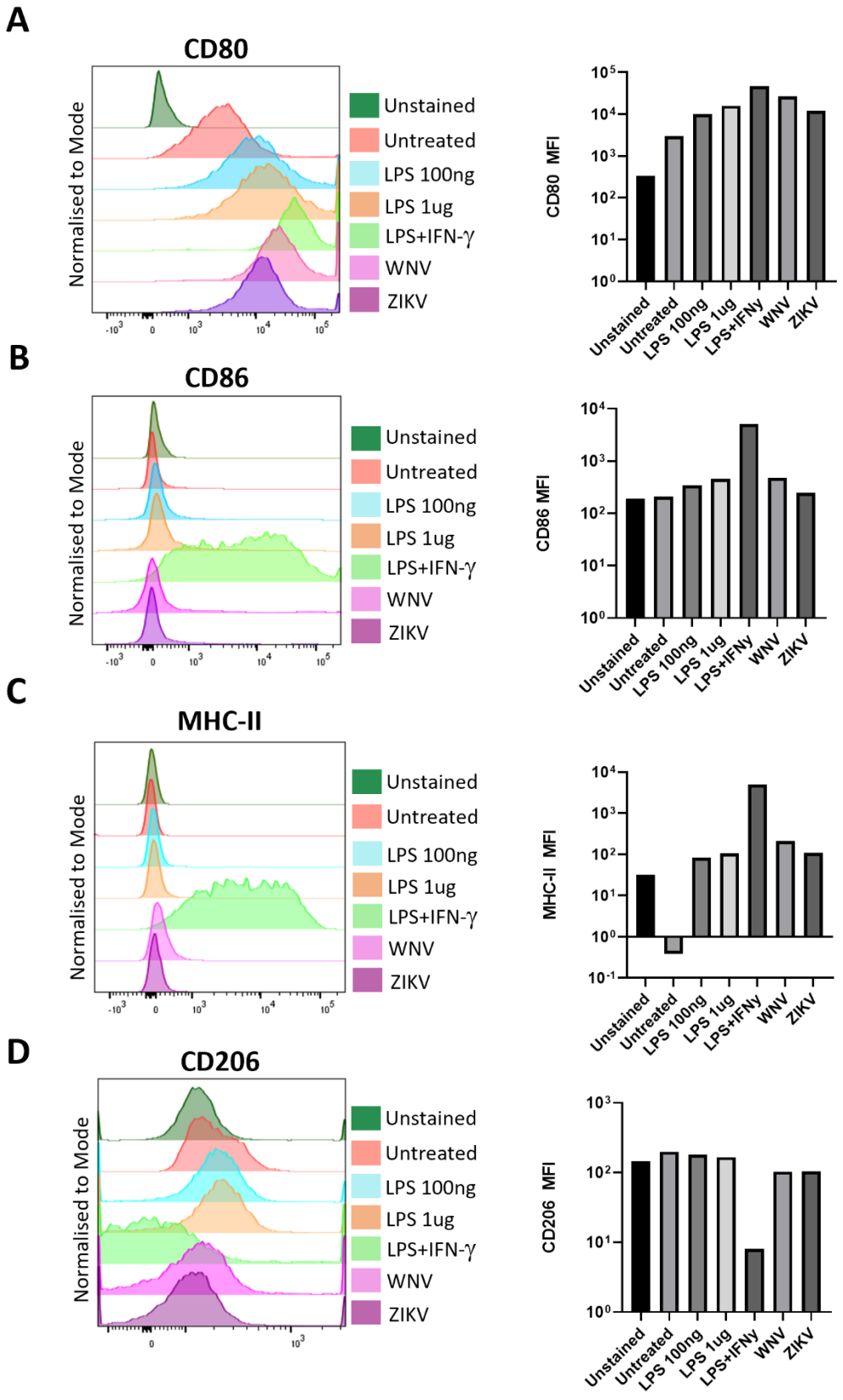
A
CD80
Normalised to Mode
Unstained
Untreated
LPS 100ng
LPS 1ug
LPS+IFN-γ
WNV
ZIKV
CD80 MFI
Unstained
Untreated
LPS 100ng
LPS 1ug
LPS+IFNγ
WNV
ZIKV
B
CD86
Normalised to Mode
Unstained
Untreated
LPS 100ng
LPS 1ug
LPS+IFN-γ
WNV
ZIKV
CD86 MFI
Unstained
Untreated
LPS 100ng
LPS 1ug
LPS+IFNγ
WNV
ZIKV
C
MHC-II
Normalised to Mode
Unstained
Untreated
LPS 100ng
LPS 1ug
LPS+IFN-γ
WNV
ZIKV
MHC-II MFI
Unstained
Untreated
LPS 100ng
LPS 1ug
LPS+IFNγ
WNV
ZIKV
D
CD206
Normalised to Mode
Unstained
Untreated
LPS 100ng
LPS 1ug
LPS+IFN-γ
WNV
ZIKV
CD206 MFI
Unstained
Untreated
LPS 100ng
LPS 1ug
LPS+IFNγ
WNV
ZIKV

Figure 49. Infection induces expression of some inflammatory macrophage markers. RAW264.7 cells were either infected with WNV or ZIKV for 48 hours at an MOI of 5, or treated with varying concentrations of LPS or LPS+IFN-γ as indicated. After 24 hours, cells were harvested and immunolabelled with antibodies to pro-inflammatory macrophage markers **(A)** CD80, **(B)** CD86 and **(C)** MHC-II, and the anti-inflammatory macrophage marker **(D)** CD206. Cells were also incubated with anti-NS1 antibody to gate for infected cells in the relevant samples. Cells were then analysed via flow cytometry BD LSR Fortessa Cell Analyser, and histograms of the fluorescent intensity values for each marker were generated using FlowJo software. n=1

4.2.16. Inhibition of de novo FAS does not affect the ability of macrophages to polarise to a pro-inflammatory state

We next aimed to determine if *de novo* FAS mediated by virus-induced activation of FASN was contributing to the pro-inflammatory state in macrophages. We hypothesised that the FASN-mediated stimulation of fatty acid synthesis by WNV and ZIKV may drive inflammatory processes, and thus inhibition of FASN activity could potentially attenuate the inflammatory response. We additionally hypothesised that by inhibiting FAO, we may be replicating the conditions of pro-inflammatory macrophages and may see an increase in M1 marker expression as a result. We again evaluated the surface expression of our nominated classic M1 and M2 markers in WNV or ZIKV-infected cells in the presence or absence of our metabolic inhibitors (namely c75, orlistat, TOFA and etomoxir). As in our previous experiment, we observed an upregulation of CD80 and MHC-II, indicating the induction of an inflammatory state by these viruses (Figure 50). Treatment with our inhibitors, however, did not significantly affect the expression of any of the markers analysed in uninfected or infected cells (Figure 50). Overall, this data suggests that the utilisation of the *de novo* FAS pathway by WNV and ZIKV, as well as FAO, is uncoupled to the polarisation of infected macrophages.

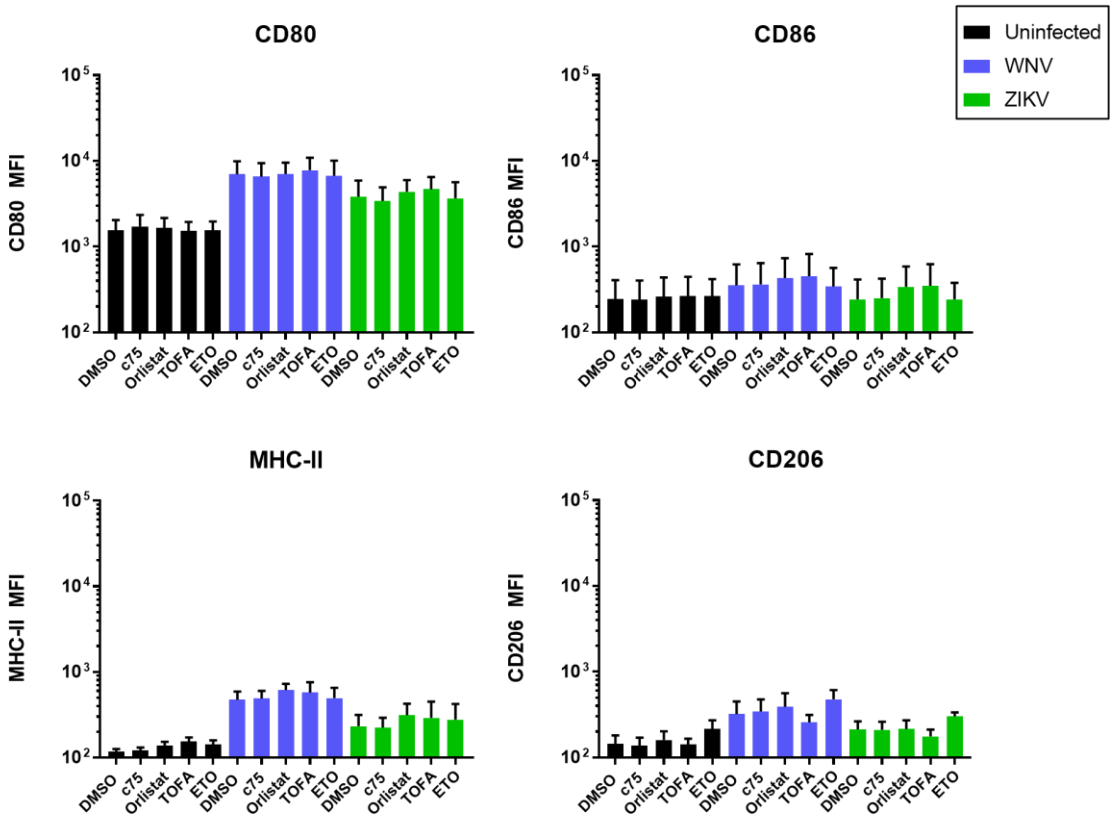

Figure 50. Inhibition of de novo fatty acid synthesis does not affect the pro-inflammatory activation of macrophages during WNV and ZIKV infection. RAW 264.7 cells were infected with either WNV or ZIKV (MOI 5) and treated with fatty acid synthesis (TOFA, c75, orlistat) or fatty acid oxidation (etomoxir or ETO) inhibitors, or DMSO as the vehicle control. After 24 hours, cells were harvested and labelled with antibodies to various macrophage markers (CD80, CD86, MHC-II or CD206), and an anti-NS1 antibody to identify infected cells. Cells were analysed using a BD LSR Fortessa Cell Analyser, and histograms were created using FlowJo. Error bars are indicative of 2 independent biological replicates (n=3, +/- SEM).

4.3. Discussion

Whilst severe Flavivirus disease is associated with inflammation, there remains much to be revealed regarding what underpins the promotion of the inflammatory processes during infection. The infection of innate immune cells, such as monocytes and macrophages, can facilitate the systemic spread of Flaviviruses, and infiltration of these cells into the CNS and release of inflammatory mediators is believed to contribute to neuropathology and severe disease. In this Chapter we aimed to investigate the drivers of inflammatory processes in macrophages during infection at a cellular level, by investigating a potential link between Flavivirus metabolic reprogramming of cells, and changes in inflammatory characteristics. We looked specifically at the involvement of *de novo* FAS and FAO, mediated via FASN activity, during both viral replication and pro-inflammatory macrophage activation. We also aimed to categorise the metabolic signature and polarisation state profile of infected macrophages, as this has not previously been determined for Flaviviruses. Our results revealed that *de novo* FAS is indispensable for viral replication, which has not been demonstrated previously in macrophages. We additionally observed that WNV and ZIKV induce an increased inflammatory state in this cell type, as determined by LD accumulation, elevated basal ECAR, and the expression of pro-inflammatory surface markers. Surprisingly, despite perturbations in mitochondrial respiration being a key facet of pro-inflammatory macrophage activation, the OCR profile of infected cells were parallel to that of uninfected cells. Whilst we hypothesised that this may dampen immune responses, we additionally observed that the promotion and utilisation of FAS and FAO pathways during infection did not markedly affect polarisation of mouse macrophages either to M1 or M2, as determined by the expression of key surface markers. Taken together, our results highlight the consistent requirement for *de novo* FAS during infection, and illustrate that these viruses are likely able to hijack this pathway without further exacerbating immune activation and response.

During this study, we demonstrated that the *de novo* FAS pathway is essential for the replication of WNV and ZIKV in macrophages. We first demonstrated this

in human macrophages, with treatment with the FASN inhibitors c75 and orlistat (Figure 33c), as well as with the knockout of the FASN gene using CRISPR-Cas9 (Figure 37), both resulting in attenuation of viral replication. The mammalian *de novo* FAS is a conserved pathway, and as mouse models of Flavivirus infection are common and can result in severe disease and encephalitis (Charlier et al, 2006; Hanners et al, 2021; Hassert et al, 2019; Hassert et al, 2018; Kimura et al, 2010; Pinto et al, 2013), we hypothesised that the dependence on FAs would likely translate to mouse macrophages. Indeed, we observed ablation of viral replication when we completely restricted *de novo* FAS with TOFA (Figure 41). This rendered both WNV and ZIKV incapable of initiating infection and proliferating replication via the construction of viral RCs (Figure 42). This indicates that these FAs are required for efficient membrane formation, which is consistent with what has been observed by us and others in different cell types (Heaton et al, 2010). Although viral replication can occur without these RCs at the early stages of infection, it is likely that preventing the formation of the membranous replication complex reduces the efficiency of replication and exposes the viral nucleic acid to immune detection resulting in subsequent clearance.

The role of FAO during infection was revealed to be more complex. Through the utilisation of etomoxir, an inhibitor of CPT-1 which facilitates transport of fatty acids to the mitochondria, we found an impact on viral protein expression for WNV, and infectious virus production for ZIKV, although there were strong trends of inhibition for both viruses in each assay (Figure 41). Our Seahorse data also clearly demonstrated an impact of etomoxir on basal and maximal OCR, indicating that these viruses do rely on FAO during their life cycle (Figure 47). As FAO provides substrates for OXPHOS, which is the most efficient energy producing pathway in humans, it is likely that inhibition of FAO is depriving the virus of energy required for replicative processes. Our cells have mechanisms in place to ensure the homeostatic regulation of metabolic processes, and the allosteric regulation of CPT-1 by malonyl-CoA ensures that FAS and FAO are not occurring simultaneously. We observed a clear role for both pathways during infection, however, suggesting that infected cells possibly undergo oscillating

periods of increased FAS and FAO over the duration of the replicative cycle. Although our metabolic analysis data showed no observable increase in OCR in infected cells, this was only assayed at 24 hours post infection, so it remains possible that FAO is increased at earlier timepoints, and these temporal analyses are something we would like to investigate in the future. It is also possible that the viruses are overriding this regulatory system and allowing FAS and FAO to concurrently occur, as has been observed in cancer cells (Koundouros & Poulogiannis, 2020).

In addition to observing an impact of CPT-1 on OCR, we unexpectedly found both orlistat and TOFA reduced OCR (Figure 47). This was less surprising for orlistat, as we observed a similar impact on metabolism in Veros (Figure 25, 26 and 27), but the result with TOFA is contradictory to what has been observed in the literature. As TOFA inhibits ACC, the enzyme responsible for converting acetyl-CoA to malonyl-CoA, treatment with this inhibitor should reduce malonyl-CoA levels. As malonyl-CoA is an inhibitor of CPT-1, TOFA should theoretically increase FAO and OCR, rather than decrease as we observed. Throughout this study we observed objectively low levels of LDs within uninfected cells (Figures 43c and 48b), so we believe that as OCR was only measured after 24 hours of infection, it is likely that any cellular FAs would have been oxidised prior to this timepoint and wouldn't be contributing to the OCR profile at the time of the assay (see Figure 51 for a model). This hypothesis would explain the absence of LDs observed during IFA with TOFA treatment (Figure 48e), and the lack of increase in OCR, but the reason for the *decrease* may be related to a reduction in free CoA levels, which is required for FAO, as TOFA is converted to ToFyl-CoA within cells. Although TOFA, orlistat and etomoxir all inhibit infectious virus production, TOFA is the only inhibitor that comprehensively suppresses viral replication. Whilst these viruses utilise OXPHOS, this data indicates that *de novo* FAS is clearly required for efficient genome replication.

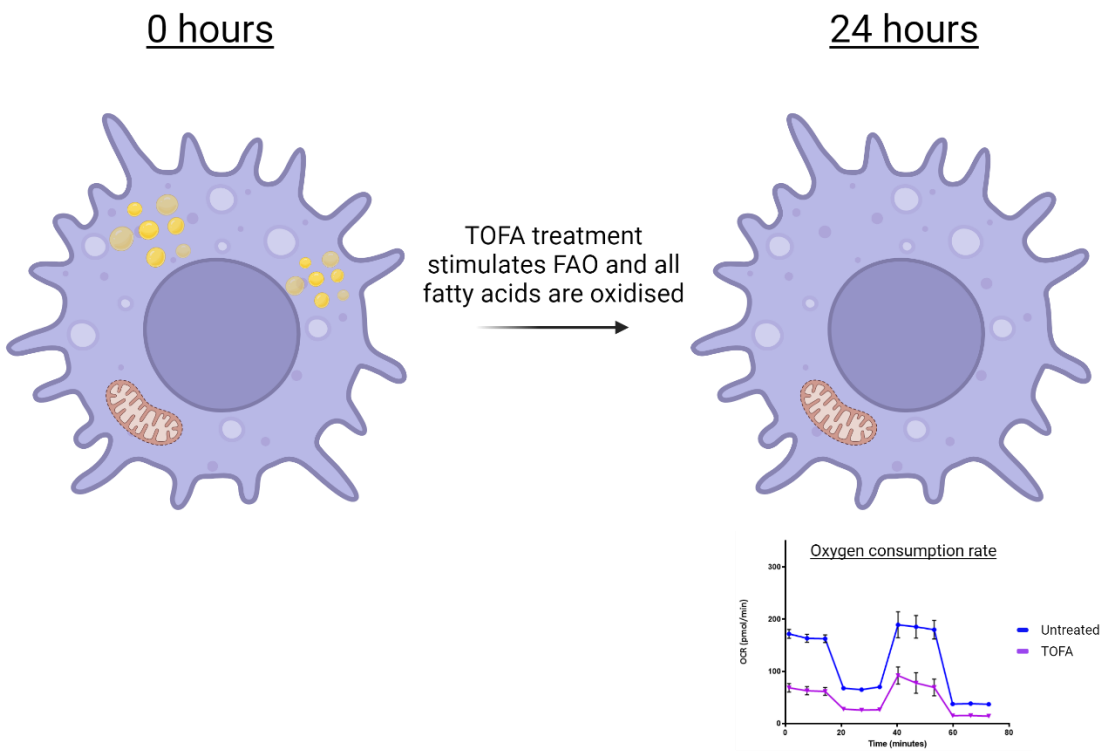

Figure 51. Model to describe the reduction in mitochondrial respiration observed during TOFA treatment in RAW264.7 cells. As TOFA is known to stimulate fatty acid oxidation (FAO) by reducing cellular malonyl-CoA levels, we hypothesise that this occurs early during treatment, and after 24 hours cellular fatty acid pools have been completely depleted, resulting in a reduction in oxygen consumption rate (OCR).

Taken together, our OCR and LD data suggest that unlike DENV, WNV and ZIKV are not upregulating the autophagy-regulated turnover of LDs to fuel mitochondrial respiration. We again cannot rule out, however, that there are oscillating periods of LD accumulation and depletion that is correlated with an increase in OCR at time points not investigated. Despite this, we observed an increase in LD content during infection at two time points that was comparable to that of LPS/IFN-γ stimulated cells (Figure 43a and b), suggesting that this upregulation may be a result of pro-inflammatory activation of these cells. Recently, it has been demonstrated that LD accumulation in classically activated (LPS +IFN-γ) macrophages is not a result of increased *de novo* FAS as had been thought, but instead arises from both increased import of serum FAs and glucose, and as a result of dysregulated mitochondrial respiration (Rosas-Ballina et al,

2020). The same report also demonstrated that the mitochondrial defects in classically activated macrophages arose from increased production of NO from iNOS, which is an inhibitor of complex IV in the ETC (Beltrán et al, 2000), and resulted in FAO inhibition and LD accumulation.

In our studies we saw LD accumulation in the absence of any mitochondrial defects, suggesting that the LD accumulation during infection is resulting either from an increase in FA import, an increase in *de novo* FAS, or both. As inflammatory lipid mediators are generally derived from dietary FAs, if the LDs induced during infection are comprised primarily of *de novo* FAs and TAGs, then the composition and potential function of these LDs could be distinct from those in pro-inflammatory macrophages. Although we observed an increase in CD36 expression during WNV infection, suggesting increased import of FAs (Figure 46), when we inhibited *de novo* FAS with TOFA we saw a strong reduction in LD content (Figure 48e). Overall, this suggests that *de novo* FAs are primarily contributing to LD formation, and the imported FAs are likely contributing to FAO. To further confirm this, we could also perform some lipidomic studies to identify possible differences in FA composition between infected and pro-inflammatory (LPS+IFN-γ) macrophages, but this is not something we could do under the time constraints. It also remains a possibility that the upregulation of the LDs is induced by the virus for the purpose of aiding in virion formation, and we did see an effect on infectious virus production with TOFA, however further work, including looking at the potential localisation of the capsid protein to LDs, is needed to confirm this. Previous work from our lab in 1997, however, did not show any links with the WNV capsid protein and cytoplasmic droplets by both IFA and IEM (Westaway et al, 1997).

Time permitting, we would have also liked to investigate further the role of iNOS during infection of these cells. As we see no mitochondrial dysfunction, we can speculate that iNOS is likely not upregulated during infection. NO is an important antiviral mediator in inflammatory macrophages (Bailey et al, 2019), and has been demonstrated previously to inhibit Flavivirus replication (King et al, 2007; Kreil & Eibl, 1996; Lin et al, 1997; Neves-Souza et al, 2005; Saxena et al, 2000).

Polyinosinic acid:polycytidylic acid (poly I:C) is a dsRNA analogue, and stimulation of RAW264.7 cells with poly I:C alone has been demonstrated to induce iNOS expression and increase NO production (Chen et al, 2016). Thus, this suggests that WNV and ZIKV may be blocking NO production, and this could be a potential immune evasion mechanism. iNOS as well as nitric oxide synthase 2 (NOS2) are activated in pro-inflammatory macrophages via IFN-γ and STAT1 (Gao et al, 2016; Salim et al, 2016; Samardzic et al, 2001). Although it has been reported that Flaviviruses induce IFN-γ production (Costa et al, 2012; Fagundes et al, 2011), Flavivirus NS proteins are known to directly interact with and degrade or block STAT1 phosphorylation (Fanunza et al, 2021a; Fanunza et al, 2021b; Liu et al, 2005; Roby et al, 2020; Roby et al, 2016), which could in turn be inhibiting NO production. Another possible explanation could have to do with the increase in FAS observed during infection; NADPH is required for both *de novo* FAS as well as NO production, so increased FAS could be sequestering available NADPH. In addition to being antiviral, NO production can also contribute to pathogenesis during infection, and it is believed that the dysregulation of the IFN-NO axis may contribute the immunopathological damage caused during encephalitis/severe disease (Ashhurst et al, 2013). In a mouse model of WNV encephalitis, inhibiting NO production in macrophages infiltrating the CNS resulted in prolonged survival (Getts et al, 2008). Similarly, in another study, dengue haemorrhage was reduced in mice lacking iNOS (Yen et al, 2008). This begs us to ask the question of whether inhibition of NO production can push macrophages towards an anti-inflammatory phenotype, which may be what is occurring in our model.

Overall, our metabolic analyses are indicative of a metabolic state during infection that is not consistent with a pro-inflammatory macrophage activation phenotype. Shifts in mitochondrial and glucose metabolism underpin the shift to a pro-inflammatory state; upregulation of glycolysis provides an immediate source of energy, and perturbations in mitochondrial respiration generate a source of microbiocidal intermediates. In this study we observed parallel mitochondrial respiration rates between infected and uninfected cells, with a significant increase in glycolytic rates only observed for WNV at the basal level (Figure 44). Although

we see no significant increase in basal or maximal respiration, an interesting observation was seen with a significant increase in spare respiratory capacity (SRC) during WNV infection (Figure 44b). SRC is a measure of metabolic fitness, and the ability of cells to respond to stress. An increase in this parameter signifies that WNV-infected cells have an increased capacity for mitochondrial energy production, and may be indicative of increased OXPHOS at time points that we did not investigate. This increase in SRC is likely supported by the increase in mitochondrial mass we observed (Figure 45b), indicating a higher number of functional mitochondria within cells, and suggesting that WNV is directly affecting mitochondrial dynamics. Furthermore, an increase in SRC is a distinctive anti-inflammatory macrophage phenotype and has been observed in IL-4 stimulated macrophages (Van den Bossche et al, 2015). Indeed, metabolic homeostasis as observed here, rather than imbalance, more closely resembles an anti-inflammatory macrophage phenotype.

Although classically activated macrophages display two breaks in the TCA cycle, this facet of metabolic reprogramming appears to be missing in our infection model. These breaks occur after citrate and again after succinate, and result in accumulation of the intermediates citrate, itaconate and succinate (Jha et al, 2015). Citrate contributes to the production of NO, ROS and prostaglandin E2, which are involved in pathogen clearance (Infantino et al, 2013). Succinate is additionally an inflammatory signal and has been demonstrated to enhance IL-1β signalling upon stimulation with LPS (Tannahill et al, 2013). As the TCA cycle occurs in the mitochondria and provides substrates for OXPHOS, we can extrapolate that infection likely does not induce these same breaks in the TCA cycle as we see no reduction in overall ATP production (Figure 47). This would likely mean less production of these antiviral metabolites and perhaps a dampening of IL-1β signalling, but this would need further investigation to confirm. In primary human macrophages WNV has been shown to attenuate the inflammatory response, including inhibiting IL-1β signalling (Kong et al, 2008b), so it is possible that blocking mitochondrial defects is a potential mechanism for this. Overall, in our cellular model we believe that the mitochondrial homeostasis

apparent during infection may be allowing the virus to negate certain pro-inflammatory functions, resulting in efficient and sustained viral replication.

Infected macrophages infiltrating the CNS during Flavivirus infection have been shown to contribute to pathogenesis, and potentially neuropathy, via the production of NO, ROS and inflammatory cytokines (Ashhurst et al, 2013; Getts et al, 2008; Yen et al, 2008). Polarization of macrophages to a pro-inflammatory state has been documented in infiltrating cells in encephalitic mice (Jhan et al, 2021), and we originally hypothesised that the stimulation of FAS could be driving this inflammatory phenotype of macrophages. We also posited that an upregulation in FAO may be flicking a 'metabolic switch', and pushing the cells to an anti-inflammatory state, which could potentially allow macrophages to cross the BBB undetected. Our flow cytometry data indicated that our infected cells demonstrated a shift towards a pro-inflammatory activation state, with the expression of CD80 and MHC-II, but surprisingly not CD86 (Figure 49). We additionally observed a slight increase in CD206 expression, which is generally an anti-inflammatory macrophage marker (Bertani et al, 2017; Orecchioni et al, 2019; Raggi et al, 2017; Smith et al, 2016). CD206 is a mannose receptor so it's possible that the viruses are upregulating the uptake of mannose, which in anti-inflammatory macrophages has been shown to supress IL-1β signalling (Torretta et al, 2020). CD206 is also a proposed receptor for Flaviviruses and facilitates DENV entry (Miller et al, 2008a). It did not appear, however, that either FAS or FAO were involved in the expression of any of these markers as inhibition of these pathways did not influence the overall macrophage phenotype during infection (Figure 50). Despite TOFA completely restricting viral replication, this inhibitor did not impact the expression of pro-inflammatory markers, indicating that their expression is induced early in infection and is sustained for at least 24 hours. Overall, our data indicates that infection does polarise macrophages towards a pro-inflammatory state, but this is independent and uncoupled from FAS and FAO.

Our results tie into the debate over the absolute necessity of FAO for M2 polarisation. Earlier reports demonstrated the requirement of this energy source

for M2 activation in murine macrophages using high concentrations of etomoxir to inhibit CPT-1 (Huang et al, 2014; Huang et al, 2016; Malandrino et al, 2015), but subsequent studies revealed no impact on M2 associated gene expression when cells were treated with lower concentrations of etomoxir (Divakaruni et al, 2018; Namgaladze & Brüne, 2014; Van den Bossche et al, 2016). Another study additionally found that deleting CPT-2 in BMDM rendered the cells incapable of oxidising FAs, but this resulted in no reduction in IL-4-induced M2 markers (Nomura et al, 2016a). A recent paper demonstrated that OXPHOS was indispensable for M2 polarisation, and the effect of high concentrations of etomoxir (~200 μM) on M2 polarisation was traced to depleted levels of free-CoA resulting from the conversion of etomoxir to etomoxiryl-CoA, and not from a loss in CPT-1 activity (Divakaruni et al, 2018). The lack of effect we see with etomoxir treatment on macrophage marker expression is therefore not entirely surprising, and FAO in our system may not be essential to M2 polarisation. An intact mitochondrial respiration complex may therefore be more of an M2 marker than increased FAO, which is what we observe in our infected cells.

This leads us to ask the question of why we do not see an increase in pro-inflammatory markers when we treat with orlistat, etomoxir or TOFA, all of which reduced mitochondrial respiration. This answer may depend on the mechanism underlying the reduction in OXPHOS by these inhibitors; mitochondrial defects in pro-inflammatory macrophages are induced by NO, and result in ROS production, however this is unlikely the case for our inhibitors. If decreased OXPHOS isn't a consequence of increased iNOS and NO, then it may not have the same effects on macrophage polarisation. It is possible that the reduction in OCR we observe is simply a result of FAS and/or FAO inhibition, and as we still see a basal OCR of >80 pmol/min, this suggests that the mitochondria are still functioning, and this may not be enough of a trigger to affect polarisation. Our observation with these inhibitors also leads us to postulate that the expression of these specific surface markers simply may not be directly, or solely induced by metabolic triggers.

Although we see some facets of pro-inflammatory macrophage polarisation during infection, we still do not know if this is accompanied by a pro-inflammatory response. Despite seeing no effect on surface marker expression, whether the levels of cytokines, ISGs or inflammatory mediators are impacted by FAS and FAO remains to be elucidated, and is something we would like to explore further. As we see such efficient replication in this cellular model, we would posit that there is blocking or evading of immune responses present to some degree. This may very well be influenced by the more or less homeostatic metabolic state we observed during infection, and may involve the downregulation of NO and IL-1β at least. The impact of Flavivirus infection of metabolism observed by other groups suggests results may be cell type specific and strain specific (Chen et al, 2020; Heaton & Randall, 2010). Although WNV_{KUN} is an encephalitic strain, it is attenuated compared to the WNV_{NY99} strain, and it may be possible that the dysregulation of metabolism, particularly mitochondrial respiration, is a contributing factor to the pathology of more severe strains. This has been observed in a mouse model of ZIKV infection, where the dysregulation of mitochondrial respiration was key to inflammation in a severe versus an attenuated strain, and predicated congenital disease (Yau et al, 2021). A side-by-side analysis of encephalitic vs non-encephalitic strains in neurons would be a useful means of investigating if there's a disruption of the metabolic axis in encephalitic strains that is driving inflammation.

To date the study of macrophage polarisation states have been predominantly performed in the context of LPS and/or IFN-γ stimulation, and have been mostly exclusive of viral infection. In this study, in addition to assessing the role of FA pathways during infection we successfully categorised, for the first time, the metabolic signature and polarisation state of Flavivirus- infected macrophages. Overall, we observed a combination of M1 and M2 markers with both viruses and believe that the activation state of infected macrophages is distinct from that of classically activated macrophages (see Figure 52). Although we observed pro-inflammatory polarisation markers for WNV and ZIKV, and a slight upregulation of glycolysis for WNV, this was not accompanied by the mitochondrial dysfunction that underpins the pro-inflammatory phenotype. As in other cell types, infection

is dependent on FAS and FAO in these macrophages, but utilisation of these pathways does not exacerbate the inflammatory phenotype. If anything, we believe metabolic manipulations in this case may be dampening immune responses, and our metabolic data is indicative of several possible attenuations of the immune response, including blockage of NO production via inhibition of STAT1, decreased ROS production, and impaired IL-1β signalling. The immediate next steps for this project are therefore to investigate iNOS expression and determine if this correlates to STAT1 inhibition in these cells, using poly I:C as a control. We would additionally like to identify the cytokine expression profile of these cells to determine if the polarisation of macrophage we observe during infection is followed by an inflammatory response, and if FAS and FAO are affecting their production.

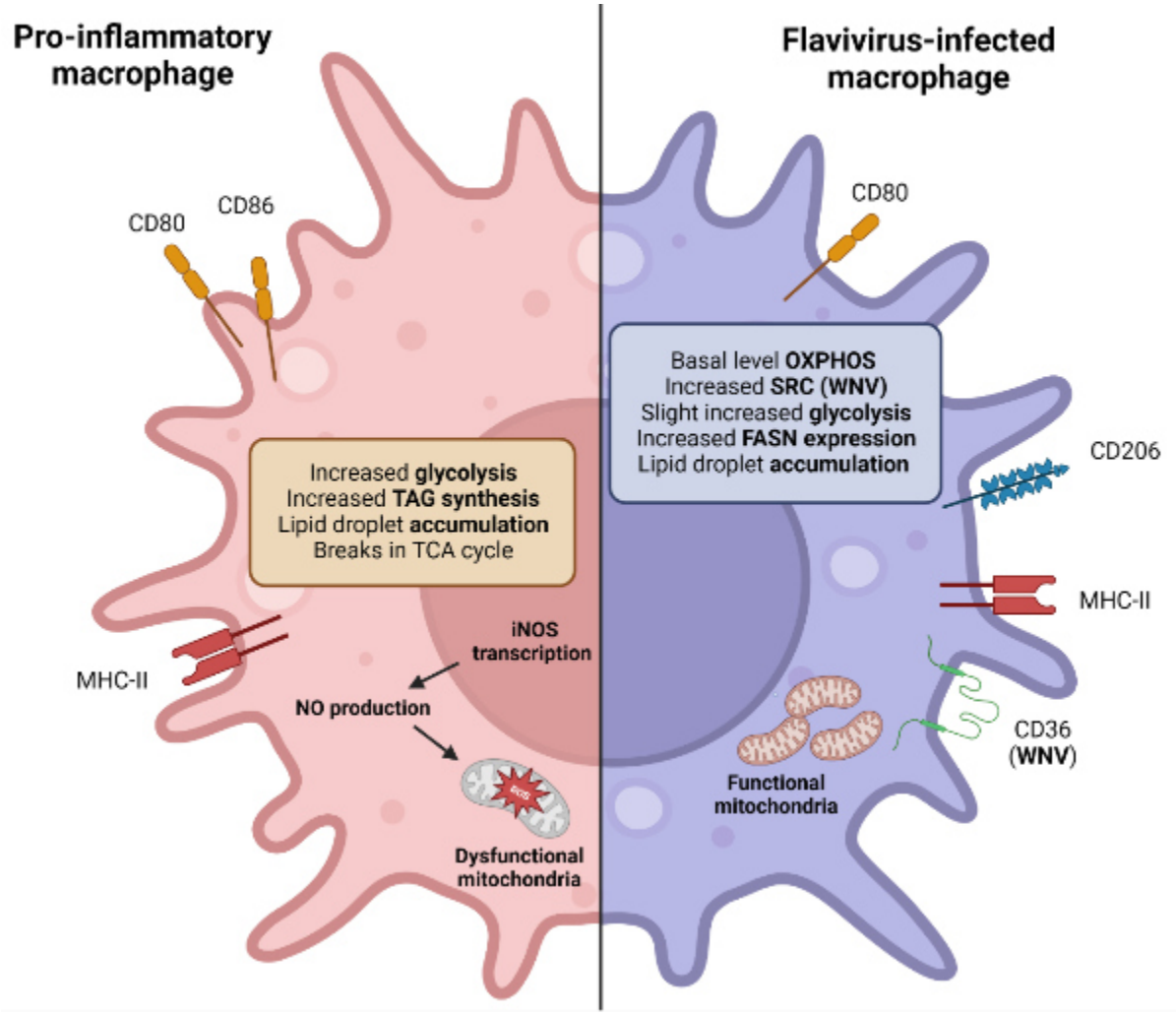

Figure 52. The metabolic signature and polarisation state of a classically activated pro-inflammatory macrophage (LPS+IFN-γ) versus a Flavivirus-infected macrophage. Classically activated pro-inflammatory macrophages generally display increased glycolysis, TAG synthesis, and dysregulated mitochondria. This dysregulation is a result of an upregulation of inducible nitric oxide-synthase (iNOS) transcription, resulting in increased nitric oxide (NO) production, which damages mitochondria and lowers OXPHOS. These macrophages also display two breaks in the TCA cycle which produce microbiocidal intermediates and is accompanied by the expression of several pro-inflammatory surface markers including CD80, CD86 and MHC-II. The results from this study with RAW264.7 macrophages indicate that macrophages infected with West Nile virus (WNV) or Zika virus (ZIKV) display a mix of pro-inflammatory and anti-inflammatory macrophage markers. They exhibit functional mitochondria and unchanged mitochondrial respiration compared to uninfected cells. WNV also displays an increase in spare respiratory capacity (SRC) and mitochondrial mass, indicative of functional changes to mitochondria. Infection results in increased FASN expression and lipid droplet accumulation, accompanied by a

mix of pro-inflammatory (CD80, MHC-II) and anti-inflammatory (CD206, CD36) macrophage surface markers.

The simplification of macrophage phenotypes using the M1/M2 model is often criticised and its usefulness questioned by some immunologists (Martinez & Gordon, 2014; Nahrendorf & Swirski, 2016). It is argued that this model is not representative of the diversity of macrophage phenotypes that have been found, and simplifies the complex nature and entanglement of metabolic pathways in macrophage activation states. Throughout this chapter we have used this model, but only as a comparative tool, which has aided us in categorising the phenotype of infected cells and allowed us to infer potential immune evasion mechanisms orchestrated by these viruses. Indeed, the profile we observe in infected cells provides only more evidence of the complex nature of macrophage phenotypes. Departure from these discrete M1/M2 profiles has been shown to be dependent on stimuli, and Flavivirus-infected cells clearly lie within the spectrum of phenotypes, as opposed to the extreme ends induced by our controls. We believe that virus-induced macrophage phenotypes comprise their own category of phenotype, which likely differs between viruses. As research in the immunometabolism field progresses, the targeting of metabolic pathways in immune cells is emerging as a promising area for therapeutics for infection and other diseases. We believe further research on this area will provide valued insight into the drivers of inflammation, as well as inform future research into therapeutics which are critically needed for Flaviviruses.

Chapter 5
General discussion and future directions

FAs play important roles in immunity and signal transduction, but they are also pro-viral. Immune cell activation and viral infection can both fundamentally alter metabolism and change the lipid landscape of cells. Targeting lipid and metabolic pathways with therapeutics has been a potential area for investigation for viral infection, cancer, and metabolic disease, but before this can be considered for Flavivirus infection, we believe it is essential to delineate the role of FAs during infection in immune cells. This understanding is integral to ensure targeting these pathways does not diminish, or exacerbate, the host immune response. We hypothesised that, as macrophage phenotypes are underpinned by specific metabolic conditions, and FAs contribute to inflammatory processes, any alteration of FA metabolism by Flaviviruses could affect the inflammatory response. Our aim was to attempt to link virus-induced changes in the metabolic and lipid landscape with inflammatory biomarkers, with the hopes of broadening our understanding of what drives inflammation at a cellular level.

As metabolism is inherently complex, we believed the relationship between FAs, infection, and immunity is likely complicated. For this reason, we investigated the FA and metabolic requirements in both an immune and a non-immune cellular background, to determine the basal metabolic requirements of these viruses, and assay if these differed in an immunity context. For immune cells such as macrophages, functionality is largely defined and driven by metabolic reprogramming, with mitochondria being integral signalling organelles capable of responding to both internal and external cues. These specialised cells require the ability to rapidly transform their metabolic state from homeostatic to highly active, to support inflammatory functions such as signal transduction and phagocytosis. Not all cells are capable of or require such plasticity, however, and are not as metabolically active. Throughout this project we utilised a kidney epithelial cell line, Veros, which are IFN-deficient and allowed us to study the relationship between Flavivirus infection and metabolism in the absence of IFN-stimulated

immune pathways. We then compared this with our results in macrophages to ascertain if there were metabolic perturbations induced by Flaviviruses that are specific to immune cells, and what consequences these may have on immune responses. Since Flaviviruses have a broad cellular tropism, and thus far the host factors required for replication have varied between cell types, we thought it essential to investigate two distinct cell types.

Overall, our investigations revealed that *de novo* FAS is a basic requirement for Flavivirus genome replication. Our data supports previous reports that FAs are indispensable for viral-induced membrane formation. As FAs are building blocks for more complex lipids, several studies have identified that chemical inhibition mediated via the compounds TOFA, c75 and orlistat can result in the decrease in not only FAs, but also ceramides, neutral lipids, and phospholipids (Jeucken & Brouwers, 2019; Jiménez de Oya et al, 2019). Each of these lipid species have been identified as integral for Flavivirus replication complex morphogenesis, and likely disrupt the curvature and fluidity of these membranes or deprive the cells completely of these membrane building blocks. We further demonstrated that the oxidation of FAs in the mitochondria was important for infectious virus production in both cell types, and that FAs contributed to OXPHOS to a greater extent in macrophages relative to epithelial cells. Despite this, our assessment of mitochondrial function revealed similar metabolic consequences of infection between cell types, in that neither WNV or ZIKV significantly alter rates of mitochondrial respiration or glycolysis relative to uninfected cells. For ZIKV, our results are in contrast with several other reports that have observed mitochondrial damage and dysfunction upon infection in placental or neuronal cells (Chen et al, 2020; Ledur et al, 2020; Rabelo et al, 2020), or an upregulation of the glycolytic pathway (Fontaine et al, 2015; Yau et al, 2021), however none of these studies were performed using the African ZIKV lineage or cell types used throughout this study. For WNV, we conversely observed modest enhancement of mitochondrial function in macrophages only, with an increase in mitochondrial mass and SRC, indicating that WNV is exerting effects on this organelle. Although we did not observe the same mitochondrial enhancement with ZIKV, this may be linked to the higher replication rate we observed for WNV in this cell type (see Figure 39a

and b). Overall, this data suggests that WNV and ZIKV usurp energy produced from FAO to fuel replication, but in macrophages this is done to a greater extent. The impact of WNV infection on host metabolism has not previously been investigated, and here we provide evidence that is consistent with WNV inducing specific functional changes in mitochondria in macrophages.

If we combine the data from this study with all current knowledge of infection in other cell types, it appears that Flaviviruses display a degree of plasticity in terms of metabolic needs. *De novo* FAS is required in every cell type thus far examined, but the manipulations of glycolytic and mitochondrial metabolism are variable, at least for DENV. This begs us to ask the question, what are the determinants of the metabolic outcome of infection in different cell types? We believe this is likely dependent on the strain of virus, the interactions between the virus and the cell-specific metabolic regulatory systems of different cells, and the metabolic microenvironment at the time of infection. We know that different cell types have distinct mechanisms of regulating metabolism, as exemplified in the regulation of OXPHOS in macrophages via NO production. The potential regulation of this metabolic pathway by Flaviviruses may therefore be specific to this cell type, or immune cells in general. Lastly, the ability of these viruses to drive metabolic pathways may depend on the availability of metabolic resources (*i.e.* lipids and glucose), and their ability to co-opt metabolic proteins (such as FASN and FA import and transport proteins). For example, in our Vero cell model, it is possible that we would observe an upregulation in OXPHOS under conditions of higher lipid content, or perhaps an increase in glycolytic rates under substantive glucose availability. It is likely a combination of these factors that determines the metabolic consequences of infection, all of which are important considerations for further research, particularly in an *in vivo* context where metabolic conditions likely differ from our *in vitro* models.

Despite our hypothesis that metabolic alterations induced by the viruses may influence immune responses, we did not observe a link between *de novo* FAS and FAO, and macrophage polarisation, indicating that WNV and ZIKV have possibly developed a sophisticated mechanism to usurp these pathways without

aggravating host immunity. Although we had hypothesised that the utilisation of FASN by these viruses may be a trigger for immune cascades, in our study FASN appeared to be exclusively pro-viral. Over the timeline of this project, several lines of evidence have emerged to support *de novo* FAS being a pro-viral host factor in macrophages. Firstly, although increased TAG synthesis is a pro-inflammatory phenotype, recent evidence has demonstrated that *de novo* FAS does not significantly contribute to TAG pools of activated macrophages, which instead rely on exogenous glucose and FAs, as well as impaired OXPHOS, to generate these TAGs and LD pools (Rosas-Ballina et al, 2020). Secondly, a recent report using *Ifnar*$^{-/-}$ BMDMs and RNA sequencing identified several metabolic genes that are downregulated by IFN-I, and identified FASN as one of these genes (Aliyari et al, 2022). They observed IFN-I downregulated FASN expression via the IFNAR/STAT1 pathway, and further demonstrated that FASN was required for the entry and replication of several viruses including SARS-CoV-2. As FASN is broadly hijacked by pathogens, it is possible that our immune system has evolved this metabolic adaptation to supress infection. Viruses, however, are masters of evolution, thus it is not surprising that they could overcome the suppression of this essential enzyme. This is evident in the cell systems studied here, where we see an upregulation of FASN in macrophages, and FAs contributing to viral RC formation as well as OXPHOS. In Figure 53 we have summarised these findings, and believe the utilisation of *de novo* FAS in infected macrophages is distinct to that of classically activated pro-inflammatory macrophages. As previously mentioned, Flaviviruses have a broad ability to inhibit IFN and STAT1, which may aid in negating this suppression of FASN and promote greater FAS. These two papers, taken together with our data, implicate the FASN pathway as pro-viral and support our observations that FASN is not required for pro-inflammatory macrophage activation.

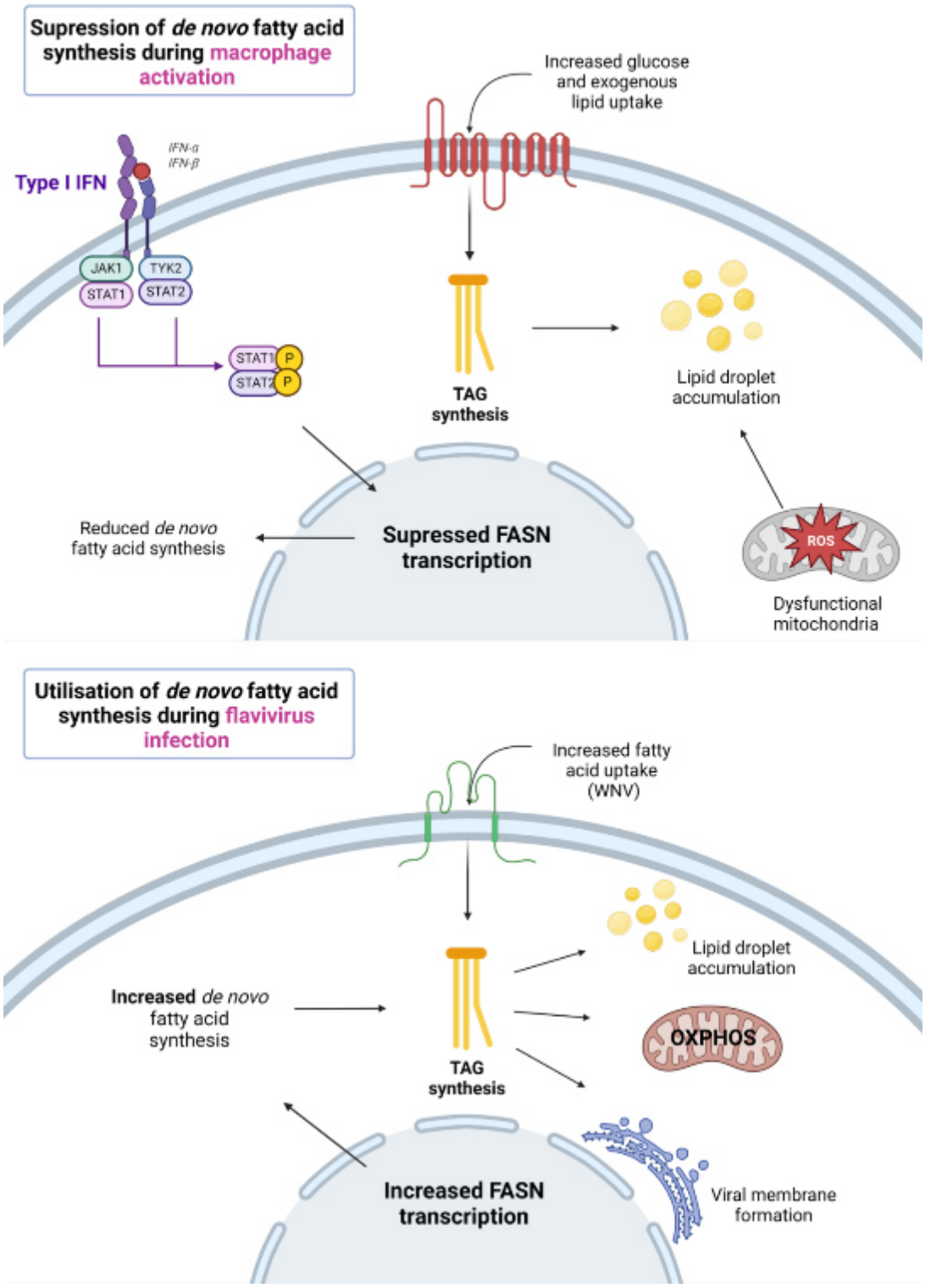

Figure 53. Model describing the suppression of de novo fatty acid synthesis during pro-inflammatory macrophage activation versus the utilisation of this pathway during Flavivirus infection. In classically activated pro-inflammatory macrophages (LPS+IFN-γ), evidence has emerged that FASN is an IFN-supressed gene *(Aliyari et al, 2022)*, and de novo fatty acids contribute very

little to lipid pools observed during activation (upper panel). Instead, synthesis of triacylglycerols is fuelled via the upregulation of glucose and exogenous lipid import *(Rosas-Ballina et al, 2020)*. Conversely, our observations in this study indicated an upregulation of FASN during infection with WNV and ZIKV in mouse macrophages, which contributed to lipid droplet formation as well as mitochondrial respiration and the formation of viral membranes.

In the previous chapter we discussed the possibility of WNV and ZIKV blocking the induction of iNOS, and subsequent NO production, which may allow these infected cells to maintain functional mitochondria and produce energy from this pathway. Several studies have implicated STAT1 activation as a requirement for the transcription of iNOS and NOS2 (Guo et al, 2007; Samardzic et al, 2001; Stempelj et al, 2007). Additionally, NO produced from these pathways in macrophages results in mitochondrial damage and drives the inflammatory phenotype. Although Flavivirus infection results in the production of type I and type II IFNs, we know these viruses are capable of interfering with downstream signalling cascades by antagonising the JAK/STAT pathway (Fanunza et al, 2021a; Fanunza et al, 2021b; Laurent-Rolle et al, 2010; Liu et al, 2005; Roby et al, 2016). Several Flavivirus proteins have been implicated in this process, with DENV NS4B expression alone inhibiting STAT1 and downstream IFN-induced signalling pathways (Muñoz-Jordán et al, 2003), and NS4B and NS2A to a lesser extent. NS5 is also capable of degrading STAT2, an observation consistent amongst Flaviviruses, although for DENV this is human-specific (Ashour et al, 2009; Grant et al, 2016; Laurent-Rolle et al, 2010; Mazzon et al, 2009; Thurmond et al, 2018). Here we propose a model, which can be visualised in Figure 54, whereby WNV and ZIKV may be simultaneously inhibiting immune signalling and promoting the desired intracellular metabolic environment.

We hypothesise that degradation of STAT1, or inhibition of STAT1 phosphorylation, by viral NS proteins, may allow the viruses to both upregulate FASN to increase FAS, and to maintain mitochondrial function via the inhibition of NO production. Inhibition of STAT1 would also likely lead to decreased ISG expression, and a reduction in inflammatory mediators associated with mitochondrial dysfunction (ROS, succinate, citrate, itaconate, IL-1β and

potentially more). To test this hypothesis, we would first assay the expression of total and phosphorylated STAT1 during infection using western blotting to determine if WNV and ZIKV are interfering with this pathway in macrophages. We have done this in the Vero cell line and observed a reduction in total and phosphorylated-STAT1 in infected cells, even in the presence of IFN (Appendix D). Subsequently we would like to attempt to correlate STAT1 inhibition with increased FASN expression and mitochondrial function, using poly I:C as a control. As poly I:C can stimulate IFN-I and IFN-II production, as well as iNOS expression, we posit that poly I:C treatment would likely result in mitochondrial dysfunction, and we would see reduced FASN expression compared to infected cells. In addition to comparing to infected cells, we would utilise gene cassettes we have in our lab containing individual viral NS proteins and transfect cells to determine the role of individual proteins in STAT1 signalling, FASN expression and mitochondrial function (using Mitotracker staining and Seahorse to assess the latter). These experiments would hopefully provide some mechanistic insight into the regulation of these metabolic pathways in macrophages by WNV and ZIKV.

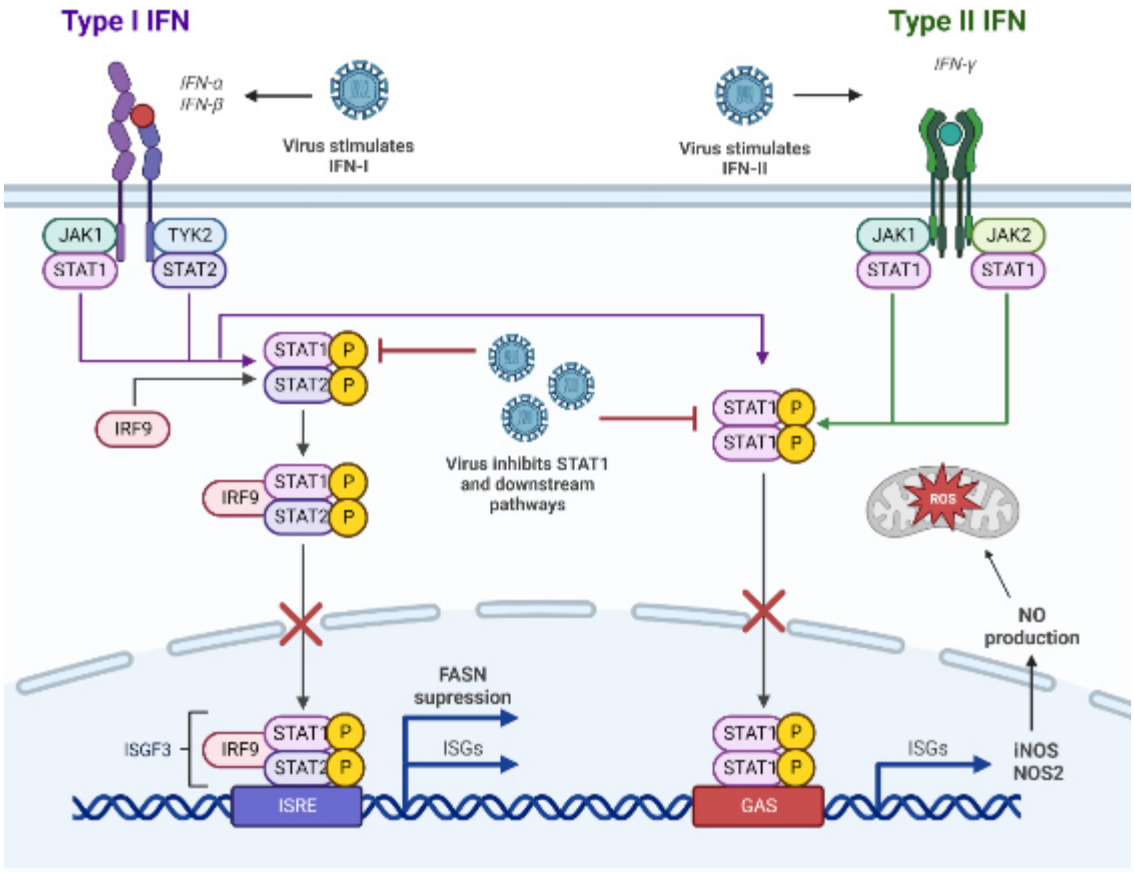

Figure 54. Proposed model for the regulation of metabolic pathways by West Nile and Zika viruses in macrophages. Fatty acid synthase (FASN) activity is essential to the replication of several Flaviviruses, including in macrophages. FASN has also been shown to be an interferon-supressed gene, with transcription being downregulated in wild-type BMDMs compared to Ifnar$^{-/-}$ BMDMs. This suppression of FASN was shown to require a functional IFNAR receptor and downstream STAT1 activation. STAT1, upon activation by IFN- g, is also necessary for the transcription of iNOS and NOS2 in pro-inflammatory macrophages. This results in increased NO production, which damages mitochondria and drives the inflammatory phenotype. In mouse macrophages (RAW264.7 cells). As numerous studies have illustrated the ability of Flaviviruses to block STAT1 signalling cascades, we hypothesise that inhibiting STAT1 in macrophages allows these viruses to promote the ideal metabolic microenvironment by increasing fatty acid synthesis and maintaining functional mitochondria and metabolic homeostasis by inhibiting NO production. Image was adapted from 'Interferon Pathway' by Biorender.com (2020).

Whilst inhibition of STAT1 seems a likely contender for the control of metabolism by these viruses, we would additionally like to explore the potential regulation of

adenosine 5'-monophosphate-activated protein kinase (AMPK) by WNV and ZIKV. AMPK is a cellular sensor of ATP, and regulates the nexus between FAO and FAS. In response to low ATP levels, AMPK is activated and can phosphorylate several metabolic proteins, to shift cells from energy consumption to energy production. Activation of AMPK results in the phosphorylation and subsequent inhibition of ACC1, ACC2, HMGCR, SREBP1 and CHREBP, and upregulates mitochondrial biogenesis and fission and increases CPT-1 activity. DENV, WNV and ZIKV all have a demonstrated ability to inhibit AMPK, resulting in increased lipid synthesis (Jiménez de Oya et al, 2018; Singh et al, 2020). ZIKV infection of endothelial cells results in a time-dependent reduction in AMPK activation, which correlated to an increase in ACC expression and an increase in glycolysis (Singh et al, 2020).

As AMPK is such a central metabolic modulator, it has also been implicated as a negative regulator of pro-inflammatory macrophage activation. Stimulation of macrophages with LPS resulted in the dephosphorylation (inactivation) of AMPK and increased TNF-a and IL-6 production (Sag et al, 2008). In endothelial and fibroblast cells, however, inactivation of AMPK resulted in the increase in of inflammatory mediators (TNF-a, CCL5, CXCL10) but reduced the expression of several antiviral genes (OAS2, ISG15, MX1, IFN-α2, IFN-β1, and IFN-γ), indicating that AMPK has an antiviral role for ZIKV (Singh et al, 2020). Based on this data, we believe it's possible that WNV and ZIKV are inactivating AMPK in both cell types as a mechanism of upregulating *de novo* FAS and supressing immune responses. Going forward, we would like to perform a similar study, whereby we investigate the impact of infection on phosphorylated AMPK expression, and potentially use common inhibitors of AMPK to extrapolate its role in viral replication and immune responses in macrophages. In these experiments, we would again utilise poly I:C as a control to dissect if alterations of AMPK are a result of general viral-induced inflammation, or inactivation of upstream kinases by these viruses.

At the beginning of this study, to fully understand the role of FAS during infection and inflammatory responses, we aimed to knockout the FASN gene, and used

inhibitors to evaluate the potential of targeting the *de novo* FAS as a therapeutic against Flaviviruses. Our results with our FASN knockout human macrophages demonstrated without a doubt the necessity of this gene for viral infection, as we observed severe impairment or complete ablation of viral production in the absence of FASN. We then utilised multiple chemical inhibitors to allow us insight into several catalytic activities involved in *de novo* FAS and FAO, which yielded some interesting and unexpected results in both cell types. Blocking FAS at three distinct points along the pathway using TOFA, c75, and orlistat, revealed differing effects on cellular processes and viral infection. Inhibiting ACC using TOFA yielded the most profound effect on viral replication in both cell types. As this enzyme catalyses the rate-limiting step in FAS, it completely inhibited initiation of FAS and gave us the clearest picture of the role of FAS in infection. Conversely, inhibiting the very last catalytic function in the FAS pathway using orlistat did not appear to impair lipid synthesis, and we believe that inhibiting only the thioesterase domain means a FA chain is still being synthesised, but the complex has lost specificity for palmitate. Overall, these results have contributed to the knowledge surrounding these inhibitors, particularly for orlistat, and in the future, we would ideally like to perform some lipidomic analyses on infected and inhibitor-treated cells, as well as a FASN activity assay, to confirm the precise impacts of these inhibitors on the lipid profile of cells. Targeting different activities even within a single metabolic pathway can result in the build-up of different metabolites and have unexpected cellular effects, as has been observed by us and others (Carroll et al, 2018b; Jeucken & Brouwers, 2019). Metabolic pathways are hugely complex and intertwined, and hopefully we have highlighted the importance of choosing the right inhibitors for a particular study, and of taking care when interpreting results.

Drug repurposing is a cost-effective alternative to both the discovery of new drugs and vaccine development, and often carries the benefit of knowing the cellular and clinical effects of these known drugs. The lack of vaccines available for Flavivirus treatment has led researchers to focus on the potential of antiviral drugs. As mentioned previously, orlistat is an FDA-approved drug, and we had hoped that our results may contribute positively to the prospect of orlistat being

used an a Flavivirus therapeutic. Although it has low systemic absorbability, it is believed that it could still be used therapeutically to reduce viral load in infected patients (Aliyari et al, 2022; Hitakarun et al, 2020). Although its antiviral effects have thus far been positive, the results obtained in this study indicate that the antiviral mechanism of orlistat, at least for Flavivirus infection, is not straight forward. We also observed orlistat induce cellular stress, even in uninfected cells, which sparked concerns for us over its clinical use, however severe adverse reactions are not common with the treatment of this drug for obesity. These results will hopefully provoke further investigation into the molecular mechanisms driving orlistat's viral inhibition in other studies, and hopefully inform a wider audience of the possible cellular consequences and off-target effects of orlistat treatment. Perhaps more promisingly, ACC inhibitor PF-05175157 has shown to be effective at reducing viral load in mice challenged with WNV (Jiménez de Oya et al, 2019). This inhibitor has also been used previously in clinical studies with both healthy patients and those with diabetes mellitus, and its safety has not proved a concern. Indeed, our results suggests that inhibition of ACC may be the most promising target for Flavivirus therapeutics.

Since the beginning of this PhD, the field has gained significant understanding of the contribution of FAs and metabolism to immune cell activation. Very recent research has indicated that *de novo* FAS, as well as FAO, are likely dispensable for macrophage polarisation. Although we have not assessed the full immune profile of infected cells, our data supports this; WNV and ZIKV are able to successfully hijack *de novo* FAS without aggravating inflammatory markers, and this may indeed be a reason that replication is so successful in this cell type. The stimulation of FAS and FAO may indeed be immunosuppressive, and our metabolic data has revealed a potential immune evasion strategy by WNV in the form of blocking STAT1 activation and NO production, thereby maintaining mitochondrial homeostasis. The next immediate steps for this project would therefore be the assessment of STAT1 and iNOS activation during infection, as previously discussed, as well as performing a cytokine array to provide an unambiguous description of the immune profile of infected cells, and the impact of our metabolic inhibitors. To strengthen the validity of the study we would further

want to recapitulate these results in human cells, including primary human macrophages. To assess if the dysregulation of the metabolic axis is a driver of severe disease, we would additionally like to study a model of hyper-inflammation/severe disease, such as primary cells from encephalitic mice (ideally cells of the CNS such as microglia and infiltrated macrophages). In these studies, we would include DENV due to its clinical importance and the divergent metabolic shifts reported by others previously.

Overall, the aim of this study was to expand on the current knowledge of the roles of fatty acids in viral replication and metabolism during infection, and to delineate the role of FAs in infection of macrophages; are they on the side of the virus, or the host? The work presented in this thesis illustrates the crucial and seemingly exclusive pro-viral role of *de novo* FAS in immune and non-immune cells. We provide evidence for *de novo* FAS being uncoupled from the activation of pro-inflammatory macrophages, and these viruses likely have a tropism for macrophages due to their high metabolic capacity, particularly when activated. Indeed, an activated macrophage with attenuated immune responses may provide the ideal cellular environment for Flavivirus replication. Although we obtained some unexpected results with our inhibitors, which may indeed broadly inform research surrounding these inhibitors, we believe that *de novo* FAS may prove an effective target for Flavivirus infection, without exacerbating or diminishing the host immune response, and this warrants more research.

References

(2012) Family - Flaviviridae, in King, A. M. Q., Adams, M. J., Carstens, E. B. & Lefkowitz, E. J. (eds), *Virus Taxonomy*. San Diego: Elsevier, 1003-1020.

Abu-Elheiga, L., Brinkley, W. R., Zhong, L., Chirala, S. S., Woldegiorgis, G. & Wakil, S. J. (2000) The subcellular localization of acetyl-CoA carboxylase 2. *Proceedings of the National Academy of Sciences of the United States of America*, 97(4), 1444-1449.

Ackermann, M. & Padmanabhan, R. (2001) De novo synthesis of RNA by the dengue virus RNA-dependent RNA polymerase exhibits temperature dependence at the initiation but not elongation phase. *J Biol Chem*, 276(43), 39926-37.

Agnello, V., Abel, G., Elfahal, M., Knight, G. B. & Zhang, Q. X. (1999) Hepatitis C virus and other flaviviridae viruses enter cells via low density lipoprotein receptor. *Proc Natl Acad Sci U S A*, 96(22), 12766-71.

Aguirre, S. & Fernandez-Sesma, A. (2017) Collateral Damage during Dengue Virus Infection: Making Sense of DNA by cGAS. *Journal of virology*, 91(14), e01081-16.

Aguirre, S., Luthra, P., Sanchez-Aparicio, M. T., Maestre, A. M., Patel, J., Lamothe, F., Fredericks, A. C., Tripathi, S., Zhu, T., Pintado-Silva, J., Webb, L. G., Bernal-Rubio, D., Solovyov, A., Greenbaum, B., Simon, V., Basler, C. F., Mulder, L. C. F., García-Sastre, A. & Fernandez-Sesma, A. (2017) Dengue virus NS2B protein targets cGAS for degradation and prevents mitochondrial DNA sensing during infection. *Nature microbiology*, 2, 17037-17037.

Ahn, A., Gibbons, D. L. & Kielian, M. (2002) The Fusion Peptide of Semliki Forest Virus Associates with Sterol-Rich Membrane Domains, 76(7), 3267-3275.

Akey, D. L., Brown, W. C., Dutta, S., Konwerski, J., Jose, J., Jurkiw, T. J., DelProposto, J., Ogata, C. M., Skiniotis, G., Kuhn, R. J. & Smith, J. L. (2014) Flavivirus NS1 structures reveal surfaces for associations with membranes and the immune system. *Science (New York, N.Y.)*, 343(6173), 881-885.

Aktepe, T. E. & Mackenzie, J. M. (2018) Shaping the flavivirus replication complex: It is curvaceous! *Cell Microbiol*, 20(8), e12884.

Aktepe, T. E., Pham, H. & Mackenzie, J. M. (2015) Differential utilisation of ceramide during replication of the flaviviruses West Nile and dengue virus. *Virology*, 484, 241-50.

Aliota, M. T., Caine, E. A., Walker, E. C., Larkin, K. E., Camacho, E. & Osorio, J. E. (2016) Characterization of Lethal Zika Virus Infection in AG129 Mice. *PLoS Negl Trop Dis*, 10(4), e0004682.

Aliyari, S. R., Ghaffari, A. A., Pernet, O., Parvatiyar, K., Wang, Y., Gerami, H., Tong, A. J., Vergnes, L., Takallou, A., Zhang, A., Wei, X., Chilin, L. D., Wu, Y., Semenkovich, C. F., Reue, K., Smale, S. T., Lee, B. & Cheng, G. (2022) Suppressing fatty acid synthase by type I interferon and chemical inhibitors as a broad spectrum anti-viral strategy against SARS-CoV-2. *Acta Pharm Sin B*, 12(4), 1624-1635.

Alvisi, G., Madan, V. & Bartenschlager, R. (2011) Hepatitis C virus and host cell lipids: an intimate connection. *RNA Biol*, 8(2), 258-69.

Ambrose, R. L. & Mackenzie, J. M. (2011a) A conserved peptide in West Nile virus NS4A protein contributes to proteolytic processing and is essential for replication. *Journal of virology*, 85(21), 11274-11282.

Ambrose, R. L. & Mackenzie, J. M. (2011b) West Nile virus differentially modulates the unfolded protein response to facilitate replication and immune evasion. *J Virol*, 85(6), 2723-32.

Amiri, M., Yousefnia, S., Seyed Forootan, F., Peymani, M., Ghaedi, K. & Nasr Esfahani, M. H. (2018) Diverse roles of fatty acid binding proteins (FABPs) in development and pathogenesis of cancers. *Gene*, 676, 171-183.

AOCS (2021) *Fatty Acid beta-Oxidation*, 2021. Available online: https://lipidlibrary.aocs.org/chemistry/physics/animal-lipids/fatty-acid-beta-oxidation [Accessed.

Aoki, C., Hidari, K. I. P. J., Itonori, S., Yamada, A., Takahashi, N., Kasama, T., Hasebe, F., Islam, M. A., Hatano, K., Matsuoka, K., Taki, T., Guo, C.-T., Takahashi, T., Sakano, Y., Suzuki, T., Miyamoto, D., Sugita, M., Terunuma, D., Morita, K. & Suzuki, Y. (2006) Identification and Characterization of Carbohydrate Molecules in Mammalian Cells Recognized by Dengue Virus Type 2. *The Journal of Biochemistry*, 139(3), 607-614.

Arias, C. F., Preugschat, F. & Strauss, J. H. (1993) Dengue 2 virus NS2B and NS3 form a stable complex that can cleave NS3 within the helicase domain. *Virology*, 193(2), 888-99.

Ashhurst, T. M., Vreden, C., Munoz-Erazo, L., Niewold, P., Watabe, K., Terry, R. L., Deffrasnes, C., Getts, D. R. & Cole King, N. J. (2013) Antiviral macrophage responses in flavivirus encephalitis. *Indian J Med Res*, 138(5), 632-47.

Ashour, J., Laurent-Rolle, M., Shi, P. Y. & García-Sastre, A. (2009) NS5 of dengue virus mediates STAT2 binding and degradation. *J Virol*, 83(11), 5408-18.

Au-Yeung, N. & Horvath, C. M. (2018) Transcriptional and chromatin regulation in interferon and innate antiviral gene expression. *Cytokine & growth factor reviews*, 44, 11-17.

Bailey, J. D., Diotallevi, M., Nicol, T., McNeill, E., Shaw, A., Chuaiphichai, S., Hale, A., Starr, A., Nandi, M., Stylianou, E., McShane, H., Davis, S., Fischer, R., Kessler, B. M., McCullagh, J., Channon, K. M. & Crabtree, M. J. (2019) Nitric Oxide Modulates Metabolic Remodeling in Inflammatory Macrophages through TCA Cycle Regulation and Itaconate Accumulation. *Cell Rep*, 28(1), 218-230.e7.

Baillie, A. G. S., Coburn, C. T. & Abumrad, N. A. (1996) Reversible Binding of Long-chain Fatty Acids to Purified FAT, the Adipose CD36 Homolog. *The Journal of Membrane Biology*, 153(1), 75-81.

Barba, G., Harper, F., Harada, T., Kohara, M., Goulinet, S., Matsuura, Y., Eder, G., Schaff, Z., Chapman, M. J., Miyamura, T. & Bréchot, C. (1997) Hepatitis C virus core protein shows a cytoplasmic localization and associates to cellular lipid storage droplets. *Proc Natl Acad Sci U S A*, 94(4), 1200-5.

Barber, M. C., Price, N. T. & Travers, M. T. (2005) Structure and regulation of acetyl-CoA carboxylase genes of metazoa. *Biochim Biophys Acta*, 1733(1), 1-28.

Barbier, V., Lang, D., Valois, S., Rothman, A. L. & Medin, C. L. (2017) Dengue virus induces mitochondrial elongation through impairment of Drp1-triggered mitochondrial fission. *Virology*, 500, 149-160.

Barton, G. M. & Medzhitov, R. (2003) Linking Toll-like receptors to IFN-α/β expression. *Nature Immunology*, 4(5), 432-433.

Baxter, E. W., Graham, A. E., Re, N. A., Carr, I. M., Robinson, J. I., Mackie, S. L. & Morgan, A. W. (2020) Standardized protocols for differentiation of THP-1 cells to macrophages with distinct M(IFNγ+LPS), M(IL-4) and M(IL-10) phenotypes. *Journal of Immunological Methods*, 478, 112721.

Beatty, P. R., Puerta-Guardo, H., Killingbeck, S. S., Glasner, D. R., Hopkins, K. & Harris, E. (2015) Dengue virus NS1 triggers endothelial permeability and vascular leak that is prevented by NS1 vaccination. *Sci Transl Med*, 7(304), 304ra141.

Beaty, N. B. & Lane, M. D. (1983) Kinetics of activation of acetyl-CoA carboxylase by citrate. Relationship to the rate of polymerization of the enzyme. *J Biol Chem*, 258(21), 13043-50.

Beltrán, B., Mathur, A., Duchen, M. R., Erusalimsky, J. D. & Moncada, S. (2000) The effect of nitric oxide on cell respiration: A key to understanding its role in cell survival or death. *Proceedings of the National Academy of Sciences*, 97(26), 14602-14607.

Ben-Nathan, D., Huitinga, I., Lustig, S., van Rooijen, N. & Kobiler, D. (1996) West Nile virus neuroinvasion and encephalitis induced by macrophage depletion in mice. *Arch Virol*, 141(3-4), 459-69.

Benfrid, S., Park, K.-H., Dellarole, M., Voss, J. E., Tamietti, C., Pehau-Arnaudet, G., Raynal, B., Brûlé, S., England, P., Zhang, X., Mikhailova, A., Hasan, M., Ungeheuer, M.-N., Petres, S., Biering, S. B., Harris, E., Sakuntabhai, A., Buchy, P., Duong, V., Dussart, P., Coulibaly, F., Bontems, F., Rey, F. A. & Flamand, M. (2022) Dengue virus NS1 protein conveys pro-inflammatory signals by docking onto high-density lipoproteins. *EMBO reports*, 23(7), e53600.

Berger, K. L., Cooper, J. D., Heaton, N. S., Yoon, R., Oakland, T. E., Jordan, T. X., Mateu, G., Grakoui, A. & Randall, G. (2009) Roles for endocytic trafficking and phosphatidylinositol 4-kinase III alpha in hepatitis C virus replication. *Proc Natl Acad Sci U S A*, 106(18), 7577-82.

Berndt, J., Kovacs, P., Ruschke, K., Klöting, N., Fasshauer, M., Schön, M. R., Körner, A., Stumvoll, M. & Blüher, M. (2007) Fatty acid synthase gene expression in human adipose tissue: association with obesity and type 2 diabetes. *Diabetologia*, 50(7), 1472-1480.

Bersuker, K. & Olzmann, J. A. (2017) Establishing the lipid droplet proteome: Mechanisms of lipid droplet protein targeting and degradation. *Biochim Biophys Acta Mol Cell Biol Lipids*, 1862(10 Pt B), 1166-1177.

Bersuker, K., Peterson, C. W. H., To, M., Sahl, S. J., Savikhin, V., Grossman, E. A., Nomura, D. K. & Olzmann, J. A. (2018) A Proximity Labeling Strategy Provides Insights into the Composition and Dynamics of Lipid Droplet Proteomes. *Developmental cell*, 44(1), 97-112.e7.

Bertani, F. R., Mozetic, P., Fioramonti, M., Iuliani, M., Ribelli, G., Pantano, F., Santini, D., Tonini, G., Trombetta, M., Businaro, L., Selci, S. & Rainer, A. (2017) Classification of M1/M2-polarized human macrophages by label-free hyperspectral reflectance confocal microscopy and multivariate analysis. *Sci Rep*, 7(1), 8965.

Bertolio, R., Napoletano, F., Mano, M., Maurer-Stroh, S., Fantuz, M., Zannini, A., Bicciato, S., Sorrentino, G. & Del Sal, G. (2019) Sterol regulatory element binding protein 1 couples mechanical cues and lipid metabolism. *Nature Communications*, 10(1), 1326.

Best, S. M. & Pierson, T. C. (2017) The Many Faces of the Flavivirus NS5 Protein in Antagonism of Type I Interferon Signaling, 91(3), e01970-16.

Bhatt, S., Gething, P. W., Brady, O. J., Messina, J. P., Farlow, A. W., Moyes, C. L., Drake, J. M., Brownstein, J. S., Hoen, A. G., Sankoh, O., Myers, M. F., George, D. B., Jaenisch, T., Wint, G. R. W., Simmons, C. P., Scott, T. W., Farrar, J. J. & Hay, S. I. (2013) The global distribution and burden of dengue. *Nature*, 496, 504.

Binnington, K. C. & Hoffmann, A. A. (1989) Wolbachia-like organisms and cytoplasmic incompatibility in Drosophila simulans. *Journal of Invertebrate Pathology*, 54(3), 344-352.

Bonen, A., Chabowski, A., Luiken, J. J. F. P. & Glatz, J. F. C. (2007) Mechanisms and Regulation of Protein-Mediated Cellular Fatty Acid Uptake: Molecular, Biochemical, and Physiological Evidence. *Physiology*, 22(1), 15-28.

Borgström, B. (1988) Mode of action of tetrahydrolipstatin: a derivative of the naturally occurring lipase inhibitor lipstatin. *Biochimica et Biophysica Acta (BBA) - Lipids and Lipid Metabolism*, 962(3), 308-316.

Borradaile, N. M., Han, X., Harp, J. D., Gale, S. E., Ory, D. S. & Schaffer, J. E. (2006) Disruption of endoplasmic reticulum structure and integrity in lipotoxic cell death. *J Lipid Res*, 47(12), 2726-37.

Bosch, M., Sánchez-Álvarez, M., Fajardo, A., Kapetanovic, R., Steiner, B., Dutra, F., Moreira, L., López, J. A., Campo, R., Marí, M., Morales-Paytuví, F., Tort, O., Gubern, A., Templin, R. M., Curson, J. E. B., Martel, N., Català, C., Lozano, F., Tebar, F., Enrich, C., Vázquez, J., Del Pozo, M. A., Sweet, M. J., Bozza, P. T., Gross, S. P., Parton, R. G. & Pol, A. (2020) Mammalian lipid droplets are innate immune hubs integrating cell metabolism and host defense, 370(6514), eaay8085.

Bowen, R. A. & Nemeth, N. M. (2007) Experimental infections with West Nile virus. *Curr Opin Infect Dis*, 20(3), 293-7.
Bowman, L. R., Donegan, S. & McCall, P. J. (2016) Is Dengue Vector Control Deficient in Effectiveness or Evidence?: Systematic Review and Meta-analysis. *PLOS Neglected Tropical Diseases*, 10(3), e0004551.
Bozza, P. T., Magalhães, K. G. & Weller, P. F. (2009) Leukocyte lipid bodies - Biogenesis and functions in inflammation. *Biochim Biophys Acta*, 1791(6), 540-51.
Brody, S., Oh, C., Hoja, U. & Schweizer, E. (1997) Mitochondrial acyl carrier protein is involved in lipoic acid synthesis in Saccharomyces cerevisiae. *FEBS Lett*, 408(2), 217-20.
Brownsey, R. W., Zhande, R. & Boone, A. N. (1997) Isoforms of acetyl-CoA carboxylase: structures, regulatory properties and metabolic functions. *Biochem Soc Trans*, 25(4), 1232-8.
Buckley, D., Duke, G., Heuer, T. S., O'Farrell, M., Wagman, A. S., McCulloch, W. & Kemble, G. (2017) Fatty acid synthase – Modern tumor cell biology insights into a classical oncology target. *Pharmacology & Therapeutics*, 177, 23-31.
Busch, A. K., Gurisik, E., Cordery, D. V., Sudlow, M., Denyer, G. S., Laybutt, D. R., Hughes, W. E. & Biden, T. J. (2005) Increased fatty acid desaturation and enhanced expression of stearoyl coenzyme A desaturase protects pancreatic beta-cells from lipoapoptosis. *Diabetes*, 54(10), 2917-24.
Byrne, S. N., Halliday, G. M., Johnston, L. J. & King, N. J. (2001) Interleukin-1beta but not tumor necrosis factor is involved in West Nile virus-induced Langerhans cell migration from the skin in C57BL/6 mice. *J Invest Dermatol*, 117(3), 702-9.
Caini, P., Guerra, C. T., Giannini, C., Giannelli, F., Gragnani, L., Petrarca, A., Solazzo, V., Monti, M., Laffi, G. & Zignego, A. L. (2007) Modifications of plasma platelet-activating factor (PAF)-acetylhydrolase/PAF system activity in patients with chronic hepatitis C virus infection. *J Viral Hepat*, 14(1), 22-8.
Campanero-Rhodes, M. A., Smith, A., Chai, W., Sonnino, S., Mauri, L., Childs, R. A., Zhang, Y., Ewers, H., Helenius, A., Imberty, A. & Feizi, T. (2007) N-glycolyl GM1 ganglioside as a receptor for simian virus 40. *J Virol*, 81(23), 12846-58.
Camus, G., Herker, E., Modi, A. A., Haas, J. T., Ramage, H. R., Farese, R. V., Jr. & Ott, M. (2013) Diacylglycerol acyltransferase-1 localizes hepatitis C virus NS5A protein to lipid droplets and enhances NS5A interaction with the viral capsid core. *J Biol Chem*, 288(14), 9915-9923.
Cao-Lormeau, V.-M., Blake, A., Mons, S., Lastère, S., Roche, C., Vanhomwegen, J., Dub, T., Baudouin, L., Teissier, A., Larre, P., Vial, A.-L., Decam, C., Choumet, V., Halstead, S. K., Willison, H. J., Musset, L., Manuguerra, J.-C., Despres, P., Fournier, E., Mallet, H.-P., Musso, D., Fontanet, A., Neil, J. & Ghawché, F. (2016) Guillain-Barré Syndrome outbreak associated with Zika virus infection in French Polynesia: a case-control study. *The Lancet*, 387(10027), 1531-1539.
Carro, S. D. & Cherry, S. (2021) Beyond the Surface: Endocytosis of Mosquito-Borne Flaviviruses. *Viruses*, 13(1).
Carroll, R. G., Zaslona, Z., Galván-Peña, S., Koppe, E. L., Sévin, D. C., Angiari, S., Triantafilou, M., Triantafilou, K., Modis, L. K. & O'Neill, L. (2018a) An unexpected link between fatty acid synthase and cholesterol synthesis in proinflammatory macrophage activation. *Journal of Biological Chemistry*, jbc. RA118. 001921.
Carroll, R. G., Zasłona, Z., Galván-Peña, S., Koppe, E. L., Sévin, D. C., Angiari, S., Triantafilou, M., Triantafilou, K., Modis, L. K. & O'Neill, L. A. (2018b) An unexpected link between fatty acid synthase and cholesterol synthesis in proinflammatory macrophage activation. *J Biol Chem*, 293(15), 5509-5521.
Cerne, D., Zitnik, I. P. & Sok, M. (2010) Increased fatty acid synthase activity in non-small cell lung cancer tissue is a weaker predictor of shorter patient survival than increased lipoprotein lipase activity. *Arch Med Res*, 41(6), 405-9.

Chakravarty, B., Gu, Z., Chirala, S. S., Wakil, S. J. & Quiocho, F. A. (2004) Human fatty acid synthase: structure and substrate selectivity of the thioesterase domain. *Proceedings of the National Academy of Sciences of the United States of America*, 101(44), 15567-15572.
Chambers, T. J., Nestorowicz, A., Amberg, S. M. & Rice, C. M. (1993) Mutagenesis of the yellow fever virus NS2B protein: effects on proteolytic processing, NS2B-NS3 complex formation, and viral replication. *J Virol*, 67(11), 6797-807.
Chanput, W., Mes, J., Vreeburg, R. A., Savelkoul, H. F. & Wichers, H. J. (2010) Transcription profiles of LPS-stimulated THP-1 monocytes and macrophages: a tool to study inflammation modulating effects of food-derived compounds. *Food Funct*, 1(3), 254-61.
Chanput, W., Mes, J. J., Savelkoul, H. F. & Wichers, H. J. (2013) Characterization of polarized THP-1 macrophages and polarizing ability of LPS and food compounds. *Food Funct*, 4(2), 266-76.
Chappell, K. J., Stoermer, M. J., Fairlie, D. P. & Young, P. R. (2008) West Nile Virus NS2B/NS3 protease as an antiviral target. *Curr Med Chem*, 15(27), 2771-84.
Charlier, N., De Clercq, E. & Neyts, J. (2006) Mouse and hamster models for the study of therapy against flavivirus infections. *Novartis Found Symp*, 277, 218-29; discussion 229-32, 251-3.
Chazal, N. & Gerlier, D. (2003) Virus entry, assembly, budding, and membrane rafts. *Microbiology and molecular biology reviews : MMBR*, 67(2), 226-237.
Che, P., Tang, H. & Li, Q. (2013) The interaction between claudin-1 and dengue viral prM/M protein for its entry. *Virology*, 446(1), 303-313.
Chen, H., Wang, D. L. & Liu, Y. L. (2016) Poly (I:C) transfection induces mitochondrial-mediated apoptosis in cervical cancer. *Mol Med Rep*, 13(3), 2689-95.
Chen, H. C., Hofman, F. M., Kung, J. T., Lin, Y. D. & Wu-Hsieh, B. A. (2007) Both virus and tumor necrosis factor alpha are critical for endothelium damage in a mouse model of dengue virus-induced hemorrhage. *J Virol*, 81(11), 5518-26.
Chen, Q., Gouilly, J., Ferrat, Y. J., Espino, A., Glaziou, Q., Cartron, G., El Costa, H., Al-Daccak, R. & Jabrane-Ferrat, N. (2020) Metabolic reprogramming by Zika virus provokes inflammation in human placenta. *Nature Communications*, 11(1), 2967.
Chen, X. & Goodman, J. M. (2017) The collaborative work of droplet assembly. *Biochim Biophys Acta Mol Cell Biol Lipids*, 1862(10 Pt B), 1205-1211.
Cheng, G., Cox, J., Wang, P., Krishnan, M. N., Dai, J., Qian, F., Anderson, J. F. & Fikrig, E. (2010) A C-Type Lectin Collaborates with a CD45 Phosphatase Homolog to Facilitate West Nile Virus Infection of Mosquitoes. *Cell*, 142(5), 714-725.
Chirala, S. S., Chang, H., Matzuk, M., Abu-Elheiga, L., Mao, J., Mahon, K., Finegold, M. & Wakil, S. J. (2003) Fatty acid synthesis is essential in embryonic development: Fatty acid synthase null mutants and most of the heterozygotes die in utero, 100(11), 6358-6363.
Chitraju, C., Mejhert, N., Haas, J. T., Diaz-Ramirez, L. G., Grueter, C. A., Imbriglio, J. E., Pinto, S., Koliwad, S. K., Walther, T. C. & Farese, R. V., Jr. (2017) Triglyceride Synthesis by DGAT1 Protects Adipocytes from Lipid-Induced ER Stress during Lipolysis. *Cell Metab*, 26(2), 407-418.e3.
Chiu, C.-F., Chu, L.-W., Liao, I.-C., Simanjuntak, Y., Lin, Y.-L., Juan, C.-C. & Ping, Y.-H. (2020) The Mechanism of the Zika Virus Crossing the Placental Barrier and the Blood-Brain Barrier, 11.
Cho, S., Park, E.-M., Febbraio, M., Anrather, J., Park, L., Racchumi, G., Silverstein, R. L. & Iadecola, C. (2005) The class B scavenger receptor CD36 mediates free radical production and tissue injury in cerebral ischemia. *The Journal of neuroscience : the official journal of the Society for Neuroscience*, 25(10), 2504-2512.
Chu, J., Xing, C., Du, Y., Duan, T., Liu, S., Zhang, P., Cheng, C., Henley, J., Liu, X., Qian, C., Yin, B., Wang, H. Y. & Wang, R.-F. (2021) Pharmacological inhibition of fatty acid synthesis blocks SARS-CoV-2 replication. *Nature Metabolism*, 3(11), 1466-1475.
Cilloniz, C., Pantin-Jackwood, M. J., Ni, C., Goodman, A. G., Peng, X., Proll, S. C., Carter, V. S., Rosenzweig, E. R., Szretter, K. J., Katz, J. M., Korth, M. J., Swayne, D. E., Tumpey, T. M. & Katze,

M. G. (2010) Lethal dissemination of H5N1 influenza virus is associated with dysregulation of inflammation and lipoxin signaling in a mouse model of infection. *Journal of virology*, 84(15), 7613-7624.
Clifford, G. M., Londos, C., Kraemer, F. B., Vernon, R. G. & Yeaman, S. J. (2000) Translocation of hormone-sensitive lipase and perilipin upon lipolytic stimulation of rat adipocytes. *J Biol Chem*, 275(7), 5011-5.
Cloherty, A. P. M., Olmstead, A. D., Ribeiro, C. M. S. & Jean, F. (2020) Hijacking of Lipid Droplets by Hepatitis C, Dengue and Zika Viruses-From Viral Protein Moonlighting to Extracellular Release. *International journal of molecular sciences*, 21(21), 7901.
Clum, S., Ebner, K. E. & Padmanabhan, R. (1997) Cotranslational membrane insertion of the serine proteinase precursor NS2B-NS3(Pro) of dengue virus type 2 is required for efficient in vitro processing and is mediated through the hydrophobic regions of NS2B. *J Biol Chem*, 272(49), 30715-23.
Cohen, B.-C., Shamay, A. & Argov-Argaman, N. (2015) Regulation of Lipid Droplet Size in Mammary Epithelial Cells by Remodeling of Membrane Lipid Composition—A Potential Mechanism. *PLOS ONE*, 10(3), e0121645.
College, O. (2013) *Electron Transport Chain and Oxidative Phosphorylation*, 2013. Available online: OpenStaxCollege/Wikimedia Commons/CC BY-SA 3.0 [Accessed.
Collins, J. M., Neville, M. J., Hoppa, M. B. & Frayn, K. N. (2010) De novo lipogenesis and stearoyl-CoA desaturase are coordinately regulated in the human adipocyte and protect against palmitate-induced cell injury. *The Journal of biological chemistry*, 285(9), 6044-6052.
Cortese, M., Goellner, S., Acosta, E. G., Neufeldt, C. J., Oleksiuk, O., Lampe, M., Haselmann, U., Funaya, C., Schieber, N., Ronchi, P., Schorb, M., Pruunsild, P., Schwab, Y., Chatel-Chaix, L., Ruggieri, A. & Bartenschlager, R. (2017) Ultrastructural Characterization of Zika Virus Replication Factories. *Cell Rep*, 18(9), 2113-2123.
Costa, V. V., Fagundes, C. T., Valadão, D. F., Cisalpino, D., Dias, A. C., Silveira, K. D., Kangussu, L. M., Ávila, T. V., Bonfim, M. R., Bonaventura, D., Silva, T. A., Sousa, L. P., Rachid, M. A., Vieira, L. Q., Menezes, G. B., de Paula, A. M., Atrasheuskaya, A., Ignatyev, G., Teixeira, M. M. & Souza, D. G. (2012) A model of DENV-3 infection that recapitulates severe disease and highlights the importance of IFN-γ in host resistance to infection. *PLoS Negl Trop Dis*, 6(5), e1663.
Coulombe, F., Jaworska, J., Verway, M., Tzelepis, F., Massoud, A., Gillard, J., Wong, G., Kobinger, G., Xing, Z., Couture, C., Joubert, P., Fritz, J. H., Powell, W. S. & Divangahi, M. (2014) Targeted prostaglandin E2 inhibition enhances antiviral immunity through induction of type I interferon and apoptosis in macrophages. *Immunity*, 40(4), 554-68.
Daker, M., Bhuvanendran, S., Ahmad, M., Takada, K. & Khoo, A. S. (2013) Deregulation of lipid metabolism pathway genes in nasopharyngeal carcinoma cells. *Mol Med Rep*, 7(3), 731-41.
Dalrymple, N. A., Cimica, V. & Mackow, E. R. (2015a) Dengue Virus NS Proteins Inhibit RIG-I/MAVS Signaling by Blocking TBK1/IRF3 Phosphorylation: Dengue Virus Serotype 1 NS4A Is a Unique Interferon-Regulating Virulence Determinant. *mBio*, 6(3), e00553-15.
Dalrymple, N. A., Cimica, V. & Mackow, E. R. (2015b) Dengue Virus NS Proteins Inhibit RIG-I/MAVS Signaling by Blocking TBK1/IRF3 Phosphorylation: Dengue Virus Serotype 1 NS4A Is a Unique Interferon-Regulating Virulence Determinant. *mBio*, 6(3), e00553.
Daniels, B. P., Kofman, S. B., Smith, J. R., Norris, G. T., Snyder, A. G., Kolb, J. P., Gao, X., Locasale, J. W., Martinez, J., Gale, M., Jr., Loo, Y. M. & Oberst, A. (2019) The Nucleotide Sensor ZBP1 and Kinase RIPK3 Induce the Enzyme IRG1 to Promote an Antiviral Metabolic State in Neurons. *Immunity*, 50(1), 64-76.e4.
Davis, C. W., Mattei, L. M., Nguyen, H. Y., Ansarah-Sobrinho, C., Doms, R. W. & Pierson, T. C. (2006a) The location of asparagine-linked glycans on West Nile virions controls their interactions

with CD209 (dendritic cell-specific ICAM-3 grabbing nonintegrin). *J Biol Chem*, 281(48), 37183-94.
Davis, C. W., Nguyen, H. Y., Hanna, S. L., Sánchez, M. D., Doms, R. W. & Pierson, T. C. (2006b) West Nile virus discriminates between DC-SIGN and DC-SIGNR for cellular attachment and infection. *J Virol*, 80(3), 1290-301.
Davison, A. M. & King, N. J. (2011) Accelerated dendritic cell differentiation from migrating Ly6C(lo) bone marrow monocytes in early dermal West Nile virus infection. *J Immunol*, 186(4), 2382-96.
Deepa, P. R., Vandhana, S., Muthukumaran, S., Umashankar, V., Jayanthi, U. & Krishnakumar, S. (2010) Chemical inhibition of fatty acid synthase: molecular docking analysis and biochemical validation in ocular cancer cells. *J Ocul Biol Dis Infor*, 3(4), 117-28.
Dierendonck, X. A. M. H. v., Vrieling, F., Smeehuijzen, L., Deng, L., Boogaard, J. P., Croes, C.-A., Temmerman, L., Wetzels, S., Biessen, E., Kersten, S. & Stienstra, R. (2022) Triglyceride breakdown from lipid droplets regulates the inflammatory response in macrophages, 119(12), e2114739119.
Divakaruni, A. S., Hsieh, W. Y., Minarrieta, L., Duong, T. N., Kim, K. K. O., Desousa, B. R., Andreyev, A. Y., Bowman, C. E., Caradonna, K., Dranka, B. P., Ferrick, D. A., Liesa, M., Stiles, L., Rogers, G. W., Braas, D., Ciaraldi, T. P., Wolfgang, M. J., Sparwasser, T., Berod, L., Bensinger, S. J. & Murphy, A. N. (2018) Etomoxir Inhibits Macrophage Polarization by Disrupting CoA Homeostasis. *Cell Metab*, 28(3), 490-503.e7.
Dowall, S. D., Graham, V. A., Rayner, E., Atkinson, B., Hall, G., Watson, R. J., Bosworth, A., Bonney, L. C., Kitchen, S. & Hewson, R. (2016) A Susceptible Mouse Model for Zika Virus Infection. *PLoS Negl Trop Dis*, 10(5), e0004658.
Dowling, S., Cox, J. & Cenedella, R. J. (2009) Inhibition of fatty acid synthase by Orlistat accelerates gastric tumor cell apoptosis in culture and increases survival rates in gastric tumor bearing mice in vivo. *Lipids*, 44(6), 489-98.
Duffy, M. R., Chen, T.-H., Hancock, W. T., Powers, A. M., Kool, J. L., Lanciotti, R. S., Pretrick, M., Marfel, M., Holzbauer, S., Dubray, C., Guillaumot, L., Griggs, A., Bel, M., Lambert, A. J., Laven, J., Kosoy, O., Panella, A., Biggerstaff, B. J., Fischer, M. & Hayes, E. B. (2009) Zika Virus Outbreak on Yap Island, Federated States of Micronesia. *New England Journal of Medicine*, 360(24), 2536-2543.
Eaton, S. (2002) Control of mitochondrial beta-oxidation flux. *Prog Lipid Res*, 41(3), 197-239.
Egger, D., Wolk, B., Gosert, R., Bianchi, L., Blum, H. E., Moradpour, D. & Bienz, K. (2002) Expression of hepatitis C virus proteins induces distinct membrane alterations including a candidate viral replication complex. *J Virol*, 76(12), 5974-84.
El-Assaad, W., Buteau, J., Peyot, M. L., Nolan, C., Roduit, R., Hardy, S., Joly, E., Dbaibo, G., Rosenberg, L. & Prentki, M. (2003) Saturated fatty acids synergize with elevated glucose to cause pancreatic beta-cell death. *Endocrinology*, 144(9), 4154-63.
El Khoury, J. B., Moore, K. J., Means, T. K., Leung, J., Terada, K., Toft, M., Freeman, M. W. & Luster, A. D. (2003) CD36 mediates the innate host response to beta-amyloid. *The Journal of experimental medicine*, 197(12), 1657-1666.
Engin, A. B. (2017) What Is Lipotoxicity? *Adv Exp Med Biol*, 960, 197-220.
Enoch, H. G., Catalá, A. & Strittmatter, P. (1976) Mechanism of rat liver microsomal stearyl-CoA desaturase. Studies of the substrate specificity, enzyme-substrate interactions, and the function of lipid. *J Biol Chem*, 251(16), 5095-103.
Episcopio, D., Aminov, S., Benjamin, S., Germain, G., Datan, E., Landazuri, J., Lockshin, R. A. & Zakeri, Z. (2019) Atorvastatin restricts the ability of influenza virus to generate lipid droplets and severely suppresses the replication of the virus. *Faseb j*, 33(8), 9516-9525.

Everts, B., Amiel, E., Huang, S. C.-C., Smith, A. M., Chang, C.-H., Lam, W. Y., Redmann, V., Freitas, T. C., Blagih, J., van der Windt, G. J. W., Artyomov, M. N., Jones, R. G., Pearce, E. L. & Pearce, E. J. (2014) TLR-driven early glycolytic reprogramming via the kinases TBK1-IKKε supports the anabolic demands of dendritic cell activation. *Nature Immunology*, 15(4), 323-332.

Eynaudi, A., Díaz-Castro, F., Bórquez, J. C., Bravo-Sagua, R., Parra, V. & Troncoso, R. (2021) Differential Effects of Oleic and Palmitic Acids on Lipid Droplet-Mitochondria Interaction in the Hepatic Cell Line HepG2, 8.

Fagone, P. & Jackowski, S. (2009) Membrane phospholipid synthesis and endoplasmic reticulum function. *Journal of lipid research*, 50 Suppl(Suppl), S311-S316.

Fagundes, C. T., Costa, V. V., Cisalpino, D., Amaral, F. A., Souza, P. R., Souza, R. S., Ryffel, B., Vieira, L. Q., Silva, T. A., Atrasheuskaya, A., Ignatyev, G., Sousa, L. P., Souza, D. G. & Teixeira, M. M. (2011) IFN-γ production depends on IL-12 and IL-18 combined action and mediates host resistance to dengue virus infection in a nitric oxide-dependent manner. *PLoS Negl Trop Dis*, 5(12), e1449.

Fanunza, E., Carletti, F., Quartu, M., Grandi, N., Ermellino, L., Milia, J., Corona, A., Capobianchi, M. R., Ippolito, G. & Tramontano, E. (2021a) Zika virus NS2A inhibits interferon signaling by degradation of STAT1 and STAT2. *Virulence*, 12(1), 1580-1596.

Fanunza, E., Grandi, N., Quartu, M., Carletti, F., Ermellino, L., Milia, J., Corona, A., Capobianchi, M. R., Ippolito, G. & Tramontano, E. (2021b) INMI1 Zika Virus NS4B Antagonizes the Interferon Signaling by Suppressing STAT1 Phosphorylation. *Viruses*, 13(12).

Farley, S. E., Kyle, J. E., Leier, H. C., Bramer, L. M., Weinstein, J. B., Bates, T. A., Lee, J.-Y., Metz, T. O., Schultz, C. & Tafesse, F. G. (2022) A global lipid map reveals host dependency factors conserved across SARS-CoV-2 variants. *Nature Communications*, 13(1), 3487.

Faustino, A. F., Carvalho, F. A., Martins, I. C., Castanho, M. A. R. B., Mohana-Borges, R., Almeida, F. C. L., Da Poian, A. T. & Santos, N. C. (2014) Dengue virus capsid protein interacts specifically with very low-density lipoproteins. *Nanomedicine: Nanotechnology, Biology and Medicine*, 10(1), 247-255.

Faustino, A. F., Guerra, G. M., Huber, R. G., Hollmann, A., Domingues, M. M., Barbosa, G. M., Enguita, F. J., Bond, P. J., Castanho, M. A. R. B., Da Poian, A. T., Almeida, F. C. L., Santos, N. C. & Martins, I. C. (2015) Understanding Dengue Virus Capsid Protein Disordered N-Terminus and pep14-23-Based Inhibition. *ACS Chemical Biology*, 10(2), 517-526.

Febbraio, M., Hajjar, D. P. & Silverstein, R. L. (2001) CD36: a class B scavenger receptor involved in angiogenesis, atherosclerosis, inflammation, and lipid metabolism. *J Clin Invest*, 108(6), 785-91.

Feingold, K. R., Shigenaga, J. K., Kazemi, M. R., McDonald, C. M., Patzek, S. M., Cross, A. S., Moser, A. & Grunfeld, C. (2012) Mechanisms of triglyceride accumulation in activated macrophages, 92(4), 829-839.

Feng, D., Witkowski, A. & Smith, S. (2009) Down-regulation of mitochondrial acyl carrier protein in mammalian cells compromises protein lipoylation and respiratory complex I and results in cell death. *The Journal of biological chemistry*, 284(17), 11436-11445.

Fernandez-Garcia, M. D., Mazzon, M., Jacobs, M. & Amara, A. (2009) Pathogenesis of flavivirus infections: using and abusing the host cell. *Cell Host Microbe*, 5(4), 318-28.

Flamand, M., Megret, F., Mathieu, M., Lepault, J., Rey, F. A. & Deubel, V. (1999) Dengue virus type 1 nonstructural glycoprotein NS1 is secreted from mammalian cells as a soluble hexamer in a glycosylation-dependent fashion. *J Virol*, 73(7), 6104-10.

Flavin, R., Peluso, S., Nguyen, P. L. & Loda, M. (2010) Fatty acid synthase as a potential therapeutic target in cancer. *Future Oncol*, 6(4), 551-62.

Fontaine, K. A., Sanchez, E. L., Camarda, R., Lagunoff, M. & Sandri-Goldin, R. M. (2015) Dengue Virus Induces and Requires Glycolysis for Optimal Replication, 89(4), 2358-2366.

Fredericksen, B. L., Keller, B. C., Fornek, J., Katze, M. G. & Gale, M., Jr. (2008) Establishment and maintenance of the innate antiviral response to West Nile Virus involves both RIG-I and MDA5 signaling through IPS-1. *J Virol*, 82(2), 609-16.
Freemerman, A. J., Johnson, A. R., Sacks, G. N., Milner, J. J., Kirk, E. L., Troester, M. A., Macintyre, A. N., Goraksha-Hicks, P., Rathmell, J. C. & Makowski, L. (2014) Metabolic Reprogramming of Macrophages: GLUCOSE TRANSPORTER 1 (GLUT1)-MEDIATED GLUCOSE METABOLISM DRIVES A PROINFLAMMATORY PHENOTYPE *. *Journal of Biological Chemistry*, 289(11), 7884-7896.
Fukuzumi, M., Shinomiya, H., Shimizu, Y., Ohishi, K., Utsumi, S. J. I. & immunity (1996) Endotoxin-induced enhancement of glucose influx into murine peritoneal macrophages via GLUT1, 64(1), 108-112.
Funk, J. L., Feingold, K. R., Moser, A. H. & Grunfeld, C. (1993) Lipopolysaccharide stimulation of RAW 264.7 macrophages induces lipid accumulation and foam cell formation. *Atherosclerosis*, 98(1), 67-82.
Gan, S. J., Leong, Y. Q., bin Barhanuddin, M. F. H., Wong, S. T., Wong, S. F., Mak, J. W. & Ahmad, R. B. (2021) Dengue fever and insecticide resistance in Aedes mosquitoes in Southeast Asia: a review. *Parasites & Vectors*, 14(1), 315.
Gao, Q., Liu, Y., Wu, Y., Zhao, Q., Wang, L., Gao, S., Wen, W., Zhang, W., Guo, N., Zhou, J. & Yuan, Z. (2016) IL-17 intensifies IFN-γ-induced NOS2 upregulation in RAW 264.7 cells by further activating STAT1 and NF-κB. *Int J Mol Med*, 37(2), 347-358.
Garcia-Tapia, D., Loiacono, C. M. & Kleiboeker, S. B. (2006) Replication of West Nile virus in equine peripheral blood mononuclear cells. *Vet Immunol Immunopathol*, 110(3-4), 229-44.
García, C. C., Vázquez, C. A., Giovannoni, F., Russo, C. A., Cordo, S. M., Alaimo, A. & Damonte, E. B. (2020) Cellular Organelles Reorganization During Zika Virus Infection of Human Cells, 11(1558).
Gebhard, L. G., Kaufman, S. B. & Gamarnik, A. V. (2012) Novel ATP-independent RNA annealing activity of the dengue virus NS3 helicase. *PLoS One*, 7(4), e36244.
Geerling, E., Steffen, T. L., Brien, J. D. & Pinto, A. K. (2020) Current Flavivirus Research Important for Vaccine Development. *Vaccines*, 8(3), 477.
Genin, M., Clement, F., Fattaccioli, A., Raes, M. & Michiels, C. (2015) M1 and M2 macrophages derived from THP-1 cells differentially modulate the response of cancer cells to etoposide. *BMC Cancer*, 15(1), 577.
Getts, D. R., Terry, R. L., Getts, M. T., Müller, M., Rana, S., Shrestha, B., Radford, J., Van Rooijen, N., Campbell, I. L. & King, N. J. (2008) Ly6c+ "inflammatory monocytes" are microglial precursors recruited in a pathogenic manner in West Nile virus encephalitis. *J Exp Med*, 205(10), 2319-37.
Gianfrancesco, M. A., Dehairs, J., L'Homme, L., Herinckx, G., Esser, N., Jansen, O., Habraken, Y., Lassence, C., Swinnen, J. V., Rider, M. H., Piette, J., Paquot, N. & Legrand-Poels, S. (2019) Saturated fatty acids induce NLRP3 activation in human macrophages through K(+) efflux resulting from phospholipid saturation and Na, K-ATPase disruption. *Biochim Biophys Acta Mol Cell Biol Lipids*, 1864(7), 1017-1030.
Gibbons, R. V. & Vaughn, D. W. (2002) Dengue: an escalating problem. *Bmj*, 324(7353), 1563-6.
Gilbert, B. E., Wilson, S. Z., Knight, V., Couch, R. B., Quarles, J. M., Dure, L., Hayes, N. & Willis, G. (1985) Ribavirin small-particle aerosol treatment of infections caused by influenza virus strains A/Victoria/7/83 (H1N1) and B/Texas/1/84. *Antimicrob Agents Chemother*, 27(3), 309-13.
Gillespie, L. K., Hoenen, A., Morgan, G. & Mackenzie, J. M. (2010) The Endoplasmic Reticulum Provides the Membrane Platform for Biogenesis of the Flavivirus Replication Complex, 84(20), 10438-10447.

Grant, A., Ponia, S. S., Tripathi, S., Balasubramaniam, V., Miorin, L., Sourisseau, M., Schwarz, M. C., Sánchez-Seco, M. P., Evans, M. J., Best, S. M. & García-Sastre, A. (2016) Zika Virus Targets Human STAT2 to Inhibit Type I Interferon Signaling. *Cell Host Microbe*, 19(6), 882-90.

Greenberg, A. S., Coleman, R. A., Kraemer, F. B., McManaman, J. L., Obin, M. S., Puri, V., Yan, Q. W., Miyoshi, H. & Mashek, D. G. (2011) The role of lipid droplets in metabolic disease in rodents and humans. *J Clin Invest*, 121(6), 2102-10.

Greseth, M. D. & Traktman, P. (2014) De novo Fatty Acid Biosynthesis Contributes Significantly to Establishment of a Bioenergetically Favorable Environment for Vaccinia Virus Infection. *PLOS Pathogens*, 10(3), e1004021.

Grunt, T. W., Wagner, R., Grusch, M., Berger, W., Singer, C. F., Marian, B., Zielinski, C. C. & Lupu, R. (2009) Interaction between fatty acid synthase- and ErbB-systems in ovarian cancer cells. *Biochem Biophys Res Commun*, 385(3), 454-9.

Gullberg, R. C., Steel, J. J., Pujari, V., Rovnak, J., Crick, D. C. & Perera, R. (2018) Stearoly-CoA desaturase 1 differentiates early and advanced dengue virus infections and determines virus particle infectivity. *PLOS Pathogens*, 14(8), e1007261.

Guo, L., Guo, H., Gao, C., Mi, Z., Russell, W. B. & Kuo, P. C. (2007) Stat1 acetylation inhibits inducible nitric oxide synthase expression in interferon-gamma-treated RAW264.7 murine macrophages. *Surgery*, 142(2), 156-62.

Guseva, N. V., Rokhlin, O. W., Glover, R. A. & Cohen, M. B. (2011) TOFA (5-tetradecyl-oxy-2-furoic acid) reduces fatty acid synthesis, inhibits expression of AR, neuropilin-1 and Mcl-1 and kills prostate cancer cells independent of p53 status. *Cancer Biol Ther*, 12(1), 80-5.

Hadváry, P., Lengsfeld, H. & Wolfer, H. (1988) Inhibition of pancreatic lipase in vitro by the covalent inhibitor tetrahydrolipstatin. *Biochem J*, 256(2), 357-61.

Hadváry, P., Sidler, W., Meister, W., Vetter, W. & Wolfer, H. (1991) The lipase inhibitor tetrahydrolipstatin binds covalently to the putative active site serine of pancreatic lipase. *J Biol Chem*, 266(4), 2021-7.

Halvorson, D. L. & McCune, S. A. (1984) Inhibition of fatty acid synthesis in isolated adipocytes by 5-(tetradecyloxy)-2-furoic acid. *Lipids*, 19(11), 851-6.

Han, H.-H., Diaz, C., Acosta, C. J., Liu, M. & Borkowski, A. (2021) Safety and immunogenicity of a purified inactivated Zika virus vaccine candidate in healthy adults: an observer-blind, randomised, phase 1 trial. *The Lancet Infectious Diseases*, 21(9), 1282-1292.

Hanners, N. W., Mar, K. B., Boys, I. N., Eitson, J. L., De La Cruz-Rivera, P. C., Richardson, R. B., Fan, W., Wight-Carter, M. & Schoggins, J. W. (2021) Shiftless inhibits flavivirus replication in vitro and is neuroprotective in a mouse model of Zika virus pathogenesis, 118(49), e2111266118.

Hannun, Y. A. & Obeid, L. M. (2018) Sphingolipids and their metabolism in physiology and disease. *Nat Rev Mol Cell Biol*, 19(3), 175-191.

Harada, N., Oda, Z., Hara, Y., Fujinami, K., Okawa, M., Ohbuchi, K., Yonemoto, M., Ikeda, Y., Ohwaki, K., Aragane, K., Tamai, Y. & Kusunoki, J. (2007) Hepatic De Novo Lipogenesis Is Present in Liver-Specific ACC1-Deficient Mice, 27(5), 1881-1888.

Harb, D., Bujold, K., Febbraio, M., Sirois, M. G., Ong, H. & Marleau, S. (2009) The role of the scavenger receptor CD36 in regulating mononuclear phagocyte trafficking to atherosclerotic lesions and vascular inflammation. *Cardiovasc Res*, 83(1), 42-51.

Harbour, D. A., Blyth, W. A. & Hill, T. J. (1978) Prostanglandins enhance spread of herpes simplex virus in cell cultures. *J Gen Virol*, 41(1), 87-95.

Hard, G. C. (1970) Some biochemical aspects of the immune macrophage. *British journal of experimental pathology*, 51(1), 97-105.

Harris, C., Herker, E., Farese, R. V., Jr. & Ott, M. (2011) Hepatitis C virus core protein decreases lipid droplet turnover: a mechanism for core-induced steatosis. *J Biol Chem*, 286(49), 42615-42625.
Hase, T., Summers, P. L., Eckels, K. H. & Baze, W. B. (1987a) An electron and immunoelectron microscopic study of dengue-2 virus infection of cultured mosquito cells: maturation events. *Arch Virol*, 92(3-4), 273-91.
Hase, T., Summers, P. L., Eckels, K. H. & Baze, W. B. (1987b) Maturation process of Japanese encephalitis virus in cultured mosquito cells in vitro and mouse brain cells in vivo. *Arch Virol*, 96(3-4), 135-51.
Hassert, M., Brien, J. D. & Pinto, A. K. (2019) Mouse Models of Heterologous Flavivirus Immunity: A Role for Cross-Reactive T Cells, 10.
Hassert, M., Wolf, K. J., Schwetye, K. E., DiPaolo, R. J., Brien, J. D. & Pinto, A. K. (2018) CD4+T cells mediate protection against Zika associated severe disease in a mouse model of infection. *PLOS Pathogens*, 14(9), e1007237.
Hayes, E. B., Komar, N., Nasci, R. S., Montgomery, S. P., O'Leary, D. R. & Campbell, G. L. (2005) Epidemiology and transmission dynamics of West Nile virus disease. *Emerging infectious diseases*, 11(8), 1167-1173.
Heaton, N. S., Perera, R., Berger, K. L., Khadka, S., Lacount, D. J., Kuhn, R. J. & Randall, G. (2010) Dengue virus nonstructural protein 3 redistributes fatty acid synthase to sites of viral replication and increases cellular fatty acid synthesis. *Proc Natl Acad Sci U S A*, 107(40), 17345-50.
Heaton, N. S. & Randall, G. (2010) Dengue virus-induced autophagy regulates lipid metabolism. *Cell host & microbe*, 8(5), 422-432.
Helbig, K. J., Eyre, N. S., Yip, E., Narayana, S., Li, K., Fiches, G., McCartney, E. M., Jangra, R. K., Lemon, S. M. & Beard, M. R. (2011) The antiviral protein viperin inhibits hepatitis C virus replication via interaction with nonstructural protein 5A. *Hepatology*, 54(5), 1506-17.
Hertig, M. (1936) The Rickettsia, Wolbachia pipientis (gen. et sp.n.) and Associated Inclusions of the Mosquito, Culex pipiens. *Parasitology*, 28(4), 453-486.
Hilgard, P. & Stockert, R. (2000) Heparan sulfate proteoglycans initiate dengue virus infection of hepatocytes. *Hepatology*, 32(5), 1069-77.
Hishiki, T., Kato, F., Nio, Y., Watanabe, S., Wen Tan, N. W., Yamane, D., Miyazaki, Y., Lin, C. C., Suzuki, R., Tajima, S., Lim, C. K., Saijo, M., Hijikata, M., Vasudevan, S. G. & Takasaki, T. (2019) Stearoyl-CoA desaturase-1 is required for flavivirus RNA replication. *Antiviral Res*, 165, 42-46.
Hitakarun, A., Khongwichit, S., Wikan, N., Roytrakul, S., Yoksan, S., Rajakam, S., Davidson, A. D. & Smith, D. R. (2020) Evaluation of the antiviral activity of orlistat (tetrahydrolipstatin) against dengue virus, Japanese encephalitis virus, Zika virus and chikungunya virus. *Scientific Reports*, 10(1), 1499.
Hlousek-Radojcic, A., Evenson, K. J., Jaworski, J. G. & Post-Beittenmiller, D. (1998) Fatty Acid Elongation Is Independent of Acyl-Coenzyme A Synthetase Activities in Leek and Brassica napus. *Plant Physiology*, 116(1), 251-258.
Hoebe, K., Georgel, P., Rutschmann, S., Du, X., Mudd, S., Crozat, K., Sovath, S., Shamel, L., Hartung, T., Zähringer, U. & Beutler, B. (2005) CD36 is a sensor of diacylglycerides. *Nature*, 433(7025), 523-7.
Hoenen, A., Liu, W., Kochs, G., Khromykh, A. A. & Mackenzie, J. M. (2007a) West Nile virus-induced cytoplasmic membrane structures provide partial protection against the interferon-induced antiviral MxA protein. *J Gen Virol*, 88(Pt 11), 3013-7.
Hoenen, A., Liu, W., Kochs, G., Khromykh, A. A. & Mackenzie, J. M. (2007b) West Nile virus-induced cytoplasmic membrane structures provide partial protection against the interferon-induced antiviral MxA protein, 88(11), 3013-3017.

Hoffmann, A. A., Montgomery, B. L., Popovici, J., Iturbe-Ormaetxe, I., Johnson, P. H., Muzzi, F., Greenfield, M., Durkan, M., Leong, Y. S., Dong, Y., Cook, H., Axford, J., Callahan, A. G., Kenny, N., Omodei, C., McGraw, E. A., Ryan, P. A., Ritchie, S. A., Turelli, M. & O'Neill, S. L. (2011) Successful establishment of Wolbachia in Aedes populations to suppress dengue transmission. *Nature*, 476(7361), 454-457.

Hollenbaugh, J. A., Munger, J. & Kim, B. (2011) Metabolite profiles of human immunodeficiency virus infected CD4+ T cells and macrophages using LC-MS/MS analysis. *Virology*, 415(2), 153-9.

Huang, J.-T., Tseng, C.-P., Liao, M.-H., Lu, S.-C., Yeh, W.-Z., Sakamoto, N., Chen, C.-M. & Cheng, J.-C. (2013) Hepatitis C Virus Replication Is Modulated by the Interaction of Nonstructural Protein NS5B and Fatty Acid Synthase, 87(9), 4994-5004.

Huang, S. C., Everts, B., Ivanova, Y., O'Sullivan, D., Nascimento, M., Smith, A. M., Beatty, W., Love-Gregory, L., Lam, W. Y., O'Neill, C. M., Yan, C., Du, H., Abumrad, N. A., Urban, J. F., Jr., Artyomov, M. N., Pearce, E. L. & Pearce, E. J. (2014) Cell-intrinsic lysosomal lipolysis is essential for alternative activation of macrophages. *Nat Immunol*, 15(9), 846-55.

Huang, S. C., Smith, A. M., Everts, B., Colonna, M., Pearce, E. L., Schilling, J. D. & Pearce, E. J. (2016) Metabolic Reprogramming Mediated by the mTORC2-IRF4 Signaling Axis Is Essential for Macrophage Alternative Activation. *Immunity*, 45(4), 817-830.

Huggins, J. W., Kim, G. R., Brand, O. M. & McKee, K. T., Jr. (1986) Ribavirin therapy for Hantaan virus infection in suckling mice. *J Infect Dis*, 153(3), 489-97.

Huss, J. M. & Kelly, D. P. (2004) Nuclear receptor signaling and cardiac energetics. *Circ Res*, 95(6), 568-78.

Iglesias, J., Lamontagne, J., Erb, H., Gezzar, S., Zhao, S., Joly, E., Truong, V. L., Skorey, K., Crane, S., Madiraju, S. R. & Prentki, M. (2016) Simplified assays of lipolysis enzymes for drug discovery and specificity assessment of known inhibitors. *J Lipid Res*, 57(1), 131-41.

Im, S. S., Yousef, L., Blaschitz, C., Liu, J. Z., Edwards, R. A., Young, S. G., Raffatellu, M. & Osborne, T. F. (2011) Linking lipid metabolism to the innate immune response in macrophages through sterol regulatory element binding protein-1a. *Cell Metab*, 13(5), 540-9.

Infantino, V., Convertini, P., Cucci, L., Panaro, M. A., Di Noia, M. A., Calvello, R., Palmieri, F. & Iacobazzi, V. (2011) The mitochondrial citrate carrier: a new player in inflammation. *Biochem J*, 438(3), 433-6.

Infantino, V., Iacobazzi, V., Palmieri, F. & Menga, A. (2013) ATP-citrate lyase is essential for macrophage inflammatory response. *Biochem Biophys Res Commun*, 440(1), 105-11.

Ishak, R., Tovey, D. G. & Howard, C. R. (1988) Morphogenesis of yellow fever virus 17D in infected cell cultures. *J Gen Virol*, 69 (Pt 2), 325-35.

Izquierdo-Useros, N., Lorizate, M., Contreras, F. X., Rodriguez-Plata, M. T., Glass, B., Erkizia, I., Prado, J. G., Casas, J., Fabriàs, G., Kräusslich, H. G. & Martinez-Picado, J. (2012) Sialyllactose in viral membrane gangliosides is a novel molecular recognition pattern for mature dendritic cell capture of HIV-1. *PLoS Biol*, 10(4), e1001315.

Jablonski, K. A., Amici, S. A., Webb, L. M., Ruiz-Rosado, J. d. D., Popovich, P. G., Partida-Sanchez, S. & Guerau-de-Arellano, M. (2015) Novel Markers to Delineate Murine M1 and M2 Macrophages. *PLOS ONE*, 10(12), e0145342.

Jackson, C. L. (2019) Lipid droplet biogenesis. *Current Opinion in Cell Biology*, 59, 88-96.

Jakobsson, A., Westerberg, R. & Jacobsson, A. (2006) Fatty acid elongases in mammals: their regulation and roles in metabolism. *Prog Lipid Res*, 45(3), 237-49.

Janabi, M., Yamashita, S., Hirano, K., Sakai, N., Hiraoka, H., Matsumoto, K., Zhang, Z., Nozaki, S. & Matsuzawa, Y. (2000) Oxidized LDL-induced NF-kappa B activation and subsequent expression of proinflammatory genes are defective in monocyte-derived macrophages from CD36-deficient patients. *Arterioscler Thromb Vasc Biol*, 20(8), 1953-60.

Jeucken, A. & Brouwers, J. F. (2019) High-Throughput Screening of Lipidomic Adaptations in Cultured Cells. *Biomolecules*, 9(2).
Jha, Abhishek K., Huang, Stanley C.-C., Sergushichev, A., Lampropoulou, V., Ivanova, Y., Loginicheva, E., Chmielewski, K., Stewart, Kelly M., Ashall, J., Everts, B., Pearce, Edward J., Driggers, Edward M. & Artyomov, Maxim N. (2015) Network Integration of Parallel Metabolic and Transcriptional Data Reveals Metabolic Modules that Regulate Macrophage Polarization. *Immunity*, 42(3), 419-430.
Jhan, M. K., Chen, C. L., Shen, T. J., Tseng, P. C., Wang, Y. T., Satria, R. D., Yu, C. Y. & Lin, C. F. (2021) Polarization of Type 1 Macrophages Is Associated with the Severity of Viral Encephalitis Caused by Japanese Encephalitis Virus and Dengue Virus. *Cells*, 10(11).
Jiang, H., Shi, H., Sun, M., Wang, Y., Meng, Q., Guo, P., Cao, Y., Chen, J., Gao, X., Li, E. & Liu, J. (2016) PFKFB3-Driven Macrophage Glycolytic Metabolism Is a Crucial Component of Innate Antiviral Defense. *J Immunol*, 197(7), 2880-90.
Jiménez, B., Volpert, O. V., Crawford, S. E., Febbraio, M., Silverstein, R. L. & Bouck, N. (2000) Signals leading to apoptosis-dependent inhibition of neovascularization by thrombospondin-1. *Nat Med*, 6(1), 41-8.
Jiménez de Oya, N., Blázquez, A. B., Casas, J., Saiz, J. C. & Martín-Acebes, M. A. (2018) Direct Activation of Adenosine Monophosphate-Activated Protein Kinase (AMPK) by PF-06409577 Inhibits Flavivirus Infection through Modification of Host Cell Lipid Metabolism. *Antimicrob Agents Chemother*, 62(7).
Jiménez de Oya, N., Esler, W. P., Huard, K., El-Kattan, A. F., Karamanlidis, G., Blázquez, A. B., Ramos-Ibeas, P., Escribano-Romero, E., Louloudes-Lázaro, A., Casas, J., Sobrino, F., Hoehn, K., James, D. E., Gutiérrez-Adán, A., Saiz, J. C. & Martín-Acebes, M. A. (2019) Targeting host metabolism by inhibition of acetyl-Coenzyme A carboxylase reduces flavivirus infection in mouse models. *Emerg Microbes Infect*, 8(1), 624-636.
Joshi, A. K., Witkowski, A., Berman, H. A., Zhang, L. & Smith, S. (2005) Effect of modification of the length and flexibility of the acyl carrier protein-thioesterase interdomain linker on functionality of the animal fatty acid synthase. *Biochemistry*, 44(10), 4100-7.
Junjhon, J., Pennington, J. G., Edwards, T. J., Perera, R., Lanman, J. & Kuhn, R. J. (2014) Ultrastructural characterization and three-dimensional architecture of replication sites in dengue virus-infected mosquito cells. *J Virol*, 88(9), 4687-97.
Kampf, J. P. & Kleinfeld, A. M. (2007) Is Membrane Transport of FFA Mediated by Lipid, Protein, or Both? *Physiology*, 22(1), 7-14.
Kastaniotis, A. J., Autio, K. J., Sormunen, R. T. & Hiltunen, J. K. (2004) Htd2p/Yhr067p is a yeast 3-hydroxyacyl-ACP dehydratase essential for mitochondrial function and morphology. *Mol Microbiol*, 53(5), 1407-21.
Kielian, M., Chanel-Vos, C. & Liao, M. (2010) Alphavirus Entry and Membrane Fusion. *Viruses*, 2(4), 796-825.
Kikkert, M. (2020) Innate Immune Evasion by Human Respiratory RNA Viruses. *J Innate Immun*, 12(1), 4-20.
Kim, T. S., Leahy, P. & Freake, H. C. (1996) Promoter usage determines tissue specific responsiveness of the rat acetyl-CoA carboxylase gene. *Biochem Biophys Res Commun*, 225(2), 647-53.
Kimura, T., Sasaki, M., Okumura, M., Kim, E. & Sawa, H. (2010) Flavivirus Encephalitis: Pathological Aspects of Mouse and Other Animal Models. *Veterinary Pathology*, 47(5), 806-818.
King, N. J., Getts, D. R., Getts, M. T., Rana, S., Shrestha, B. & Kesson, A. M. (2007) Immunopathology of flavivirus infections. *Immunol Cell Biol*, 85(1), 33-42.

Klemm, E. J., Spooner, E. & Ploegh, H. L. (2011) Dual role of ancient ubiquitous protein 1 (AUP1) in lipid droplet accumulation and endoplasmic reticulum (ER) protein quality control. *J Biol Chem*, 286(43), 37602-14.
Ko, J. & Small, D. M. (1997) Behavior of tetrahydrolipstatin in biological model membranes and emulsions. *J Lipid Res*, 38(8), 1544-52.
Kong, K. F., Delroux, K., Wang, X., Qian, F., Arjona, A., Malawista, S. E., Fikrig, E. & Montgomery, R. R. (2008a) Dysregulation of TLR3 impairs the innate immune response to West Nile virus in the elderly. *J Virol*, 82(15), 7613-23.
Kong, K. F., Wang, X., Anderson, J. F., Fikrig, E. & Montgomery, R. R. (2008b) West nile virus attenuates activation of primary human macrophages. *Viral Immunol*, 21(1), 78-82.
Koonen, D. P., Jacobs, R. L., Febbraio, M., Young, M. E., Soltys, C. L., Ong, H., Vance, D. E. & Dyck, J. R. (2007) Increased hepatic CD36 expression contributes to dyslipidemia associated with diet-induced obesity. *Diabetes*, 56(12), 2863-71.
Koundouros, N. & Poulogiannis, G. (2020) Reprogramming of fatty acid metabolism in cancer. *British Journal of Cancer*, 122(1), 4-22.
Koyuncu, E., Purdy, J. G., Rabinowitz, J. D. & Shenk, T. (2013) Saturated Very Long Chain Fatty Acids Are Required for the Production of Infectious Human Cytomegalovirus Progeny. *PLOS Pathogens*, 9(5), e1003333.
Krahmer, N., Farese, R. V., Jr. & Walther, T. C. (2013) Balancing the fat: lipid droplets and human disease. *EMBO Mol Med*, 5(7), 973-83.
Krahmer, N., Guo, Y., Wilfling, F., Hilger, M., Lingrell, S., Heger, K., Newman, H. W., Schmidt-Supprian, M., Vance, D. E., Mann, M., Farese, R. V., Jr. & Walther, T. C. (2011) Phosphatidylcholine synthesis for lipid droplet expansion is mediated by localized activation of CTP:phosphocholine cytidylyltransferase. *Cell Metab*, 14(4), 504-15.
Kreil, T. R. & Eibl, M. M. (1996) Nitric oxide and viral infection: NO antiviral activity against a flavivirus in vitro, and evidence for contribution to pathogenesis in experimental infection in vivo. *Virology*, 219(1), 304-6.
Kridel, S. J., Axelrod, F., Rozenkrantz, N. & Smith, J. W. (2004) Orlistat is a novel inhibitor of fatty acid synthase with antitumor activity. *Cancer Res*, 64(6), 2070-5.
Krishnan, M. N., Ng, A., Sukumaran, B., Gilfoy, F. D., Uchil, P. D., Sultana, H., Brass, A. L., Adametz, R., Tsui, M., Qian, F., Montgomery, R. R., Lev, S., Mason, P. W., Koski, R. A., Elledge, S. J., Xavier, R. J., Agaisse, H. & Fikrig, E. (2008) RNA interference screen for human genes associated with West Nile virus infection. *Nature*, 455(7210), 242-5.
Krzak, G., Willis, C. M., Smith, J. A., Pluchino, S. & Peruzzotti-Jametti, L. (2021) Succinate Receptor 1: An Emerging Regulator of Myeloid Cell Function in Inflammation. *Trends in Immunology*, 42(1), 45-58.
Kuhajda, F. P., Jenner, K., Wood, F. D., Hennigar, R. A., Jacobs, L. B., Dick, J. D. & Pasternack, G. R. (1994) Fatty acid synthesis: a potential selective target for antineoplastic therapy. *Proceedings of the National Academy of Sciences of the United States of America*, 91(14), 6379-6383.
Kuhajda, F. P., Pizer, E. S., Li, J. N., Mani, N. S., Frehywot, G. L. & Townsend, C. A. (2000) Synthesis and antitumor activity of an inhibitor of fatty acid synthase, 97(7), 3450-3454.
Kuhn, R. J., Zhang, W., Rossmann, M. G., Pletnev, S. V., Corver, J., Lenches, E., Jones, C. T., Mukhopadhyay, S., Chipman, P. R., Strauss, E. G., Baker, T. S. & Strauss, J. H. (2002) Structure of dengue virus: implications for flavivirus organization, maturation, and fusion. *Cell*, 108(5), 717-25.
Kulkarni, R., Wiemer, E. A. C. & Chang, W. (2022) Role of Lipid Rafts in Pathogen-Host Interaction - A Mini Review, 12.

Kumar, A., Hou, S., Airo, A. M., Limonta, D., Mancinelli, V., Branton, W., Power, C. & Hobman, T. C. (2016) Zika virus inhibits type-I interferon production and downstream signaling. *EMBO Rep*, 17(12), 1766-1775.
Kumar, P. & Bhandari, U. (2015) Obesity pharmacotherapy: current status. *Excli j*, 14, 290-3.
Kummerer, B. M. & Rice, C. M. (2002) Mutations in the yellow fever virus nonstructural protein NS2A selectively block production of infectious particles. *J Virol*, 76(10), 4773-84.
Laurent-Rolle, M., Boer, E. F., Lubick, K. J., Wolfinbarger, J. B., Carmody, A. B., Rockx, B., Liu, W., Ashour, J., Shupert, W. L., Holbrook, M. R., Barrett, A. D., Mason, P. W., Bloom, M. E., García-Sastre, A., Khromykh, A. A. & Best, S. M. (2010) The NS5 protein of the virulent West Nile virus NY99 strain is a potent antagonist of type I interferon-mediated JAK-STAT signaling. *J Virol*, 84(7), 3503-15.
Laureti, M., Narayanan, D., Rodriguez-Andres, J., Fazakerley, J. K. & Kedzierski, L. (2018) Flavivirus Receptors: Diversity, Identity, and Cell Entry, 9.
Lazear, Helen M., Govero, J., Smith, Amber M., Platt, Derek J., Fernandez, E., Miner, Jonathan J. & Diamond, Michael S. (2016) A Mouse Model of Zika Virus Pathogenesis. *Cell Host & Microbe*, 19(5), 720-730.
Lazear, H. M., Pinto, A. K., Ramos, H. J., Vick, S. C., Shrestha, B., Suthar, M. S., Gale, M., Jr. & Diamond, M. S. (2013) Pattern recognition receptor MDA5 modulates CD8+ T cell-dependent clearance of West Nile virus from the central nervous system. *J Virol*, 87(21), 11401-15.
Le Breton, M., Meyniel-Schicklin, L., Deloire, A., Coutard, B., Canard, B., de Lamballerie, X., Andre, P., Rabourdin-Combe, C., Lotteau, V. & Davoust, N. (2011) Flavivirus NS3 and NS5 proteins interaction network: a high-throughput yeast two-hybrid screen. *BMC Microbiol*, 11, 234.
Ledur, P. F., Karmirian, K., Pedrosa, C. d. S. G., Souza, L. R. Q., Assis-de-Lemos, G., Martins, T. M., Ferreira, J. d. C. C. G., de Azevedo Reis, G. F., Silva, E. S., Silva, D., Salerno, J. A., Ornelas, I. M., Devalle, S., Madeiro da Costa, R. F., Goto-Silva, L., Higa, L. M., Melo, A., Tanuri, A., Chimelli, L., Murata, M. M., Garcez, P. P., Filippi-Chiela, E. C., Galina, A., Borges, H. L. & Rehen, S. K. (2020) Zika virus infection leads to mitochondrial failure, oxidative stress and DNA damage in human iPSC-derived astrocytes. *Scientific Reports*, 10(1), 1218.
Lee, Y.-R., Lei, H.-Y., Liu, M.-T., Wang, J.-R., Chen, S.-H., Jiang-Shieh, Y.-F., Lin, Y.-S., Yeh, T.-M., Liu, C.-C. & Liu, H.-S. (2008) Autophagic machinery activated by dengue virus enhances virus replication. *Virology*, 374(2), 240-248.
Leier, H. C., Messer, W. B. & Tafesse, F. G. (2018) Lipids and pathogenic flaviviruses: An intimate union. *PLoS Pathog*, 14(5), e1006952.
Leis, A. A., Grill, M. F., Goodman, B. P., Sadiq, S. B., Sinclair, D. J., Vig, P. J. S. & Bai, F. (2020) Tumor Necrosis Factor-Alpha Signaling May Contribute to Chronic West Nile Virus Post-infectious Proinflammatory State, 7.
Lescar, J., Luo, D., Xu, T., Sampath, A., Lim, S. P., Canard, B. & Vasudevan, S. G. (2008) Towards the design of antiviral inhibitors against flaviviruses: the case for the multifunctional NS3 protein from Dengue virus as a target. *Antiviral Res*, 80(2), 94-101.
Leung, J. Y., Pijlman, G. P., Kondratieva, N., Hyde, J., Mackenzie, J. M. & Khromykh, A. A. (2008) Role of nonstructural protein NS2A in flavivirus assembly. *J Virol*, 82(10), 4731-41.
Levi, M. E. (2017) Zika virus: a cause of concern in transplantation? *Curr Opin Infect Dis*, 30(4), 340-345.
Li, X.-D., Deng, C.-L., Ye, H.-Q., Zhang, H.-L., Zhang, Q.-Y., Chen, D.-D., Zhang, P.-T., Shi, P.-Y., Yuan, Z.-M. & Zhang, B. (2016) Transmembrane Domains of NS2B Contribute to both Viral RNA Replication and Particle Formation in Japanese Encephalitis Virus. *Journal of Virology*, 90(12), 5735.

Liebscher, S., Ambrose, R. L., Aktepe, T. E., Mikulasova, A., Prier, J. E., Gillespie, L. K., Lopez-Denman, A. J., Rupasinghe, T. W. T., Tull, D., McConville, M. J. & Mackenzie, J. M. (2018) Phospholipase A2 activity during the replication cycle of the flavivirus West Nile virus. *PLOS Pathogens*, 14(4), e1007029.

Lima, R. G., Moreira, L., Paes-Leme, J., Barreto-de-Souza, V., Castro-Faria-Neto, H. C., Bozza, P. T. & Bou-Habib, D. C. (2006) Interaction of macrophages with apoptotic cells enhances HIV Type 1 replication through PGE2, PAF, and vitronectin receptor. *AIDS Res Hum Retroviruses*, 22(8), 763-9.

Limsuwat, N., Boonarkart, C., Phakaratsakul, S., Suptawiwat, O. & Auewarakul, P. (2020) Influence of cellular lipid content on influenza A virus replication. *Archives of Virology*, 165(5), 1151-1161.

Lin, C. Y. & Smith, S. (1978) Properties of the thioesterase component obtained by limited trypsinization of the fatty acid synthetase multienzyme complex. *J Biol Chem*, 253(6), 1954-62.

Lin, Y. L., Huang, Y. L., Ma, S. H., Yeh, C. T., Chiou, S. Y., Chen, L. K. & Liao, C. L. (1997) Inhibition of Japanese encephalitis virus infection by nitric oxide: antiviral effect of nitric oxide on RNA virus replication. *J Virol*, 71(7), 5227-35.

Lindenbach, B., Murray, C., Thiel, H. & Rice, C. J. F. v. (2013) Flaviviridae, 1.

Lindenbach, B., Thiel, H. J. & Rice, C. M. (2007) Flaviviridae: The viruses and their replication. *Fields Virology*, 1101-1151.

Listenberger, L. L., Han, X., Lewis, S. E., Cases, S., Farese, R. V., Jr., Ory, D. S. & Schaffer, J. E. (2003) Triglyceride accumulation protects against fatty acid-induced lipotoxicity. *Proc Natl Acad Sci U S A*, 100(6), 3077-82.

Little, J. L., Wheeler, F. B., Fels, D. R., Koumenis, C. & Kridel, S. J. (2007) Inhibition of fatty acid synthase induces endoplasmic reticulum stress in tumor cells. *Cancer Res*, 67(3), 1262-9.

Liu, W. J., Wang, X. J., Mokhonov, V. V., Shi, P. Y., Randall, R. & Khromykh, A. A. (2005) Inhibition of interferon signaling by the New York 99 strain and Kunjin subtype of West Nile virus involves blockage of STAT1 and STAT2 activation by nonstructural proteins. *J Virol*, 79(3), 1934-42.

Liu, Y. Y., Liang, X. D., Liu, C. C., Cheng, Y., Chen, H., Baloch, A. S., Zhang, J., Go, Y. Y. & Zhou, B. (2021) Fatty Acid Synthase Is Involved in Classical Swine Fever Virus Replication by Interaction with NS4B. *J Virol*, 95(17), e0078121.

Long, S., Zhou, Y., Bai, D., Hao, W., Zheng, B., Xiao, S. & Fang, L. (2019) Fatty Acids Regulate Porcine Reproductive and Respiratory Syndrome Virus Infection via the AMPK-ACC1 Signaling Pathway. *Viruses*, 11(12).

Lopaschuk, G. D., Ussher, J. R., Folmes, C. D., Jaswal, J. S. & Stanley, W. C. (2010) Myocardial fatty acid metabolism in health and disease. *Physiol Rev*, 90(1), 207-58.

Lu, G. & Gong, P. (2013) Crystal Structure of the full-length Japanese encephalitis virus NS5 reveals a conserved methyltransferase-polymerase interface. *PLoS pathogens*, 9(8), e1003549-e1003549.

Lubick, K. J., Robertson, S. J., McNally, K. L., Freedman, B. A., Rasmussen, A. L., Taylor, R. T., Walts, A. D., Tsuruda, S., Sakai, M., Ishizuka, M., Boer, E. F., Foster, E. C., Chiramel, A. I., Addison, C. B., Green, R., Kastner, D. L., Katze, M. G., Holland, S. M., Forlino, A., Freeman, A. F., Boehm, M., Yoshii, K. & Best, S. M. (2015) Flavivirus Antagonism of Type I Interferon Signaling Reveals Prolidase as a Regulator of IFNAR1 Surface Expression. *Cell Host Microbe*, 18(1), 61-74.

Luo, H., Winkelmann, E. R., Fernandez-Salas, I., Li, L., Mayer, S. V., Danis-Lozano, R., Sanchez-Casas, R. M., Vasilakis, N., Tesh, R., Barrett, A. D., Weaver, S. C. & Wang, T. (2018) Zika, dengue and yellow fever viruses induce differential anti-viral immune responses in human monocytic and first trimester trophoblast cells. *Antiviral Res*, 151, 55-62.

Lv, R., Bao, Q. & Li, Y. (2017) Regulation of M1-type and M2-type macrophage polarization in RAW264.7 cells by Galectin-9. *Mol Med Rep*, 16(6), 9111-9119.

Lyn, R. K., Singaravelu, R., Kargman, S., O'Hara, S., Chan, H., Oballa, R., Huang, Z., Jones, D. M., Ridsdale, A., Russell, R. S., Partridge, A. W. & Pezacki, J. P. (2014) Stearoyl-CoA desaturase inhibition blocks formation of hepatitis C virus-induced specialized membranes. *Scientific reports*, 4, 4549-4549.

Ma, S., Mao, Q., Chen, W., Zhao, M., Wu, K., Song, D., Li, X., Zhu, E., Fan, S., Yi, L., Ding, H., Zhao, M. & Chen, J. (2019) Serum Lipidomics Analysis of Classical Swine Fever Virus Infection in Piglets and Emerging Role of Free Fatty Acids in Virus Replication in vitro, 9.

Macdonald, J., Tonry, J., Hall, R. A., Williams, B., Palacios, G., Ashok, M. S., Jabado, O., Clark, D., Tesh, R. B., Briese, T. & Lipkin, W. I. (2005) NS1 protein secretion during the acute phase of West Nile virus infection. *J Virol*, 79(22), 13924-33.

Mackenzie, J. (2005) Wrapping things up about virus RNA replication. *Traffic*, 6(11), 967-77.

Mackenzie, J. M., Jones, M. K. & Westaway, E. G. (1999) Markers for trans-Golgi membranes and the intermediate compartment localize to induced membranes with distinct replication functions in flavivirus-infected cells. *J Virol*, 73(11), 9555-67.

Mackenzie, J. M., Jones, M. K. & Young, P. R. (1996a) Immunolocalization of the dengue virus nonstructural glycoprotein NS1 suggests a role in viral RNA replication. *Virology*, 220(1), 232-40.

Mackenzie, J. M., Jones, M. K. & Young, P. R. (1996b) Improved membrane preservation of flavivirus-infected cells with cryosectioning. *J Virol Methods*, 56(1), 67-75.

Mackenzie, J. M., Khromykh, A. A., Jones, M. K. & Westaway, E. G. (1998) Subcellular localization and some biochemical properties of the flavivirus Kunjin nonstructural proteins NS2A and NS4A. *Virology*, 245(2), 203-15.

Mackenzie, J. M., Khromykh, A. A. & Parton, R. G. (2007) Cholesterol manipulation by West Nile virus perturbs the cellular immune response. *Cell Host Microbe*, 2(4), 229-39.

Mackenzie, J. M., Khromykh, A. A. & Westaway, E. G. (2001) Stable expression of noncytopathic Kunjin replicons simulates both ultrastructural and biochemical characteristics observed during replication of Kunjin virus. *Virology*, 279(1), 161-72.

Mackenzie, J. M. & Westaway, E. G. (2001) Assembly and Maturation of the Flavivirus Kunjin Virus Appear To Occur in the Rough Endoplasmic Reticulum and along the Secretory Pathway, Respectively. *Journal of Virology*, 75(22), 10787.

Magnus, M. M., Espósito, D. L. A., Costa, V. A. d., Melo, P. S. d., Costa-Lima, C., Fonseca, B. A. L. d. & Addas-Carvalho, M. (2018) Risk of Zika virus transmission by blood donations in Brazil. *Hematology, transfusion and cell therapy*, 40(3), 250-254.

Malandrino, M. I., Fucho, R., Weber, M., Calderon-Dominguez, M., Mir, J. F., Valcarcel, L., Escoté, X., Gómez-Serrano, M., Peral, B., Salvadó, L., Fernández-Veledo, S., Casals, N., Vázquez-Carrera, M., Villarroya, F., Vendrell, J. J., Serra, D. & Herrero, L. (2015) Enhanced fatty acid oxidation in adipocytes and macrophages reduces lipid-induced triglyceride accumulation and inflammation. *Am J Physiol Endocrinol Metab*, 308(9), E756-69.

Mantovani, A., Biswas, S. K., Galdiero, M. R., Sica, A. & Locati, M. (2013) Macrophage plasticity and polarization in tissue repair and remodelling. *J Pathol*, 229(2), 176-85.

Martín-Acebes, M. A., Blázquez, A.-B., Jiménez de Oya, N., Escribano-Romero, E. & Saiz, J.-C. (2011a) West Nile Virus Replication Requires Fatty Acid Synthesis but Is Independent on Phosphatidylinositol-4-Phosphate Lipids. *PLOS ONE*, 6(9), e24970.

Martín-Acebes, M. A., Blázquez, A. B., Jiménez de Oya, N., Escribano-Romero, E. & Saiz, J. C. (2011b) West Nile virus replication requires fatty acid synthesis but is independent on phosphatidylinositol-4-phosphate lipids. *PLoS One*, 6(9), e24970.

Martin-Acebes, M. A., Vazquez-Calvo, A. & Saiz, J. C. (2016) Lipids and flaviviruses, present and future perspectives for the control of dengue, Zika, and West Nile viruses. *Prog Lipid Res*, 64, 123-137.

Martinez, F. O. & Gordon, S. (2014) The M1 and M2 paradigm of macrophage activation: time for reassessment. *F1000Prime Rep*, 6, 13.
Martins, A. S., Carvalho, F. A., Faustino, A. F., Martins, I. C. & Santos, N. C. (2019) West Nile Virus Capsid Protein Interacts With Biologically Relevant Host Lipid Systems, 9.
Mateo, R., Nagamine, C. M., Spagnolo, J., Méndez, E., Rahe, M., Gale, M., Jr., Yuan, J. & Kirkegaard, K. (2013) Inhibition of cellular autophagy deranges dengue virion maturation. *J Virol*, 87(3), 1312-21.
Matsuo, S., Yang, W. L., Aziz, M., Kameoka, S. & Wang, P. (2014) Fatty acid synthase inhibitor C75 ameliorates experimental colitis. *Mol Med*, 20(1), 1-9.
Mattick, J. S., Nickless, J., Mizugaki, M., Yang, C. Y., Uchiyama, S. & Wakil, S. J. (1983) The architecture of the animal fatty acid synthetase. II. Separation of the core and thioesterase functions and determination of the N-C orientation of the subunit. *J Biol Chem*, 258(24), 15300-4.
Mazzon, M., Jones, M., Davidson, A., Chain, B. & Jacobs, M. (2009) Dengue virus NS5 inhibits interferon-alpha signaling by blocking signal transducer and activator of transcription 2 phosphorylation. *J Infect Dis*, 200(8), 1261-70.
McCarthy, A. D. & Hardie, D. G. (1984) Fatty acid synthase — an example of protein evolution by gene fusion. *Trends in Biochemical Sciences*, 9(2), 60-63.
McCune, S. A. & Harris, R. A. (1979) Mechanism responsible for 5-(tetradecyloxy)-2-furoic acid inhibition of hepatic lipogenesis. *J Biol Chem*, 254(20), 10095-101.
McLean, J. E., Wudzinska, A., Datan, E., Quaglino, D. & Zakeri, Z. (2011) Flavivirus NS4A-induced autophagy protects cells against death and enhances virus replication. *J Biol Chem*, 286(25), 22147-59.
Means, T. K., Mylonakis, E., Tampakakis, E., Colvin, R. A., Seung, E., Puckett, L., Tai, M. F., Stewart, C. R., Pukkila-Worley, R., Hickman, S. E., Moore, K. J., Calderwood, S. B., Hacohen, N., Luster, A. D. & El Khoury, J. (2009) Evolutionarily conserved recognition and innate immunity to fungal pathogens by the scavenger receptors SCARF1 and CD36. *J Exp Med*, 206(3), 637-53.
Medigeshi, G. R., Hirsch, A. J., Streblow, D. N., Nikolich-Zugich, J. & Nelson, J. A. (2008) West Nile virus entry requires cholesterol-rich membrane microdomains and is independent of alphavbeta3 integrin. *J Virol*, 82(11), 5212-9.
Merino-Ramos, T., Vázquez-Calvo, Á., Casas, J., Sobrino, F., Saiz, J.-C. & Martín-Acebes, M. A. (2015) Modification of the Host Cell Lipid Metabolism Induced by Hypolipidemic Drugs Targeting the Acetyl Coenzyme A Carboxylase Impairs West Nile Virus Replication. *Antimicrobial agents and chemotherapy*, 60(1), 307-315.
Michelucci, A., Cordes, T., Ghelfi, J., Pailot, A., Reiling, N., Goldmann, O., Binz, T., Wegner, A., Tallam, A., Rausell, A., Buttini, M., Linster, C. L., Medina, E., Balling, R. & Hiller, K. (2013) Immune-responsive gene 1 protein links metabolism to immunity by catalyzing itaconic acid production. *Proc Natl Acad Sci U S A*, 110(19), 7820-5.
Michl, J., Ohlbaum, D. J. & Silverstein, S. C. (1976) 2-Deoxyglucose selectively inhibits Fc and complement receptor-mediated phagocytosis in mouse peritoneal macrophages II. Dissociation of the inhibitory effects of 2-deoxyglucose on phagocytosis and ATP generation. *J Exp Med*, 144(6), 1484-93.
Miinalainen, I. J., Chen, Z. J., Torkko, J. M., Pirilä, P. L., Sormunen, R. T., Bergmann, U., Qin, Y. M. & Hiltunen, J. K. (2003) Characterization of 2-enoyl thioester reductase from mammals. An ortholog of YBR026p/MRF1'p of the yeast mitochondrial fatty acid synthesis type II. *J Biol Chem*, 278(22), 20154-61.
Mikulasova, A., Gillespie, L. K., Ambrose, R. L., Aktepe, T. E., Trenerry, A. M., Liebscher, S. & Mackenzie, J. M. (2021) A Putative Lipid-Associating Motif in the West Nile Virus NS4A Protein Is Required for Efficient Virus Replication. *Front Cell Dev Biol*, 9, 655606.

Miller, J. L., de Wet, B. J., Martinez-Pomares, L., Radcliffe, C. M., Dwek, R. A., Rudd, P. M. & Gordon, S. (2008a) The mannose receptor mediates dengue virus infection of macrophages. *PLoS Pathog*, 4(2), e17.
Miller, J. L., deWet, B. J. M., Martinez-Pomares, L., Radcliffe, C. M., Dwek, R. A., Rudd, P. M. & Gordon, S. (2008b) The Mannose Receptor Mediates Dengue Virus Infection of Macrophages. *PLOS Pathogens*, 4(2), e17.
Miller, S., Kastner, S., Krijnse-Locker, J., Buhler, S. & Bartenschlager, R. (2007) The non-structural protein 4A of dengue virus is an integral membrane protein inducing membrane alterations in a 2K-regulated manner. *J Biol Chem*, 282(12), 8873-82.
Millet, P., Vachharajani, V., McPhail, L., Yoza, B. & McCall, C. E. (2016) GAPDH Binding to TNF-α mRNA Contributes to Posttranscriptional Repression in Monocytes: A Novel Mechanism of Communication between Inflammation and Metabolism. *J Immunol*, 196(6), 2541-51.
Mills, E. L., Kelly, B., Logan, A., Costa, A. S. H., Varma, M., Bryant, C. E., Tourlomousis, P., Däbritz, J. H. M., Gottlieb, E., Latorre, I., Corr, S. C., McManus, G., Ryan, D., Jacobs, H. T., Szibor, M., Xavier, R. J., Braun, T., Frezza, C., Murphy, M. P. & O'Neill, L. A. (2016) Succinate Dehydrogenase Supports Metabolic Repurposing of Mitochondria to Drive Inflammatory Macrophages. *Cell*, 167(2), 457-470.e13.
Miner, J. J., Cao, B., Govero, J., Smith, A. M., Fernandez, E., Cabrera, O. H., Garber, C., Noll, M., Klein, R. S., Noguchi, K. K., Mysorekar, I. U. & Diamond, M. S. (2016) Zika Virus Infection during Pregnancy in Mice Causes Placental Damage and Fetal Demise. *Cell*, 165(5), 1081-1091.
Miorin, L., Romero-Brey, I., Maiuri, P., Hoppe, S., Krijnse-Locker, J., Bartenschlager, R. & Marcello, A. (2013) Three-dimensional architecture of tick-borne encephalitis virus replication sites and trafficking of the replicated RNA. *J Virol*, 87(11), 6469-81.
Mittal, A., Ranganath, V. & Nichani, A. (2010) Omega fatty acids and resolution of inflammation: A new twist in an old tale. *J Indian Soc Periodontol*, 14(1), 3-7.
Miyanari, Y., Atsuzawa, K., Usuda, N., Watashi, K., Hishiki, T., Zayas, M., Bartenschlager, R., Wakita, T., Hijikata, M. & Shimotohno, K. (2007) The lipid droplet is an important organelle for hepatitis C virus production. *Nat Cell Biol*, 9(9), 1089-97.
Modhiran, N., Watterson, D., Blumenthal, A., Baxter, A. G., Young, P. R. & Stacey, K. J. (2017) Dengue virus NS1 protein activates immune cells via TLR4 but not TLR2 or TLR6. *Immunology And Cell Biology*, 95, 491.
Moesker, B., Rodenhuis-Zybert, I. A., Meijerhof, T., Wilschut, J. & Smit, J. M. (2010) Characterization of the functional requirements of West Nile virus membrane fusion. *J Gen Virol*, 91(Pt 2), 389-93.
Moessinger, C., Klizaite, K., Steinhagen, A., Philippou-Massier, J., Shevchenko, A., Hoch, M., Ejsing, C. S. & Thiele, C. (2014) Two different pathways of phosphatidylcholine synthesis, the Kennedy Pathway and the Lands Cycle, differentially regulate cellular triacylglycerol storage. *BMC Cell Biology*, 15(1), 43.
Molfino, A., Amabile, M. I., Monti, M. & Muscaritoli, M. (2017) Omega-3 Polyunsaturated Fatty Acids in Critical Illness: Anti-Inflammatory, Proresolving, or Both? *Oxid Med Cell Longev*, 2017, 5987082.
Monson, E. A., Crosse, K. M., Duan, M., Chen, W., O'Shea, R. D., Wakim, L. M., Carr, J. M., Whelan, D. R. & Helbig, K. J. (2021a) Intracellular lipid droplet accumulation occurs early following viral infection and is required for an efficient interferon response. *Nat Commun*, 12(1), 4303.
Monson, E. A., Trenerry, A. M., Laws, J. L., Mackenzie, J. M. & Helbig, K. J. (2021b) Lipid droplets and lipid mediators in viral infection and immunity. *FEMS microbiology reviews*, 45(4), fuaa066.
Moon, J. S., Hisata, S., Park, M. A., DeNicola, G. M., Ryter, S. W., Nakahira, K. & Choi, A. M. K. (2015a) mTORC1-Induced HK1-Dependent Glycolysis Regulates NLRP3 Inflammasome Activation. *Cell Rep*, 12(1), 102-115.

Moon, J. S., Lee, S., Park, M. A., Siempos, II, Haslip, M., Lee, P. J., Yun, M., Kim, C. K., Howrylak, J., Ryter, S. W., Nakahira, K. & Choi, A. M. (2015b) UCP2-induced fatty acid synthase promotes NLRP3 inflammasome activation during sepsis. *J Clin Invest*, 125(2), 665-80.
Moon, J. S., Nakahira, K., Chung, K. P., DeNicola, G. M., Koo, M. J., Pabon, M. A., Rooney, K. T., Yoon, J. H., Ryter, S. W., Stout-Delgado, H. & Choi, A. M. (2016) NOX4-dependent fatty acid oxidation promotes NLRP3 inflammasome activation in macrophages. *Nat Med*, 22(9), 1002-12.
Moreira, L. A., Iturbe-Ormaetxe, I., Jeffery, J. A., Lu, G., Pyke, A. T., Hedges, L. M., Rocha, B. C., Hall-Mendelin, S., Day, A., Riegler, M., Hugo, L. E., Johnson, K. N., Kay, B. H., McGraw, E. A., van den Hurk, A. F., Ryan, P. A. & O'Neill, S. L. (2009) A Wolbachia symbiont in Aedes aegypti limits infection with dengue, Chikungunya, and Plasmodium. *Cell*, 139(7), 1268-78.
Morita, M., Kuba, K., Ichikawa, A., Nakayama, M., Katahira, J., Iwamoto, R., Watanebe, T., Sakabe, S., Daidoji, T., Nakamura, S., Kadowaki, A., Ohto, T., Nakanishi, H., Taguchi, R., Nakaya, T., Murakami, M., Yoneda, Y., Arai, H., Kawaoka, Y., Penninger, J. M., Arita, M. & Imai, Y. (2013) The lipid mediator protectin D1 inhibits influenza virus replication and improves severe influenza. *Cell*, 153(1), 112-25.
Morrison, J., Laurent-Rolle, M., Maestre, A. M., Rajsbaum, R., Pisanelli, G., Simon, V., Mulder, L. C., Fernandez-Sesma, A. & García-Sastre, A. (2013) Dengue virus co-opts UBR4 to degrade STAT2 and antagonize type I interferon signaling. *PLoS Pathog*, 9(3), e1003265.
Munday, M. R. (2002) Regulation of mammalian acetyl-CoA carboxylase. *Biochemical Society Transactions*, 30(6), 1059-1064.
Munoz-Jordan, J. L., Sanchez-Burgos, G. G., Laurent-Rolle, M. & Garcia-Sastre, A. (2003) Inhibition of interferon signaling by dengue virus. *Proc Natl Acad Sci U S A*, 100(24), 14333-8.
Muñoz-Jordán, J. L., Sánchez-Burgos, G. G., Laurent-Rolle, M. & García-Sastre, A. (2003) Inhibition of interferon signaling by dengue virus. *Proceedings of the National Academy of Sciences*, 100(24), 14333-14338.
Musso, D., Nhan, T., Robin, E., Roche, C., Bierlaire, D., Zisou, K., Shan Yan, A., Cao-Lormeau, V. M. & Broult, J. (2014) Potential for Zika virus transmission through blood transfusion demonstrated during an outbreak in French Polynesia, November 2013 to February 2014. *Euro Surveill*, 19(14).
Muthumani, K., Griffin, B. D., Agarwal, S., Kudchodkar, S. B., Reuschel, E. L., Choi, H., Kraynyak, K. A., Duperret, E. K., Keaton, A. A., Chung, C., Kim, Y. K., Booth, S. A., Racine, T., Yan, J., Morrow, M. P., Jiang, J., Lee, B., Ramos, S., Broderick, K. E., Reed, C. C., Khan, A. S., Humeau, L., Ugen, K. E., Park, Y. K., Maslow, J. N., Sardesai, N. Y., Joseph Kim, J., Kobinger, G. P. & Weiner, D. B. (2016) In vivo protection against ZIKV infection and pathogenesis through passive antibody transfer and active immunisation with a prMEnv DNA vaccine. *npj Vaccines*, 1(1), 16021.
Nahrendorf, M. & Swirski, F. K. (2016) Abandoning M1/M2 for a Network Model of Macrophage Function. *Circ Res*, 119(3), 414-7.
Nakajima, S., Gotoh, M., Fukasawa, K., Murakami-Murofushi, K. & Kunugi, H. (2019) Oleic acid is a potent inducer for lipid droplet accumulation through its esterification to glycerol by diacylglycerol acyltransferase in primary cortical astrocytes. *Brain Res*, 1725, 146484.
Namgaladze, D. & Brüne, B. (2014) Fatty acid oxidation is dispensable for human macrophage IL-4-induced polarization. *Biochim Biophys Acta*, 1841(9), 1329-35.
Nasheri, N., Joyce, M., Rouleau, Y., Yang, P., Yao, S., Tyrrell, D. L. & Pezacki, John P. (2013) Modulation of Fatty Acid Synthase Enzyme Activity and Expression during Hepatitis C Virus Replication. *Chemistry & Biology*, 20(4), 570-582.
Nasirudeen, A. M., Wong, H. H., Thien, P., Xu, S., Lam, K. P. & Liu, D. X. (2011) RIG-I, MDA5 and TLR3 synergistically play an important role in restriction of dengue virus infection. *PLoS Negl Trop Dis*, 5(1), e926.

Naujoks, J., Tabeling, C., Dill, B. D., Hoffmann, C., Brown, A. S., Kunze, M., Kempa, S., Peter, A., Mollenkopf, H. J., Dorhoi, A., Kershaw, O., Gruber, A. D., Sander, L. E., Witzenrath, M., Herold, S., Nerlich, A., Hocke, A. C., van Driel, I., Suttorp, N., Bedoui, S., Hilbi, H., Trost, M. & Opitz, B. (2016) IFNs Modify the Proteome of Legionella-Containing Vacuoles and Restrict Infection Via IRG1-Derived Itaconic Acid. *PLoS Pathog*, 12(2), e1005408.

Neves-Souza, P. C., Azeredo, E. L., Zagne, S. M., Valls-de-Souza, R., Reis, S. R., Cerqueira, D. I., Nogueira, R. M. & Kubelka, C. F. (2005) Inducible nitric oxide synthase (iNOS) expression in monocytes during acute Dengue Fever in patients and during in vitro infection. *BMC Infect Dis*, 5, 64.

Ng, M. L. (1987) Ultrastructural studies of Kunjin virus-infected Aedes albopictus cells. *J Gen Virol*, 68 (Pt 2), 577-82.

Ng, M. L. & Hong, S. S. (1989) Flavivirus infection: essential ultrastructural changes and association of Kunjin virus NS3 protein with microtubules. *Arch Virol*, 106(1-2), 103-20.

Nguyen, L. N., Lim, Y. S., Pham, L. V., Shin, H. Y., Kim, Y. S. & Hwang, S. B. (2014) Stearoyl coenzyme A desaturase 1 is associated with hepatitis C virus replication complex and regulates viral replication. *J Virol*, 88(21), 12311-25.

Nguyen, T. B. & Olzmann, J. A. (2017) Lipid droplets and lipotoxicity during autophagy. *Autophagy*, 13(11), 2002-2003.

Nicholls, C. M. R., Sevvana, M. & Kuhn, R. J. (2020) Structure-guided paradigm shifts in flavivirus assembly and maturation mechanisms. *Advances in virus research*, 108, 33-83.

Nio, Y., Hasegawa, H., Okamura, H., Miyayama, Y., Akahori, Y. & Hijikata, M. (2016) Liver-specific mono-unsaturated fatty acid synthase-1 inhibitor for anti-hepatitis C treatment. *Antiviral Res*, 132, 262-7.

Nolan, C. J. & Larter, C. Z. (2009) Lipotoxicity: why do saturated fatty acids cause and monounsaturates protect against it? *J Gastroenterol Hepatol*, 24(5), 703-6.

Nomura, M., Liu, J., Rovira, II, Gonzalez-Hurtado, E., Lee, J., Wolfgang, M. J. & Finkel, T. (2016a) Fatty acid oxidation in macrophage polarization. *Nat Immunol*, 17(3), 216-7.

Nomura, M., Liu, J., Rovira, I. I., Gonzalez-Hurtado, E., Lee, J., Wolfgang, M. J. & Finkel, T. (2016b) Fatty acid oxidation in macrophage polarization. *Nature immunology*, 17(3), 216-217.

O'Leary, D. R., Marfin, A. A., Montgomery, S. P., Kipp, A. M., Lehman, J. A., Biggerstaff, B. J., Elko, V. L., Collins, P. D., Jones, J. E. & Campbell, G. L. (2004) The epidemic of West Nile virus in the United States, 2002. *Vector Borne Zoonotic Dis*, 4(1), 61-70.

O'Neill, Luke A. J. (2011) A critical role for citrate metabolism in LPS signalling. *Biochemical Journal*, 438(3), e5-e6.

Octave, M., Pirotton, L., Lepropre, S., Ginion, A., Robaux, V., Kautbally, S., Darley-Usmar, V. M., Ambroise, J., Guigas, B., Foretz, M., Bertrand, L., Beauloye, C. & Horman, S. (2020) Pharmacological ACC inhibition decreases thrombin-induced platelet aggregation by a mechanism independent of lipid content. *Archives of Cardiovascular Diseases Supplements*, 12(2), 204.

Odegaard, J. I. & Chawla, A. (2011) Alternative macrophage activation and metabolism. *Annu Rev Pathol*, 6, 275-97.

Oem, J. K., Jackel-Cram, C., Li, Y. P., Zhou, Y., Zhong, J., Shimano, H., Babiuk, L. A. & Liu, Q. (2008) Activation of sterol regulatory element-binding protein 1c and fatty acid synthase transcription by hepatitis C virus non-structural protein 2. *J Gen Virol*, 89(Pt 5), 1225-1230.

Oh, Y. S., Bae, G. D., Baek, D. J., Park, E.-Y. & Jun, H.-S. (2018) Fatty Acid-Induced Lipotoxicity in Pancreatic Beta-Cells During Development of Type 2 Diabetes, 9.

Ohol, Y. M., Wang, Z., Kemble, G. & Duke, G. (2015) Direct Inhibition of Cellular Fatty Acid Synthase Impairs Replication of Respiratory Syncytial Virus and Other Respiratory Viruses. *PloS one*, 10(12), e0144648-e0144648.

Olofsson, S. O., Andersson, L., Haversen, L., Olsson, C., Myhre, S., Rutberg, M., Mobini, R., Li, L., Lu, E., Boren, J. & Bostrom, P. (2011) The formation of lipid droplets: possible role in the development of insulin resistance/type 2 diabetes. *Prostaglandins Leukot Essent Fatty Acids*, 85(5), 215-8.
Olzmann, J. A. & Carvalho, P. (2019) Dynamics and functions of lipid droplets. *Nat Rev Mol Cell Biol*, 20(3), 137-155.
Orecchioni, M., Ghosheh, Y., Pramod, A. B. & Ley, K. (2019) Macrophage Polarization: Different Gene Signatures in M1(LPS+) vs. Classically and M2(LPS-) vs. Alternatively Activated Macrophages. *Front Immunol*, 10, 1084.
Ortega-Prieto, P. & Postic, C. (2019) Carbohydrate Sensing Through the Transcription Factor ChREBP, 10.
Otto, D. A., Chatzidakis, C., Kasziba, E. & Cook, G. A. (1985) Reciprocal effects of 5-(tetradecyloxy)-2-furoic acid on fatty acid oxidation. *Archives of Biochemistry and Biophysics*, 242(1), 23-31.
Overby, A. K., Popov, V. L., Niedrig, M. & Weber, F. (2010) Tick-borne encephalitis virus delays interferon induction and hides its double-stranded RNA in intracellular membrane vesicles. *J Virol*, 84(17), 8470-83.
Padwal, R. S. & Majumdar, S. R. (2007) Drug treatments for obesity: orlistat, sibutramine, and rimonabant. *Lancet*, 369(9555), 71-7.
Palmer, C. S., Anzinger, J. J., Zhou, J., Gouillou, M., Landay, A., Jaworowski, A., McCune, J. M. & Crowe, S. M. (2014) Glucose Transporter 1–Expressing Proinflammatory Monocytes Are Elevated in Combination Antiretroviral Therapy–Treated and Untreated HIV⁺ Subjects. *The Journal of Immunology*, 193(11), 5595.
Palmer, C. S., Henstridge, D. C., Yu, D., Singh, A., Balderson, B., Duette, G., Cherry, C. L., Anzinger, J. J., Ostrowski, M. & Crowe, S. M. (2016) Emerging Role and Characterization of Immunometabolism: Relevance to HIV Pathogenesis, Serious Non-AIDS Events, and a Cure. *The Journal of Immunology*, 196(11), 4437.
Parisi, L., Gini, E., Baci, D., Tremolati, M., Fanuli, M., Bassani, B., Farronato, G., Bruno, A. & Mortara, L. (2018) Macrophage Polarization in Chronic Inflammatory Diseases: Killers or Builders? *J Immunol Res*, 2018, 8917804.
Park, C.-Y., Jun, H.-J., Wakita, T., Cheong, J. H. & Hwang, S. B. (2009a) Hepatitis C Virus Nonstructural 4B Protein Modulates Sterol Regulatory Element-binding Protein Signaling via the AKT Pathway *. *Journal of Biological Chemistry*, 284(14), 9237-9246.
Park, Y. M., Febbraio, M. & Silverstein, R. L. (2009b) CD36 modulates migration of mouse and human macrophages in response to oxidized LDL and may contribute to macrophage trapping in the arterial intima. *The Journal of clinical investigation*, 119(1), 136-145.
Pastorino, B., Nougairède, A., Wurtz, N., Gould, E. & de Lamballerie, X. (2010) Role of host cell factors in flavivirus infection: Implications for pathogenesis and development of antiviral drugs. *Antiviral Research*, 87(3), 281-294.
Paton, C. M. & Ntambi, J. M. (2009) Biochemical and physiological function of stearoyl-CoA desaturase. *American journal of physiology. Endocrinology and metabolism*, 297(1), E28-E37.
Paul, D. & Bartenschlager, R. (2015) Flaviviridae Replication Organelles: Oh, What a Tangled Web We Weave. *Annu Rev Virol*, 2(1), 289-310.
Pavlou, S., Wang, L., Xu, H. & Chen, M. (2017) Higher phagocytic activity of thioglycollate-elicited peritoneal macrophages is related to metabolic status of the cells. *J Inflamm (Lond)*, 14, 4.
Pazirandeh, M., Chirala, S. S., Huang, W. Y. & Wakil, S. J. (1989) Characterization of recombinant thioesterase and acyl carrier protein domains of chicken fatty acid synthase expressed in Escherichia coli. *J Biol Chem*, 264(30), 18195-201.

Pealer, L. N., Marfin, A. A., Petersen, L. R., Lanciotti, R. S., Page, P. L., Stramer, S. L., Stobierski, M. G., Signs, K., Newman, B., Kapoor, H., Goodman, J. L. & Chamberland, M. E. (2003) Transmission of West Nile virus through blood transfusion in the United States in 2002. *N Engl J Med*, 349(13), 1236-45.

Pennathur, S., Pasichnyk, K., Bahrami, N. M., Zeng, L., Febbraio, M., Yamaguchi, I. & Okamura, D. M. (2015) The macrophage phagocytic receptor CD36 promotes fibrogenic pathways on removal of apoptotic cells during chronic kidney injury. *Am J Pathol*, 185(8), 2232-45.

Penzo, D., Tagliapietra, C., Colonna, R., Petronilli, V. & Bernardi, P. (2002) Effects of fatty acids on mitochondria: implications for cell death. *Biochimica et Biophysica Acta (BBA) - Bioenergetics*, 1555(1), 160-165.

Perera, R., Riley, C., Isaac, G., Hopf-Jannasch, A. S., Moore, R. J., Weitz, K. W., Pasa-Tolic, L., Metz, T. O., Adamec, J. & Kuhn, R. J. (2012) Dengue Virus Infection Perturbs Lipid Homeostasis in Infected Mosquito Cells. *PLOS Pathogens*, 8(3), e1002584.

Petersen, L. R. & Marfin, A. A. (2002) West Nile virus: a primer for the clinician. *Ann Intern Med*, 137(3), 173-9.

Phalen, T. & Kielian, M. (1991) Cholesterol is required for infection by Semliki Forest virus. *Journal of Cell Biology*, 112(4), 615-623.

Pinto, A. K., Richner, J. M., Poore, E. A., Patil, P. P., Amanna, I. J., Slifka, M. K. & Diamond, M. S. (2013) A Hydrogen Peroxide-Inactivated Virus Vaccine Elicits Humoral and Cellular Immunity and Protects against Lethal West Nile Virus Infection in Aged Mice, 87(4), 1926-1936.

Pireaux, V., Sauvage, A., Bihin, B., Van Steenbrugge, M., Rousseau, A., Van Antwerpen, P., Zouaoui Boudjeltia, K. & Raes, M. (2016) Myeloperoxidase-Oxidized LDLs Enhance an Anti-Inflammatory M2 and Antioxidant Phenotype in Murine Macrophages. *Mediators Inflamm*, 2016, 8249476.

Pombo, J. P. & Sanyal, S. (2018) Perturbation of Intracellular Cholesterol and Fatty Acid Homeostasis During Flavivirus Infections, 9.

Posokhova, E. N., Khoshchenko, O. M., Chasovskikh, M. I., Pivovarova, E. N. & Dushkin, M. I. (2008) Lipid synthesis in macrophages during inflammation in vivo: Effect of agonists of peroxisome proliferator activated receptors α and γ and of retinoid X receptors. *Biochemistry (Moscow)*, 73(3), 296-304.

Potisopon, S., Priet, S., Collet, A., Decroly, E., Canard, B. & Selisko, B. (2014) The methyltransferase domain of dengue virus protein NS5 ensures efficient RNA synthesis initiation and elongation by the polymerase domain. *Nucleic acids research*, 42(18), 11642-11656.

Puig, T., Turrado, C., Benhamú, B., Aguilar, H., Relat, J., Ortega-Gutiérrez, S., Casals, G., Marrero, P. F., Urruticoechea, A., Haro, D., López-Rodríguez, M. L. & Colomer, R. (2009) Novel Inhibitors of Fatty Acid Synthase with Anticancer Activity. *Clinical Cancer Research*, 15(24), 7608-7615.

Rabelo, K., de Souza, L. J., Salomão, N. G., Machado, L. N., Pereira, P. G., Portari, E. A., Basílio-de-Oliveira, R., Dos Santos, F. B., Neves, L. D., Morgade, L. F., Provance, D. W., Jr., Higa, L. M., Tanuri, A., de Carvalho, J. J. & Paes, M. V. (2020) Zika Induces Human Placental Damage and Inflammation. *Front Immunol*, 11, 2146.

Raggi, F., Pelassa, S., Pierobon, D., Penco, F., Gattorno, M., Novelli, F., Eva, A., Varesio, L., Giovarelli, M. & Bosco, M. C. (2017) Regulation of Human Macrophage M1-M2 Polarization Balance by Hypoxia and the Triggering Receptor Expressed on Myeloid Cells-1. *Front Immunol*, 8, 1097.

Rajan, S., de Guzman, H. C., Palaia, T., Goldberg, I. J. & Hussain, M. M. (2021) A simple, rapid, and sensitive fluorescence-based method to assess triacylglycerol hydrolase activity. *J Lipid Res*, 62, 100115.

Rajasagi, N. K., Reddy, P. B., Mulik, S., Gjorstrup, P. & Rouse, B. T. (2013) Neuroprotectin D1 reduces the severity of herpes simplex virus-induced corneal immunopathology. *Invest Ophthalmol Vis Sci*, 54(9), 6269-79.
Randall, R. E. & Goodbourn, S. (2008) Interferons and viruses: an interplay between induction, signalling, antiviral responses and virus countermeasures. *J Gen Virol*, 89(Pt 1), 1-47.
Rey, F. A., Heinz, F. X., Mandl, C., Kunz, C. & Harrison, S. C. (1995) The envelope glycoprotein from tick-borne encephalitis virus at 2 A resolution. *Nature*, 375(6529), 291-8.
Richardson, J. Y., Ottolini, M. G., Pletneva, L., Boukhvalova, M., Zhang, S., Vogel, S. N., Prince, G. A. & Blanco, J. C. (2005) Respiratory syncytial virus (RSV) infection induces cyclooxygenase 2: a potential target for RSV therapy. *J Immunol*, 174(7), 4356-64.
Riegler, M., Sidhu, M., Miller, W. J. & O'Neill, S. L. (2005) Evidence for a Global *Wolbachia* Replacement in *Drosophila melanogaster*. *Current Biology*, 15(15), 1428-1433.
Ripa, I., Andreu, S., López-Guerrero, J. A. & Bello-Morales, R. (2021) Membrane Rafts: Portals for Viral Entry, 12.
Ritter, J. B., Wahl, A. S., Freund, S., Genzel, Y. & Reichl, U. (2010) Metabolic effects of influenza virus infection in cultured animal cells: Intra- and extracellular metabolite profiling. *BMC Systems Biology*, 4(1), 61.
Roby, J. A., Esser-Nobis, K., Dewey-Verstelle, E. C., Fairgrieve, M. R., Schwerk, J., Lu, A. Y., Soveg, F. W., Hemann, E. A., Hatfield, L. D., Keller, B. C., Shapiro, A., Forero, A., Stencel-Baerenwald, J. E., Savan, R. & Gale, M., Jr. (2020) Flavivirus Nonstructural Protein NS5 Dysregulates HSP90 to Broadly Inhibit JAK/STAT Signaling. *Cells*, 9(4).
Roby, J. A., Keller, B. C., Ramos, H. J., Diamond, M. S. & Gale, M. J. (2016) The JAK/STAT signaling cascades of multiple cytokines are dysregulated during West Nile virus infection. *The Journal of Immunology*, 196(1 Supplement), 217.38.
Rohwedder, A., Zhang, Q., Rudge, S. A. & Wakelam, M. J. (2014) Lipid droplet formation in response to oleic acid in Huh-7 cells is mediated by the fatty acid receptor FFAR4. *J Cell Sci*, 127(Pt 14), 3104-15.
Romano, A. H. & Conway, T. (1996) Evolution of carbohydrate metabolic pathways. *Res Microbiol*, 147(6-7), 448-55.
Roosendaal, J., Westaway, E. G., Khromykh, A. & Mackenzie, J. M. (2006a) Regulated cleavages at the West Nile virus NS4A-2K-NS4B junctions play a major role in rearranging cytoplasmic membranes and Golgi trafficking of the NS4A protein. *Journal of virology*, 80(9), 4623-4632.
Roosendaal, J., Westaway, E. G., Khromykh, A. & Mackenzie, J. M. (2006b) Regulated cleavages at the West Nile virus NS4A-2K-NS4B junctions play a major role in rearranging cytoplasmic membranes and Golgi trafficking of the NS4A protein. *J Virol*, 80(9), 4623-32.
Rosas-Ballina, M., Guan, X. L., Schmidt, A. & Bumann, D. (2020) Classical Activation of Macrophages Leads to Lipid Droplet Formation Without de novo Fatty Acid Synthesis, 11(131).
Rossen, J. W., Bouma, J., Raatgeep, R. H., Büller, H. A. & Einerhand, A. W. (2004) Inhibition of cyclooxygenase activity reduces rotavirus infection at a postbinding step. *J Virol*, 78(18), 9721-30.
Rossi, S. L., Tesh, R. B., Azar, S. R., Muruato, A. E., Hanley, K. A., Auguste, A. J., Langsjoen, R. M., Paessler, S., Vasilakis, N. & Weaver, S. C. (2016) Characterization of a Novel Murine Model to Study Zika Virus. *Am J Trop Med Hyg*, 94(6), 1362-1369.
Roth, S. L. & Whittaker, G. R. (2011) Promotion of vesicular stomatitis virus fusion by the endosome-specific phospholipid bis(monoacylglycero)phosphate (BMP). *FEBS Lett*, 585(6), 865-9.
Rothwell, C., Lebreton, A., Young Ng, C., Lim, J. Y., Liu, W., Vasudevan, S., Labow, M., Gu, F. & Gaither, L. A. (2009) Cholesterol biosynthesis modulation regulates dengue viral replication. *Virology*, 389(1-2), 8-19.

Royle, J., Donald, C. L., Merits, A., Kohl, A. & Varjak, M. (2017) Differential effects of lipid biosynthesis inhibitors on Zika and Semliki Forest viruses. *Veterinary journal (London, England : 1997)*, 230, 62-64.
Sag, D., Carling, D., Stout, R. D. & Suttles, J. (2008) Adenosine 5'-monophosphate-activated protein kinase promotes macrophage polarization to an anti-inflammatory functional phenotype. *J Immunol*, 181(12), 8633-41.
Saitoh, T., Satoh, T., Yamamoto, N., Uematsu, S., Takeuchi, O., Kawai, T. & Akira, S. (2011) Antiviral protein Viperin promotes Toll-like receptor 7- and Toll-like receptor 9-mediated type I interferon production in plasmacytoid dendritic cells. *Immunity*, 34(3), 352-63.
Salas-Benito, J., Reyes-Del Valle, J., Salas-Benito, M., Ceballos-Olvera, I., Mosso, C. & del Angel, R. M. (2007) Evidence that the 45-kD glycoprotein, part of a putative dengue virus receptor complex in the mosquito cell line C6/36, is a heat-shock related protein. *Am J Trop Med Hyg*, 77(2), 283-90.
Salim, T., Sershen, C. L. & May, E. E. (2016) Investigating the Role of TNF-α and IFN-γ Activation on the Dynamics of iNOS Gene Expression in LPS Stimulated Macrophages. *PLOS ONE*, 11(6), e0153289.
Samardzic, T., Jankovic, V., Stosic-Grujicic, S. & Trajkovic, V. (2001) STAT1 is required for iNOS activation, but not IL-6 production in murine fibroblasts. *Cytokine*, 13(3), 179-82.
Samsa, M. M., Mondotte, J. A., Iglesias, N. G., Assuncao-Miranda, I., Barbosa-Lima, G., Da Poian, A. T., Bozza, P. T. & Gamarnik, A. V. (2009) Dengue virus capsid protein usurps lipid droplets for viral particle formation. *PLoS Pathog*, 5(10), e1000632.
Samuel, M. A. & Diamond, M. S. (2006) Pathogenesis of West Nile Virus infection: a balance between virulence, innate and adaptive immunity, and viral evasion. *Journal of virology*, 80(19), 9349-9360.
Samuel, M. A., Whitby, K., Keller, B. C., Marri, A., Barchet, W., Williams, B. R. G., Silverman, R. H., Gale, M., Jr. & Diamond, M. S. (2006) PKR and RNase L contribute to protection against lethal West Nile Virus infection by controlling early viral spread in the periphery and replication in neurons. *Journal of virology*, 80(14), 7009-7019.
Sarkar, R., Sharma, K. B., Kumari, A., Asthana, S. & Kalia, M. (2021) Japanese encephalitis virus capsid protein interacts with non-lipidated MAP1LC3 on replication membranes and lipid droplets. *J Gen Virol*, 102(1).
Saxena, S. K., Singh, A. & Mathur, A. (2000) Antiviral effect of nitric oxide during Japanese encephalitis virus infection. *Int J Exp Pathol*, 81(2), 165-72.
Schaeffer, B. E. & Curtis, A. S. (1977) Effects on cell adhesion and membrane fluidity of changes in plasmalemmal lipids in mouse L929 cells. *J Cell Sci*, 26, 47-55.
Schmidt, T. L., Barton, N. H., Rašić, G., Turley, A. P., Montgomery, B. L., Iturbe-Ormaetxe, I., Cook, P. E., Ryan, P. A., Ritchie, S. A., Hoffmann, A. A., O'Neill, S. L. & Turelli, M. (2017) Local introduction and heterogeneous spatial spread of dengue-suppressing Wolbachia through an urban population of Aedes aegypti. *PLOS Biology*, 15(5), e2001894.
Schott, M. B., Weller, S. G., Schulze, R. J., Krueger, E. W., Drizyte-Miller, K., Casey, C. A. & McNiven, M. A. (2019) Lipid droplet size directs lipolysis and lipophagy catabolism in hepatocytes. *Journal of Cell Biology*, 218(10), 3320-3335.
Schulz, H. (1994) Regulation of Fatty Acid Oxidation in Heart. *The Journal of Nutrition*, 124(2), 165-171.
Sen, S., Kaminiski, R., Deshmane, S., Langford, D., Khalili, K., Amini, S. & Datta, P. K. (2015) Role of Hexokinase-1 in the survival of HIV-1-infected macrophages. *Cell Cycle*, 14(7), 980-989.
Senkal, C. E., Salama, M. F., Snider, A. J., Allopenna, J. J., Rana, N. A., Koller, A., Hannun, Y. A. & Obeid, L. M. (2017) Ceramide Is Metabolized to Acylceramide and Stored in Lipid Droplets. *Cell Metab*, 25(3), 686-697.

Sergi, D., Luscombe-Marsh, N., Naumovski, N., Abeywardena, M. & O'Callaghan, N. (2021) Palmitic Acid, but Not Lauric Acid, Induces Metabolic Inflammation, Mitochondrial Fragmentation, and a Drop in Mitochondrial Membrane Potential in Human Primary Myotubes, 8.

Serhan, C. N. (2014) Pro-resolving lipid mediators are leads for resolution physiology. *Nature*, 510(7503), 92-101.

Shang, Z., Song, H., Shi, Y., Qi, J. & Gao, G. F. (2018) Crystal Structure of the Capsid Protein from Zika Virus. *Journal of Molecular Biology*, 430(7), 948-962.

Shapouri-Moghaddam, A., Mohammadian, S., Vazini, H., Taghadosi, M., Esmaeili, S. A., Mardani, F., Seifi, B., Mohammadi, A., Afshari, J. T. & Sahebkar, A. (2018) Macrophage plasticity, polarization, and function in health and disease. *J Cell Physiol*, 233(9), 6425-6440.

Shavinskaya, A., Boulant, S., Penin, F., McLauchlan, J. & Bartenschlager, R. (2007) The lipid droplet binding domain of hepatitis C virus core protein is a major determinant for efficient virus assembly. *J Biol Chem*, 282(51), 37158-69.

Shimano, H. & Sato, R. (2017) SREBP-regulated lipid metabolism: convergent physiology — divergent pathophysiology. *Nature Reviews Endocrinology*, 13(12), 710-730.

Shirey, K. A., Lai, W., Pletneva, L. M., Karp, C. L., Divanovic, S., Blanco, J. C. G. & Vogel, S. N. (2014) Role of the lipoxygenase pathway in RSV-induced alternatively activated macrophages leading to resolution of lung pathology. *Mucosal immunology*, 7(3), 549-557.

Silva, E. M., Conde, J. N., Allonso, D., Ventura, G. T., Coelho, D. R., Carneiro, P. H., Silva, M. L., Paes, M. V., Rabelo, K., Weissmuller, G., Bisch, P. M. & Mohana-Borges, R. (2019) Dengue virus nonstructural 3 protein interacts directly with human glyceraldehyde-3-phosphate dehydrogenase (GAPDH) and reduces its glycolytic activity. *Scientific Reports*, 9(1), 2651.

Simmonds, P., Becher, P., Bukh, J., Gould, E. A., Meyers, G., Monath, T., Muerhoff, S., Pletnev, A., Rico-Hesse, R., Smith, D. B., Stapleton, J. T. & Ictv Report, C. (2017) ICTV Virus Taxonomy Profile: Flaviviridae. *The Journal of general virology*, 98(1), 2-3.

Singh, N., Wakil, S. J. & Stoops, J. K. (1984) On the question of half- or full-site reactivity of animal fatty acid synthetase. *J Biol Chem*, 259(6), 3605-11.

Singh, S., Singh, P. K., Suhail, H., Arumugaswami, V., Pellett, P. E., Giri, S. & Kumar, A. (2020) AMP-Activated Protein Kinase Restricts Zika Virus Replication in Endothelial Cells by Potentiating Innate Antiviral Responses and Inhibiting Glycolysis. *The Journal of Immunology*, 204(7), 1810.

Smith, G. M., Garton, A. J., Aitken, A. & Yeaman, S. J. (1996) Evidence for a multi-domain structure for hormone-sensitive lipase. *FEBS Lett*, 396(1), 90-4.

Smith, T. D., Tse, M. J., Read, E. L. & Liu, W. F. (2016) Regulation of macrophage polarization and plasticity by complex activation signals. *Integr Biol (Camb)*, 8(9), 946-55.

Souza, D. G., Fagundes, C. T., Sousa, L. P., Amaral, F. A., Souza, R. S., Souza, A. L., Kroon, E. G., Sachs, D., Cunha, F. Q., Bukin, E., Atrasheuskaya, A., Ignatyev, G. & Teixeira, M. M. (2009) Essential role of platelet-activating factor receptor in the pathogenesis of Dengue virus infection. *Proc Natl Acad Sci U S A*, 106(33), 14138-43.

Stempelj, M., Kedinger, M., Augenlicht, L. & Klampfer, L. (2007) Essential Role of the JAK/STAT1 Signaling Pathway in the Expression of Inducible Nitric-oxide Synthase in Intestinal Epithelial Cells and Its Regulation by Butyrate *. *Journal of Biological Chemistry*, 282(13), 9797-9804.

Stiasny, K. & Heinz, F. X. (2004) Effect of membrane curvature-modifying lipids on membrane fusion by tick-borne encephalitis virus. *J Virol*, 78(16), 8536-42.

Stone, A. E. L., Green, R., Wilkins, C., Hemann, E. A. & Gale, M., Jr. (2019) RIG-I-like receptors direct inflammatory macrophage polarization against West Nile virus infection. *Nat Commun*, 10(1), 3649.

Storch, J. & Thumser, A. E. (2010) Tissue-specific functions in the fatty acid-binding protein family. *J Biol Chem*, 285(43), 32679-32683.
Suzuki, M., Shinohara, Y., Ohsaki, Y. & Fujimoto, T. (2011) Lipid droplets: size matters. *Journal of Electron Microscopy*, 60(suppl_1), S101-S116.
Sviridov, D. & Bukrinsky, M. (2014) Interaction of pathogens with host cholesterol metabolism. *Current Opinion in Lipidology*, 25(5), 333-338.
Taber, L. H., Knight, V., Gilbert, B. E., McClung, H. W., Wilson, S. Z., Norton, H. J., Thurson, J. M., Gordon, W. H., Atmar, R. L. & Schlaudt, W. R. (1983) Ribavirin aerosol treatment of bronchiolitis associated with respiratory syncytial virus infection in infants. *Pediatrics*, 72(5), 613-8.
Taciak, B., Białasek, M., Braniewska, A., Sas, Z., Sawicka, P., Kiraga, Ł., Rygiel, T. & Król, M. (2018) Evaluation of phenotypic and functional stability of RAW 264.7 cell line through serial passages. *PLoS One*, 13(6), e0198943.
Taguwa, S., Maringer, K., Li, X., Bernal-Rubio, D., Rauch, J. N., Gestwicki, J. E., Andino, R., Fernandez-Sesma, A. & Frydman, J. (2015) Defining Hsp70 Subnetworks in Dengue Virus Replication Reveals Key Vulnerability in Flavivirus Infection. *Cell*, 163(5), 1108-1123.
Tandon, N. N., Kralisz, U. & Jamieson, G. A. (1989) Identification of glycoprotein IV (CD36) as a primary receptor for platelet-collagen adhesion. *J Biol Chem*, 264(13), 7576-83.
Tannahill, G. M., Curtis, A. M., Adamik, J., Palsson-McDermott, E. M., McGettrick, A. F., Goel, G., Frezza, C., Bernard, N. J., Kelly, B., Foley, N. H., Zheng, L., Gardet, A., Tong, Z., Jany, S. S., Corr, S. C., Haneklaus, M., Caffrey, B. E., Pierce, K., Walmsley, S., Beasley, F. C., Cummins, E., Nizet, V., Whyte, M., Taylor, C. T., Lin, H., Masters, S. L., Gottlieb, E., Kelly, V. P., Clish, C., Auron, P. E., Xavier, R. J. & O'Neill, L. A. J. (2013) Succinate is an inflammatory signal that induces IL-1β through HIF-1α. *Nature*, 496(7444), 238-242.
Taube, S., Jiang, M. & Wobus, C. E. (2010) Glycosphingolipids as receptors for non-enveloped viruses. *Viruses*, 2(4), 1011-49.
Tebas, P., Roberts, C. C., Muthumani, K., Reuschel, E. L., Kudchodkar, S. B., Zaidi, F. I., White, S., Khan, A. S., Racine, T., Choi, H., Boyer, J., Park, Y. K., Trottier, S., Remigio, C., Krieger, D., Spruill, S. E., Bagarazzi, M., Kobinger, G. P., Weiner, D. B. & Maslow, J. N. (2017) Safety and Immunogenicity of an Anti–Zika Virus DNA Vaccine. *New England Journal of Medicine*, 385(12), e35.
Tedesco, S., De Majo, F., Kim, J., Trenti, A., Trevisi, L., Fadini, G. P., Bolego, C., Zandstra, P. W., Cignarella, A. & Vitiello, L. (2018) Convenience versus Biological Significance: Are PMA-Differentiated THP-1 Cells a Reliable Substitute for Blood-Derived Macrophages When Studying in Vitro Polarization?, 9.
Thombare, K., Ntika, S., Wang, X. & Krizhanovskii, C. (2017) Long chain saturated and unsaturated fatty acids exert opposing effects on viability and function of GLP-1-producing cells: Mechanisms of lipotoxicity. *PLOS ONE*, 12(5), e0177605.
Thupari, J. N., Landree, L. E., Ronnett, G. V. & Kuhajda, F. P. (2002) C75 increases peripheral energy utilization and fatty acid oxidation in diet-induced obesity. *Proc Natl Acad Sci U S A*, 99(14), 9498-502.
Thurmond, S., Wang, B., Song, J. & Hai, R. (2018) Suppression of Type I Interferon Signaling by Flavivirus NS5. *Viruses*, 10(12), 712.
Tiwari, S. K., Dang, J., Qin, Y., Lichinchi, G., Bansal, V. & Rana, T. M. (2017) Zika virus infection reprograms global transcription of host cells to allow sustained infection. *Emerg Microbes Infect*, 6(4), e24.
Tong, L. & Harwood, H. J., Jr. (2006) Acetyl-coenzyme A carboxylases: versatile targets for drug discovery. *J Cell Biochem*, 99(6), 1476-88.

Tongluan, N., Ramphan, S., Wintachai, P., Jaresitthikunchai, J., Khongwichit, S., Wikan, N., Rajakam, S., Yoksan, S., Wongsiriroj, N., Roytrakul, S. & Smith, D. R. (2017) Involvement of fatty acid synthase in dengue virus infection. *Virology Journal*, 14(1), 28.
Torretta, S., Scagliola, A., Ricci, L., Mainini, F., Di Marco, S., Cuccovillo, I., Kajaste-Rudnitski, A., Sumpton, D., Ryan, K. M. & Cardaci, S. (2020) D-mannose suppresses macrophage IL-1β production. *Nature Communications*, 11(1), 6343.
Tsai, B., Gilbert, J. M., Stehle, T., Lencer, W., Benjamin, T. L. & Rapoport, T. A. (2003) Gangliosides are receptors for murine polyoma virus and SV40. *Embo j*, 22(17), 4346-55.
Tse, E. K., Salehi, A., Clemenzi, M. N. & Belsham, D. D. (2018) Role of the saturated fatty acid palmitate in the interconnected hypothalamic control of energy homeostasis and biological rhythms. *Am J Physiol Endocrinol Metab*, 315(2), E133-e140.
Turelli, M. & Hoffmann, A. A. (1991) Rapid spread of an inherited incompatibility factor in California Drosophila. *Nature*, 353(6343), 440-442.
Uchida, L., Espada-Murao, L. A., Takamatsu, Y., Okamoto, K., Hayasaka, D., Yu, F., Nabeshima, T., Buerano, C. C. & Morita, K. (2014) The dengue virus conceals double-stranded RNA in the intracellular membrane to escape from an interferon response. *Scientific Reports*, 4, 7395.
Umashankar, M., Sánchez-San Martín, C., Liao, M., Reilly, B., Guo, A., Taylor, G. & Kielian, M. (2008) Differential cholesterol binding by class II fusion proteins determines membrane fusion properties. *J Virol*, 82(18), 9245-53.
Utarini, A., Indriani, C., Ahmad, R. A., Tantowijoyo, W., Arguni, E., Ansari, M. R., Supriyati, E., Wardana, D. S., Meitika, Y., Ernesia, I., Nurhayati, I., Prabowo, E., Andari, B., Green, B. R., Hodgson, L., Cutcher, Z., Rancès, E., Ryan, P. A., O'Neill, S. L., Dufault, S. M., Tanamas, S. K., Jewell, N. P., Anders, K. L. & Simmons, C. P. (2021) Efficacy of Wolbachia-Infected Mosquito Deployments for the Control of Dengue, 384(23), 2177-2186.
Valle, J. R.-d., Chávez-Salinas, S., Medina, F. & Angel, R. M. d. (2005) Heat Shock Protein 90 and Heat Shock Protein 70 Are Components of Dengue Virus Receptor Complex in Human Cells, 79(8), 4557-4567.
Van den Bossche, J., Baardman, J. & de Winther, M. P. (2015) Metabolic Characterization of Polarized M1 and M2 Bone Marrow-derived Macrophages Using Real-time Extracellular Flux Analysis. *J Vis Exp*(105).
Van den Bossche, J., Baardman, J., Otto, N. A., van der Velden, S., Neele, A. E., van den Berg, S. M., Luque-Martin, R., Chen, H. J., Boshuizen, M. C., Ahmed, M., Hoeksema, M. A., de Vos, A. F. & de Winther, M. P. (2016) Mitochondrial Dysfunction Prevents Repolarization of Inflammatory Macrophages. *Cell Rep*, 17(3), 684-696.
Van den Bossche, J., O'Neill, L. A. & Menon, D. (2017) Macrophage Immunometabolism: Where Are We (Going)? *Trends Immunol*, 38(6), 395-406.
van den Elsen, K., Quek, J. P. & Luo, D. (2021) Molecular Insights into the Flavivirus Replication Complex. *Viruses*, 13(6), 956.
van der Schaar, H. M., Rust, M. J., Chen, C., van der Ende-Metselaar, H., Wilschut, J., Zhuang, X. & Smit, J. M. (2008) Dissecting the cell entry pathway of dengue virus by single-particle tracking in living cells. *PLoS pathogens*, 4(12), e1000244-e1000244.
Varshney, P., Yadav, V. & Saini, N. (2016) Lipid rafts in immune signalling: current progress and future perspective. *Immunology*, 149(1), 13-24.
Vastag, L., Koyuncu, E., Grady, S. L., Shenk, T. E. & Rabinowitz, J. D. (2011) Divergent Effects of Human Cytomegalovirus and Herpes Simplex Virus-1 on Cellular Metabolism. *PLOS Pathogens*, 7(7), e1002124.
Ventura, R., Mordec, K., Waszczuk, J., Wang, Z., Lai, J., Fridlib, M., Buckley, D., Kemble, G. & Heuer, T. S. (2015) Inhibition of de novo Palmitate Synthesis by Fatty Acid Synthase Induces

Apoptosis in Tumor Cells by Remodeling Cell Membranes, Inhibiting Signaling Pathways, and Reprogramming Gene Expression. *EBioMedicine*, 2(8), 808-24.
Villani, A., Cirino, N. M., Baldi, E., Kester, M., McFadden, E. R., Jr. & Panuska, J. R. (1991) Respiratory syncytial virus infection of human mononuclear phagocytes stimulates synthesis of platelet-activating factor. *J Biol Chem*, 266(9), 5472-9.
Viola, A., Munari, F., Sánchez-Rodríguez, R., Scolaro, T. & Castegna, A. (2019) The Metabolic Signature of Macrophage Responses, 10.
Wakil, S. J., Stoops, J. K. & Joshi, V. C. (1983) FATTY ACID SYNTHESIS AND ITS REGULATION. *Annual Review of Biochemistry*, 52(1), 537-579.
Wan, S.-W., Wu-Hsieh, B. A., Lin, Y.-S., Chen, W.-Y., Huang, Y. & Anderson, R. (2018) The monocyte-macrophage-mast cell axis in dengue pathogenesis. *Journal of Biomedical Science*, 25(1), 77.
Wang, H., Yang, P., Liu, K., Guo, F., Zhang, Y., Zhang, G. & Jiang, C. (2008) SARS coronavirus entry into host cells through a novel clathrin- and caveolae-independent endocytic pathway. *Cell Research*, 18(2), 290-301.
Wang, L., Chen, R. F., Liu, J. W., Yu, H. R., Kuo, H. C. & Yang, K. D. (2007) Implications of dynamic changes among tumor necrosis factor-alpha (TNF-alpha), membrane TNF receptor, and soluble TNF receptor levels in regard to the severity of dengue infection. *Am J Trop Med Hyg*, 77(2), 297-302.
Wang, T., Town, T., Alexopoulou, L., Anderson, J. F., Fikrig, E. & Flavell, R. A. (2004) Toll-like receptor 3 mediates West Nile virus entry into the brain causing lethal encephalitis. *Nat Med*, 10(12), 1366-73.
Wang, W., Li, G., De, W., Luo, Z., Pan, P., Tian, M., Wang, Y., Xiao, F., Li, A., Wu, K., Liu, X., Rao, L., Liu, F., Liu, Y. & Wu, J. (2018) Zika virus infection induces host inflammatory responses by facilitating NLRP3 inflammasome assembly and interleukin-1β secretion. *Nature Communications*, 9(1), 106.
Wei, X., Song, H., Yin, L., Rizzo, M. G., Sidhu, R., Covey, D. F., Ory, D. S. & Semenkovich, C. F. (2016) Fatty acid synthesis configures the plasma membrane for inflammation in diabetes. *Nature*, 539(7628), 294-298.
Weiss, L., Hoffmann, G. E., Schreiber, R., Andres, H., Fuchs, E., Körber, E. & Kolb, H. J. (1986) Fatty-acid biosynthesis in man, a pathway of minor importance. Purification, optimal assay conditions, and organ distribution of fatty-acid synthase. *Biol Chem Hoppe Seyler*, 367(9), 905-12.
Welsch, S., Miller, S., Romero-Brey, I., Merz, A., Bleck, C. K., Walther, P., Fuller, S. D., Antony, C., Krijnse-Locker, J. & Bartenschlager, R. (2009) Composition and three-dimensional architecture of the dengue virus replication and assembly sites. *Cell Host Microbe*, 5(4), 365-75.
Wen, C., Yu, Y., Gao, C., Qi, X., Cardona, C. J. & Xing, Z. (2022) Concomitant pyroptotic and apoptotic cell death triggered in macrophages infected by Zika virus. *PLOS ONE*, 17(4), e0257408.
Wen, H., Gris, D., Lei, Y., Jha, S., Zhang, L., Huang, M. T., Brickey, W. J. & Ting, J. P. (2011) Fatty acid-induced NLRP3-ASC inflammasome activation interferes with insulin signaling. *Nat Immunol*, 12(5), 408-15.
Wengler, G. & Wengler, G. (1989) Cell-associated West Nile flavivirus is covered with E+pre-M protein heterodimers which are destroyed and reorganized by proteolytic cleavage during virus release. *J Virol*, 63(6), 2521-6.
Westaway, E. G., Khromykh, A. A. & Mackenzie, J. M. (1999) Nascent flavivirus RNA colocalized in situ with double-stranded RNA in stable replication complexes. *Virology*, 258(1), 108-17.

Westaway, E. G., Mackenzie, J. M., Kenney, M. T., Jones, M. K. & Khromykh, A. A. (1997) Ultrastructure of Kunjin virus-infected cells: colocalization of NS1 and NS3 with double-stranded RNA, and of NS2B with NS3, in virus-induced membrane structures. *J Virol*, 71(9), 6650-61.
Westaway, E. G., Mackenzie, J. M. & Khromykh, A. A. (2002) Replication and gene function in Kunjin virus. *Curr Top Microbiol Immunol*, 267, 323-51.
Widmer, J., Fassihi, K. S., Schlichter, S. C., Wheeler, K. S., Crute, B. E., King, N., Nutile-McMenemy, N., Noll, W. W., Daniel, S., Ha, J., Kim, K. H. & Witters, L. A. (1996) Identification of a second human acetyl-CoA carboxylase gene. *The Biochemical journal*, 316 (Pt 3)(Pt 3), 915-922.
Wilentz, R. E., Witters, L. A. & Pizer, E. S. (2000) Lipogenic enzymes fatty acid synthase and acetyl-coenzyme A carboxylase are coexpressed with sterol regulatory element binding protein and Ki-67 in fetal tissues. *Pediatr Dev Pathol*, 3(6), 525-31.
Wilfling, F., Wang, H., Haas, J. T., Krahmer, N., Gould, T. J., Uchida, A., Cheng, J. X., Graham, M., Christiano, R., Fröhlich, F., Liu, X., Buhman, K. K., Coleman, R. A., Bewersdorf, J., Farese, R. V., Jr. & Walther, T. C. (2013) Triacylglycerol synthesis enzymes mediate lipid droplet growth by relocalizing from the ER to lipid droplets. *Dev Cell*, 24(4), 384-99.
Winston, D. J., Vikram, H. R., Rabe, I. B., Dhillon, G., Mulligan, D., Hong, J. C., Busuttil, R. W., Nowicki, M. J., Mone, T., Civen, R., Tecle, S. A., Trivedi, K. K., Hocevar, S. N. & West Nile Virus Transplant-Associated Transmission Investigation, T. (2014) Donor-derived West Nile virus infection in solid organ transplant recipients: report of four additional cases and review of clinical, diagnostic, and therapeutic features. *Transplantation*, 97(9), 881-889.
Witkowski, A., Thweatt, J. & Smith, S. (2011) Mammalian ACSF3 protein is a malonyl-CoA synthetase that supplies the chain extender units for mitochondrial fatty acid synthesis. *The Journal of biological chemistry*, 286(39), 33729-33736.
Woo, M. S., Yang, J., Beltran, C. & Cho, S. (2016) Cell Surface CD36 Protein in Monocyte/Macrophage Contributes to Phagocytosis during the Resolution Phase of Ischemic Stroke in Mice. *J Biol Chem*, 291(45), 23654-23661.
Xie, G., Luo, H., Tian, B., Mann, B., Bao, X., McBride, J., Tesh, R., Barrett, A. D. & Wang, T. (2015) A West Nile virus NS4B-P38G mutant strain induces cell intrinsic innate cytokine responses in human monocytic and macrophage cells. *Vaccine*, 33(7), 869-78.
Xie, M., Yu, Y., Kang, R., Zhu, S., Yang, L., Zeng, L., Sun, X., Yang, M., Billiar, T. R., Wang, H., Cao, L., Jiang, J. & Tang, D. (2016) PKM2-dependent glycolysis promotes NLRP3 and AIM2 inflammasome activation. *Nat Commun*, 7, 13280.
Yang, W., Hood, B. L., Chadwick, S. L., Liu, S., Watkins, S. C., Luo, G., Conrads, T. P. & Wang, T. (2008) Fatty acid synthase is up-regulated during hepatitis C virus infection and regulates hepatitis C virus entry and production. *Hepatology*, 48(5), 1396-403.
Yao, C. H., Liu, G. Y., Wang, R., Moon, S. H., Gross, R. W. & Patti, G. J. (2018) Identifying off-target effects of etomoxir reveals that carnitine palmitoyltransferase I is essential for cancer cell proliferation independent of β-oxidation. *PLoS Biol*, 16(3), e2003782.
Yasser, B., Ala, I., Mohammad, M., Mohammad, H., Khalid, T., Hatim, A., Ihab, A. & Bashar, A.-K. (2010) Inhibition of hormone sensitive lipase and pancreatic lipase by Rosmarinus officinalis extract and selected phenolic constituents. *Journal of Medicinal Plants Research*, 4(21), 2235-2242.
Yau, C., Low, J. Z. H., Gan, E. S., Kwek, S. S., Cui, L., Tan, H. C., Mok, D. Z. L., Chan, C. Y. Y., Sessions, O. M., Watanabe, S., Vasudevan, S. G., Lee, Y. H., Chan, K. R. & Ooi, E. E. (2021) Dysregulated metabolism underpins Zika-virus-infection-associated impairment in fetal development. *Cell Reports*, 37(11).
Yen, Y. T., Chen, H. C., Lin, Y. D., Shieh, C. C. & Wu-Hsieh, B. A. (2008) Enhancement by tumor necrosis factor alpha of dengue virus-induced endothelial cell production of reactive nitrogen and oxygen species is key to hemorrhage development. *J Virol*, 82(24), 12312-24.

Yeung, A. W., Wu, W., Freewan, M., Stocker, R., King, N. J. & Thomas, S. R. (2012) Flavivirus infection induces indoleamine 2,3-dioxygenase in human monocyte-derived macrophages via tumor necrosis factor and NF-κB. *J Leukoc Biol*, 91(4), 657-66.
Yockey, L. J., Varela, L., Rakib, T., Khoury-Hanold, W., Fink, S. L., Stutz, B., Szigeti-Buck, K., Van den Pol, A., Lindenbach, B. D., Horvath, T. L. & Iwasaki, A. (2016) Vaginal Exposure to Zika Virus during Pregnancy Leads to Fetal Brain Infection. *Cell*, 166(5), 1247-1256.e4.
Zaitseva, E., Yang, S.-T., Melikov, K., Pourmal, S. & Chernomordik, L. V. (2010a) Dengue Virus Ensures Its Fusion in Late Endosomes Using Compartment-Specific Lipids. *PLOS Pathogens*, 6(10), e1001131.
Zaitseva, E., Yang, S. T., Melikov, K., Pourmal, S. & Chernomordik, L. V. (2010b) Dengue virus ensures its fusion in late endosomes using compartment-specific lipids. *PLoS Pathog*, 6(10), e1001131.
Zang, Y., Wang, T., Xie, W., Wang-Fischer, Y.-L., Getty, L., Han, J., Corkey, B. E. & Guo, W. (2005) Regulation of Acetyl CoA Carboxylase and Carnitine Palmitoyl Transferase-1 in Rat Adipocytes, 13(9), 1530-1539.
Zhang, H.-L., Ye, H.-Q., Liu, S.-Q., Deng, C.-L., Li, X.-D., Shi, P.-Y. & Zhang, B. (2017) West Nile Virus NS1 Antagonizes Interferon Beta Production by Targeting RIG-I and MDA5. *Journal of virology*, 91(18), e02396-16.
Zhao, Y., Soh, T. S., Lim, S. P., Chung, K. Y., Swaminathan, K., Vasudevan, S. G., Shi, P. Y., Lescar, J. & Luo, D. (2015) Molecular basis for specific viral RNA recognition and 2'-O-ribose methylation by the dengue virus nonstructural protein 5 (NS5). *Proc Natl Acad Sci U S A*, 112(48), 14834-9.
Zhou, Y., Niu, C., Li, Y., Gao, B., Zheng, J., Guo, X. & Ma, W. (2012) Fatty acid synthase expression and esophageal cancer. *Mol Biol Rep*, 39(10), 9733-9.
Zou, J., Lee, L. T., Wang, Q. Y., Xie, X., Lu, S., Yau, Y. H., Yuan, Z., Geifman Shochat, S., Kang, C., Lescar, J. & Shi, P.-Y. (2015) Mapping the Interactions between the NS4B and NS3 Proteins of Dengue Virus. *Journal of Virology*, 89(7), 3471.
Zuo, H. & Wan, Y. (2020) Metabolic Reprogramming in Mitochondria of Myeloid Cells. *Cells*, 9(1).
Zuo, Z., Liew, O. W., Chen, G., Chong, P. C., Lee, S. H., Chen, K., Jiang, H., Puah, C. M. & Zhu, W. (2009) Mechanism of NS2B-mediated activation of NS3pro in dengue virus: molecular dynamics simulations and bioassays. *J Virol*, 83(2), 1060-70.

APPENDICES

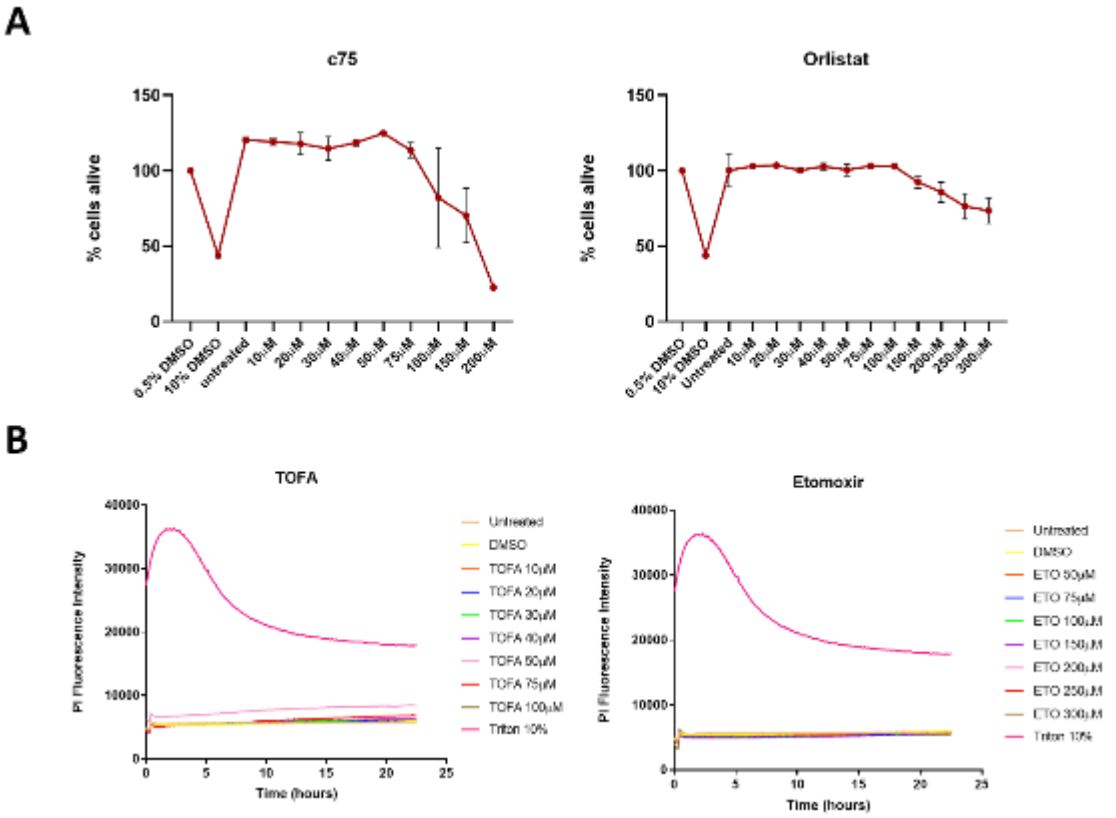

Appendix A. Cytotoxicity of fatty acid synthesis and fatty acid oxidation inhibitors in Vero cells. Vero cells were treated with inhibitors at varying concentrations as indicated, for 24 hours in media supplemented with 2 % FCS. All drugs were diluted in DMSO, at or below a final concentration of 0.5 %, and as such this concentration was used as a control to test the toxicity of DMSO. 10 % DMSO or Triton-X was also used as a control for total cell death. **(A)** After 24 hours, toxicity of c75 and orlistat was determined by measuring the release of lactate dehydrogenase using the CytoTox 96® Non-Radioactive Cytotoxicity Assay kit as per the manufacturer's protocol. GraphPad Prism 8 was used to graph the final results, and each data point represents 3 technical replicates in 3 independent biological replicates (n=3, +/- S.E.M.). **(B)** Cells were seeded in black-walled 96-well plates, and after adhesion were treated with varying concentrations of TOFA and etomoxir, as indicated. Propidium iodide was added to each well at a final concentration of 1 μg/mL, and PI fluorescence was measured using a ClarioStar Plus Microplate Reader over a 24-hour period at 37 °C and 5 % CO_2. Fluorescent intensity was then graphed using GraphPad Prism 8 (n=3).

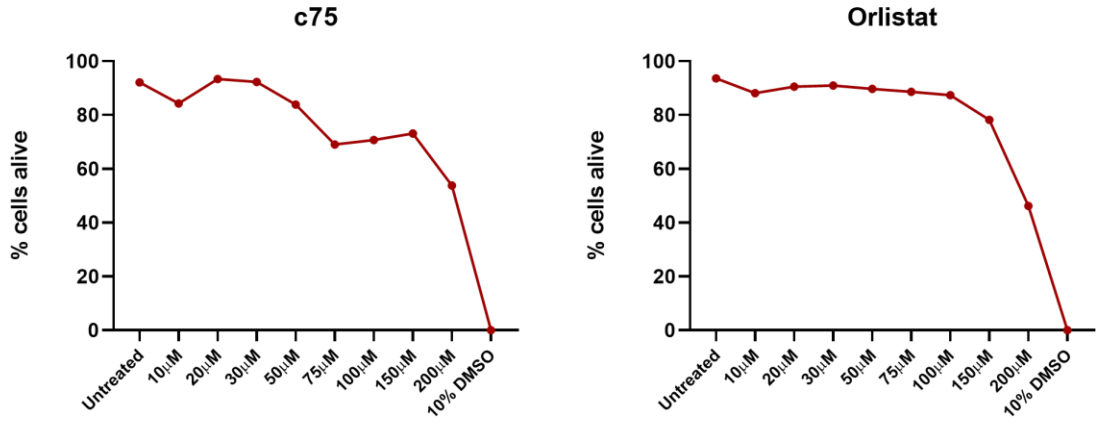

Appendix B. Cytotoxicity of fatty acid synthesis inhibitors in THP-1 cells. THP-1 monocytes were differentiated to a macrophage-like state with 25 ng/mL of PMA for 24 hours, followed by 24 hours of rest. Differentiated cells were then treated with c75 or orlistat at varying concentrations as indicated, for 3 days in media supplemented with 2 % FCS. All drugs were diluted in DMSO, at or below a final concentration of 0.5 %, and as such this concentration was used as a control to test the toxicity of DMSO. After 3 days, toxicity of c75 and orlistat was determined by measuring the release of lactate dehydrogenase using the CytoTox 96® Non-Radioactive Cytotoxicity Assay kit as per the manufacturer's protocol. GraphPad Prism 8 was used to graph the final results.

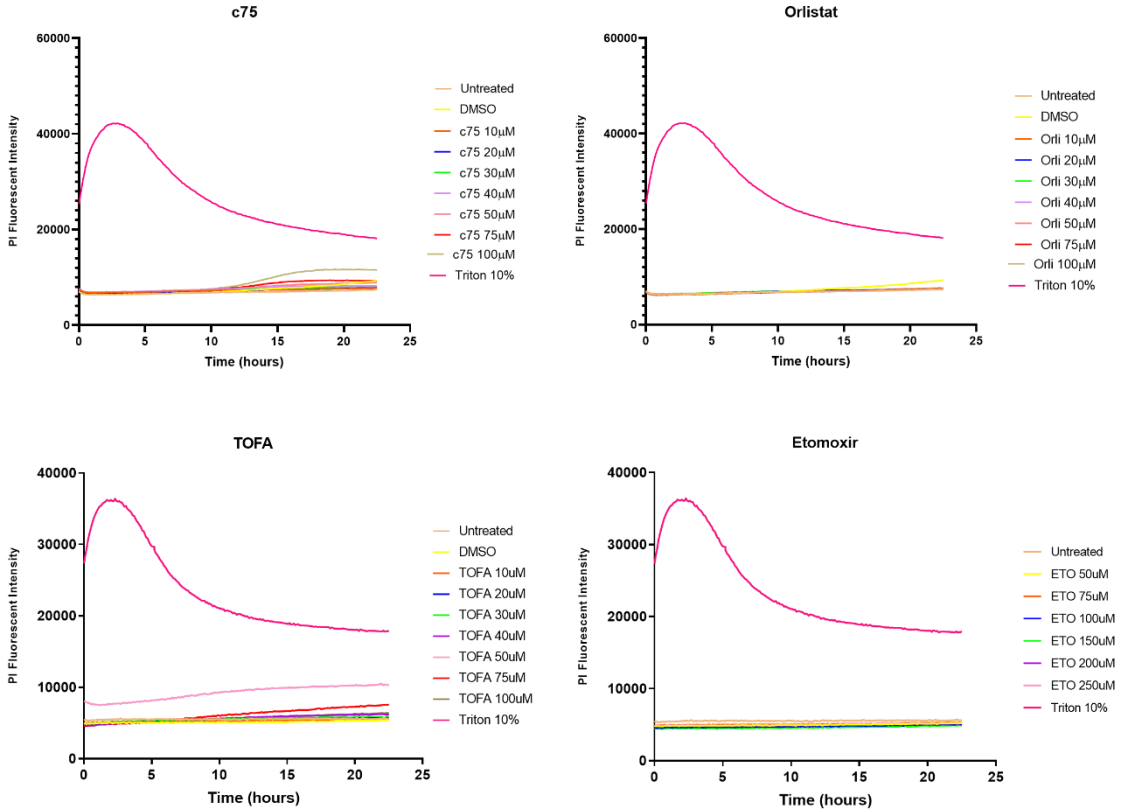

Appendix C. Cytotoxicity of fatty acid synthesis and fatty acid oxidation inhibitors in RAW264.7 cells. RAW264.7 cells were seeded in black-walled 96-well plates, left to attach for 24 hours, and then treated with inhibitors at varying concentrations as indicated, for 24 hours in media supplemented with 2 % FCS. All drugs were diluted in DMSO, at or below a final concentration of 0.5 %, and as such this concentration was used as a control to test the toxicity of DMSO. 10 % Triton-X was also used as a control for total cell death. Propidium iodide was added to each well at a final concentration of 1 μg/mL, and PI fluorescence was measured using a ClarioStar Plus Microplate Reader over a 24-hour period at 37 °C and 5 % CO_2. Fluorescent intensity was then graphed using GraphPad Prism 8 (n=3).

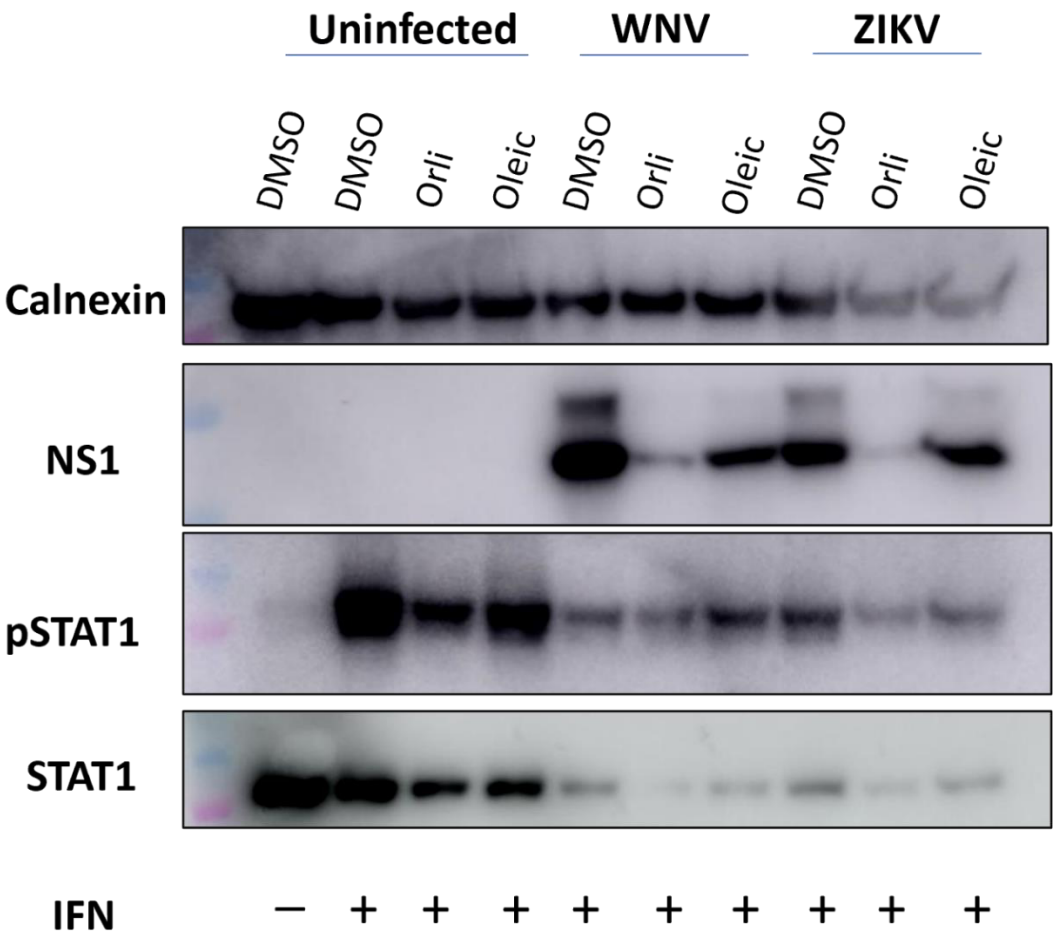

Appendix D. Infection with WNV and ZIKV reduces levels of total and phosphorylated STAT1 in Vero cells. Vero cells were infected and either left untreated, or treated with FASN inhibitors c75 (30 μM) or orlistat (100 μM) for 24 hours. Human IFN-α was used to stimulate cells for 45 minutes (at 37 °C) prior to this 24 hour timepoint, after which cell lysates were harvested. Western blotting and specific antibodies to calnexin (loading control), NS1 (viral marker), total STAT1 and phosphorlated STAT1 (pSTAT1) were used to visualise the relative amounts of each protein. This western blot is representative of 2 independent replicates (n=2).